2020

# Solvolytic Lignocellulosic Biomass Liquefaction

Mustafa Alluhaibi
*South Dakota State University*

# SOLVOLYTIC LIGNOCELLULOSIC BIOMASS LIQUEFACTION

By

MUSTAFA ALLUHAIBI

A dissertation submitted in partial fulfillment of the requirements for the

Doctor of Philosophy

Major in Chemistry

South Dakota State University

2020

DISSERTATION ACCEPTANCE PAGE

Mustafa Alluhaibi

This dissertation is approved as a creditable and independent investigation by a candidate for the Doctor of Philosophy degree and is acceptable for meeting the dissertation requirements for this degree. Acceptance of this does not imply that the conclusions reached by the candidate are necessarily the conclusions of the major department.

Cheng Zhang
Advisor Date

Douglas Raynie
Department Head Date

Nicole Lounsbery, PhD
Director, Graduate School Date

# ACKNOWLEDGEMENTS

I want to take this opportunity to thank the people who have helped me during my study at South Dakota State University. First and foremost, I would like to thank my advisor, Dr. Cheng Zhang, for his guidance, support, patience, and encouragement in every aspect of this work. I would like to thank my committee members, Dr. Douglas Raynie, Dr. Surtaj Iram, and Dr. Ross Abraham, for their time and valuable discussions.

I am grateful to Dr. Zheng Gu and Dr. Quinn Qiao for the allowance of using their labs to do the characterization of my samples. I would also like to thank my previous group members Dr. Jianyuan Sun, Dr. Logan Sanow, and Manik Gudimani for collaborations. I am grateful to all the faculty members, postdocs, and graduate students in the Chemistry and Biochemistry department for valuable discussions, help in experiments and friendship.

This dissertation is dedicated to my late parents for their unfailing love, support, faith, and motivation, which provided me with the power to persist in completing my Ph.D. successfully. My sincere thanks to my dear wife for her utmost care, support, and wise suggestions to handle all of my obstacles during my stay in the U.S. I would like to acknowledge the NSF EPSCoR Track II, Dakota Bioprocessing Consortium (DakotaBioCon) Award #: IIA-1330842 for supporting this work.

Finally, I much appreciate and recognize the scholarship received from Umm Al-Qura University, which is without it, I cannot pursue my education in Chemistry field and get the academic experience that I have now.

CONTENTS

# ABSTRACT

SOLVOLYTIC LIGNOCELLULOSIC BIOMASS LIQUEFACTION

MUSTAFA ALLUHAIBI

2020

Increasing energy demand, petroleum prices, global warming, and depleting fossil fuel resources are the main challenges faced by the human beings. Many scientists are searching for sustainable and alternative sources of fossil fuels as solutions to these challenges. Lignocellulosic biomass is one of the renewable and eco-friendly abundant sources that has been considered by both academia and industry sectors as a renewable source for bio-oil and chemicals. Direct liquefaction of biomass in the sub-/super-critical solvent has considered a practical method to convert lignocellulosic material into liquid fuel. However, undesirable properties such as poor stability, low energy value, and high acidity and heteroatoms content are the main drawbacks of bio-oil generated by the liquefaction method. Elimination of these undesirable properties is necessary before the bio-oil can be utilized for co-processing in refineries alongside petroleum crude oil or used as transportation and engine fuels directly. To improve the biomass liquefaction process, the research presented in this dissertation focuses on the chemistry of direct biomass liquefaction in terms of product distribution and yields of liquefaction, the influence of liquefaction parameters, and role of catalysts. In chapter 2, pine sawdust liquefaction was catalyzed by different concentrations of NaOH, metals, and metallic salts in $H_2O$, EtOH, and a mixture of EtOH and $H_2O$. The liquefaction results showed that liquefaction in $H_2O$ at 200 °C gave low bio-oil yields. While in the co-solvent liquefaction, higher yields of bio-oil were obtained at 240 °C and 260 °C in comparison

with that achieved at 200 °C. In solvolytic liquefaction (only EtOH used as solvent), pine sawdust was effectively liquefied, and higher production of bio-oil was generated by metals with high reduction power. Based on the results revealed in this chapter, outcomes of pine sawdust liquefaction are highly determined by solvent and temperature more than other parameters. In chapter 3, many investigations were conducted to determine the influence of residence time, biomass: base ratio, metal oxide, and Ni metals for the development of a catalytic system for corn stover liquefaction. The results suggested that high bio-oil yields could be obtained using Ni metal combined with $Fe_2O_3$ under the basic condition at (8:1) ratio of biomass/base. In chapter 4, liquefaction of different biomass such as corn stover, birch, switchgrass, pine sawdust, and sugarcane bagasse using various catalytic systems were investigated. The synergistic effect of Ni metal-metal oxide in the presence of NaOH showed a more significant influence on biomass liquefaction, depending on the type of biomass and metal oxide used. The results are consistent with what was presented in chapter 3. Bio-oil production was more promoted under basic than neutral conditions. Lower percentages of protons attributed to aromatic and oxygenated species were measured in bio-oils generated under basic conditions compared to those measured under neutral conditions. The distribution of bio-oil components is highly determined by the type of biomass and catalysts used. In chapter 5, to achieve better improvements in the quality and cost-effectiveness of bio-oils generated from direct liquefaction, Fe, Zn, and Ni metals were used in combination with a salt for liquefaction of corn stover under different conditions. KOAc was found to be a more effective base than NaOH. High bio-oils (>40%) and low SR (<6%) yields with low

oxygen content were achieved from corn stover liquefaction at 300 $^{o}$C for < 4 hr using Ni metal-$Fe_2O_3$- KOAc and Zn metal, $Ni(OAc)_2$, KOAc.

# CHAPTER 1: INTRODUCTION

## 1.1 Importance of biofuels

Today, fossil fuels are the dominant energy sources and provide > 80% of the world's energy supply. However, fossil fuels are non-renewable, and their resources are limited. According to the current consumption rates, petroleum, natural gas, and coal will only last for 45, 60, 120 years, respectively.[1] The diminishing supply and increasing greenhouse gas levels owing to the combustion of fossil fuels for the production of heat and power compel the world to develop renewable energy alternatives.[2-4] Thus, the development of clean technologies to utilize a sustainably produced feedstock is one of the current research interests in chemistry, engineering, agriculture, and environmental society.[5]

In the present day, the entirety of energy supply is met by a single source (*i.e.*, petroleum) in many countries. Consequently, a more flexible system drawing from multiple sources should be an attractive long-term solution for energy production. For instance, vehicles powered by electricity, water, wind, and solar energy, and hydrogen fuel cells are highly researched to reduce our dependence on petroleum as a source of energy. However, these new technologies especially hydrogen fuel cells have not yet been economically and technically viable. In contrast, due to their similarity to the currently preferred fuel sources, liquid biofuels derived from renewable biomass are a better option. Their implementation does not require extensive changes to the transportation infrastructure and the internal combustion engine. Thus, the use of biomass feedstocks as a sustainable source of carbon for biofuels and chemicals is a realizable and promising alternative.[6] Currently, commercial production of electricity and liquid

transportation fuels from biomass feedstocks is practiced in most nations. The U.S. bioenergy production reached $4.76x10^{15}$ J in 2011, accounting for 48.8% of the renewable energy and 5.8% of the total energy produced in the year. In 2012, 49 billion liters of bioethanol were generated from 42% of the U.S. corn grains, representing 94% of the liquid biofuels produced and replaced 10% of the nation's demanded gasoline fuel. The U.S. Energy Independence and Security Act of 2007 mandates to increase annual biofuel addition to gasoline from 34 billion liters in 2008 to136 billion liters by 2022, with 60 billion liters of the biofuel from lignocellulosic biomass.[1]

**1.2 Lignocellulosic biomass**

Biomass can be any organic by-product with a biological origin such as woody plants, agriculture and forestry residues, municipal and industrial wastes, and aquatic plants.[7, 8] Biomass has a relatively higher ratio of H/C compared to coal.[9] Among the elements (carbon, hydrogen, nitrogen, sulfur, and oxygen) present in biomass,[10] carbon accounted for 34.1-53.5 wt%, which represents the major contribution to the overall heating value of biomass.[9] Hydrogen is another major element of biomass, constituting 5.5-6 wt% in herbaceous and 6-8 wt% in woody biomass. Nitrogen and sulfur contents accounted for < 1.8 wt% and 0.1–0.6 wt% of the biomass, respectively, which are lower than those of fossil fuels. The heating value of the bio-oil obtained via any processing technique is highly determined by the oxygen content.[10] Carbohydrates, lignin, protein, and lipids are the basic representative components of various biomass feedstocks. Based on compositions and structures, the biomass can be classified into lignocellulosic biomass, microalgae, and organic wastes. Lignocellulosic materials are the most widespread type of biomass used for bio-oil production through liquefaction.[11] The cell

walls of lignocellulosic biomass are composed of cellulose (40 – 50%) microfibrils frameworks, hemicellulose (25–35%), and lignin (15 – 20%).[6] These structures are interlaced, as illustrated in Figure 1.1.

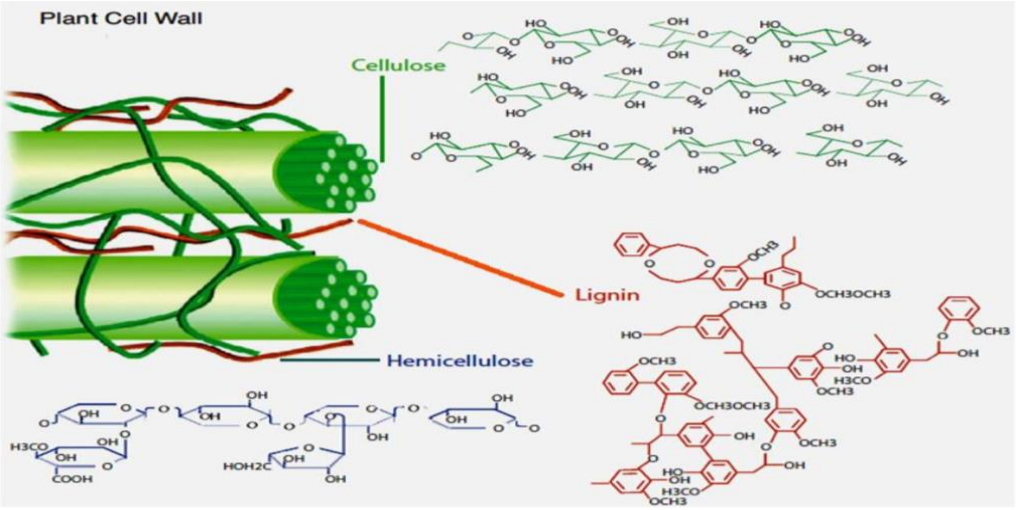


Figure 1.1: Structure of lignocellulosic biomass.[12]

Cellulose is a major component of the primary cell wall of lignocellulose. It is composed of polysaccharide polymer consisting of D-glucose units with β-1,4 glycosidic bonds. The hydroxyl groups on one chain form hydrogen bonds with nearby oxygen to form a very stable molecule with a high degree of polymerization. Hydrogen bonding makes cellulose insoluble in either polar or non-polar solvents at ambient temperature but tends to be soluble with the increment in the temperature.[6, 10] Hemicellulose component is interlaced with cellulose strands and bound to lignin via hydrogen bonds. It is an amorphous polymer of five different sugar monomers including D-xylose, L-arabinose, D-galactose, D-glucose, and D-mannose, with xylose being the most abundant.[6] Lignin is an amorphous polymer comprising coniferyl, sinapyl, and coumaryl alcohols having different functional groups such as hydroxyl, methoxy, carbonyl, and carboxyl. These

alcohols are connected by various interunit linkages such as β-O-4, α-O-4, β-5, 4-O-5, 5-5, β-1, β-β, as illustrated in Figure 1.2.

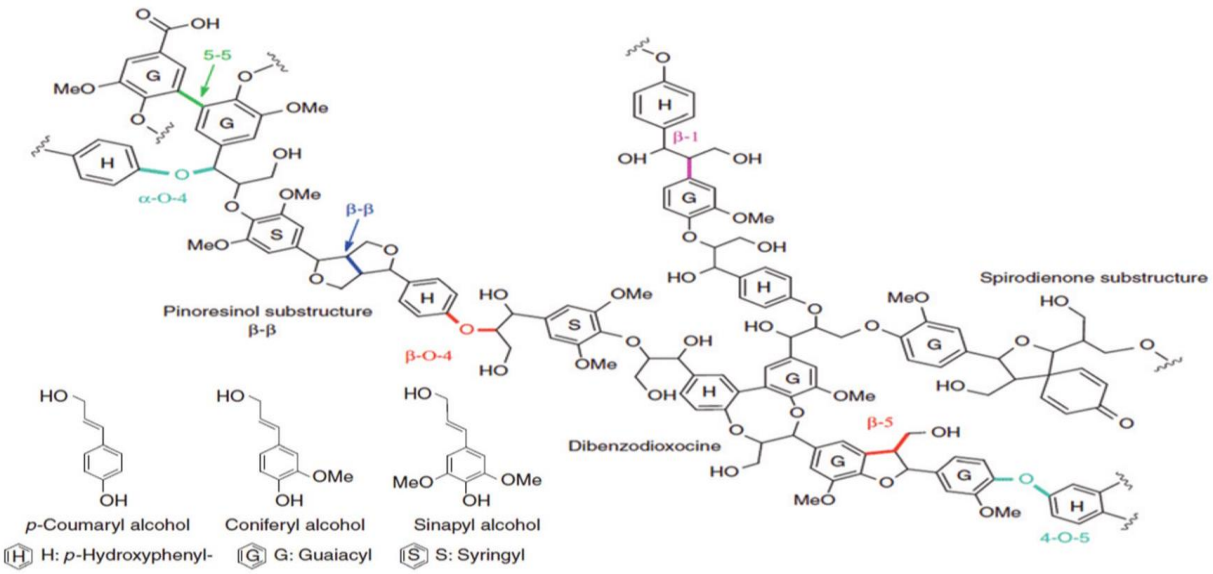


Figure 1.2: Schematic representation of the building blocks of lignin with common linkages.[13]

Compared to other linkages, β-O-4 and α-O-4 ether bonds are the most abundant in lignin, making up about 70% of the linkages found in native lignin. Hence, the cleavage of β-O-4 linkages is the most targeted among others for the depolymerization of lignin.[14-16]

### 1.3 Biomass conversion technologies

Biomass can be converted to biofuels and biopower via thermochemical and biochemical conversion processes. Thermochemical conversion is a significant route for bio-methanol, biodiesel, bio-oil, bio-syngas, and bio-hydrogen. While in biochemical conversion, liquid or gaseous fuels can be produced through fermentation or anaerobic respiration. The production of biofuels via thermochemical conversion processes has

drawn the most attention in the world. The thermochemical methods show a superior ability to degrade diverse biomass in shorter time than the biochemical process.[8, 17, 18] The main routes of biomass conversion through thermochemical technologies involve combustion, gasification, pyrolysis, and liquefaction.[19]

### 1.3.1 Combustion and gasification

Combustion is the most direct and technically most straightforward process for producing heat, carbon dioxide, and water from biomass using an oxidant. Gasification is a biomass conversion process that involves complex reactions, pressure changes, and heat and mass transfer processes. In this method, gasifying agents such as oxygen, air, and steam are necessary to convert biomass into gaseous fuels (syngas or producer gas), which typically have some quantity of $CO_2$, CO, $CH_4$, and $N_2$. Syngas can be upgraded to liquid fuels such as diesel and gasoline by Fischer–Tropsch (FT) synthesis. The gasification process is carried out through various steps, including drying, devolatilization, combustion, and reduction. Biomass is first dried at 150 °C to evaporate the moisture. Then, it is subjected to devolatilization in the temperature range of 150–700 °C to liberate the volatile species followed by the combustion of biomass in 700–1500 °C. In the combustion step, fuel constituents oxidize, and exothermic reactions are triggered. While in the last reduction step (800–1100 °C), fuel constituents reduce, and endothermic reactions are involved. Gasification has many advantages over combustion. It can use low-value feedstock and convert them into electricity and vehicle fuels. It is expected that gasification will serve as a significant technology for complementing the energy demands of the world within the coming years.[6, 19, 20]

### 1.3.2 Pyrolysis

Pyrolysis is a thermal degradation of biomass in the absence of oxygen to form gases, pyrolytic oil (bio-oil), and char. Pyrolysis processes are classified into slow and fast based on operating parameters such as reaction temperature, reaction time, and heating rate on which the yields of products depend. Slow pyrolysis works at a temperature range of 400–600 °C at 0.1–1 °C/s heating rate for 5–30 min residence time. In slow pyrolysis, biochar is formed in higher amounts in comparison to gases and bio-oil produced. However, fast pyrolysis can provide a higher yield of bio-oil and lower char. Fast pyrolysis is operated at a higher temperature range of 850-1250 °C at a 10–20 °C/s heating rate, and short residence time of 1–10 s. In fast pyrolysis, biomass with low moisture content requires a high temperature and heating rate. The bio-oil formed through pyrolysis cannot be served as a transportation fuel due to its high oxygen value (40-50 wt%), low pH value, high water content (15-30 wt%), and low H/C ratios. Therefore, the upgrading of bio-oil is necessary before its utilization.[7, 8, 19, 21]

### 1.3.3 Liquefaction

Liquefaction is a suitable process for converting a variety of wet feedstocks, unlike pyrolysis and gasification, where the biomass has to be dried before use.[22] Direct liquefaction is seen as a promising technology for the production of biofuel and chemicals from biomass feedstock.[23] With this process, various solvents and operation conditions have been employed. For instance, the hydrothermal liquefaction (HTL) process converts biomass into a liquid product in the presence of water at 250–400 °C and 5–25 MPa pressures.[7] In the HTL process, water has been used as the primary solvent for being cheap and eco-friendly. Water in the HTL process acts as a reactant and

solvent. Bio-oil is the main product of the HTL process, whereas water-soluble products, hydro-char, and gases are considered as by-products. Biomass components (cellulose and hemicellulose) can be hydrolyzed easily in water at elevated temperatures and pressures.[8, 9] Various organic solvents have been employed in solvent liquefaction instead of water to liquefy biomass at 120–500 °C temperature.[9] Due to their unique characteristics, among other solvents, the effect of alcoholic solvents has been studied broadly in lignocellulosic biomass liquefaction. Unlike water, alcohol can dissolve decomposed products under both ambient and supercritical conditions. Bio-oil is more easily separated in alcohol compared to the case of sub and supercritical water. Moreover, alcohols have a lower corrosive risk than water and can provide hydrogen during liquefaction reaction. The use of alcohol as a hydrogen donor can suppress repolymerization and carbonization reactions, which improves the bio-oil yield.[24] The effect of a co-solvent system consisting of organic solvent and water on lignocellulosic biomass liquefaction has been explored at a temperature range of 200–340 °C.[9] Pan et al.[25] reported that the synergistic effect of organic solvent and water showed high solubility and gave a high yield and good quality of bio-oil in mild reaction conditions. The individual roles of ethanol and water in co-solvent liquefaction of lignocellulosic biomass have been examined by Feng et al. [26] Based on their investigation, carbohydrate decomposition was accelerated by water, while lignin depolymerization was facilitated in ethanol by dissolving lignin fragments and impeding the re-condensation of the reaction intermediates. Bio-oil produced from liquefaction method at lower temperature has higher heating value and moderate oxygen content compared with other thermochemical processes such as gasification and pyrolysis.[19, 24] The process schematic of bio-oil production from biomass liquefaction is

illustrated in Figure 1.3. Biomass depolymerizes into simpler monomers, which in turn decompose through cleavage, dehydration, decarboxylation, and deamination into small light fragments. These fragments, through condensation, cyclization, and polymerization, can rearrange to form bio-oil.[11, 27]

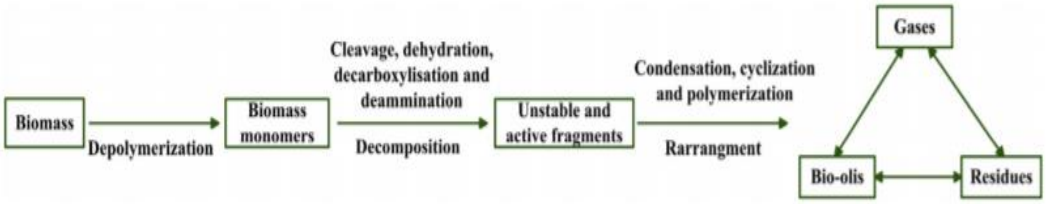


Figure 1.3: The process schematic of liquefaction biomass. [11]

# CHAPTER 2: LIQUEFACTION OF PINE SAWDUST: A COMPARATIVE STUDY OF DIFFERENT CATALYSTS AND EFFECTS OF SOLVENT, TEMPERATURE, AND RESIDENCE TIME ON BIO-OIL PRODUCTION

## 2.1 Introduction

The depletion of finite resources of fossil fuels, environmental pollution, and energy crisis are driving the global society to search for cheap, clean, efficient, and sustainable energy production. [28-30] Biomass is a renewable and abundant resource of carbon-based fuel that can be exploited to produce bio-oil. Lignocellulosic biomass (agricultural by-products) has been utilized as a viable carbon feedstock for liquid fuel production. Lignocellulosic agriculture wastes are composed of cellulose, hemicellulose, and lignin. Cellulose is a straight-chain polymer of poly-glucose units, while hemicellulose is a polymer comprising different C5 and C6 sugars. Lignin is composed of a complex polymer of propyl–phenol groups bound together by ether and carbon-carbon bonds. The biomass component's structural complexity increases from cellulose to hemicellulose to lignin, which means that the energy required for converting biomass increases as the complexity of the biomass component increases.[31, 32]

Various thermochemical conversion processes have been used to liquefy biomass,[33] but direct thermochemical liquefaction is potentially more competitive as the process typically requires low temperature and can produce a liquid fuel with low-oxygen in one step. Many attempts have been made to improve the direct biomass liquefaction through increasing bio-oil production and reducing char formation. Different alkali solutions of NaOH, $Ca(OH)_2$, $K_2CO_3$, RbOH, CsOH, KOH, and $Ba(OH)_2$ have been

employed as catalysts for the production of heavy bio-oil from the biomass liquefaction in sub/near-critical water.[34-37] Most metals catalysts such as cobalt (Co), molybdenum (Mo), nickel (Ni), titanium (Ti), tungsten (W), Zinc (Zn), antimony (Sb), bismuth (Bi), cerium (Ce), Vanadium (V), niobium (Nb), tantalum (Ta), chromium (Cr), manganese (Mn), rhenium (Re), iron (Fe), platinum (Pt), iridium (Ir), palladium (Pd), osmium (Os), rhodium (Rh) and ruthenium (Ru) along with other metal compounds are employed by petroleum industries in refining processes.[38, 39] For biomass upgrade, metal salts are often employed as catalysts in non-aqueous solvents.[40-43] Extensive research on the biomass liquefaction using different catalysts has been made to enhance liquid fuel yield and quality. However, the bio-oil produced by liquefaction process has not been commercialized yet. High cost, undesirable properties, and low yield are considered the main obstacles for the commercialization of bio-oil production by this method. It is crucial to study the liquefaction behavior of biomass by different metals without using an external reducing agent to gain improvements in the quality and quantity of bio-oils from cost-effective liquefaction.

Indeed, different catalysts are needed for biomass liquefaction. Transition metals as an electron donor and hydrogen transfer can facilitate the reduction and hydrogenation processes of oxygenated species resulted from biomass liquefaction. Alkaline earth metals such as NaOH are an essential catalyst to promote the hydrolysis of biomass and decarboxylation reactions. Moreover, metal oxides as Lewis acids can enhance oxygen removal through dehydration and dehydrogenation reactions. This study aims to investigate how the synergy of Ni metal + ZnO + NaOH can influence the yield and quality of bio-oils from hydrothermal and co-solvent liquefaction of pine sawdust at a

low temperature of 200 °C. Moreover, the synergy of different metals (ex; Ni, Pd, Co, Cu, Mo, Fe, Ag, Ru) + metal oxides (ex; ZnO, MgO, FeO, PbO, MnO) + NaOH was investigated on solvolytic pine sawdust liquefaction in 100% EtOH at a moderate temperature of 260 °C. The intensity of aromatic and aliphatic protons in bio-oil are measured by $^{1}$H-NMR, and volatile components in the bio-oil products are identified by GC-MS. To gain better understanding of how oxygen atoms got removed from biomass, the decomposition pathways for the formation of significant liquefaction products were proposed.

## 2.2 Experimental

### 2.2.1 Materials

Pine sawdust was obtained from a local farm and reduced in size using a blender to 18-50 mesh. The chemical composition of pine sawdust has cellulose ( 45-50 wt.%), hemi-cellulose (25-35 wt.%) and lignin (25-35 wt.%). All metallic salts, metals, and reagents throughout the whole experiments were commercially available, analytical grade, and used as received. Sodium hydroxide and ethanol were purchased from Fisher Scientific and Pharmco-AAPER company, respectively.

### 2.2.2 Liquefaction procedure

The general procedure of pine sawdust liquefaction: To a stainless-steel pressure reactor in a nitrogen glovebox were added a magnetic stirring bar, catalyst, 400 mg of pine sawdust, and solvent. Then, the closed reactor was transferred into a fume-hood and heated in a molten salt bath at the desired temperature and time. After the reactor was cooled down, the reactor was opened, and liquid-solid products were separated and extracted as seen in Figure 2.1. The reaction mixture was thoroughly rinsed out of the

reactor with EtOH. Then, the suspension solution was filtered at a reduced pressure using a pre-weighed filter paper. The Zn cake remaining on the filter paper was washed with HCl solution (6N) to make sure all Zn reacted, and cellulose fibers precipitated. The resulted suspension was filtrated to collect and measure the remained cellulose, while aqueous filtrate was evaporated to remove EtOH and then $NaHCO_3$ solution was added to precipitate the repolymerized lignin. Subsequently, the lignin suspension was filtered, and the resulted aqueous phase was extracted three times using 2 mL of dichloromethane each time. For liquefaction in pure EtOH, the liquid-solid mixture was filtered and washed with EtOH. The ethanol solution was condensed by rotary evaporation under a reduced pressure of 80 mbar using a 50°C water bath. To the residue, 1 mL of $CH_2Cl_2$ (DCM) and 0.5 ml of water were added. The DCM solution was separated, and the water phase was extracted by DCM (0.5 mL × 2). The combined DCM solution was neutralized with $NaHCO_3$, dried with $MgSO_4$ powder, and condensed on a rotary evaporator to yield an oil.

The percentage yield of oil, solid bio-residue, and pine sawdust conversion was calculated based on the weight of pine sawdust feed by the following formula:

$$\text{Bio oil yield (wt\%)} = \frac{\text{Weight of bio-oil}}{\text{Biomass weight}} \times 100\%$$

$$\text{Solid bio residue (SR) yield (wt\%)} = \frac{\text{Weight of solid bio residue}}{\text{Biomass wieght}} \times 100\%$$

$$\text{Un repolymerization yield (wt\%) of bio oil} = 100\% - \text{Solid bio residue \%}$$

$$\text{Gas + water soluble species (wt\%)} = 100\% - \text{Bio oil \%} - \text{Solid bio residue \%}$$

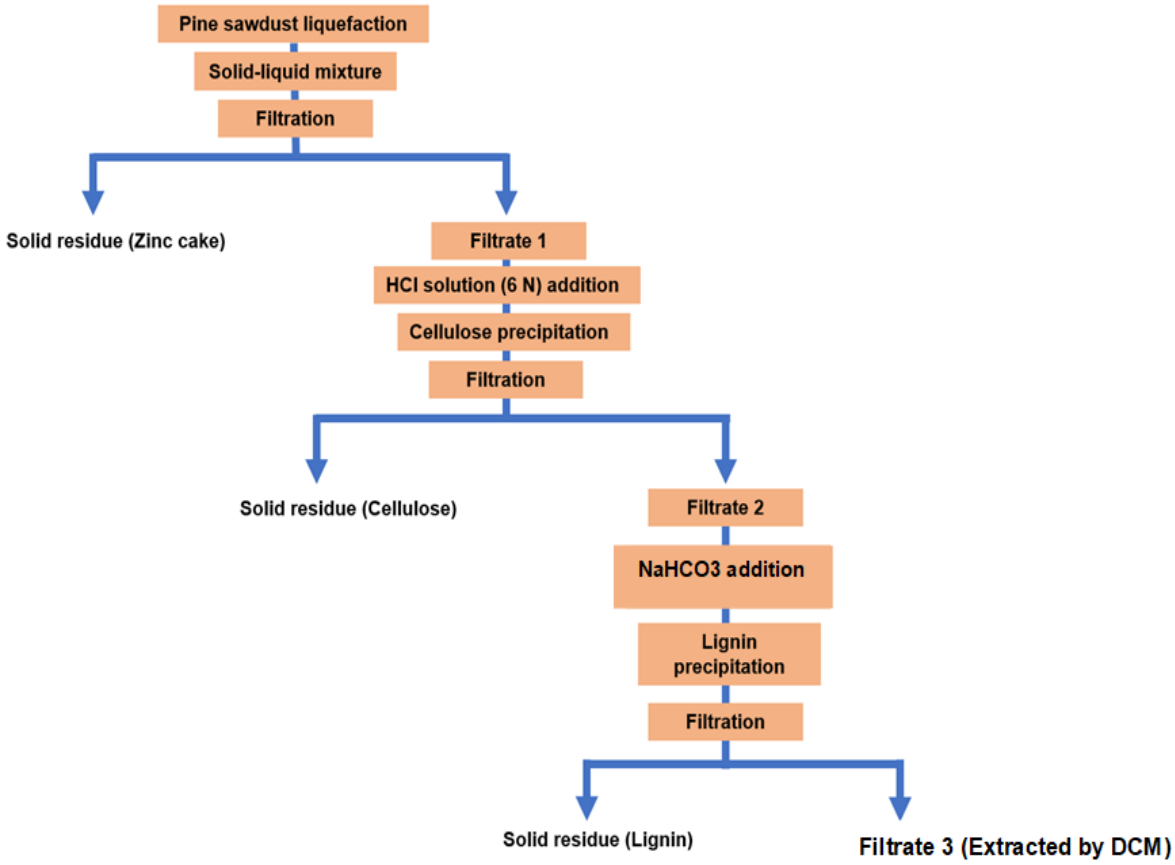


Figure 2.1. Procedure for separation and extraction of hydro- and co-solvent liquefaction products.

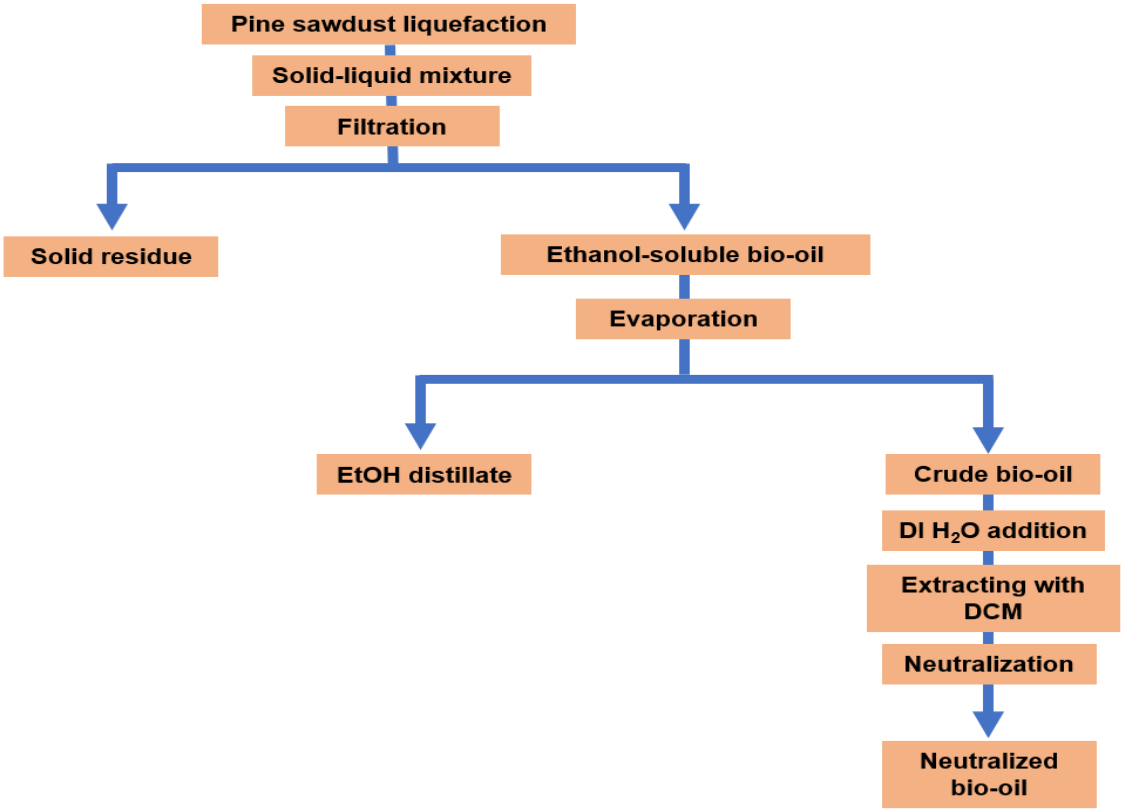


Figure 2.2. Procedure for separation and extraction of solvolytic liquefaction products.

### 2.2.3 Characterization

$^1$H-NMR analysis was performed for bio-oil obtained from each pine sawdust liquefaction on a Bruker AVANCE- 400 and 600 MHz NMR spectrometer in $CDCl_3$ using TMS as the internal standard. GC-MS analysis was performed on a Shimadzu GCMS-QP2010SE. GC column temperature program was set as follows: the temperature was held at 40 $^o$C for 1 minute, then increased to 240 $^o$C at a heating rate of 25 $^o$C/min, and then maintained at 240 $^o$C for 3 minutes. To facilitate the bio-oil derivatization, the bio-oil samples were treated with a common TMS derivatizing reagent - N,O-bis(trimethylsilyl)trifluoroacetamide – BSTFA.

## 2.3 Liquefaction reaction results and discussion

### 2.3.1 Hydrothermal liquefaction using Zn metal and $Ni(OAc)_2$

In this study, we investigated hydrothermal liquefaction of pine sawdust catalyzed by Ni metal produced by the reduction of $Ni^{2+}$ ions in $Ni(OAc)_2$ using Zn metal, which in turn is oxidized into ZnO, and NaOH under different conditions. The effect of the catalyst system on product distribution from liquefaction at 200 ℃ is shown in Table 2.1. The biomass conversion yield reached 60.13%, 61.33%, and 72.48%, and the bio-oil production was 7.43%, 6.33%, and 8.65% by using 100, 200, 300 mg of NaOH for liquefaction runs 2.2, 2.5, and 2.6, respectively. The effect of NaOH showed a significant impact on the conversion of cellulose and lignin. Hydrolysis of cellulose was more promoted, while the decomposition of lignin into phenolic monomers was more depressed by increasing NaOH loading. In contrast, 6.05%, and 51.25%, 72.48%, 83.88%, and 64.25% of biomass conversion was achieved by increasing the time from 2-20 hr for liquefaction runs 2.1-2.4, giving 8.65%, 10.73%, and 14.25% of bio-oil, respectively. Besides, increasing the time from 6-24 hr for liquefaction runs 2.6-2.8 enhanced the conversion yield to 60.13%, 69%, and 71.13%, producing 7.43%, 12.9%, and 13.28% of bio-oil, respectively. The yields of lignin and cellulose were greatly reduced by increasing the time, achieving 16.13%, which is the minimum content of solid residue obtained from liquefaction run 2.3. The last experiment (run 2.9) gave 16.45% of bio-oil, which is higher than what achieved in other runs. According to Cheng, D'cruz et al.,[44] hydro-liquefaction of pine sawdust at 300 °C and 1:10 of biomass: $H_2O$ ratio gave 70 wt% biomass conversion and 40 wt% bio-oil yield, which are higher than what was achieved in our investigation. Xu and Lad[34] found that both heavy oil and water-soluble

oil increase as temperature increased from 280 to 300 °C for the Jack pine sawdust liquefaction in sub/near-critical water at 280 to 380 °C and 1:10 ratio of biomass: solvent. And further increment in temperature resulted in a slight decline in their yields. In contrast, the liquefaction results of our investigation were found comparable to those reported by Singh, Balagurumurthy et al. from catalytic hydrothermal liquefaction of water hyacinth using $K_2CO_3$ and KOH at a temperature range of 250 to 300 °C.[45] The previous results under this investigation indicate that the biomass liquefaction in a high ratio of biomass:$H_2O$ can improve oil yield remarkably as the temperature increases compared to other factors such as time and catalyst.

Table 2.1: The products yields of 400 mg pine sawdust liquefaction using Ni metal and ZnO in 8 mL $H_2O$ at 200°C.

| Reaction run | Catalyst | Liquefaction time (h) | Bio-oil% | Un-repolymerization% | Solid residue% | | Gas + water-soluble species% |
|---|---|---|---|---|---|---|---|
| | | | | | Lignin% | Cellulose% | |
| 2.1 | 901 mg Zn, 40 mg $Ni(OAc)_2$, 300 mg NaOH | 2 | 6.05 | 51.25 | 21 | 27.75 | 45.2 |
| 2.2 | 901 mg Zn, 40 mg $Ni(OAc)_2$, 300 mg NaOH | 6 | 8.65 | 72.475 | 16.65 | 10.875 | 63.825 |
| 2.3 | 901 mg Zn, 40 mg $Ni(OAc)_2$, 300 mg NaOH | 12 | 10.725 | 83.875 | 13.75 | 2.375 | 73.15 |
| 2.4 | 901 mg Zn, 40 mg $Ni(OAc)_2$, 300 mg NaOH | 20 | 14.25 | 64.25 | 31.5 | 4.25 | 50 |
| 2.5 | 901 mg Zn, 40 mg $Ni(OAc)_2$, 200 mg NaOH | 6 | 6.325 | 61.375 | 21.425 | 17.2 | 55.05 |
| 2.6 | 901 mg Zn, 40 mg $Ni(OAc)_2$, 100 mg NaOH | 6 | 7.425 | 60.125 | 4.125 | 35.75 | 52.7 |
| 2.7 | 901 mg Zn, 40 mg $Ni(Oac)_2$, 100 mg NaOH | 12 | 12.9 | 69 | 3 | 28 | 56.1 |
| 2.8 | 901 mg Zn, 40 mg $Ni(Oac)_2$, 100 mg NaOH | 24 | 13.275 | 71.125 | 1.625 | 27.25 | 57.85 |
| 2.9 | 901 mg Zn, 100 mg NaOH | 15 | 16.45 | 68.15 | 5.875 | 25.975 | 51.7 |

### 2.3.2 Liquefaction using Zn metal and $Ni(OAc)_2$ in ethanol-water

The effect of ZnO and Ni metal on pine sawdust liquefaction in the mixture of EtOH and $H_2O$ was investigated under different conditions, as shown in Table 2.2. The biomass liquefaction at 200°C for six hours gave an irregular profile by increasing NaOH loading in liquefaction runs 2.11-2.13. The yields of bio-oil and biomass conversion declined while the SR yield increased to 62.85%, with NaOH rising from 30 mg to 50 mg. As NaOH was further increased to above 50 mg, bio-oil production rose to 21.18%, and SR yield decreased to 40%.

From runs 2.14 and 2.15, the $H_2O$: EtOH ratio was changed from 1:1 to 1:3. As a result, less cellulose and lignin were recovered, and a lower yield of bio-oil was obtained. So, biomass liquefaction is unfavored in a less aqueous medium at low temperatures. The time elongation influence was investigated, as seen in liquefaction runs 2.17-2.20. Bio-oil production was enhanced while SR was reduced by increasing the time of liquefaction, achieving 91.5% of bio-oil, which is the highest yield obtained from liquefaction at 200 °C. Compared to run 2.20, lower bio-oil and higher gas production happened in run 2.21. This result may suggest that cracking and dehydration reactions could be promoted by ZnO and NaOH in the absence of Ni metal at a long time of co-solvent liquefaction. High bio-oil yields were made from liquefaction 2.10 and 2.22 at 260°C and 240°C in the presence of NaOH. From the above results, it can be concluded that cellulose hydrolysis was quite slow at low temperature irrespective of whether a catalyst was present or not, and liquefaction at high temperatures (260°C and 240°C) produced higher yields of bio-oil.

Table 2.2: The product yields from 400 mg pine sawdust liquefaction using Ni metal and ZnO in mixture of EtOH and $H_2O$.[a]

| Run | Catalyst | Liquefaction condition | Bio-oil% | Un-repolymerization% | Solid residue% | | Gas + water-soluble species% |
|---|---|---|---|---|---|---|---|
| | | | | | Lignin% | Cellulose% | |
| 2.10 | 901 mg Zn, 40 mg $Ni(OAc)_2$, 100 mg NaOH | 260°C, 6 h | 52.23 | 95.25 | 0.5 | 4.25 | 43.02 |
| 2.11 | 901 mg Zn, 40 mg $Ni(OAc)_2$, 100 mg NaOH | 200°C, 6 h | 21.18 | 60 | 4.75 | 35.25 | 38.82 |
| 2.12 | 901 mg Zn, 40 mg $Ni(OAc)_2$, 50 mg NaOH | 200°C, 6 h | 7.1 | 37.15 | 4.25 | 58.6 | 30.05 |
| 2.13 | 901 mg Zn, 40 mg $Ni(OAc)_2$, 30 mg NaOH | 200°C, 6 h | 9.7 | 95 | 5 | 0 | 85.3 |
| 2.14 | 901 mg Zn, 40 mg $Ni(OAc)_2$ | 200°C, 6 h | 18.93 | 64.5 | 3.25 | 32.25 | 45.57 |

| | | | | | | | |
|---|---|---|---|---|---|---|---|
| 2.15 | 901 mg Zn, 40 mg $Ni(OAc)_2$ | 200°C, 6 h | 15.03 | 43.7 | 5.5 | 50.8 | 28.67 |
| 2.16 | 901 mg Zn, 40 mg $Ni(OAc)_2$, 100 mg NaOH | 200°C, 2 h | 5.88 | 29.87 | 2.12 | 68 | 24 |
| 2.17 | 901 mg Zn, 40 mg $Ni(OAc)_2$, 100 mg NaOH | 200°C, 2 h | 7.5 | 34.85 | 0 | 65.15 | 27.35 |
| 2.18 | 901 mg Zn, 40 mg $Ni(OAc)_2$, 100 mg NaOH | 200°C, 13 h | 17.975 | 62.275 | 0 | 37.725 | 44.3 |
| 2.19 | 901 mg Zn, 40 mg $Ni(OAc)_2$, 100 mg NaOH | 200°C, 44 h | 91.5 | 79.425 | 0 | 20.57 | - |
| 2.20 | 901 mg Zn, 40 mg $Ni(OAc)_2$, 100 mg NaOH | 200°C, 20 h | 33.875 | 61.55 | 5.575 | 32.875 | 27.675 |
| 2.21 | 901 mg Zn, 100 mg NaOH | 200°C, 20 h | 24.15 | 79.25 | 2.275 | 18.475 | 55.1 |

| | | | | | | | |
|---|---|---|---|---|---|---|---|
| | 901 mg Zn, 40 mg | | | | | | |
| 2.22 | $Ni(OAc)_2$, 100 mg | 240°C, 16 h | 78.25 | 87.2 | 0 | 12.8 | 8.95 |
| | NaOH | | | | | | |

[a] Solvent: (2/6), (7.5/0.5), (8/0.5), and (4/4) mL of EtOH/$H_2O$ mixture were used under reaction runs (2.15), (2.16), (2.17 and 2.18), and (2.10-2.14 and 2.19-2.22), respectively.

### 2.3.3 Solvolytic liquefaction catalyzed by metals and metallic salts

The synergistic effect of Cu, Pd, Co, Ag, Ru, Mo, and Fe metals, produced by the full reduction of their metallic salts using Zn metal, with ZnO and NaOH was investigated on liquefaction of pine sawdust in EtOH in runs 2.23-2.26 and 2.28-2.30, as illustrated in Table 2.3. The bio-oil yields obtained from runs 2.23-2.25 by Cu, Pd, Co metals with ZnO and NaOH is ranked in the following order: Pd (135.1%) > Co (64.65%) > Cu (58.9%) metal and the lower SR yield was achieved by Pd metal. This result is consistent with the fact that metal with a larger atomic radius tends to be a better reductant because the more influential the reducing agent, the higher is its tendency to donate electrons. When a higher amount of Sb (745 mg, run 2.34) was employed with Pd metal, produced by the reduction of $Pd^{+2}$ ions via Sb metal, and NaOH, the bio-oil dropped to 20%, the lowest production achieved. So, Sb metalloid as a reducing agent is inferior to Zn (run 2.24). Among Ag, Ru, Fe and Mo metals used with ZnO and NaOH (runs 2.26 and 2.28-2.30), Ru gave higher yield (80.08%) of bio-oil and lower yields (3.83% and 16.1%) of SR, gas, and water.

The synergy of Ni metal, generated by the reduction of $Ni^{+2}$ via Mg, Fe, Pb, and Mn metals, with their oxides and NaOH on pine sawdust liquefaction was also examined as seen in runs 2.31, 2.33, 2.35, and 2.36. The results showed how biomass liquefaction was greatly affected by the reducing character of metal applied because the reduction surface of Ni metal depends on the number of electrons donated by the reducing agent. When a lower number of moles of electrons (0.012 mol e-) was supplied by Mn metal to $Ni^{+2}$ ions compared to the electrons added of Fe (0.021 mol e-) and Mg (0.05 mol e-), the yields of bio-oil and un-repolymerization were high. Similar trends were observed by

comparing the results achieved from runs 2.27 and 2.32. The addition of 0.012 mole e- of Zn metal showed better results from biomass liquefaction than Fe metal. Furthermore, because Pb is not higher active to reduce Ni ions, the same moles number of electrons of Pb (0.012 mol e-) in run 2.35 gave lower bio-oil and higher yields of SR, gas, and water-soluble species, indicating that Fe and Pb are not suitable catalysts as Ni metal.

| Run | Catalyst | Bio-oil% | Un-repolymerization% | Solid residue% | | Gas + water-soluble species% |
|---|---|---|---|---|---|---|
| | | | | Lignin% | Cellulose% | |
| 2.23 | 20 mg $Cu(OAc)_2$. $H_2O$, 400 mg Zn, 50 mg NaOH | 58.9 | 79.85 | 0 | 20.15 | 20.95 |
| 2.24 | 20 mg $Pd(OAc)_2$, 400 mg Zn, 50 mg NaOH | 135.1 | 89.875 | 0 | 10.125 | - |
| 2.25 | 20.7 mg $Co(OAc)_2$, 400 mg Zn, 50 mg NaOH | 64.65 | 83.75 | 0.5 | 15.75 | 19.1 |
| 2.26 | 13.7 mg $AgNO_3$, 400 mg Zn, 50 mg NaOH | 48.925 | 77.1 | 0 | 22.9 | 28.175 |
| 2.27 | 7.7 mg Mo, 400 mg Zn, 50 mg NaOH | 54.85 | 73.7 | 0 | 26.3 | 18.85 |
| 2.28 | 24.9 mg $Ru(NH_3)_6$ $Cl_3$, 400 mg Zn, 55 mg NaOH | 80.075 | 96.175 | 0 | 3.825 | 16.1 |
| 2.29 | 13.0 mg $FeCl_3$, 400 mg Zn, 55 mg NaOH | 54.975 | 84.3 | 0 | 15.7 | 29.325 |

| | | | | | | |
|---|---|---|---|---|---|---|
| 2.30 | 16.5 mg $Na_2MoO_4$, 400 mg Zn, 50 mg NaOH | 45.2 | 83.625 | 7.25 | 9.125 | 38.425 |
| 2.31 | 20 mg $Ni(OAc)_2$, 594.8 mg Mg, 50 mg NaOH | 34 | 87.175 | 0 | 12.825 | 53.175 |
| 2.32 | 600 mg Fe, 50 mg NaOH | 45.15 | 69.425 | 17.625 | 12.95 | 24.275 |
| 2.33 | 20 mg $Ni(OAc)_2$. $H_2O$, 600 mg Fe, 50 mg NaOH | 78.375 | 92.525 | 0.05 | 7.425 | 14.15 |
| 2.34 | 20 mg $Pd(OAc)_2$, 745 mg Sb, 50 mg NaOH | 20 | 52.925 | 14.375 | 32.7 | 32.925 |
| 2.35 | 20 mg $Ni(OAc)_2$, 1267.9 mg Pb, 50 mg NaOH | 43.625 | 79.5 | 0 | 20.5 | 35.875 |
| 2.36 | 20 mg $Ni(OAc)_2$, 336.1 mg Mn, 50 mg NaOH | 75.825 | 92.5 | 0 | 7.5 | 16.675 |

Table 2.3: The liquefaction yields from 400 mg pine sawdust using diverse metals and metallic salts in EtOH.[a]

[a] Liquefaction condition: 400 mg pine sawdust, 4 mL EtOH, 260°C, 8 h.

### 2.3.4 Characterization of bio-oil composition

#### 2.3.4.1 $^{1}$H-NMR analysis of bio-oil

To investigate the chemical structural changes of bio-oil produced, $^{1}$H-NMR analysis was carried out. The percentages of proton type were calculated on the basis of the integration values obtained from the $^{1}$H NMR spectra. The region of spectrum from 0.5 to 3.0 ppm represents aliphatic protons of non-oxygenated carbon atoms (—$CH_3$, —$CH_n$—) , 3.0 to 4.0 ppm represents protons on oxygenated aliphatic carbon atoms (alcohol and ether), (.1 to 4.3 ppm represents protons of ester group (—$COOCH_n$—), 5.0-6.0 ppm corresponds to protons of unsaturated carbon (=CH—) and 6.0 to 8.0 ppm corresponds to the aromatic protons ( Ar—H).

$^{1}$H-NMR analysis of bio-oils from hydrothermal (runs 2.1-2.9), co-solvent ( runs 2.10-2.22), and solvolytic ( runs 2.23-2.36) liquefaction of pine sawdust is presented in Figures 2.3, 2.4, and 2.5, respectively ($^{1}$H-NMR spectra are shown in S1-S37). Based on the proton distributions, Zn metal + $Ni(OAc)_2$ + NaOH showed a good synergistic effect of on reduction of oxygenated species resulted from cellulose and hemicellulose decomposition. In all bio-oils except that from run 2.15, the percentage of protons in 0.5-3.0 ppm was higher than that of located in the other regions, which indicates a high degree of reduction of the biomass decomposition products. The bio-oils produced by hydrothermal liquefaction the low temperature of 200 °C contained 34.94%-48% of protons in the region of 6-8 and 3-4 ppm, which is considered the lowest quality compared to bio-oils generated by co-solvent and solvolytic liquefaction. On the other hand, for co-solvent liquefaction, the relative proton intensity of non-oxygenated carbons was highly enhanced under runs 2.10, 2.19, 2.20, and 2.22 of Figure 2.4, which indicates

that increasing time and temperature was more effective on the reduction of aromatic and oxygenated species compared to the loading effect of NaOH. In contrast, the influence of Zn metal and $Ni(OAc)_2$ in the absence of NaOH showed lower effectiveness on their reduction under 2.14 and 2.15, which may be ascribed that the reduction reactions are less promoted under neutral conditions.

Liquefaction of pine sawdust using different metallic salts and metals in EtOH gave percentages lower than 20% of protons bound to aromatic and oxygenated carbons with the exception under run 2.35. Consequently, most protons in bio-oils produced are of non-oxygenated carbons. Among metals used with $Ni(OAc)_2$ and NaOH under runs 2.31, 2.33, 2.35, and 2.36 of Figure 2.5, Fe gave 10.71% of protons linked to aromatic and oxygenated carbons. The metallic acetate salts used with Zn or Sb under runs 2.23-2.25 and 2.34 gave close proton percentages of non-oxygenated carbons. On the other hand, Ru metal gave a higher portion of protons located in the region of 0.5-3.0 ppm among inorganic metallic salts used with Zn metal.

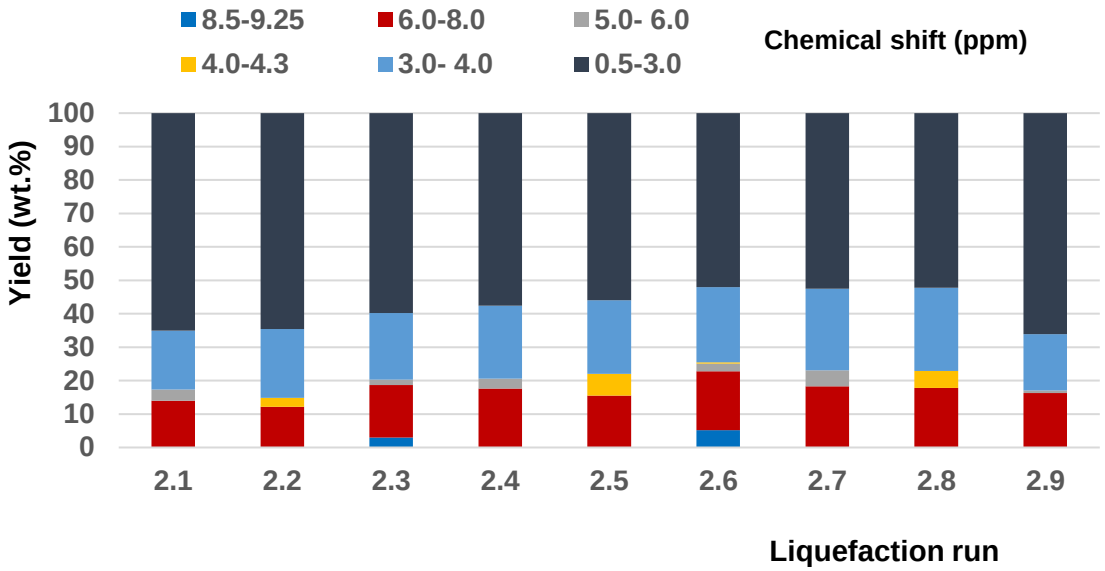


Figure 2.3: $^{1}$H-NMR analysis of bio-oil produced from Hydrothermal liquefaction of pine sawdust in runs 2.1-2.9 using Zn metal and $Ni(OAc)_2$.

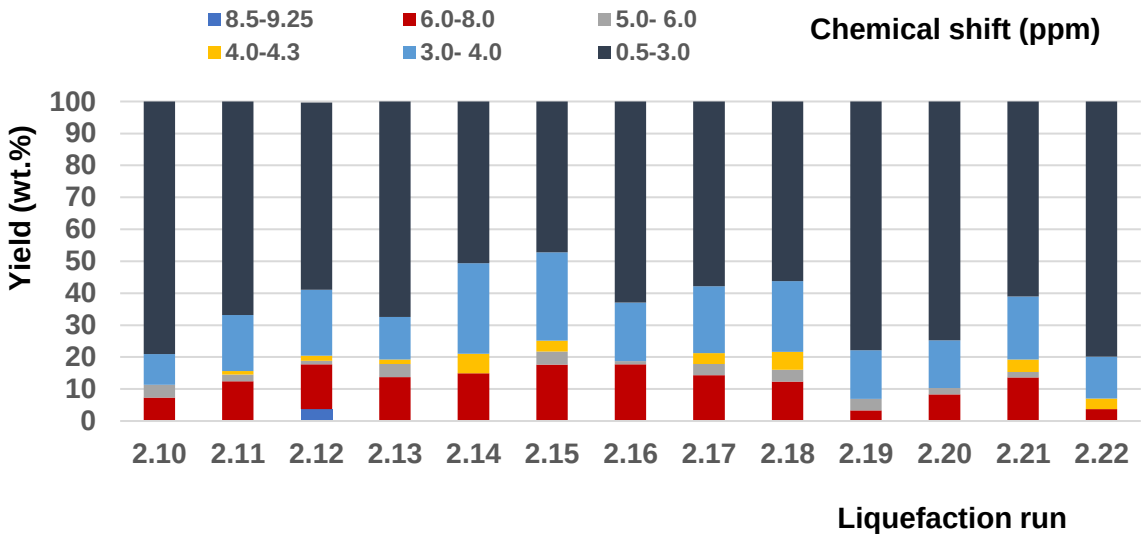


Figure 2.4: $^{1}$H-NMR analysis of bio-oil produced from liquefaction of pine sawdust in runs 2.10-2.22 using Zn metal and $Ni(OAc)_2$ in a mixture of EtOH and $H_2O$.

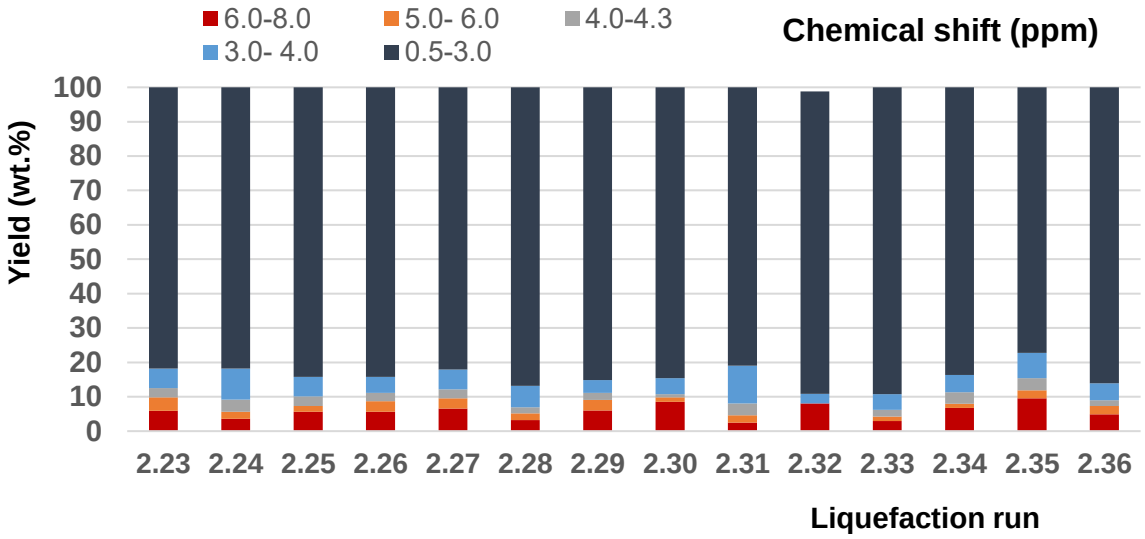


Figure 2.5: $^{1}$H-NMR analysis of bio-oil produced from liquefaction of pine sawdust in runs 2.23-2.36 using diverse metallic salts and metals in EtOH.

### 2.3.4.2 GC-MS analysis of bio-oil

The GC−MS analysis was carried out to identify the volatile components of the bio-oils from the biomass liquefaction using a NIST mass spectral database. The relative percent area of a compound identified was determined by the area percentage of the compound out of the total area. Only compounds in the bio-oil that are volatile and can pass through the GC column show up in the GC-MS chromatograms (S38-S48).

As illustrated in Tables 2.4, 2.5, and 2.6, the major compounds in the bio-oil generated in aqueous media under runs 2.1, 2.2, and 2.9, respectively were phenolic products (>91%) and some minor species of alcohol. The bio-oils from co-solvent liquefaction under runs 2.10, 2.17, 2.18, and 2.22 were analyzed, as presented in Tables 2.7, 2.8, 2.9, and 2.10, respectively. Aromatics account for 86.45%, which is the highest content of the compounds identified under run 2.17. In contrast, alcoholic derivatives constituted the most elevated amount (80.53%) of the compounds identified under run 2.22. For runs

2.10 and 2.18, the major compounds detected were attributed to both aromatic and alcohol, which are present in close proportions. The composition of bio-oils produced from biomass liquefaction using metals and metallic salts was analyzed, as seen in Tables 2.11, 2.12, 2.13, and 2.14. Alcoholic products were the dominant category detected in runs 2.24, 2.31, 2.33 and 2.36, and other categories such as ester, ether, aldehyde, ketone, hydrocarbon, and acid were also found in lower abundances. No aromatic derivatives were observed in bio-oils produced by metals and metallic salts.

Table 2.4: Main compounds identified and their contents in bio-oils generated from biomass liquefaction in $H_2O$ under run 2.1.

| Ret. Time (min) | Area% | Similarity% | Compound name |
|---|---|---|---|
| 4.072 | 0.913618 | 95 | Propane-1,2-diol |
| 4.508 | 1.094572 | 97 | Butane-2,3-diol |
| 4.709 | 0.728392 | 97 | Phenol |
| 5.165 | 0.814123 | 96 | Butane-1,2-diol |
| 5.582 | 0.788948 | 92 | 2-Methyl-butane |
| 5.987 | 0.414507 | 72 | 2-Methylene-butane-1,4-diol |
| 6.348 | 7.958543 | 95 | 2-Methoxy-phenol |
| 6.449 | 13.01567 | 90 | 4-Isopropyl-phenol |
| 7.049 | 2.337122 | 87 | 2-Methoxy-4-methylphenol |
| 7.581 | 23.00698 | 84 | 4-Hydroxy-3-methoxy-benzaldehyde |
| 8.091 | 1.246251 | 69 | 2-Methoxybenzenacetic acid |
| 8.901 | 5.349935 | 92 | 1-(4-Hydroxy-3-methoxy-phenyl)-ethanone |

| | | | |
|---|---|---|---|
| 9.295 | 14.56649 | 94 | 4-(2-Hydroxy-ethyl)-2-methoxy-phenol |
| 9.363 | 7.006329 | 80 | 2-Hydroxy-2-(4-methoxy-phenyl)-propionic acid |
| 9.828 | 17.51399 | 93 | 4-(3-Hydroxy-propyl)-2-methoxy-phenol |
| 10.233 | 0.690252 | 93 | 3-(4-Hydroxy-3-methoxy-phenyl)-propionic acid |
| 10.58 | 0.701 | 87 | 3-(4-Hydroxy-3-methoxy-phenyl)-propane-1,2-diol |
| 11.703 | 1.853278 | 68 | 2-Hydroxy-3-(4-hydroxy-3-methoxy-phenyl)-propionic acid |

Table 2.5: Main compounds identified and their contents in bio-oils generated from biomass liquefaction in $H_2O$ under run 2.2.

| Ret. Time (min) | Area% | Similarity% | Compound name |
|---|---|---|---|
| 3.941 | 0.876139 | 95 | Ethane-1,2-diol |
| 4.077 | 2.824533 | 96 | Propane-1,2-diol |
| 4.512 | 2.164902 | 97 | Butane-2,3-diol |
| 5.289 | 1.414481 | 88 | 1,2-Butanediol |
| 5.584 | 1.504618 | 93 | 2-Methylbutane |
| 6.349 | 12.62569 | 95 | 2-Methoxyphenol |

| | | | |
|---|---|---|---|
| 6.451 | 10.35903 | 89 | 4-Isopropylphenol |
| 7.05 | 3.487997 | 89 | 2-Methoxy-4-methylphenol |
| 7.583 | 25.00713 | 83 | 4-Hydroxy-3-methoxy-benzaldehyde |
| 8.901 | 3.837468 | 93 | 1-(4-Hydroxy-3-methoxy-phenyl)-ethanone |
| 9.295 | 14.61353 | 92 | 4-(2-Hydroxy-ethyl)-2-methoxy-phenol |
| 9.363 | 6.368222 | 79 | 2-Hydroxy-2-(4-methoxy-phenyl)-propionic acid |
| 9.828 | 14.91626 | 93 | 3-Vanilpropanol |

Table 2.6: Main compounds identified and their contents in bio-oils generated from biomass liquefaction in $H_2O$ under run 2.9.

| **Ret. Time (min)** | **Area%** | **Similarity%** | **Compound name** |
|---|---|---|---|
| 4.716 | 2.408969 | 97 | Phenol |
| 5.293 | 1.115254 | 81 | 1,2-Butanediol |
| 6.356 | 33.92353 | 96 | 2-Methoxyphenol |
| 6.455 | 14.85751 | 91 | 4-Isopropylphenol |
| 6.57 | 1.683196 | 63 | Pentane-1,5-diol |
| 7.053 | 2.104002 | 88 | 2-Methoxy-4-methylphenol |
| 7.584 | 19.33667 | 81 | 3-Hydroxy-4-methoxy-benzaldehyde |
| 8.093 | 5.220068 | 70 | (2-Methoxy-phenyl)-acetic acid |
| 8.464 | 1.602646 | 95 | 4-Hydroxy-3-methoxy-benzaldehyde |
| 8.903 | 6.854123 | 93 | 1-(4-Hydroxy-3-methoxy-phenyl)-ethanone |

| | | | |
|---|---|---|---|
| 9.297 | 1.978745 | 86 | 4-(2-Hydroxy-ethyl)-2-methoxy-phenol |
| 9.83 | 8.915287 | 93 | 3-Vanilpropanol |

Table 2.7: Main compounds identified and their contents in bio-oils generated from biomass liquefaction in ethanol-water mixture under run 2.10.

| Ret. Time (min) | Area% | Similarity% | Compound name |
|---|---|---|---|
| 3.708 | 2.2467148 | 95 | Isobutyric acid |
| 4.23 | 2.3702807 | 95 | 2-Methyl-butyric acid |
| 4.458 | 3.2509833 | 96 | 3-Methyl-pentan-1-ol |
| 4.852 | 0.6359555 | 88 | 2,2-Dimethyl-pentan-3-ol |
| 4.968 | 0.7114835 | 90 | 3,3-Dimethyl-butan-2-ol |
| 5.081 | 0.7388323 | 97 | Pentanoic acid |
| 5.157 | 0.458143 | 95 | Ethane-1,2-diol |
| 5.264 | 13.785242 | 97 | Hexan-1-ol |
| 5.402 | 0.630594 | 95 | Propane-1,2-diol |
| 5.443 | 0.4242305 | 88 | 3-Methyl-pentanoic acid |
| 5.496 | 0.7195944 | 87 | Hexanoic acid |
| 5.827 | 0.5093598 | 85 | Cyclohexanol |
| 5.954 | 1.2485568 | 94 | Butane-2,3-diol |
| 6.259 | 1.3156621 | 89 | 2,2-Dimethyl-pentan-3-ol |
| 7.309 | 8.0311481 | 95 | 2-Ethyl-hexan-1-ol |
| 7.493 | 1.3582757 | 88 | Butane-1,2-diol |

| | | | |
|---|---|---|---|
| 7.71 | 4.3390692 | 88 | 4-Methyl-3-heptanol |
| 8.088 | 2.6978901 | 71 | 2-Ethyl-hexan-1-ol |
| 8.213 | 0.8385302 | 91 | 4-Ethoxy-butyric acid |
| 8.713 | 9.8175451 | 96 | Octan-1-ol |
| 8.813 | 0.9163095 | 85 | 2,3-Dimethyl-butane-2,3-diol |
| 8.94 | 0.9953556 | 90 | 2-Hydroxy-3-methyl-butyric acid |
| 9.045 | 1.8692416 | 86 | 2,4-Dimethyl-pentan-3-ol |
| 9.421 | 6.1529052 | 92 | 2-Methoxyphenol |
| 10.292 | 1.7667414 | 85 | Decan-1-ol |
| 10.656 | 3.4914495 | 91 | 2-Methoxy-4-methylphenol |
| 11.338 | 4.2959653 | 95 | Decan-1-ol |
| 11.555 | 8.9661445 | 83 | 4-Hydroxy-3-methoxy-benzaldehyde |
| 12.226 | 2.8002649 | 74 | 2-(2-Hydroxy-ethyl)-phenol |
| 12.407 | 2.8836096 | 60 | 1-Phenyl-propan-1-ol |
| 13.209 | 2.8840587 | 74 | 2-tert-Butyl-benzene-1,4-diol |
| 14.231 | 3.290273 | 92 | 4-(2-Hydroxy-ethyl)-2-methoxy-phenol |
| 14.888 | 3.5595902 | 91 | 3-Vanilpropanol |

Table 2.8: Main compounds identified and their contents in bio-oils generated from biomass liquefaction in ethanol-water mixture under run 2.17.

| **Ret. Time (min)** | **Area%** | **Similarity%** | **Compound name** |
|---|---|---|---|

| | | | |
|---|---|---|---|
| 4.711 | 1.3840384 | 96 | Phenol |
| 4.821 | 5.2877372 | 83 | 4-Methyl-heptan-3-ol |
| 5.598 | 2.8057922 | 80 | Isobutyric acid 2-hydroxy-3-isobutyryloxy-propyl ester |
| 5.786 | 2.7972658 | 82 | 2-Methyl-3-buten-2-ol |
| 6.345 | 2.6501173 | 70 | 2-Ethyl-butan-1-ol |
| 6.45 | 33.788497 | 91 | 4-Isopropylphenol |
| 8.09 | 12.586424 | 71 | 1-(4-Hydroxy-3-methoxy-phenyl)-ethanone |
| 8.624 | 16.471575 | 93 | 4-Allyl-2-methoxy-phenol |
| 9.421 | 5.8527119 | 57 | Matairesinol |
| 9.513 | 6.7079783 | 69 | (4-Hydroxy-3-methoxy-phenyl)-acetic acid ethyl ester |
| 9.826 | 9.6678638 | 92 | 3-Vanilpropanol |

Table 2.9: Main compounds identified and their contents in bio-oils generated from biomass liquefaction in ethanol-water mixture under run 2.18.

| **Ret. Time (min)** | **Area%** | **Similarity%** | **Compound name** |
|---|---|---|---|
| 3.939 | 4.3362514 | 95 | Ethane-1,2-diol |
| 4.403 | 1.9995655 | 91 | Propane-1,2-diol |
| 4.51 | 3.5045439 | 97 | Butane-2,3-diol |
| 4.821 | 10.137715 | 83 | 4-Methyl-3-heptanol |

| | | | |
|---|---|---|---|
| 5.164 | 2.1800791 | 88 | Pentane-1,3-diol |
| 5.287 | 2.6411278 | 80 | Butane-1,2-diol |
| 5.596 | 9.3290224 | 81 | Isobutyric acid 2-hydroxy-3-isobutyryloxy-propyl ester |
| 5.906 | 1.6313262 | 84 | 2-Methyl-butane |
| 6.344 | 7.3423393 | 75 | 2-Ethyl-butan-1-ol |
| 6.449 | 7.5023675 | 92 | 4-Isopropylphenol |
| 6.731 | 1.2830927 | 78 | 2-Methyl-propane-1,2,3-triol |
| 6.891 | 1.9637392 | 79 | Butan-2-ol |
| 7.045 | 1.7086277 | 66 | 2-Methoxy-4-methylphenol |
| 7.578 | 2.6794091 | 61 | 4-Hydroxy-3-methoxy-benzaldehyde |
| 8.002 | 3.5885354 | 81 | Pentane-1,2,5-triol |
| 8.09 | 19.147931 | 69 | Benzeneacetic acid, 2-methoxy- |
| 8.527 | 2.1602012 | 75 | 2H-Pyran, 2-ethoxytetrahydro- |
| 9.293 | 8.9144228 | 92 | 4-(2-Hydroxy-ethyl)-2-methoxy-phenol |
| 9.825 | 7.9497025 | 93 | 3-Vanilpropanol |

Table 2.10: Main compounds identified and their contents in bio-oils generated from biomass liquefaction in ethanol-water mixture under run 2.22.

| Ret. Time (min) | Area% | Similarity% | Compound name |
|---|---|---|---|
| 3.423 | 0.8750995 | 96 | 2-Methyl-butyric acid |

| | | | |
|---|---|---|---|
| 3.559 | 15.024444 | 95 | 2-Ethyl-butan-1-ol |
| 4.022 | 25.062458 | 97 | Hexan-1-ol |
| 4.408 | 1.4441465 | 78 | Hexanoic acid |
| 4.878 | 1.3213591 | 81 | 4,4-Dimethoxy-2-methyl-butan-2-ol |
| 5.203 | 12.957992 | 97 | 2-Ethyl-hexan-1-ol |
| 5.611 | 4.3709781 | 77 | 2-Propyl-pentan-1-ol |
| 5.936 | 10.474362 | 96 | Octan-1-ol |
| 6.123 | 1.0452256 | 85 | 2,4-Dimethyl-pentan-3-ol |
| 6.357 | 4.498981 | 92 | 2-Methoxyphenol |
| 6.457 | 5.69995 | 89 | 4-Isopropylphenol |
| 7.436 | 5.1891792 | 89 | Decan-1-ol |
| 7.586 | 4.5626479 | 82 | 4-Hydroxy-3-methoxy-benzaldehyde |
| 8.081 | 2.2297395 | 82 | 2-Ethyl-decan-1-ol |
| 8.184 | 0.8706861 | 78 | 10-Methyl-undecan-1-ol |
| 8.589 | 2.1153095 | 71 | Dodecan-1-ol |
| 9.105 | 1.1919298 | 58 | Tetradecan-1-ol |
| 9.299 | 1.0655119 | 88 | 4-(2-Hydroxy-ethyl)-2-methoxy-phenol |

Table 2.11: Main compounds identified and their contents in bio-oils generated from biomass liquefaction by metals and metallic salts under run 2.24.

| Ret. Time (min) | Area% | Similarity% | Compound name |
|---|---|---|---|
| 1.942 | 0.3814004 | 89 | Butane, 2,3-dimethyl- |

| | | | |
|---|---|---|---|
| 2.005 | 0.5633886 | 97 | Pentane, 3-methyl- |
| 2.075 | 3.0960231 | 97 | n-Hexane |
| 2.437 | 73.361672 | 96 | 1-Butanol |
| 2.61 | 9.9715066 | 96 | Dimethyl ether |
| 2.75 | 3.0665402 | 91 | Propanoic acid, ethyl ester |
| 2.88 | 2.6879998 | 97 | Ethane, 1,1-diethoxy- |
| 3.163 | 1.2530945 | 98 | Butanal, 2-ethyl- |
| 3.447 | 2.6939606 | 98 | Butanoic acid, ethyl ester |
| 3.553 | 1.2998275 | 97 | Acetic acid, butyl ester |
| 3.794 | 0.2810203 | 95 | 1-Butanol, 2-ethyl- |
| 4.244 | 0.2960494 | 80 | Butane, 1,1-diethoxy- |
| 4.988 | 1.0475174 | 96 | Hexanoic acid, ethyl ester |

Table 2.12: Main compounds identified and their contents in bio-oils generated from biomass liquefaction by metals and metallic salts under run 2.31.

| **Ret. Time (min)** | **Area%** | **Similarity%** | **Compound name** |
|---|---|---|---|
| 1.575 | 0.528429699 | 96 | Acetaldehyde |
| 1.939 | 1.116285113 | 84 | 1-Propanol, 2-methyl- |
| 2.006 | 0.983429866 | 96 | Pentane, 3-methyl- |
| 2.076 | 8.164205504 | 97 | n-Hexane |
| 2.439 | 85.62002466 | 96 | 1-Butanol |
| 2.883 | 1.759041202 | 97 | Ethane, 1,1-diethoxy- |

| | | | |
|---|---|---|---|
| 3.165 | 0.51976067 | 90 | Butanal, 2-ethyl- |
| 3.451 | 1.30882329 | 95 | Butanoic acid, ethyl ester |

Table 2.13: Main compounds identified and their contents in bio-oils generated from biomass liquefaction by metals and metallic salts under run 2.33.

| Ret. Time (min) | Area% | Similarity% | Compound name |
|---|---|---|---|
| 1.573 | 1.9833217 | 98 | Acetaldehyde |
| 1.941 | 3.2770793 | 89 | Pentane, 2-methyl- |
| 2.004 | 4.0498148 | 97 | Pentane, 3-methyl- |
| 2.075 | 31.186399 | 97 | n-Hexane |
| 2.442 | 37.402923 | 88 | 1-Butanol |
| 2.596 | 0.9107757 | 91 | 2-Pentanone |
| 2.754 | 3.2165674 | 96 | Propanoic acid, ethyl ester |
| 2.883 | 5.3357299 | 96 | Ethane, 1,1-diethoxy- |
| 3.166 | 2.9686449 | 96 | Butanal, 2-ethyl- |
| 3.329 | 1.2865228 | 85 | 3-Hexanone |
| 3.453 | 6.3037185 | 96 | Butanoic acid, ethyl ester |
| 4.248 | 2.0785029 | 82 | Pentanoic acid, ethyl ester |

Table 2.14: Main compounds identified and their contents in bio-oils generated from biomass liquefaction by metals and metallic salts under run 2.36.

| Ret. Time (min) | Area% | Similarity% | Compound name |
|---|---|---|---|

| | | | |
|---|---|---|---|
| 2.826 | 7.095284 | 92 | Acetic acid |
| 3.418 | 19.92677 | 97 | Butan-1-ol |
| 4.115 | 3.184334 | 92 | Butanoic acid |
| 4.516 | 6.8371 | 96 | 2-Methyl-pentan-1-ol |
| 4.787 | 3.188646 | 80 | 3-Methyl-but-2-en-1-ol |
| 4.818 | 2.465291 | 91 | Pentanoic acid |
| 4.893 | 27.62632 | 96 | Hexan-1-ol |
| 5.015 | 6.041377 | 86 | cis-2-Hexen-1-ol |
| 5.481 | 4.971713 | 89 | Hexanoic acid |
| 5.537 | 0.884015 | 70 | 2-Methyl-butan-2-ol |
| 5.69 | 3.170788 | 91 | 2-Ethyl-hexan-1-ol |
| 5.806 | 1.873957 | 77 | 2-Hexenoic acid |
| 5.895 | 2.906247 | 70 | Oct-3-en-2-ol |
| 6.187 | 2.294016 | 89 | Octan-1-ol |
| 10.382 | 5.039991 | 72 | Dehydroabietic acid |
| 10.58 | 2.49415 | 73 | Dehydroabietic acid methyl ester |

### 2.3.5 Proposed decomposition paths for the formation of significant liquefaction products

#### 2.3.5.1 Proposed pathways of phenolic monomers

The dominant linkage in the lignin polymer and easier to be cleaved than condensed linkages during the lignin depolymerization and conversion[46] is β-aryl ether (β-O-4), accounting for more than 50% and 60% of total linkages in softwood and hardwood, respectively.[47] Thus, the cleavage of the β-O-4 is considered a critical step of

raw lignin depolymerization to produce phenolic monomers. To understand how the oxygen atoms of the lignin carbon side chain were removed, we propose decomposition paths of the significant phenolic monomers detected via GC-MS. The β-O-4 linkage is employed in the paths proposed for the formation of 3-(4-Hydroxy-3-methoxy-phenyl)-propane-1,2-diol (Table 2.4), 1-(4-Hydroxy-3-methoxy-phenyl)-ethanone (Tables 2.4, 2.5, 2.9, and 2.17), 3-Vanilpropanol (Tables 2.5-2.9), 4-Allyl-2-methoxy-phenol (Table 2.8), 2-Methoxy-phenol (Table 2.4), 2-Methoxy-4-methylphenol (Tables 2.4-2.7 and 2.9), 4-(2-Hydroxy-ethyl)-2-methoxy-phenol (Tables 2.4-2.7, 2.9, and 2.10).

**The decomposition path to 3-(4-Hydroxy-3-methoxy-phenyl)-propane-1,2-diol (Scheme 1).** The deprotonation of OH of the Cα of the lignin side chain can take place under basic condition leading to heterolytic β-O-4 linkage cleavage and α,β-epoxide intermediate **1** formation via intramolecular substitution $S_N2$. The phenol of this intermediate can get deprotonation, resulting in the opening of epoxide ring and forming the quinone methide intermediate **2**, which is likely reduced by Ni metal. As a result, the radical intermediate **3** is reduced and yield 3-(4-Hydroxy-3-methoxy-phenyl)-propane-1,2-diol **4.**

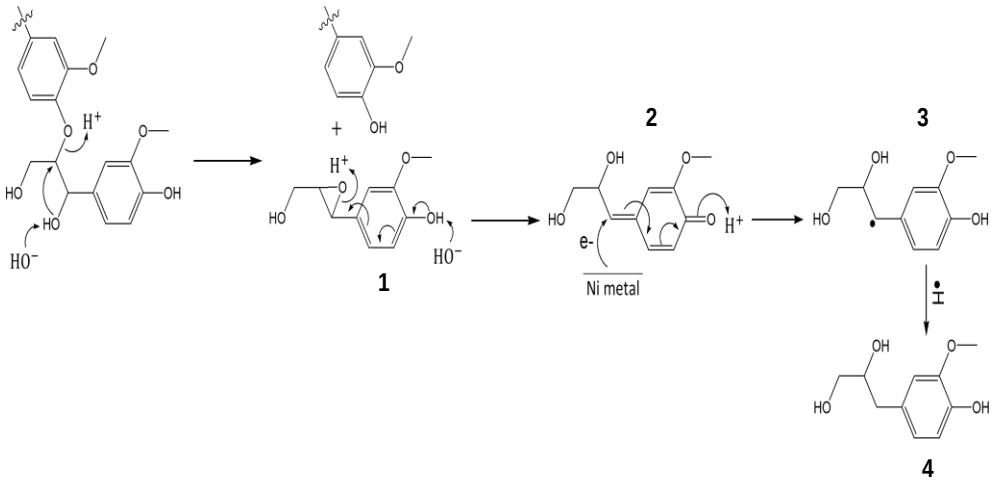


Scheme 1: The formation of 3-(4-Hydroxy-3-methoxy-phenyl)-propane-1,2-diol **4.**

**The decomposition path to 1-(4-Hydroxy-3-methoxy-phenyl)-ethanone.** The β -O-4 linkage can undergo cleavage via intermolecular elimination across Cα-Cβ resulting in propene-1,3-diol intermediate, which is tautomerized into 3-Hydroxy-propan-1-one intermediate **5**. γ-OH of Keto intermediate **5** can undergo intermolecular deprotonation followed by retro-aldol Cβ-Cγ bond cleavage giving 1-(4-Hydroxy-3-methoxy-phenyl)-ethanone **6**, as depicted in Scheme 2.

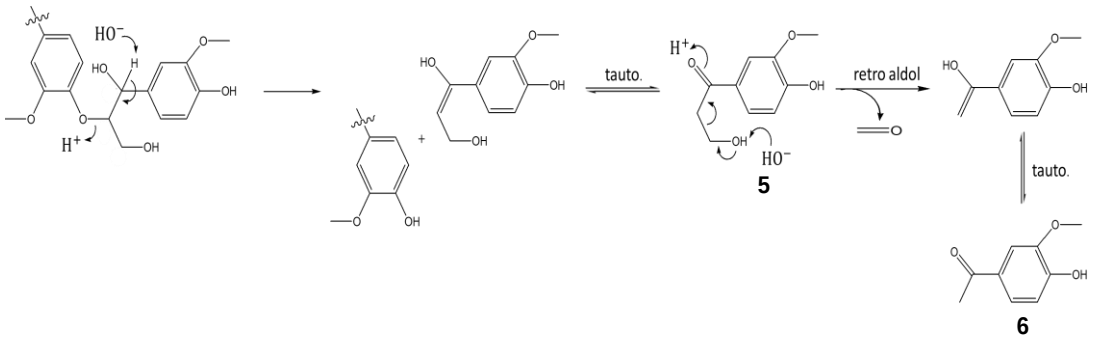


Scheme 2: The formation of 1-(4-Hydroxy-3-methoxy-phenyl)-ethanone **6.**

**The decomposition paths to 3-Vanilpropanol and 4-Allyl-2-methoxy-phenol (Scheme 3 and 4).** The α-OH elimination of lignin side chain can take place under basic condition via the deprotonation of phenol and form quinone methide intermediate **7**. The β -O-4 linkage of intermediate **7** can undergo heterolytic cleavage over the reduction surface of Ni metal yielding radical intermediate **8**, which subjects to different resonance forming a coniferyl alcohol radical. Thereafter, the reduction of radical intermediate **9** into 3-Hydroxy-propenyl intermediate **10** can take place followed by hydrogenation producing 3-Vanilpropanol **11**. γ-OH of coniferyl alcohol **10** can undergo hydrogenolysis by Ni metal resulted in eugenol radical **12**, which is reduced to 4-Allyl-2-methoxy-phenol **13**.

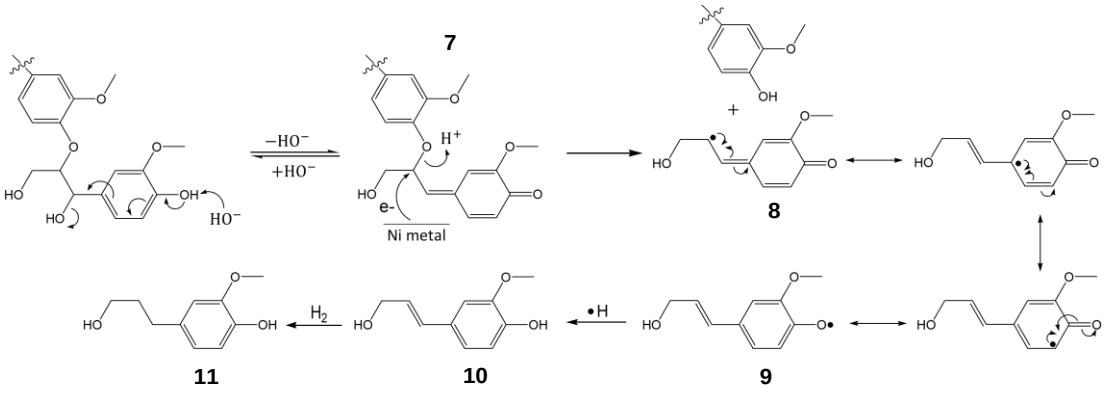


Scheme 3: The formation of 3-Vanilpropanol **11**.

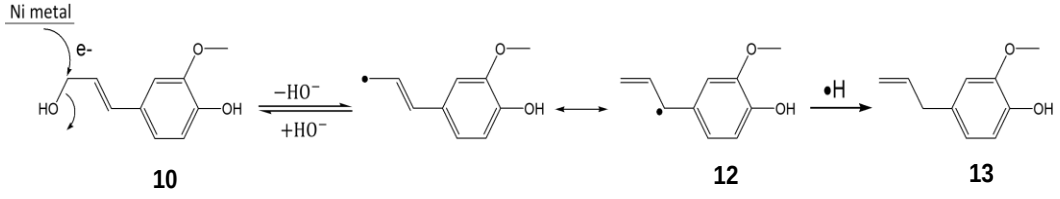


Scheme 4: The formation of 4-Allyl-2-methoxy-phenol **13**.

**The decomposition path to 2-Methoxy-phenol (Scheme 5).** The deprotonation of γ-OH can facilitate β-O-4 linkage cleavage through intramolecular substitution $S_N2$, producing β,γ -epoxide intermediate **14**. This intermediate **14** can undergo retro-aldol Cα-Cβ bond cleavage and β,γ-epoxide ring-opening via the deprotonation of phenol to form the enol intermediate **15**, which is tautomerized to benzaldehyde intermediate **16**. This intermediate **16** can be oxidized to benzoic acid intermediate **17** followed by decarboxylation and form 2-Methoxy-phenol **18**.

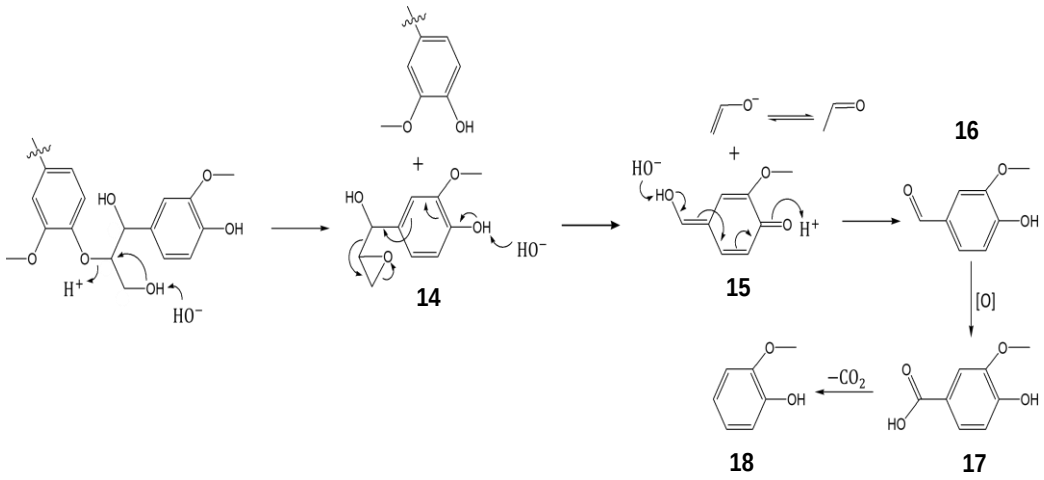


Scheme 5: The formation of 2-Methoxy-phenol **18**.

**The decomposition paths to 2-Methoxy-4-methyl-phenol and 4-(2-Hydroxy-ethyl)-2-methoxy-phenol (Scheme 6).** The lignin side chain can undergo the elimination of α-OH group by forming the quinone methide, which undergoes retro-aldol Cβ-Cγ bond cleavage producing vinyl ether intermediate **19**. Vinyl ether **19** can be hydrolyzed to acetaldehyde intermediate **20**, which is either hydrogenated to form 4-(2-Hydroxy-ethyl)-2-methoxy-phenol **20c** or oxidized and decarboxylated sequentially to form 2-Methoxy-4-methyl-phenol **20b**.

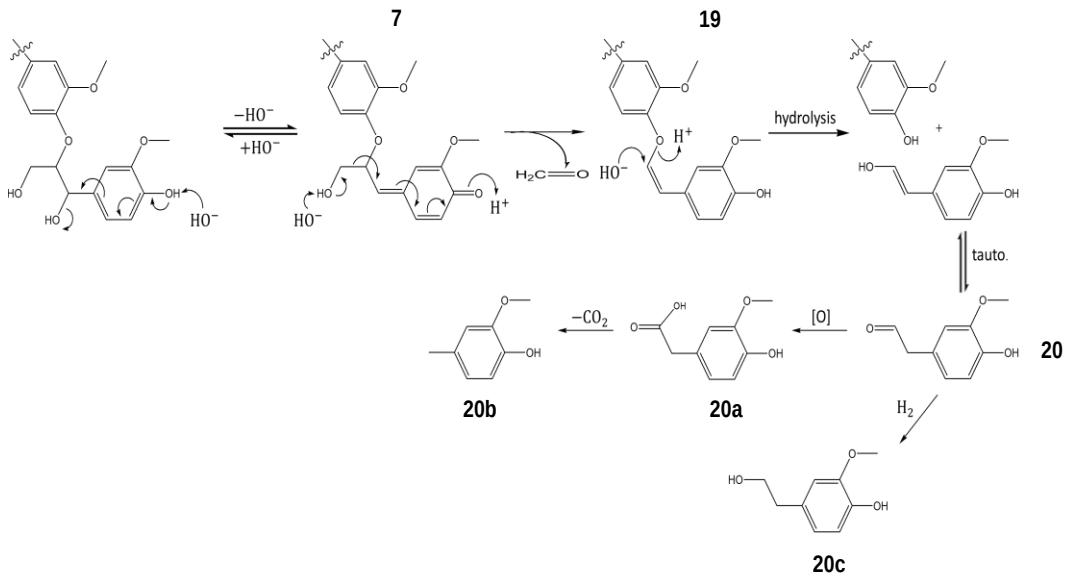


Scheme 6: The formation of 2-Methoxy-4-methyl-phenol **20b** and 4-(2-Hydroxy-ethyl)-2-methoxy-phenol **20c**.

### 2.3.5.2 Proposed pathways of hydrocarbon, ketone, and sugar alcohols

To get a clear insight into the oxygen removal of liquefaction products from the hydrolysis of cellulose and hemicellulose and explore the dominant reactions involved in their formation, we propose the formation paths of hydrocarbon, ketone, and sugar alcohols identified by GC-MS, including 2-methylbutane (Table 2.5), 3-hexanone (Table 2.13), 2-pentanone (Table 2.13), propane-1,2-diol (Tables 2.4, 2.5, 2.7, and 2.9), pentane-1,3-diol (Table 2.9), pentane-1,2,5-triol (Table 2.9), butane-1,2-diol (Table 2.4, 2.7, and 2.9), and Butane-2,3-diol (Table 2.4, 2.5, 2.7, and 2.9).

**The formation pathways of 2-methylbutane.** The β or α-branched and unbranched aldehyde can be formed under basic conditions via aldol addition-condensation reactions and ketonic decarboxylation (ketonization) reactions, as depicted in Scheme 8. The resulted aldehydes are likely to reduce into corresponding alcohol,

which can undergo dehydration and hydrogenation reactions sequentially, forming the downstream product, which is 2-methylbutane.

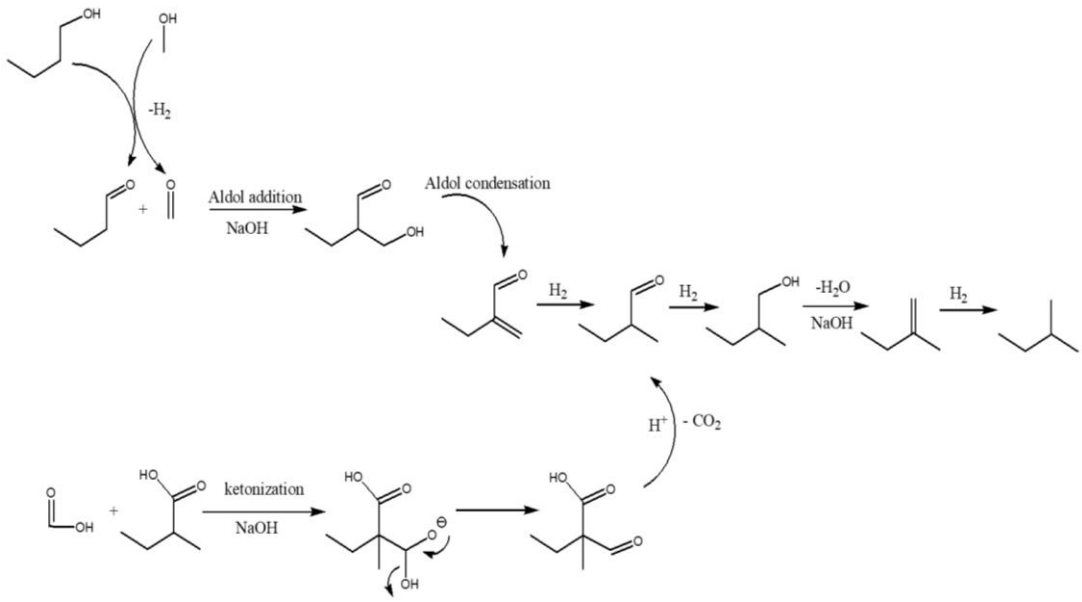


Scheme 8: Hydrocarbon formation through aldol addition-condensation reactions and ketonic decarboxylation (ketonization) reactions.

**The formation pathways of 3-Hexanone and 2-Pentanone via ketonization reactions of acids.** Another example that can clarify how oxygen removal reactions can occur over metal oxide is ketonization reactions of two acids, as shown in Scheme 9. The one or two oxygen atoms of carboxylate/aldehyde can bind to the metal cation (Lewis acid site) through different coordination structures (monodentate, bridging, and chelating bidentate). In contrast, the dissociated hydrogen atom from acid can bind weakly to the surface oxygen anion (Lewis base site). The adsorbed carboxylate undergoes a bimolecular elimination reaction (E2) at the α -carbon to give an enolate that attacks another carboxylate and forms β-hydroxy carboxylate intermediate. This intermediate

undergoes monomolecular dehydration and forms the β-ketoacid, which, as mentioned above, can readily decarboxylate to generate the ketone product.

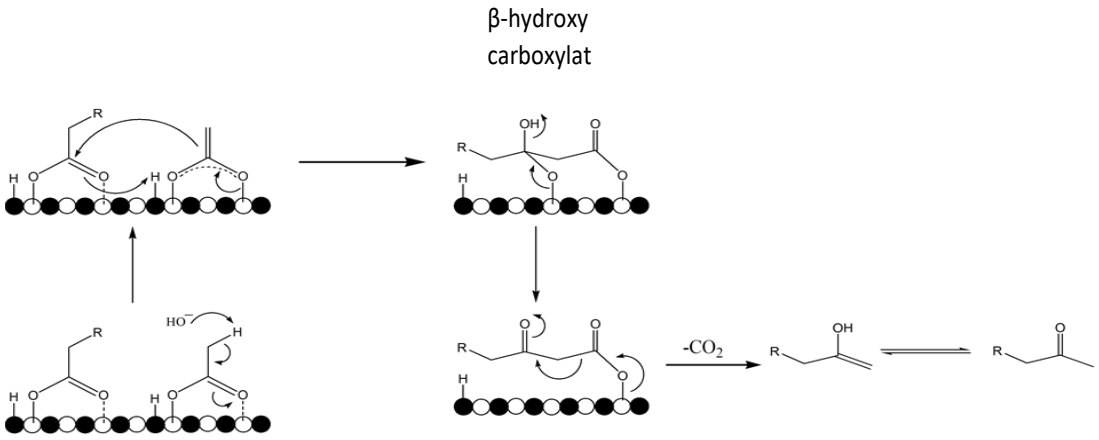


Scheme 9: Ketonization reactions of two acids over metal oxide.

**The formation pathways of butan-2-ol, pentane-1,3-diol, pentane-1,2,5-triol, butane-1,2-diol, and butane-2,3-diol.** Sugar molecules generated from biomass during the liquefaction process may undergo the selective oxygen removal. Therefore, it is reasonable to state that detected compounds such as butan-2-ol, pentane-1,3-diol, pentane-1,2,5-triol, butane-1,2-diol, and butane-2,3-diol, may form from other sugar molecules through a series of selective oxidation and reduction reactions. To illustrate how these reactions would occur, three proposed mechanisms of the selective removal of oxygen in erythritol were proposed, as presented in Scheme 10. Erythritol undergoes dehydrogenation, dehydration, keto-enol tautomerization, and hydrogenation (path A); dehydration, keto-enol tautomerization, and hydrogenation (path B); direct protonation, deprotonation, dehydrogenation, and hydrogenation (path C), respectively.

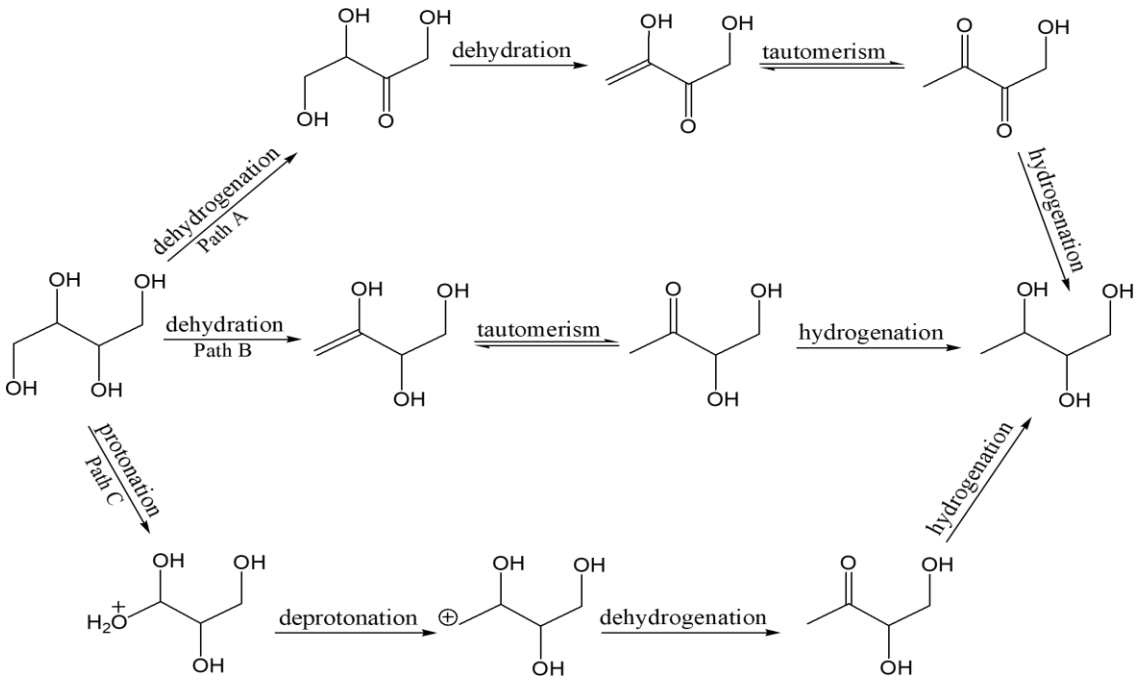


Scheme 10: Proposed pathways of selective removal of oxygen over metal oxide.

This selectivity was also observed for erythritol over an Ir-ReOx/$SiO_2$ catalyst generating two butanetriols, four butanediols, and two butanols.[48, 49] However, they formed through the hydrodeoxygenation (hydrogenolysis) of erythritol as erythritol conversion was conducted in the presence of $H_2$ under acidic condition. As the oxygen removal via hydrodeoxygenation can occur by hydrogenolysis catalysts in the reductive condition, it is expected that the synergy of Ni metal + metal oxide may play a role in the selective removal of the C−OH bond. Ni metal plays a role in keto-enol tautomerization by providing hydrogen and functions as Lewis base as it is an electron donor. In contrast, the metal oxide can promote dehydrogenation and dehydration reaction based on their basic and acidic characters. Thus, the hydrogenolysis of C−O bonds can occur over a metallic surface adjacent to the metal oxide, as presented in Scheme 11. Herein, Ni metal can donate an electron to a carbon atom bound to hydroxyl, facilitating the removal of

hydroxyl. Consequently, the reduction of the formed radical would take place, forming alcohol with fewer hydroxyl groups.

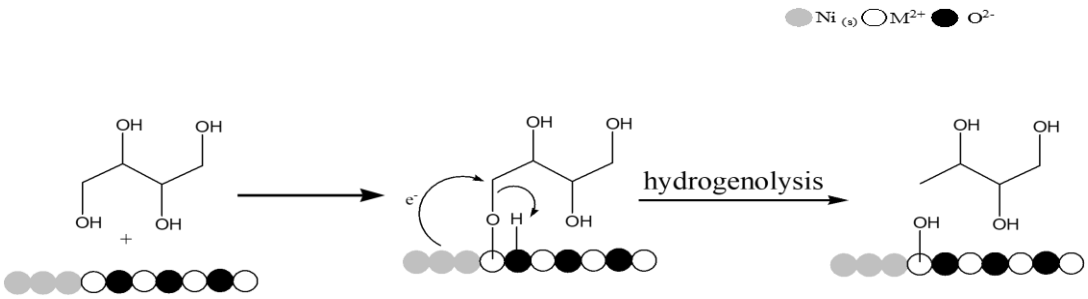


Scheme 11: O—H bond hydrogenolysis over metallic surface adjacent to metal oxide.

As depicted in Scheme 12, cellulose and hemicellulose are hydrolyzed into C6, C5, and C4 sugars. Cellulose is hydrolyzed to glucose undergoing C4-C5 bond cleavage to form erythrose and glycolaldehyde, while hemicellulose is hydrolyzed to xylose undergoing hydrogenation and produces xylitol. These sugars may undergo removal selectivity of oxygen via dehydration, dehydrogenation, and hydrogenolysis, as described above. OHs of Erythritol undergo elimination to give butane-1,2,3-triol followed by butane-1,2-diol and butane-2,3-diol. In contrast, OH groups of xylitol were removed, producing pentane-1,2,5-triol followed by pentane-1,2-diol.

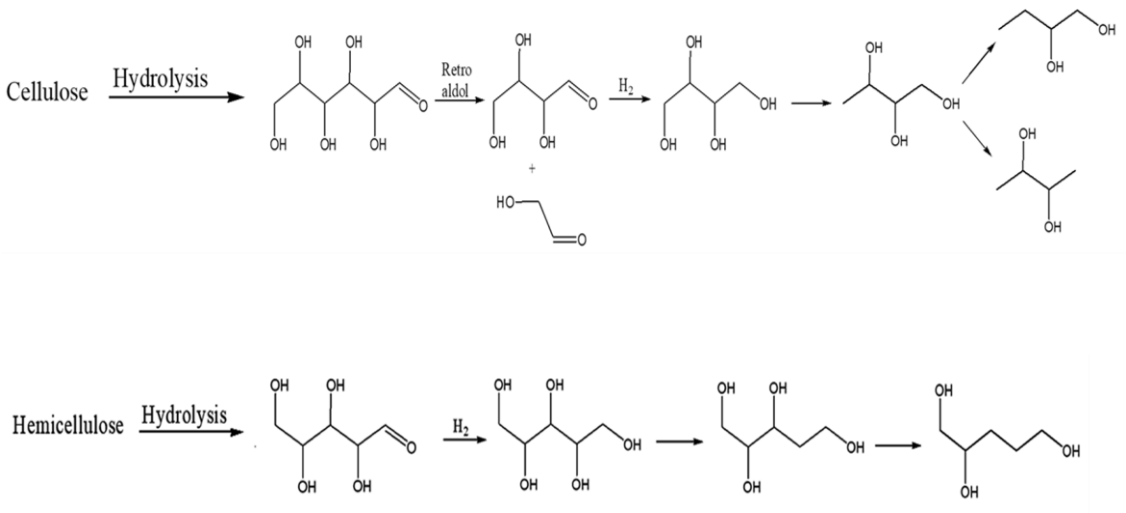


Scheme 12: Alcoholic products formation from cellulose and hemicellulose via selective catalytic reduction.

## 2.4 Conclusions

The catalytic liquefaction of pine sawdust using Ni metal + ZnO +NaOH was conducted in the presence of different amounts of NaOH in 100% $H_2O$ and in 50% of both EtOH and $H_2O$ for different reaction times at 200 °C. Thereafter, pine sawdust liquefaction was conducted using

different metals such as Ni, Pd, Co, Cu, Mo, Fe, Ag, Ru + metal oxides such as ZnO, MgO, FeO, PbO, MnO + NaOH in 100% EtOH at 260 °C. Based on the liquefaction results obtained from this work, the following specific conclusions can be summarized:

- Hydrolysis of biomass in water as a co-/solvent occurs so rapidly caused the decomposed molecules to undergo cracking more than liquefaction reactions.
- Cracking and dehydration are the dominant reactions in hydrothermal and co-solvent liquefactions, regardless of catalysts employed.
- Increasing the amount of NaOH enhances the repolymerization of lignin derivatives and hydrolysis of repolymerized cellulose.

- Bio-oils generated from hydrothermal and co-solvent liquefactions contained high percentages of aromatic and oxygenated protons.
- 14.25% and 33.88% of bio-oil were the highest yields achieved from hydrothermal and co-solvent liquefaction, respectively for a reaction time of 20 h.
- The combinations of Ni-MnO-NaOH, Ni-FeO-NaOH, Ru-ZnO-NaOH, and Pd-ZnO-NaOH showed strong synergistic effect, producing > 75% of bio-oil and ≤ 10% of solid bio-residue, for solvolytic liquefaction of pine sawdust.

Based on the solvolytic liquefaction results, the development of cheaper catalytic system consisting of Ni metal, metal oxide, and NaOH should be further investigated in future work.

## 2.5 Appendix

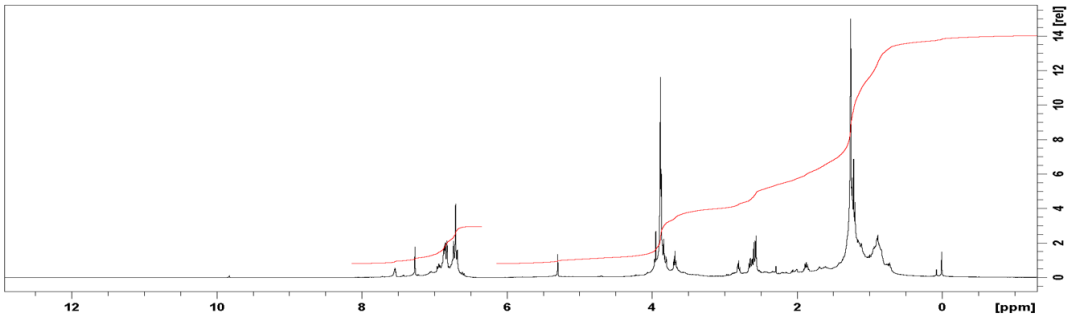


Figure S1 : The H-NMR spectrum of bio-oil product of hydrothermal pine sawdust liquefaction of run 2.1.

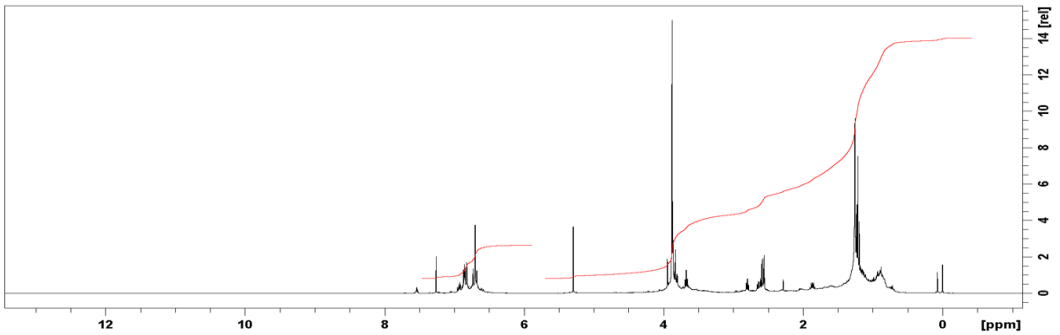


Figure S2: The H-NMR spectrum of bio-oil product of hydrothermal pine sawdust liquefaction of run 2.2.

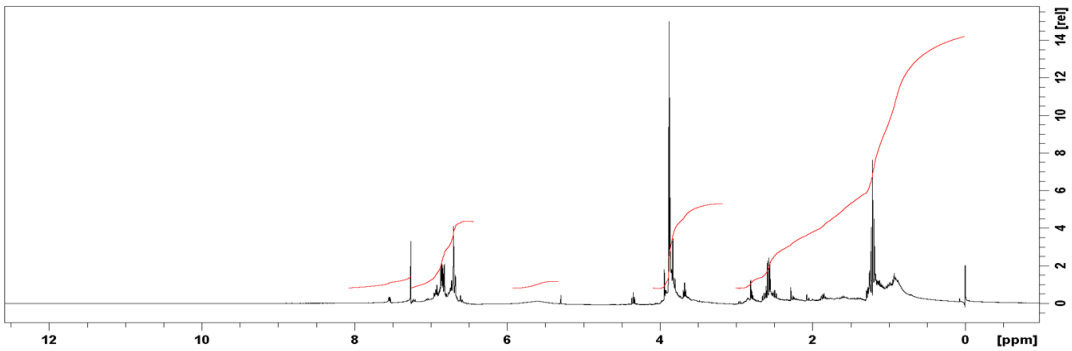


Figure S3: The H-NMR spectrum of bio-oil product of hydrothermal pine sawdust liquefaction of run 2.3.

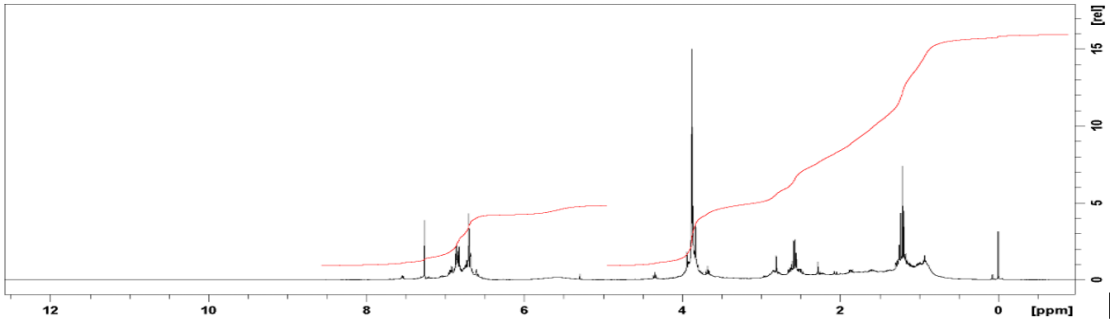


Figure S4: The H-NMR spectrum of bio-oil product of hydrothermal pine sawdust liquefaction of run 2.4.

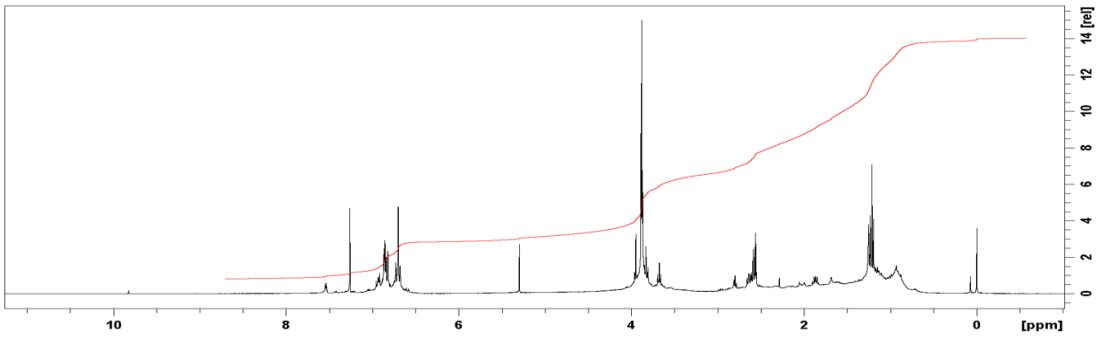


Figure S5: The H-NMR spectrum of bio-oil product of hydrothermal pine sawdust liquefaction of run 2.5.

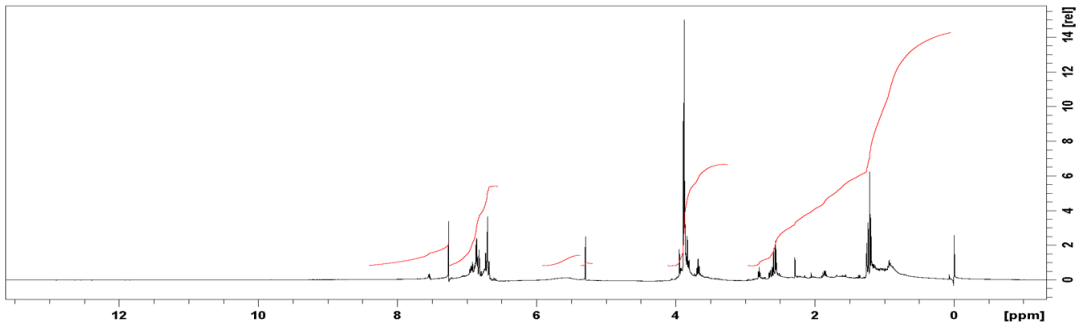


Figure S6: The H-NMR spectrum of bio-oil product of hydrothermal pine sawdust liquefaction of run 2.6.

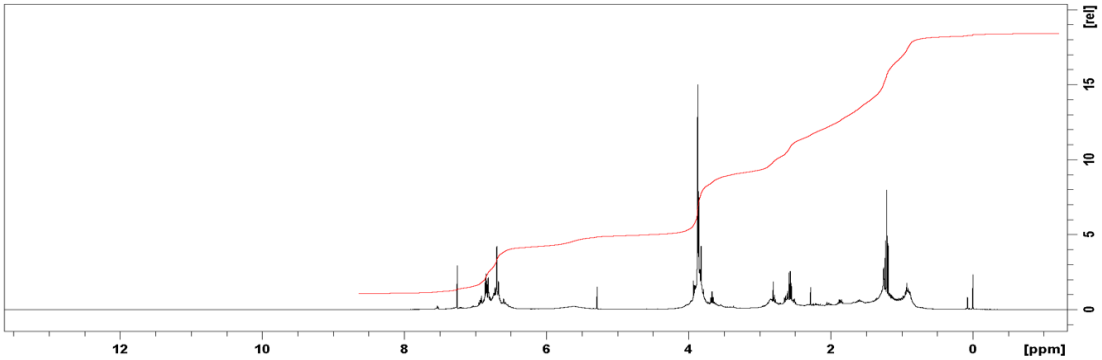


Figure S7: The H-NMR spectrum of bio-oil product of hydrothermal pine sawdust liquefaction of run 2.7.

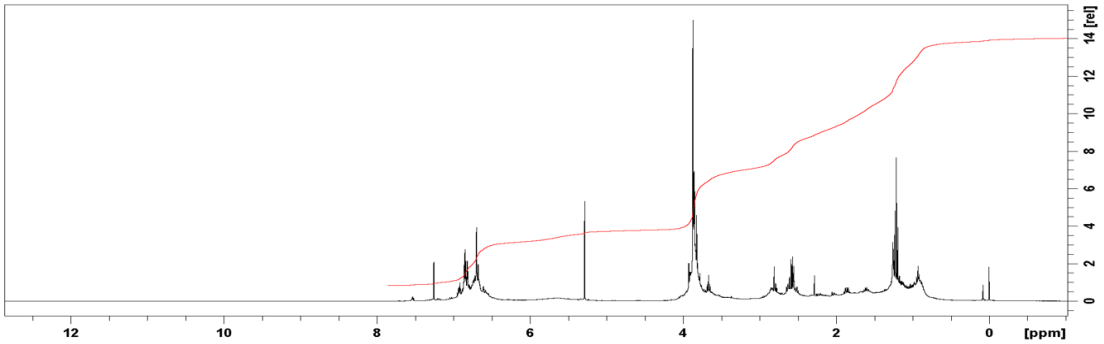


Figure S8: The H-NMR spectrum of bio-oil product of hydrothermal pine sawdust liquefaction of run 2.8.

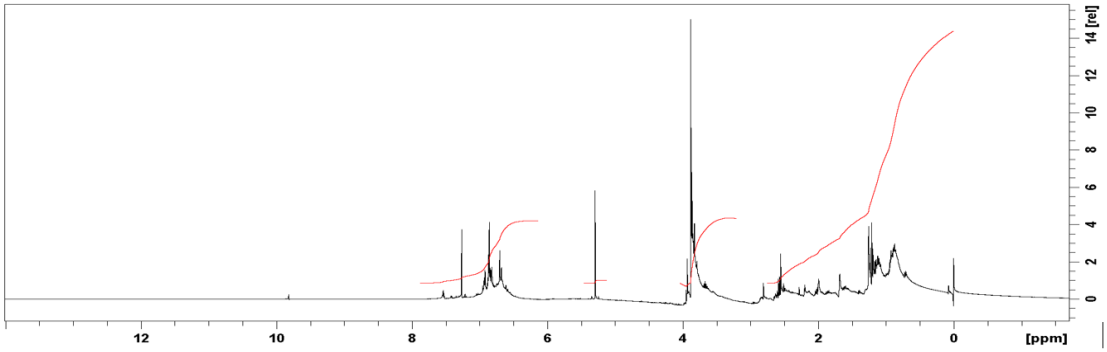


Figure S9: The H-NMR spectrum of bio-oil product of hydrothermal pine sawdust liquefaction of run 2.9.

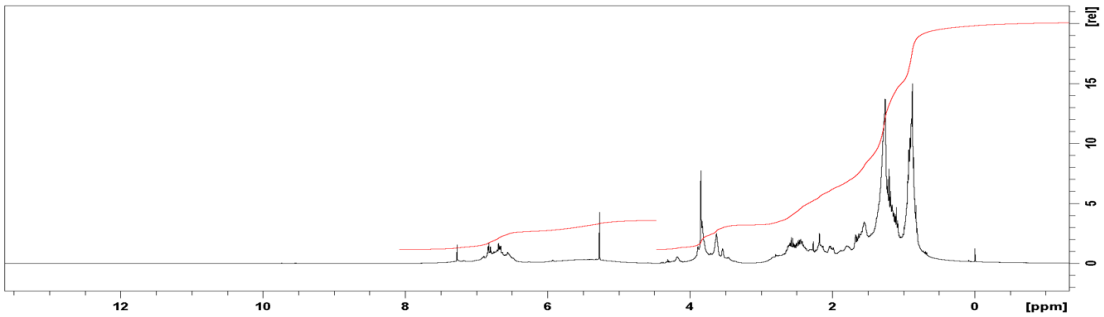


Figure S10: The H-NMR spectrum of bio-oil product of pine sawdust liquefaction in

EtOH-$H_2O$ mixture of run 2.10.

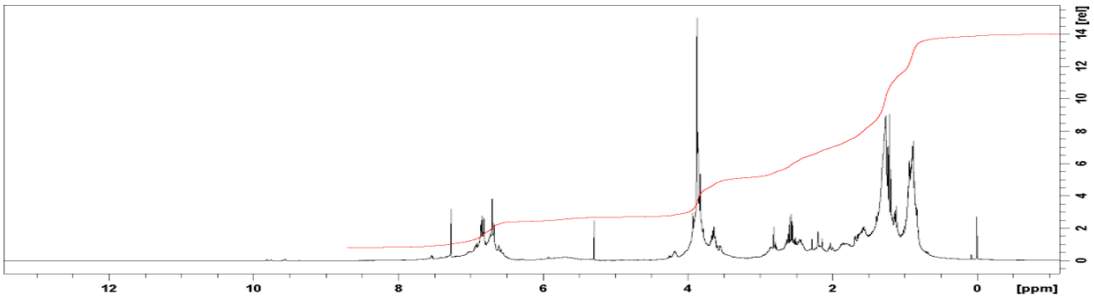


Figure S11: The H-NMR spectrum of bio-oil product of pine sawdust liquefaction in EtOH-$H_2O$ mixture of run 2.11.

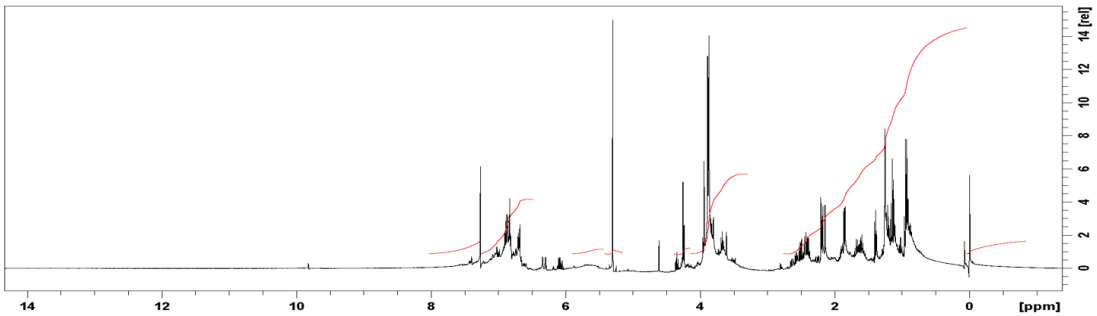


Figure S12: The H-NMR spectrum of bio-oil product of pine sawdust liquefaction in EtOH-$H_2O$ mixture of run 2.12.

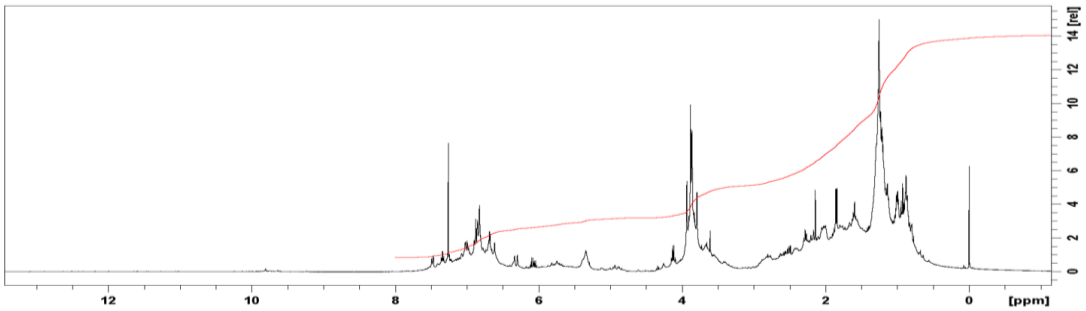


Figure S13: The H-NMR spectrum of bio-oil product of pine sawdust liquefaction in EtOH-$H_2O$ mixture of run 2.13.

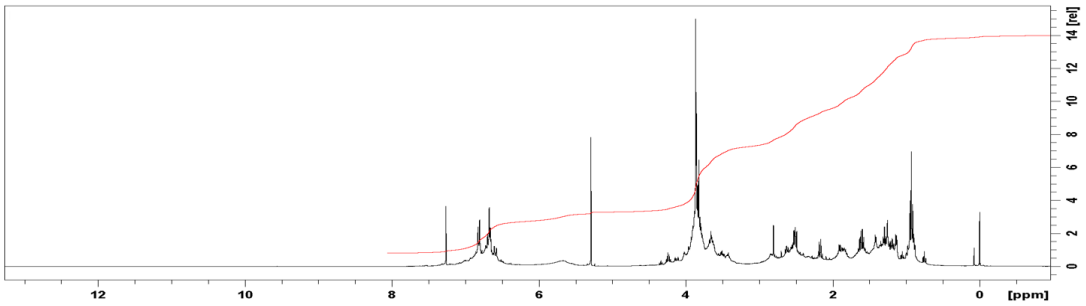


Figure S14: The H-NMR spectrum of bio-oil product of pine sawdust liquefaction in EtOH-$H_2O$ mixture of run 2.14.

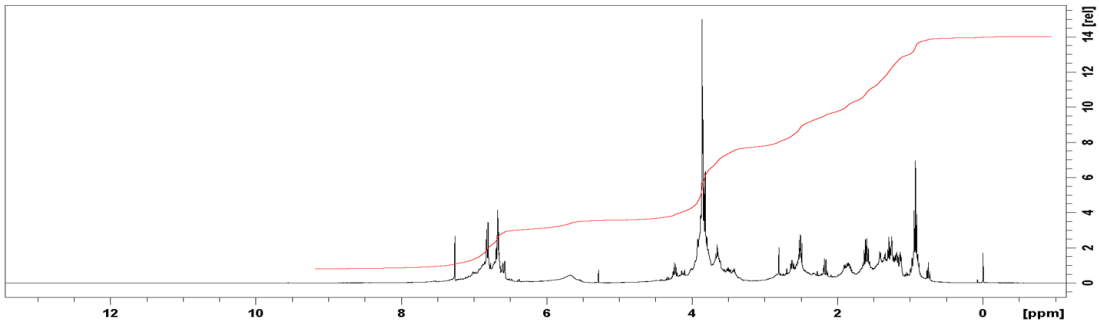


Figure S15: The H-NMR spectrum of bio-oil product of pine sawdust liquefaction in EtOH-$H_2O$ mixture of run 2.15.

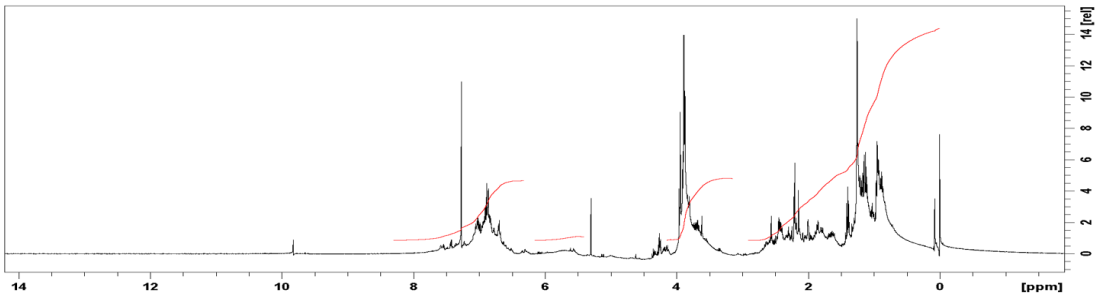


Figure S16: The H-NMR spectrum of bio-oil product of pine sawdust liquefaction in EtOH-$H_2O$ mixture of run 2.16.

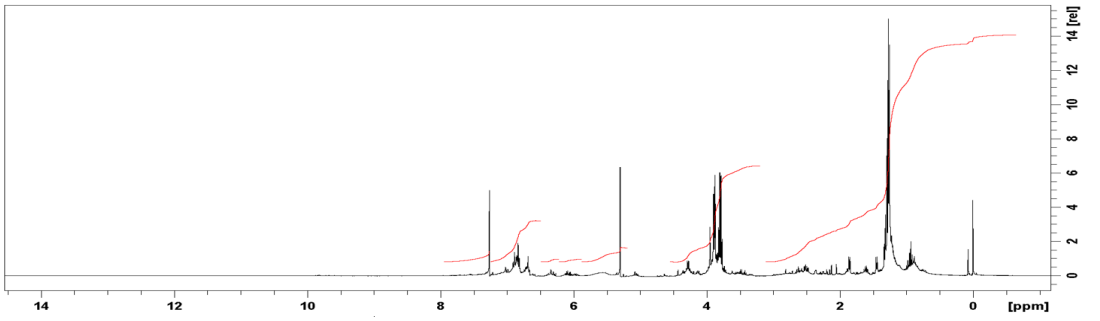


Figure S17: The H-NMR spectrum of bio-oil product of pine sawdust liquefaction in EtOH-$H_2O$ mixture of run 2.17.

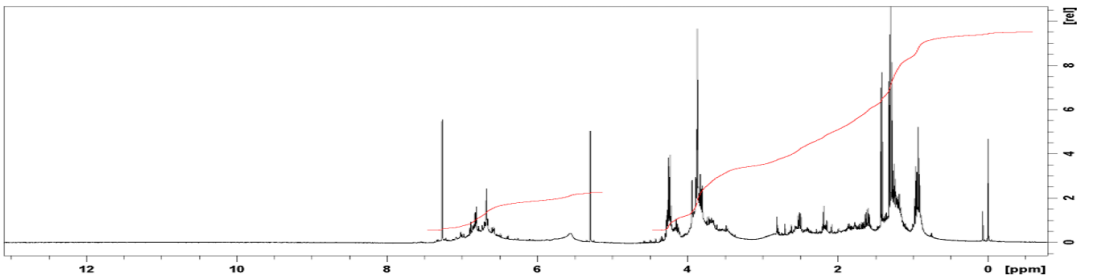


Figure S18: The H-NMR spectrum of bio-oil product of pine sawdust liquefaction in EtOH-$H_2O$ mixture of run 2.18.

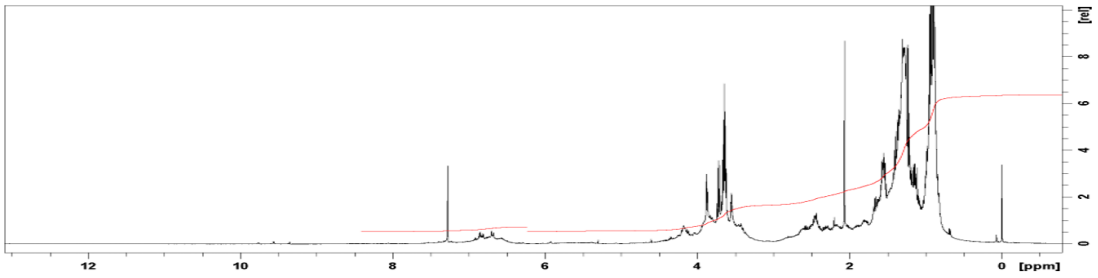


Figure S19: The H-NMR spectrum of bio-oil product of pine sawdust liquefaction in EtOH-$H_2O$ mixture of run 2.19.

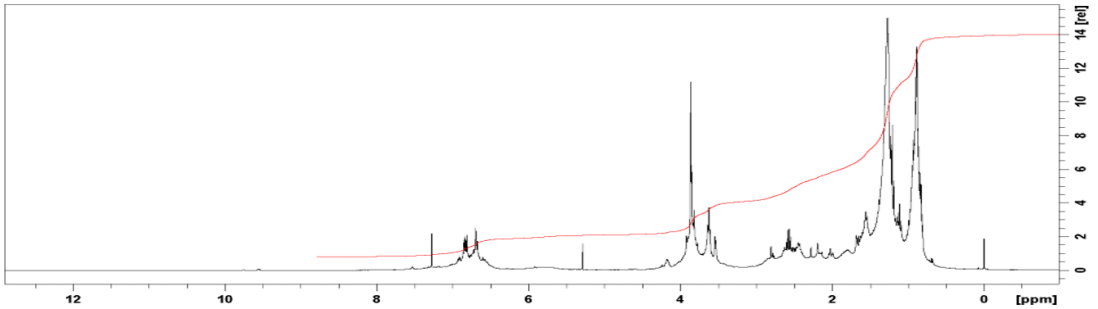


Figure S20: The H-NMR spectrum of bio-oil product of pine sawdust liquefaction in EtOH-$H_2O$ mixture of run 2.20.

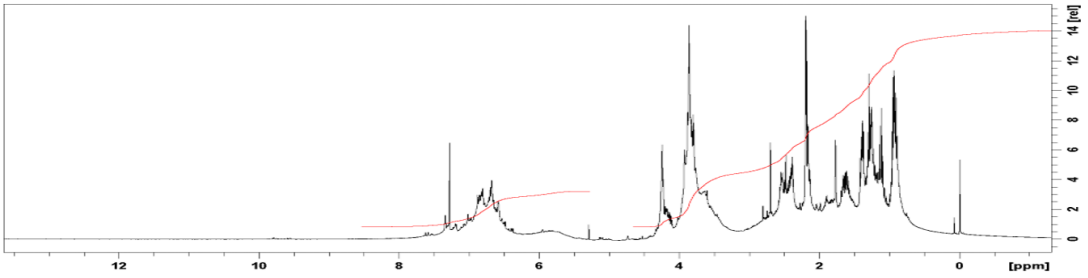


Figure S21: The H-NMR spectrum of bio-oil product of pine sawdust liquefaction in EtOH-$H_2O$ mixture of run 2.21.

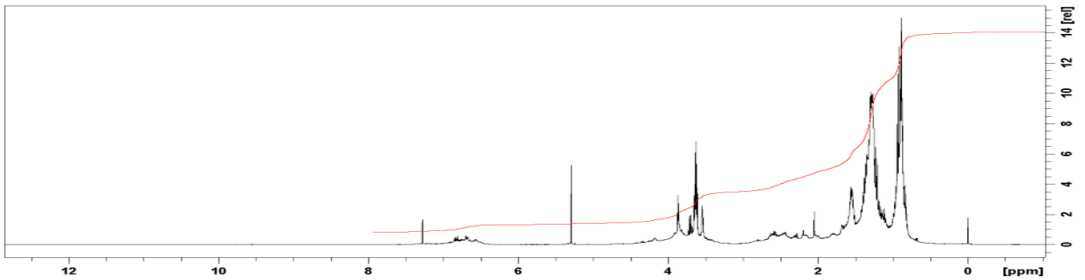


Figure S22: The H-NMR spectrum of bio-oil product of pine sawdust liquefaction in EtOH-$H_2O$ mixture of run 2.22.

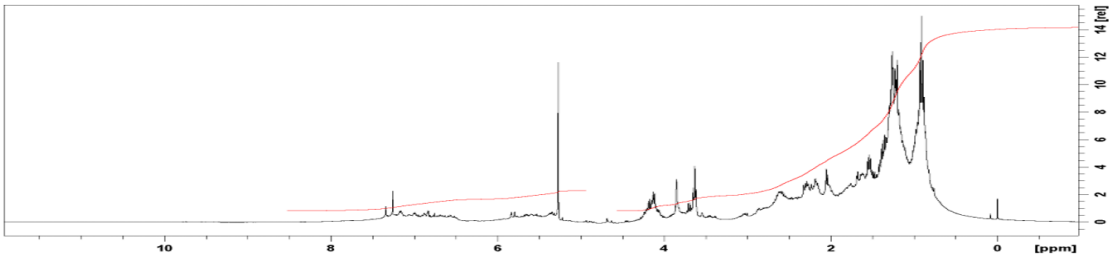


Figure S23: The H-NMR spectrum of bio-oil product of pine sawdust liquefaction using diverse metals and metallic salts of run 2.23.

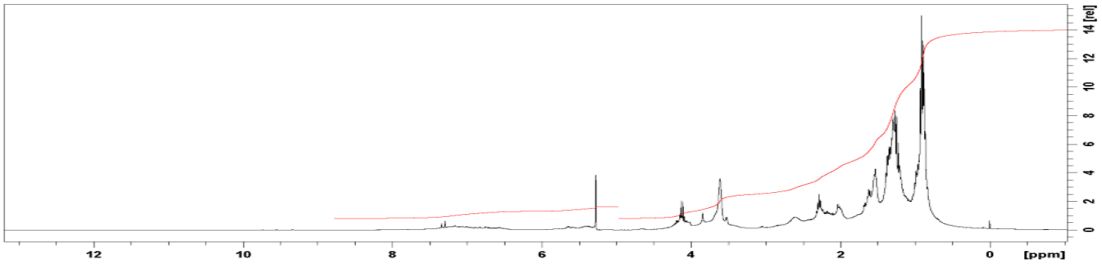


Figure S24: The H-NMR spectrum of bio-oil product of pine sawdust liquefaction using diverse metals and metallic salts of run 2.24.

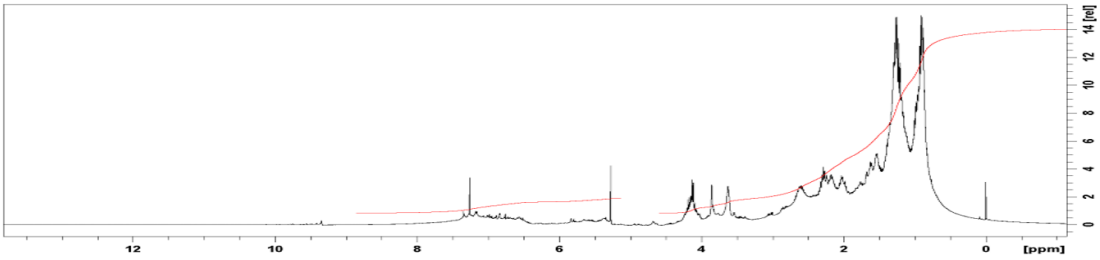


Figure S25: The H-NMR spectrum of bio-oil product of pine sawdust liquefaction using diverse metals and metallic salts of run 2.25.

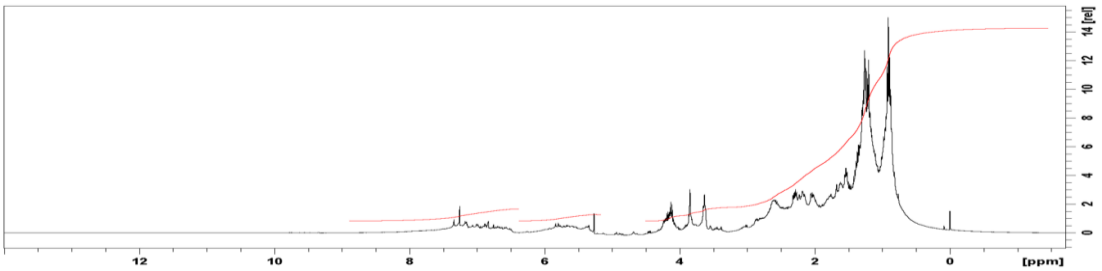


Figure S26: The H-NMR spectrum of bio-oil product of pine sawdust liquefaction using diverse metals and metallic salts of run 2.26.

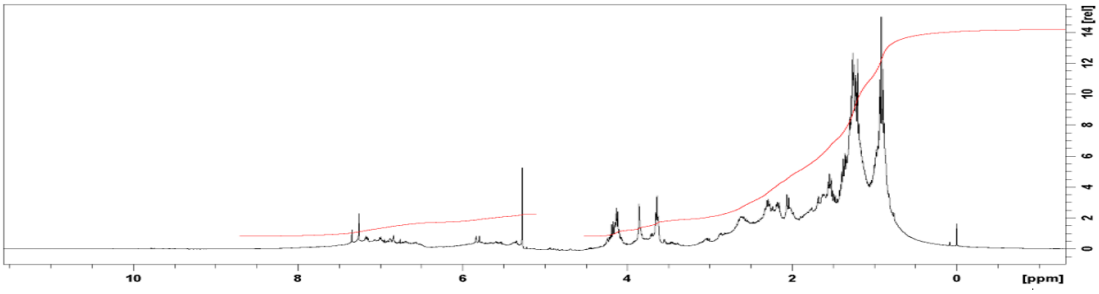


Figure S27: The H-NMR spectrum of bio-oil product of pine sawdust liquefaction using diverse metals and metallic salts of run 2.27.

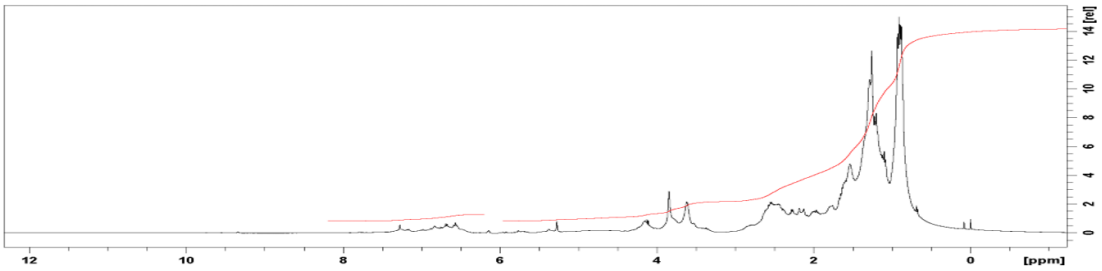


Figure S28: The H-NMR spectrum of bio-oil product of pine sawdust liquefaction using diverse metals and metallic salts of run 2.28.

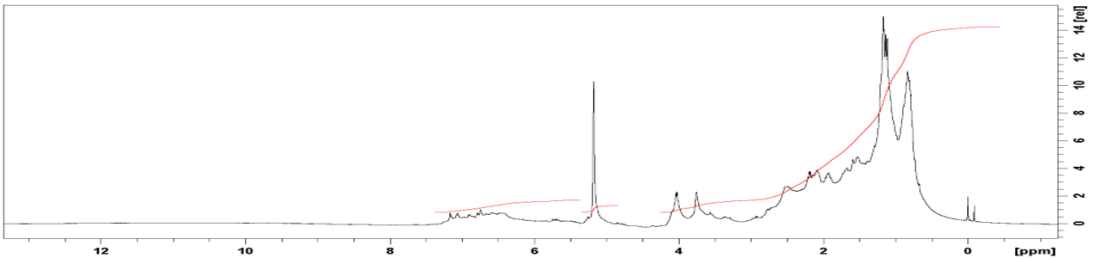


Figure S29: The H-NMR spectrum of bio-oil product of pine sawdust liquefaction using diverse metals and metallic salts of run 2.29.

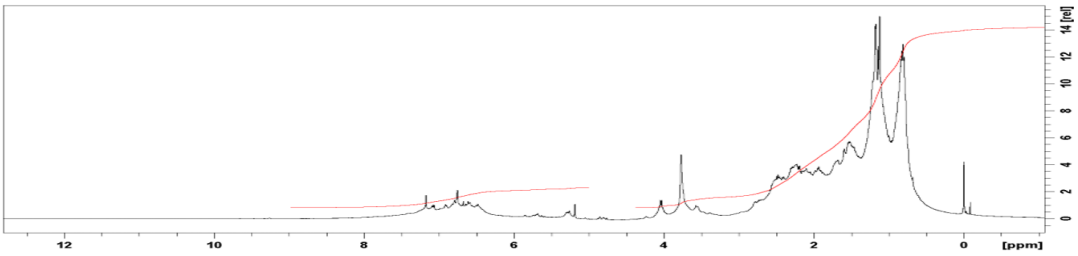


Figure S30: The H-NMR spectrum of bio-oil product of pine sawdust liquefaction using diverse metals and metallic salts of run 2.30.

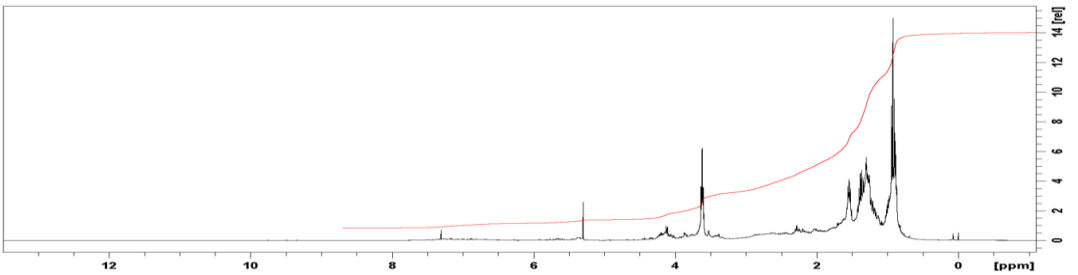

Figure S31: The H-NMR spectrum of bio-oil product of pine sawdust liquefaction using diverse metals and metallic salts of run 2.31.

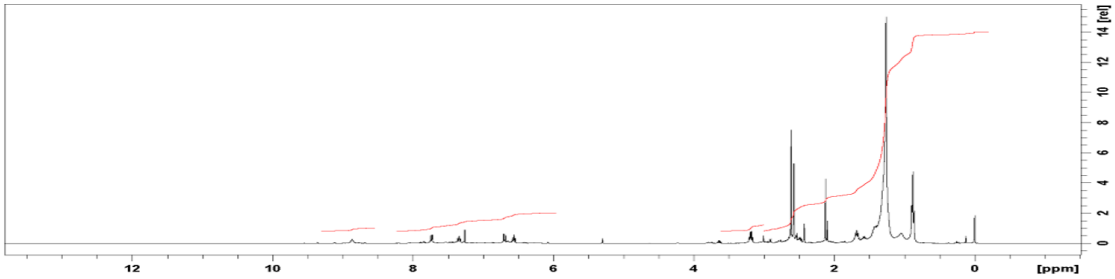


Figure S32: The H-NMR spectrum of bio-oil product of pine sawdust liquefaction using diverse metals and metallic salts of run 2.32.

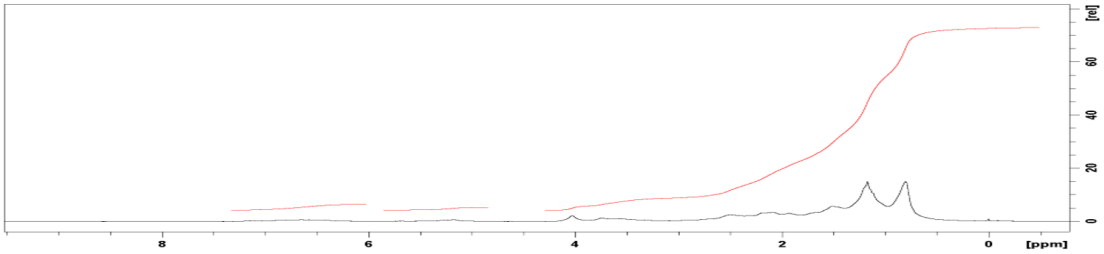


Figure S33: The H-NMR spectrum of bio-oil product of pine sawdust liquefaction using diverse metals and metallic salts of run 2.33.

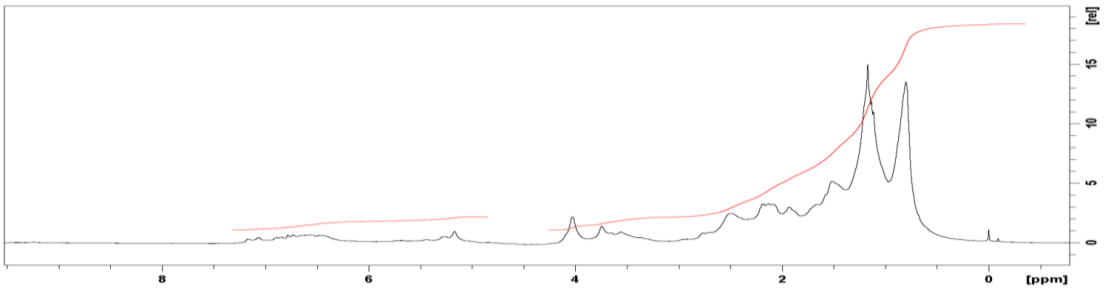


Figure S34: The H-NMR spectrum of bio-oil product of pine sawdust liquefaction using diverse metals and metallic salts of Run 12.

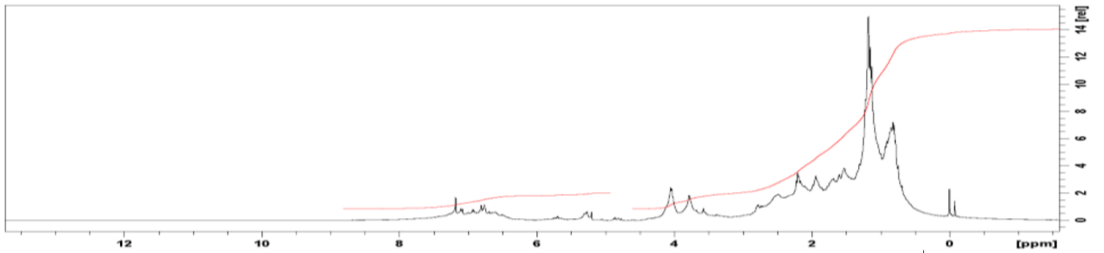


Figure S35: The H-NMR spectrum of bio-oil product of pine sawdust liquefaction using

diverse metals and metallic salts of run 2.34.

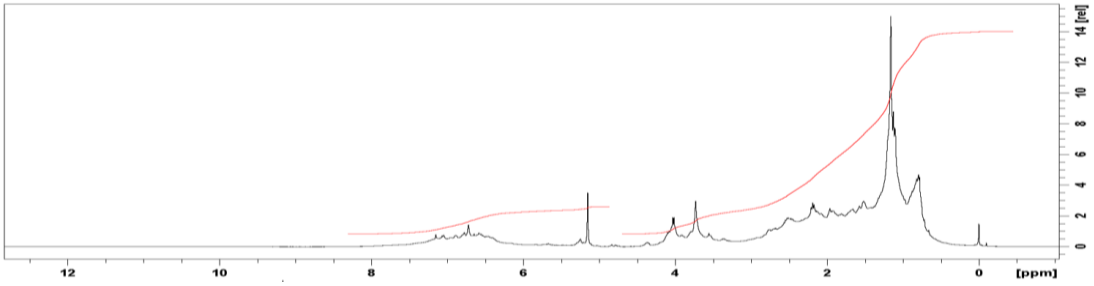


Figure S36: The H-NMR spectrum of bio-oil product of pine sawdust liquefaction using diverse metals and metallic salts of run 2.35.

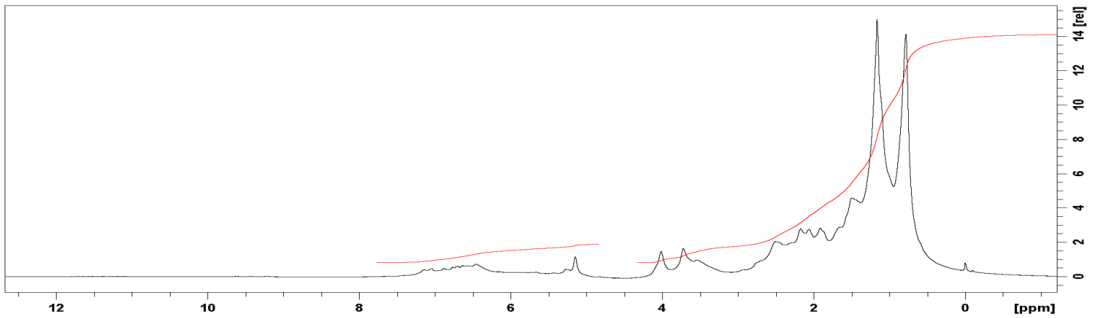


Figure S37: The H-NMR spectrum of bio-oil product of pine sawdust liquefaction using diverse metals and metallic salts of run 2.36.

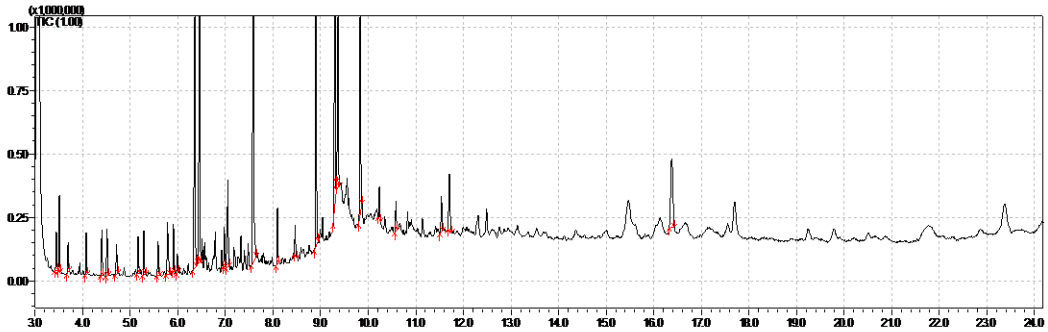


Figure S38: The GC-MS chromatogram of bio-oil product of hydrothermal pine sawdust liquefaction of run 2.1.

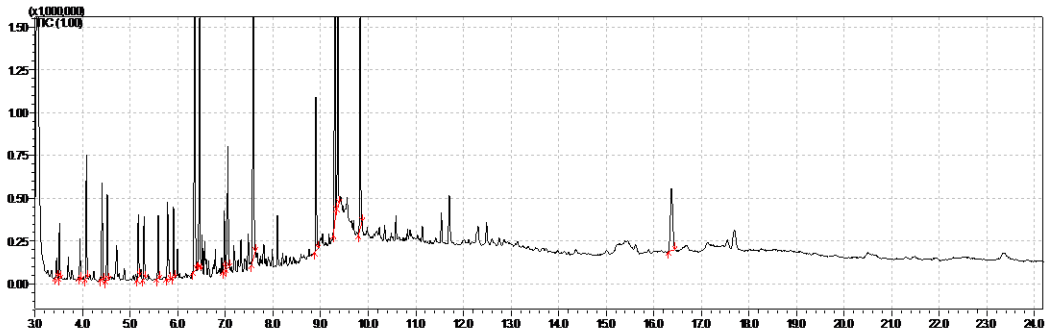


Figure S39: The GC-MS chromatogram of bio-oil product of hydrothermal pine sawdust liquefaction of run 2.2.

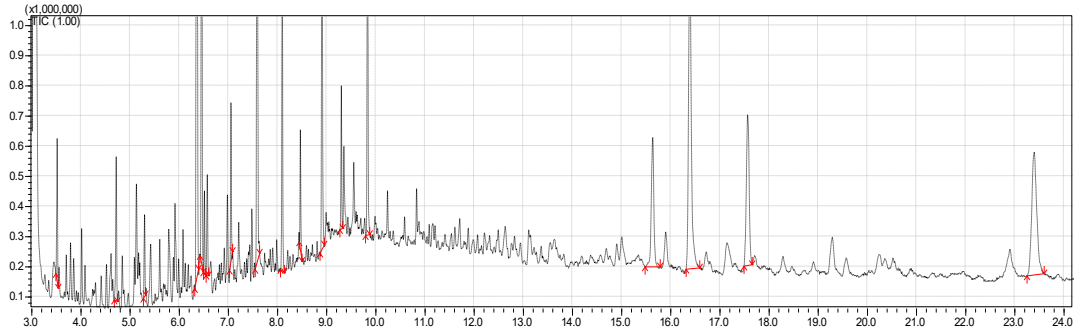


Figure S40: The GC-MS chromatogram of bio-oil product of hydrothermal pine sawdust liquefaction of run 2.9.

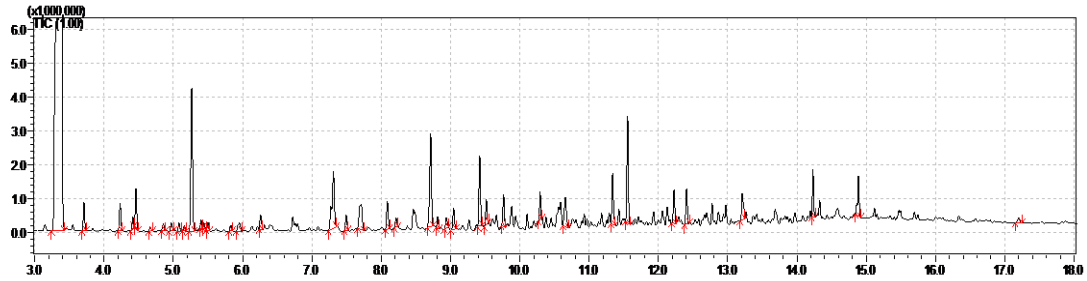


Figure S41: The GC-MS chromatogram of bio-oil product of pine sawdust liquefaction in EtOH-$H_2O$ mixture of run 2.10.

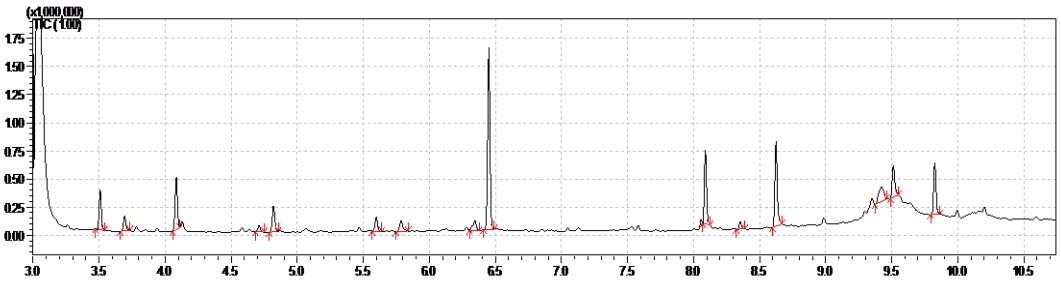


Figure S42: The GC-MS chromatogram of bio-oil product of pine sawdust liquefaction in EtOH-$H_2O$ mixture of run 2.17.

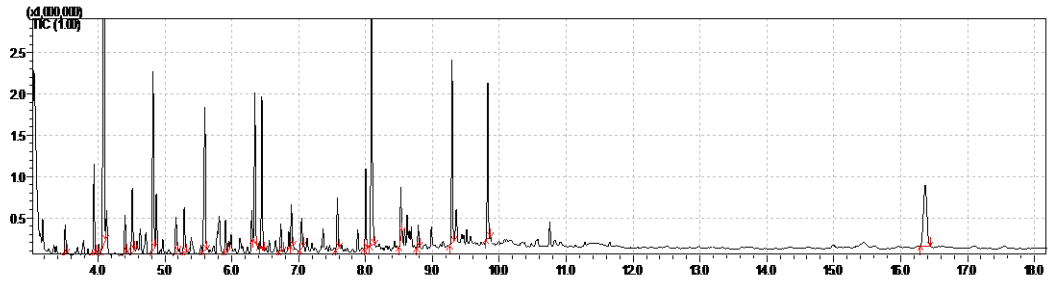


Figure S43: The GC-MS chromatogram of bio-oil product of pine sawdust liquefaction in EtOH-$H_2O$ mixture of run 2.18.

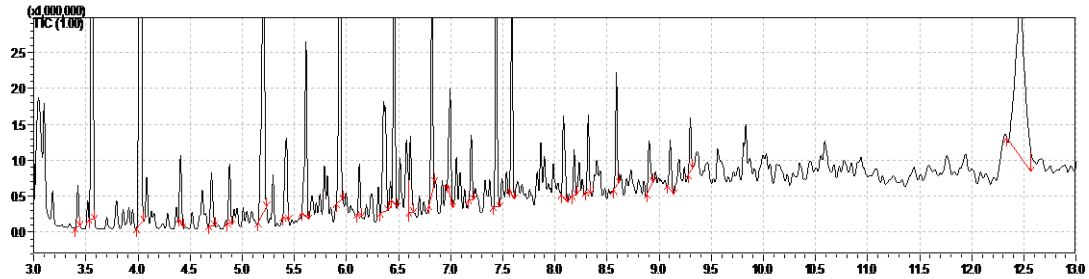


Figure S44: The GC-MS chromatogram of bio-oil product of pine sawdust liquefaction in EtOH-$H_2O$ mixture of run 2.22.

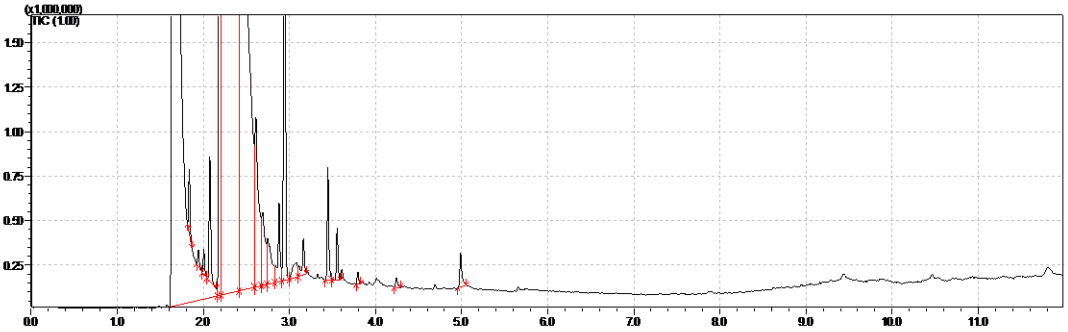


Figure S45: The GC-MS chromatogram of bio-oil product of pine sawdust liquefaction using diverse metals and metallic salts of run 2.24.

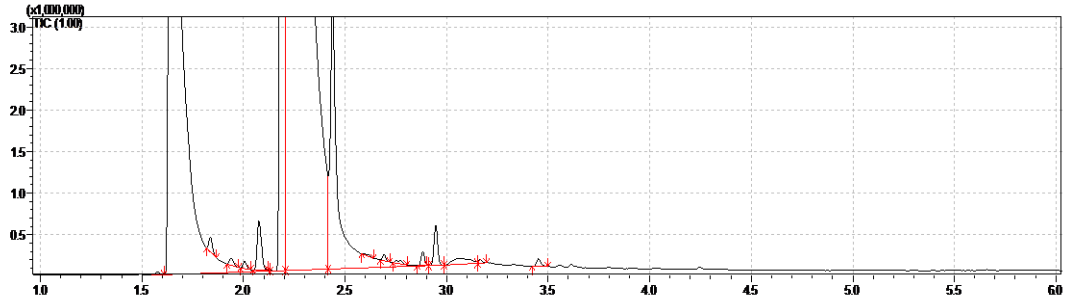


Figure S46: The GC-MS chromatogram of bio-oil product of pine sawdust liquefaction using diverse metals and metallic salts of run 2.31.

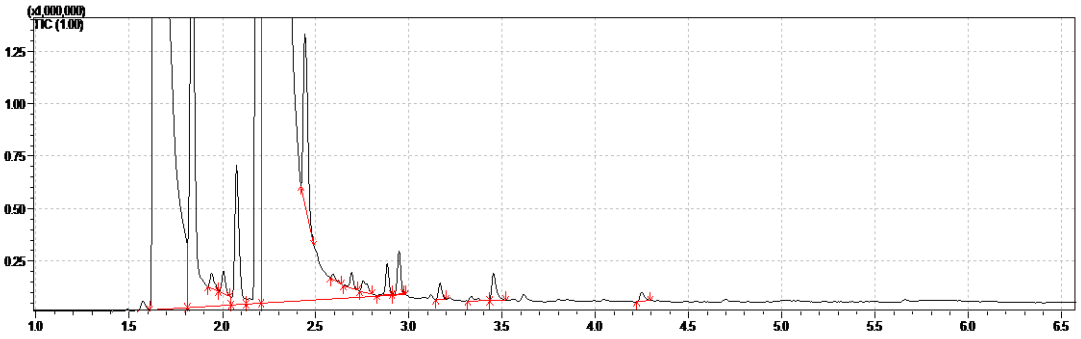


Figure S47: The GC-MS chromatogram of bio-oil product of pine sawdust liquefaction using diverse metals and metallic salts of run 2.33.

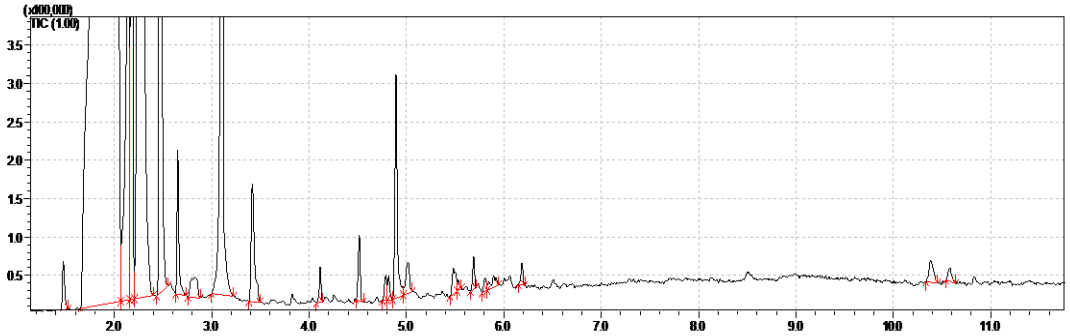


Figure S48: The GC-MS chromatogram of bio-oil product of pine sawdust liquefaction using diverse metals and metallic salts of run 2.36.

# CHAPTER 3: THE CATALYTIC EFFECTS OF Ni METALS, NiO, $Fe_2O_3$, AND THEIR SYNERGY IN CORN STOVER LIQUEFACTION

## 3.1 Introduction

Lignocellulosic biomass is considered the only sustainable feedstock of carbon that can be exploited for liquid transportation fuels and chemicals production.[50, 51] However, the conversion of biomass into liquid fuels is still challenging due to the original complexity and high oxygen content of lignocellulose.[52-54] Thus, the resulting products from the thermochemical processes are highly oxygenated and require further upgrading before use as a fuel. Besides, these processes depend on hydrodeoxygenation to reduce O/C and increase H/C molar ratio in the bio-oil under the facilitate of $H_2$. These issues make the conversion of biomass to fuel grade bio-oil unpractical and uneconomical on a large scale.[55] Among conversion processes, direct liquefaction is considered to be the most promising method for the production of low molecular weight liquid fuels.[56] In biomass liquefaction, different reactions, such as depolymerization, thermal decomposition, dehydration, decarboxylation, hydrogenolysis, and hydrogenation, can occur. Among them, dehydration, decarboxylation, and hydrogenation are considered responsible reactions to increase the H/C ratio and decrease the O/C ratio.[57] The depolymerization of biomass is a dominant reaction during earlier stages of liquefaction, while at later stages, repolymerization becomes active, leading to the formation of char.[58]

To enhance the yield and improve the quality of bio-oil, many efforts were made to explore the catalytic performance on the biomass conversion. For instance, the hydrolysis-hydrogenation of cellulose using a carbon black -supported Ni catalyst to

hexitols in $H_2O$ in the presence of $H_2$ (g) provided a hexitol yield of 64% with a cellulose conversion of 90%.[59] In contrast, Ni catalysts loaded on $SiO_2$, γ-$Al_2O_3$, $TiO_2$ and $ZrO_2$ supports gave much lower yields of the hexitols (28%–43%) and higher yields of numerous degradation products, including propylene glycol and ethylene glycol.[59] The basicity of the metal oxides could play a significant role in enhancing the hydrogenolysis of sugar alcohols. Non-noble metal catalysts, including Ni[60-65], Cu[66-68], and Mo[69-71] catalysts have been used extensively for the hydrogenolysis of lignin and model lignin compounds with molecular $H_2$ or some other source of hydrogen because of their low cost and availability. According to Qi, Jiaying, et al.,[72] Ni/C metal showed high performance for the hydrogenolysis of both aryl–alkyl (C–O–C) and hydroxyl (–OH) bonds and gave 85% of the selectivity for the C–O bond cleavage products which are higher than that achieved over Ru/C and Pd/C.

To the best of our knowledge, there are few studies carried out to investigate the catalytic activities of nickel metal catalysts prepared by different methods for corn stover liquefaction at a moderate temperature under basic conditions. Corn stover has been chosen as the starting material due to one of the most important resources worldwide for bio-fuels production. Also, metal oxides with difference Lewis acid strength, are expected to have different effect on corn stover liquefaction due to their catalysis for oxygen migration in carbon-chain molecules which leads to the desired decarboxylation. Different oxides including $Fe_2O_3$, $Cu_2O$, ZnO, $TiO_2$, MgO and $V_2O_5$ were screened. A suitable metal oxide was chosen to explore the influence of reaction time, type of base and solvent, ratio of base/metal oxide, and type of catalyst on the liquefaction behavior of corn stover. The chemical structure of bio-oils was characterized by proton nuclear

magnetic resonance ($^1$H-NMR) and Fourier transform infrared spectroscopy (FT-IR). X-ray diffraction (XRD) and scanning electron microscopy (SEM) equipped with an energy dispersive X-ray (EDX) were utilized to characterize crystal structure and surface morphology and composition of the catalysts, respectively. Gas chromatography with both flame ionization (FID) and thermal conductivity (TCD) detectors was used to analysis the chemical composition of the gas out of ethanol condensation catalyzed by Ni (270 °C ) and Ni/C.

## 3.2 Experimental

### 3.2.1 Materials

Corn stover was obtained from a local farm and reduced in size using a blender to 18-50 mesh. Corn stover has cellulose ( 28-51.2 wt.%), hemi-cellulose (19.1-30.7 wt.%) and lignin (11-16.9 wt.%) [73].

### 3.2.2 Preparation of catalysts

**Ni/C:** To a 50-mL beaker were added 17 mmol, 4.24g of $Ni(OAc)_2.4H_2O$, 14 ml of DI water and 9 g of activated carbon (Aldrich 161551, 100 mesh). The mixture was thoroughly mixed, and then transferred to a glass surface, which was heated on a hot plate (~70 $^oC$). The paste was stirred while the water was evaporating. After the paste turned into powder, it was heated in an oven at 120 $^oC$ for 3h, and then at 110 $^oC$ for 15h. The powder was transferred to a 250 mL flask, then 40mL of DI water and 6 eq, 6 g of $H_2NNH_2.1.5H_2O$ were added while the mixture was vigorously stirred in a 78 $^oC$ oil bath. 1.49 g of NaOH/5 ml of water was added over 5 minutes. The reaction started when 82% of the NaOH solution was added. After bubbling stopped in 10 minutes, the flask was transfered into a $N_2$ glovebox. The product was collected by filtration, washed with EtOH, and vacuum dried in the transfer chamber at RT.

**NiO:** Nickel (II) carbonate hydroxide hydrate powder (9.2614g, Fisher Scientific, AC223160010, ca 45-47% Ni) in a 50mL flask was heated in a 270 °C molten salt bath for 2 hrs 40 min. The gas from the composition was released through a bubbler, so the system was free of air. The formed NiO was ground and passed through a 500-mesh sieve.

**Ni (270 °C):** NiO was heated in the presence of organic acid at 270 °C in $N_2$ for 1 h to obtain Ni (270 °C) catalyst.

**Ni ($H_2$):** 6.108 g of NiO was loaded in a test tube. Hydrogen gas was introduced to the bottom of the the tube via a needle. The tube was stoppered and connected to a bubbler. The tube was then heated in a 300 $^oC$ molten salt bath untill no more water was coming out (taking 75 min). Without exposing the Ni to air, the tube was transfered to a $N_2$ glovebox. Yield: 4.7824 g. In the glove box, the Ni powder was ground and passed through a 500-mesh sieve.

All metal salt and base chemicals were purchased from Fisher Scientific and ethanol purchased from Pharmco-AAPER company.

### 3.2.3 Liquefaction procedure

The general procedure of corn stover liquefaction: To a stainless-steel pressure reactor in a glovebox were added a magnet stirring bar, catalyst, 400 mg of corn stover, and 4 ml of EtOH. The closed reactor was transferred into a fume-hood and heated in a 260°C molten salt bath for 8 hours. After reactor was cooled down, the mixture was filtered and washed with EtOH. The ethanol solution was condensed by rotary evaporation under a reduced pressure of 80 mbar using a 50°C water bath. To the residue, 1 mL of $CH_2Cl_2$ (DCM) and 0.5 ml of water were added. The DCM solution was separated out and the water phase was extracted by DCM (0.5 mL × 2). The combined

DCM solution was neutralized with $NaHCO_3$, dried with $MgSO_4$ powder, and condensed on a rotary evaporator to yield oil product.

The percentage yield of oil, solid residue, and corn stover conversion was calculated based on the weight of corn stover feed by the following formula [74]:

$$\text{Bio oil yield (wt\%)} = \frac{\text{Weight of bio-oil}}{\text{Biomass weight}} \times 100\%$$

$$\text{Solid bio residue (SR) yield (wt\%)} = \frac{\text{Weight of solid bio residue}}{\text{Biomass wieght}} \times 100\%$$

$$\text{Un repolymerization yield (wt\%) of bio oil} = 100\% - \text{Solid bio residue \%}$$

$$\text{Gas + water soluble species (wt\%)} = 100\% - \text{Bio oil \%} - \text{Solid bio residue \%}$$

### 3.2.4 Characterization

**$^1$H-NMR analysis** was performed for oil obtained from each corn stover liquefaction on a Bruker AVANCE-400 MHz NMR spectrometer in CDCl3 using TMS as the internal standard. Percentage of protons in different types of chemical groups were calculated from the relative intensity of protons.

**GC-TCD and GC-FID analysis** was performed for gaseous products from liquefaction reactions (Agilent GC 7890A with a 50 m × 0.53 mm × 15 μm 19095P-S25 column). The column initial temperature in GC is 60°C (at this temperature holding time 3 min), then increased at 5 °C/min to 100 °C (holding time 0 min) and then increased at 10 °C/min to 180 °C (holding time 3 min). The final temperature is 180 °C.

**XRD analysis** of catalysts was carried out on Rigaku SmartLab diffractometer (Cu *Kα*, *k* = 0.1540 nm; 40 kV and 44 mA) .

**SEM-EDX analysis** was conducted on a Hitachi S-3400 N Scanning Electron Microscope to study the morphology of the catalysts and their composition was examined by EDX.

**FTIR** spectra of oil coated on a KBr crystal were obtained using Perkin-Elmer Spectrum Two FTIR Spectrometer.

### 3.3 Liquefaction reaction results and discussion

#### 3.3.1 Effect of reaction time in the presence and absence of $Fe_2O_3$

To investigate the effect of reaction time and $Fe_2O_3$ on liquefaction of corn stover, the reaction was conducted in the absence and presence of $Fe_2O_3$ with the residence time from 2 to 12 h and from 4 to 12 h, respectively. The reaction results are shown in Table 3.1. It is obvious that the residence time had a significant effect on the bio-oil yield. The bio-oil yield increased from 19.25 % to 35.15% and from 27.1% to 34.53% in the absence and presence of $Fe_2O_3$, respectively as the reaction time increased from 4 to 8 h. With further elongation of reaction time from 8 to 12 h, the bio-oil yield in the absence/presence of $Fe_2O_3$ significantly declined. Two reactions may be responsible for the drop in oil yield with elongated reaction time: cracking reaction to give volatile compounds and repolymerization of oil molecules into insoluble polymers. The fact that drop in oil yield was accompanied by also a drop in the yield of solid residue suggests that cracking to form gas molecules (including $CO_2$) was more likely the reason for the drop in oil yield. We obtained the highest yield of bio-oil either in the presence or absence of $Fe_2O_3$ with the same amount of reaction time (8 h). The oils of these runs were analyzed using $^1$H-NMR as seen in Figure 3.1 (S1-S4). In comparison with the bio-oils obtained in the presence and absence of $Fe_2O_3$ we found that the bio-oils obtained in the presence of $Fe_2O_3$ have lower contents of protons on oxygenated carbons indicating that $Fe_2O_3$ catalyze the reduction of oxygenated species and/or oxygen removal by decarboxylation. With long reaction time(8 and 12 h) lower oxygenated and aromatic carbons were obtained in the presence of $Fe_2O_3$. Moreover, a lower percentage of

oxygenated carbons for a shorter reaction time (4 h) than an 8h reaction was observed, which may be ascribed to insufficient time.

| Reaction run | $Fe_2O_3$ (mg) | Reaction time (h) | Bio-oil% | Un-repolymerization% | Solid bio-residue% |
|---|---|---|---|---|---|
| 3.1 | - | 2 | 14.5 | 10 | 90 |
| 3.2 | - | 4 | 19.25 | 24.25 | 75.75 |
| 3.3 | - | 8 | 35.15 | 70.95 | 29.05 |
| 3.4 | - | 12 | 27.25 | 74 | 26 |
| 3.5 | 300 | 4 | 27.1 | 28 | 72 |
| 3.6 | 300 | 8 | 34.53 | 68.45 | 31.55 |
| 3.7 | 300 | 12 | 32.95 | 69.52 | 30.48 |

Table 3.1: Product profile of non-catalytic and catalytic solvent liquefaction of corn stover under different times.

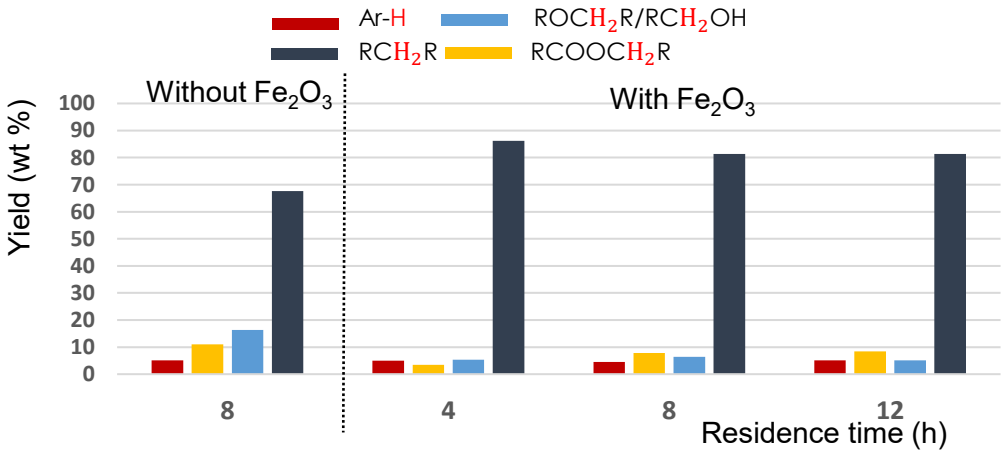


Figure 3.1: $^1$H-NMR data analysis of bio-oils produced from runs 3 and 5-7.

### 3.3.2 The influence of base, solvent, and metal oxide

The effect of the amount of NaOH on liquefaction of corn stover was tested in runs 3.8-3.11 with $Fe_2O_3$ at 260 °C in 4 mL of mixture of 3/1 EtOH/$H_2O$ for 8 h with the mass of added NaOH varying from 20 to 80 mg as shown in Table 3.2. The yield of bio-oil maximized at 32.1% when 40 mg of NaOH was used (run 3.9). When the solvent was

changed to pure EtOH and the amount to NaOH varied from 30 mg to 50 mg to 100 mg (runs 3.12-3.14), the oil yield maximized at 50mg (run 3.13). When 50 mg of NaOH was replaced by 50 mg of $Ca(OH)_2$, the oil yield decreased.

| Reaction run | Base (mg) | | Solvent (ml) | | Bio-oil% | Un-repolymerization% | Solid bio-residue% |
|---|---|---|---|---|---|---|---|
| | NaOH | $Ca(OH)_2$ | EtOH | $H_2O$ | | | |
| 3.8 | 20 | - | 3 | 1 | 28.7 | 84.05 | 15.95 |
| 3.9 | 40 | - | 3 | 1 | 32.1 | 89.13 | 10.87 |
| 3.10 | 60 | - | 3 | 1 | 15.43 | 78.1 | 21.9 |
| 3.11 | 80 | - | 3 | 1 | 18.98 | 79.65 | 20.35 |
| 3.12 | 30 | - | 4 | - | 24.98 | 75.3 | 24.7 |
| 3.13 | 50 | - | 4 | - | 34.93 | 66.25 | 33.75 |
| 3.14 | 100 | - | 4 | - | 25.75 | 55.32 | 44.68 |
| 3.15 | - | 50 | 4 | - | 30.08 | 48 | 52 |

Table 3.2: Products yields of solvent and co-solvent liquefaction of corn stover catalyzed by different masses of NaOH/$Ca(OH)_2$ + 300 mg $Fe_2O_3$.

After optimization of corn stover liquefaction using $Fe_2O_3$ under basic condition, the effect of various metal oxides/ metal on direct liquefaction of corn stover was investigated. The results are presented in Figure 3.2 a & b. The reaction was carried out under the previous optimized condition (run 3.13, Table 3.2) using various metal oxides and Fe. Yield of bio-oil ranged 16.5%-34.1%. The highest bio-oil yield of 34.1% was obtained in the presence of Fe, which indicates that Fe can be used to produce iron oxide in-situ and also serve as a reducing agent. The $^1$H-NMR data analysis of bio-oils (Fig. 3.2b, S5-S12) showed different relative weights of aromatic, ether and ester derivatives contained in bio-oils and these metal oxides gave a significant decrease in the yield of bio-oil except $Fe_2O_3$. The oil yields of reactions using $Fe_3O_4$, $MnO_2$, ZnO, $TiO_2$, MgO and $V_2O_5$ as catalyst are all lower than the 35% yield obtained with $Fe_2O_3$. Thus, $Fe_2O_3$ was selected as co-catalyst of Ni metal and NiO for optimization corn stover liquefaction

processes. The results of $^{1}$H-NMR showed that all metal oxides gave higher protons of none-oxygenated carbons and lower protons of oxygenated carbons compared to none catalyst used. It is found that liquefaction of corn stover under basic condition produced bio-oil with lower lignin and ester contents than the reaction under a neutral condition. From these experiments, it is very clear that metal oxide has a more significant effect on ratios of O/C and H/C than bio-oil yield.

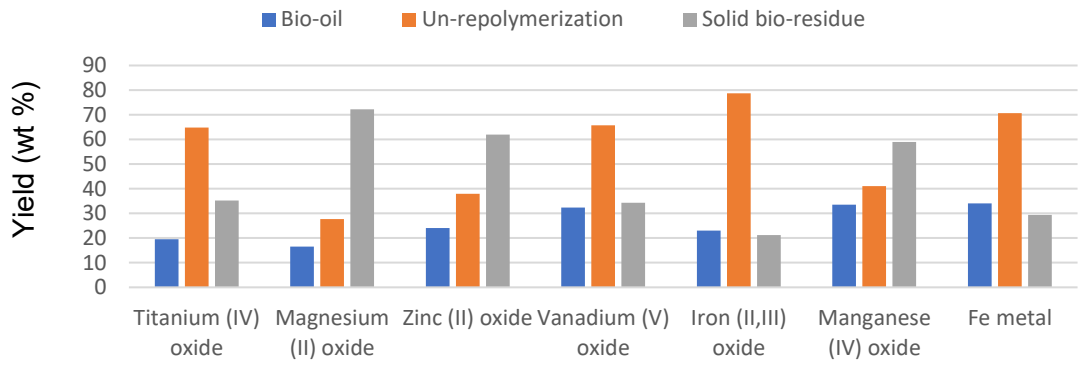


Figure 3.2 (a): Effect of metal oxide type and Fe metal on the products yields of corn stover liquefaction.

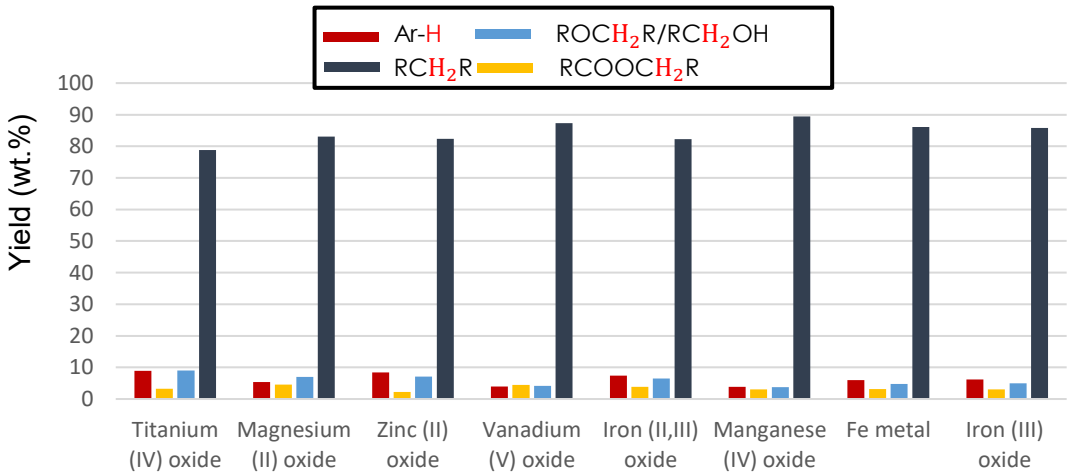


Figure 3.2 (b): The relative intensity of phenolic, ether and ester protons in bio-oil obtained by different metal oxides and Fe was measured using $^{1}$H-NMR.

### 3.3.3 Effect of Ni/C and Ni (270 °C) alone on condensation and liquefaction reactions

The effect of Ni/C and Ni (270 °C ) alone in the presence and absence of NaOH was also investigated on corn stover liquefaction from run 3.16 to 3.19. The results of this investigation are shown in Table 3.3. Initially, Ni (270 °C ) was used to liquefy corn stover under neutral condition (run 3.18) and the yield of bio-oil was 36.7%. This yield is a little bit higher than the one obtained in the absence of any catalyst. When we added a base (50 mg NaOH, run 3.17) the yield went up to 85.13%. Then when we decreased the amount of this metal catalyst to the half (50 mg, run 3.19), the yield of bio-oil also decreased to 61%. It is so clear that NaOH activated Ni (270 °C ) to condense more ethanol which increased the yield of bio-oil obtained under basic conditions. However, when we added the same amount of the base, Ni/C (run 3.16) performed poorly producing an oil yield of only 35%. Generally, Ni metal catalyst can be more catalyzed by a base to liquefy biomass than under neutral condition. So that high yield of bio-oil is expected to get under a basic condition. However, under a basic condition, the catalytic power of these catalyst can also be activated toward ethanol condensation.

Ethanol acts as solvent as well as reactant in the presence of nickel catalysts during the liquefaction reaction. To determine the contribution to oil yield from condensation of ethanol, the reactions from runs 3.20-3.23 were repeated in absence of the biomass to give the results shown in Table 3.3. The yield of condensed ethanol products was higher in NaOH than in the absence of NaOH for both Ni/C and Ni (270 °C ). Still, the latter showed lower activity toward ethanol condensation in both basic and non-basic conditions compared to Ni/C. In addition to that, gas coming from ethanol condensation was analyzed by GC (Table 3.4). $H_2$, $CH_4$, $CO_2$, CO, $CH_4$, $C_2H_6$, and $C_3H_8$

were the gas products detected, similar to those obtained from ethanol steam reforming (ESR)[75-77]. Thus, EtOH is expected to decompose into volatile species in a similar mechanism of ESR. As illustrated in Scheme 1, EtOH may undergo various bonds cleavage of O—H and C—H during ethanol condensation forming these volatile species as by-products. Molecular hydrogen is expected to generate through the combination of free hydrides and protons or neutral hydrogen atoms, which were generated from the dissociation of the O—H and C—H bonds. According to GC analysis, the production of hydrogen was more activated under the basic condition as compared to its production under neutral condition. The presence of CO indicated that EtOH undergoes multi-dissociation of C-C, C-H, and O-H bonds. Consequently, the formation of CO2 was undoubtedly coming from CO via Water Gas Shift (WGS) in which water is involved, and hydrogen is produced. It is interesting to note that no $CH_2=CH_2$ was detected among the gas products, which confirm that no dehydration reaction would occur over the metallic surface of the Ni catalyst. Moreover, the evolution of the CH species during EtOH decomposition can cause carbon accumulation on the catalyst surface, which leads to rapid catalyst deactivation.[75, 76] Analysis of gases produced by solvent condensation gave unexpected results compared to that obtained for biomass liquefaction catalyzed by Ni metals alone. Unlike Ni (270 °C), Ni/C produced more $H_2$ (g), and the solvent was more consumed, likely due to its higher surface area. It remains a question why a higher oil yield was obtained in the presence of Ni (270 °C).

| Run | Catalyst | Reaction time (h) | Bio-oil% | Un-repolymerization% | SR% |
|---|---|---|---|---|---|
| 3.16 | 69 mg Ni/C + 50 mg NaOH | 6 | 34.75 | 90.48 | 9.5 |
| 3.17 | 100 mg Ni (270 °C ) + 50 mg NaOH | 8 | 85.13 | 79.75 | 20.52 |

| | | | | | |
|---|---|---|---|---|---|
| 3.18 | 100 mg Ni (270 °C ) | 7 | 36.7 | 83.83 | 16.18 |
| 3.19 | 50 mg Ni (270 °C ) + 50 mg NaOH | 6 | 61.15 | 81.85 | 18.15 |
| 3.20 | 69 mg Ni/C + 50 mg NaOH | 8 | 7.73 | - | - |
| 3.21 | 60 mg Ni (270 °C ) + 50 mg NaOH | 8 | 3.07 | - | - |
| 3.22 | 69 mg Ni/C | 8 | 0.70 | - | - |
| 3.23 | 60 mg Ni (270 °C ) | 8 | 0.25 | - | - |

Table 3.3: The influence of Ni (270 °C ) and Ni/C alone on corn stover liquefaction and ethanol condensation under neutral and basic conditions.

| **Run** | **Catalyst** | **Total gas volume (mL)** | **GC-TCD (V%)** | | | | | **GC-FID (V%)** | | |
|---|---|---|---|---|---|---|---|---|---|---|
| | | | **$H_2$** | **$N_2$** | **$CH_4$** | **$CO_2$** | **CO** | **$CH_4$** | **$C_2H_6$** | **$C_3H_8$** |
| 3.20 | Ni/C | 239.8 | 69.8 | 7.90 | 17.63 | 8.60 | 0.7 | 19.8 | 0.16 | 0.69 |
| 3.21 | Ni (270 °C ) | 416.3 | 49.3 | 4.3 | 35.4 | 14.8 | 2.3 | 40.2 | 0.246 | 0.27 |
| 3.22 | Ni/C | 81.1 | 55.76 | 16.0 | 16.22 | 3.08 | 13.25 | 18.4 | 0.22 | 0.30 |
| 3.23 | Ni (270 °C ) | 234.8 | 33.7 | 7.3 | 32.1 | 2.1 | 21.0 | 36.2 | 0.20 | 0.18 |

Table 3.4: GC results of ethanol condensation using Ni/C and Ni (270 °C ) under the following condition: with/without 50mg NaOH, 260°C, 8 h.

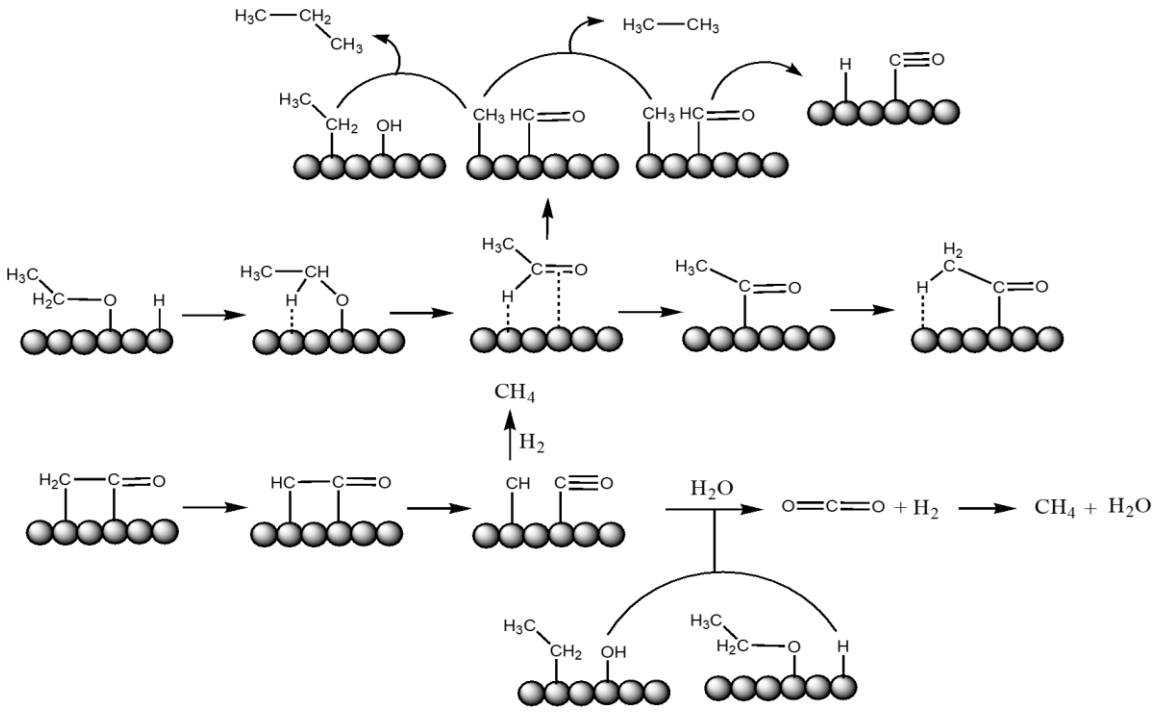

Scheme 1: EtOH decomposition over Ni metal in the presence/absence of NaOH.

### 3.3.4 The synergistic influence of Ni-based catalysts + $Fe_2O_3$ + NaOH

Effect of catalysts (Ni ($H_2$), Ni (270 °C), Ni/C, and NiO) on liquefaction of corn stover in presence of $Fe_2O_3$ and NaOH was investigated and the results are shown in Figure 3.3 a. The resulting bio-oil yields are 109.6%, 63.05% 126.1%, 64.1%, and 34.5% for reactions employing Ni ($H_2$), Ni (270 °C), Ni/C, and NiO, respectively. Ni metal, $Fe_2O_3$, and NaOH combination can catalyze dehydroxylation, decarboxylation, and hydrogenation resulting in a higher oil yield compared to $Fe_2O_3$ + NaOH and Ni metal + NaOH. Ethanol condensation could also be enhanced by this combination. Consequently, more than 100% of the oil with 2% and 40% of solid bio-residue was obtained using Ni ($H_2$) and Ni (270°C) metals, respectively. The different catalytic performance of the two Ni metals may be attributed to their different preparation methods. With NiO, the bio-oil

yield was slightly decreased compared to the corn stover liquefaction with no catalyst added. No significant changes in the un-repolymerized oil molecules and solid bio-residue yields were observed with NiO compared to other metal oxides.

As illustrated in Figure 3.3b (S13-S16), $^{1}$H -NMR analysis of bio-oils generated under this investigation showed that Ni ($H_2$), Ni (270°C), and Ni/C gave 2.15%, 1.20%, and 2.66% of phenolic protons, 86.71 %, 81.63%, and 89.73% of non-oxygenated methylene protons, 2.85%, 1.91%, and 1.97% of ester protons, and 8.29%, 15.26%, and 5.64% of ether/alcohol protons, respectively. Higher percentages of alcohol and ether protons were measured for the bio-oils generated using Ni ($H_2$) and Ni (270°C) compared to that measured using Ni/C, indicating that more solvent condensation reaction occurred. The lowest proton percentage of non-oxygenated carbons was observed in bio-oil generated using NiO. Based on H-NMR analysis, the bio-oil quality is ranked based on Ni-based catalyst applied in the following order: Ni/C > Ni ($H_2$) > Ni (270°C) > NiO.

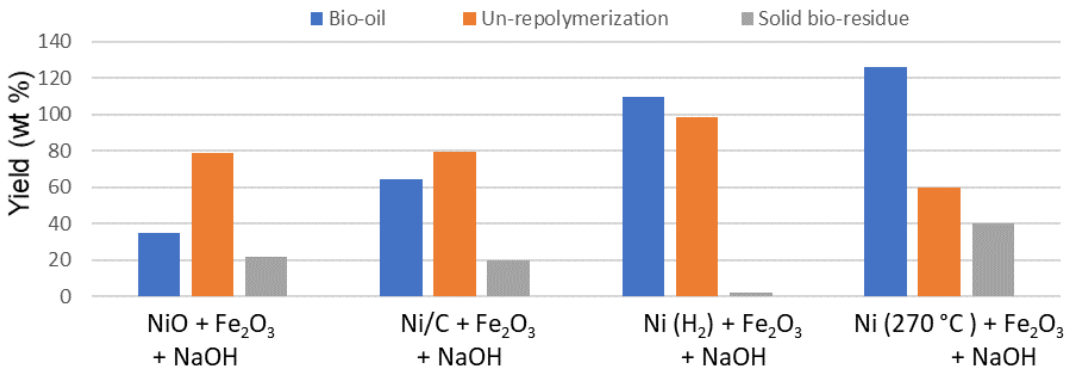


Figure 3.3a: The product profile of 400 mg corn stover liquefaction catalyzed by 100 mg Ni- based catalyst + 300 mg $Fe_2O_3$ + 50 mg NaOH in 4 mL EtOH at 260°C for 8h.

FTIR spectra of bio-oils obtained by this investigation are illustrated in Fig.3.3 c. The absorption bands of bio-oil in IR spectra were identified using Infrared spectroscopy correlation table and reported researches related to characterization of corn stover using FTIR. [78, 79] The absorption bands of O—H stretching bands (3432 $cm^{-1}$), C—H stretch (2877 $cm^{-1}$ ), C=O (1718 $cm^{-1}$), and $SP^2$ and $SP^3$-hybridized O—C (1209 and 1070 $cm^{-1}$) were observed in IR spectra of bio-oils. These bands indicate that bio-oil products can be alcohol, aldehyde, ether and ester. In FTIR spectrum of bio-oil obtained in the absence of any catalyst, the absorption band of benzene ring (1603 $cm^{-1}$) was significant. This band almost disappeared for bio-oil obtained in the presence of Ni metals and metal oxide indicating that reduction of lignin products to this catalytic system. Also, higher intensity of $CH_2$ and $CH_3$ (1463 and 1381 $cm^{-1}$, respectively) bending bands appeared in bio-oils obtained by Ni metal and hematite compared to bio-oils produced in the presence of metal oxide/ non-catalyst used giving a second evidence that biomass components can be reduced effectively by Ni metals in the presence of hematite. In contrast, the bio-oil from NiO-catalyzed liquefaction shows smaller $CH_2$ and $CH_3$ bending bands.

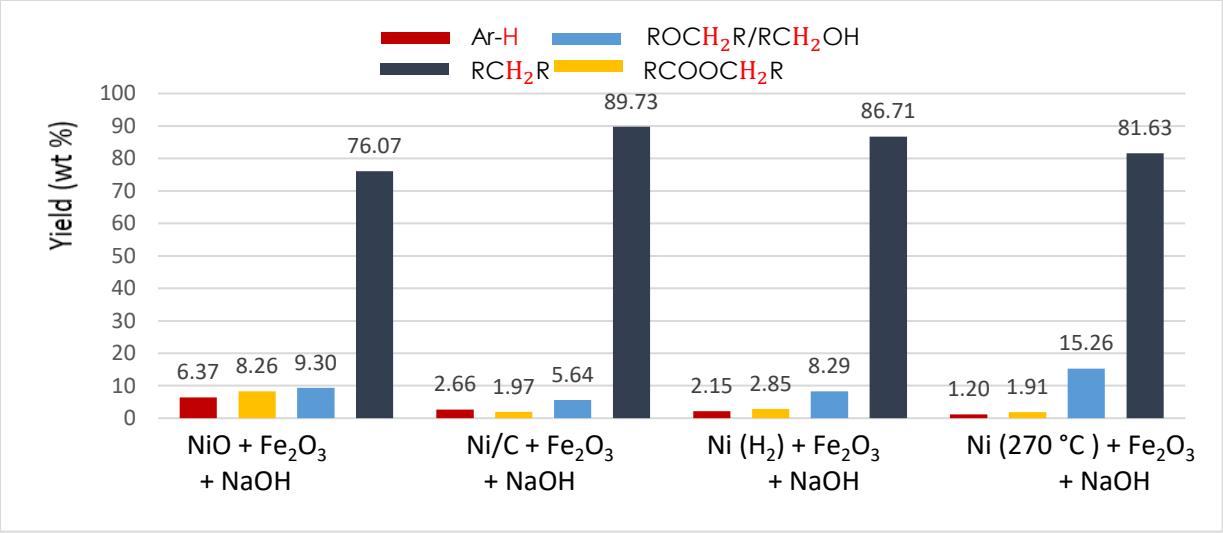

Figure 3.3b: The relative intensity of protons in bio-oil using Ni-based catalysts combined with hematite and NaOH was measured using $^{1}$H-NMR.

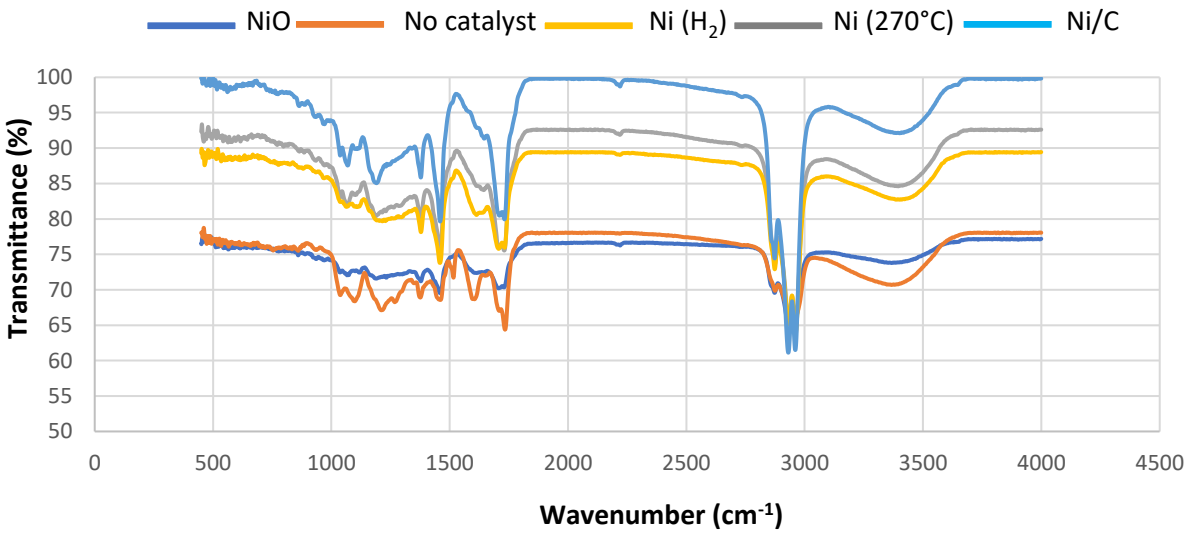


Figure 3.3c: The chemical composition of bio-oil obtained by Ni-based catalysts combined with hematite and NaOH was characterized using FTIR.

### 3.3.5 Catalyst characterization

#### 3.3.5.1 Morphology and Composition of Catalysts

Figure 3.4 shows the surface morphology of the four catalysts. The surface morphologies were analyzed using a field emission scanning electron microscope (Hitachi S-3400 N Scanning Electron Microscope) equipped with an energy dispersive X-ray (EDX) feature. Ni ($H_2$) was reduced from Ni (270°C), however, Ni ($H_2$) particles are 3-4 times larger in length and have clearer particle boundary than the particles of Ni (270°C), indicating that NiO and Ni (270°C) have similar morphology. The catalysts composition was detected using EDX analysis. From the chosen area of the Ni/NiO catalysts, the percentage of nickel element in Ni/C, Ni (270°C), Ni ($H_2$) and NiO is 18%, 95%, 99.6% and 95%, respectively. Oxygen was not detected in Ni ($H_2$), so it is fully

reduced. A similar Ni wt% in Ni (270°C) was determined by measuring $H_2$ (g) produced from reacting with HCl. Nickel metal on carbon is well distributed and deposited on the surface as shown by the green-colored dots under EDX analysis in Fig 3.4.

### 3.3.5.2 XRD analysis of Ni catalysts

The crystallinity of the catalysts was determined by X-ray diffraction method and the XRD patterns of the synthesized catalysts are given in Figure 3.5. The XRD pattern of catalysts were analyzed. The three sharp Ni (111, 200, and 220) diffraction peaks were observed at $2\theta$ = 44.49°, 51.84°, and 76.40° for Ni ($H_2$), Ni (270°C) and Ni/C and broad C (002) diffraction peak (2θ = 15-30°) is attributed to the carbon of Ni/C. Five characteristic diffraction peaks of Ni/O were observed at 37.27°, 43.27°, 62.78°, 75.31°, and 79.35°, corresponding to the (111), (200), (220), (311), and (222) planes of the fcc phase of NiO.[80, 81] NiO show the lowest crystallinity compared to other catalysts; in contrast, Ni ($H_2$) show higher crystallinity compared to Ni (270°C) indicating that reduction of metal oxide by $H_2$ (g) into metal not only increase the metal content but also improve the crystallinity. The crystallinity of Ni in Ni/C is weaker than Ni (270°C).

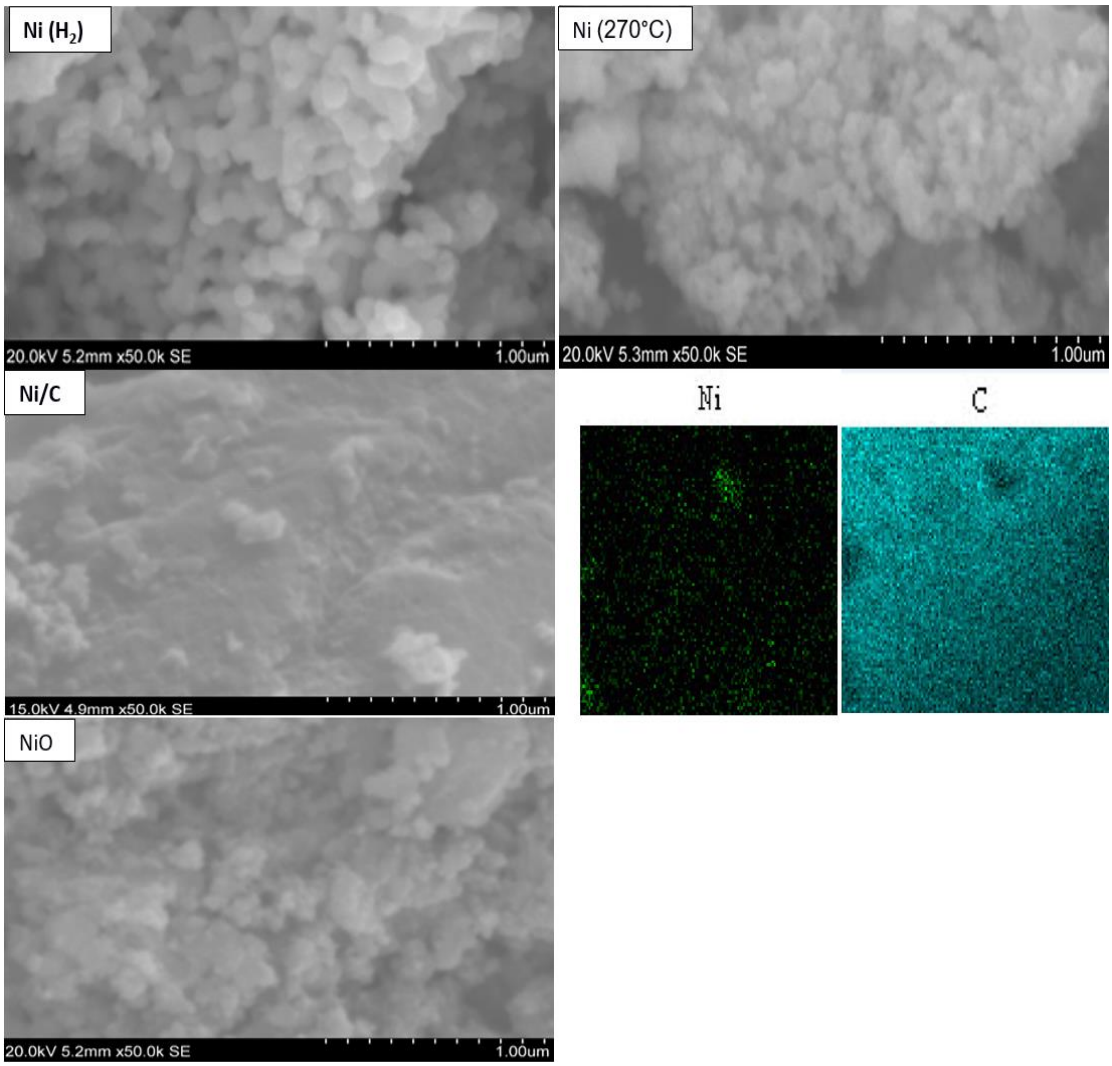


Figure 3.4: SEM images of Ni ($H_2$), Ni (270°C) , Ni/C and NiO.

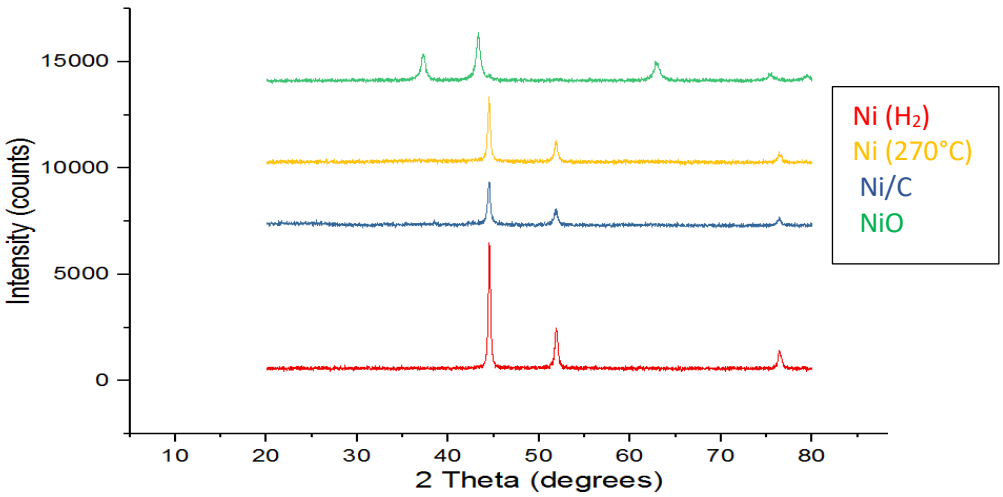


Figure 3.5: XRD patterns of Ni ($H_2$), Ni (270°C), Ni/C and NiO.

## 3.4 Conclusions

In this study, corn stover was effectively liquefied using cheap catalytic system consisted of Ni metal and metal oxide in ethanol in the presence of NaOH at 260 °C. Based on the results above, the following specific conclusions can be made:

- The yields of bio-oil increased significantly as the NaOH concentration increased from 20 mg to 50 mg, but the profile of bio-oil yield became irregular when the concentration was increased further from 60 to 100 mg. These results suggested that the highest bio-oil yield could be obtained under basic condition at (8:1) ratio of biomass/base.
- 400mg Corn stover, 300mg $Fe_2O_3$, 4ml ethanol, 50mg NaOH, 260°C, 8 h was found to be the optimized condition for direct liquefaction of corn stover to produce the bio-oil using the synthesized catalysts.
- The descending order of bio-oil yield from corn stover liquefaction was achieved using Ni ($H_2$), Ni/C, Ni (270°C), and NiO at an identical condition, respectively.

- NiO catalyst showed similar catalytic activity to metal oxides.
- Based on H-NMR and FTIR, the chemical composition of liquid fuel obtained by Ni ($H_2$) showed the lowest ratio of O/C compared to others; in contrast, the morphos shape, the highest crystallinity and thermal corn stover decomposition were also assigned to Ni ($H_2$).
- The future work will be directed to liquefy different biomass using Ni metal + metal oxide's synergy in the presence and absence of NaOH under different conditions.

## 3.5 Appendix

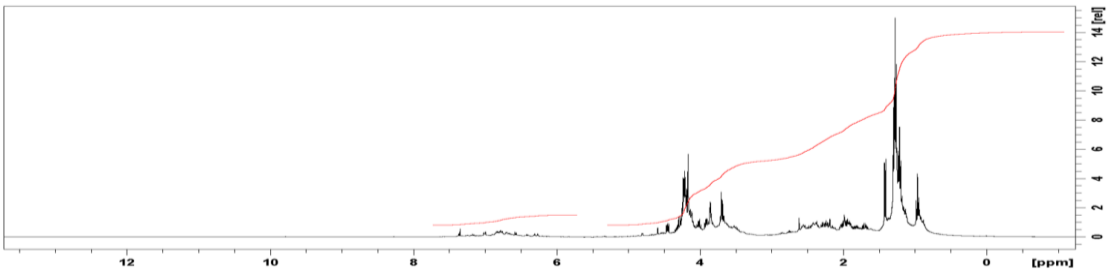


Figure S1: $^{1}$H-NMR spectrum of bio-oil from corn stover liquefaction for 8 hr with no catalyst added.

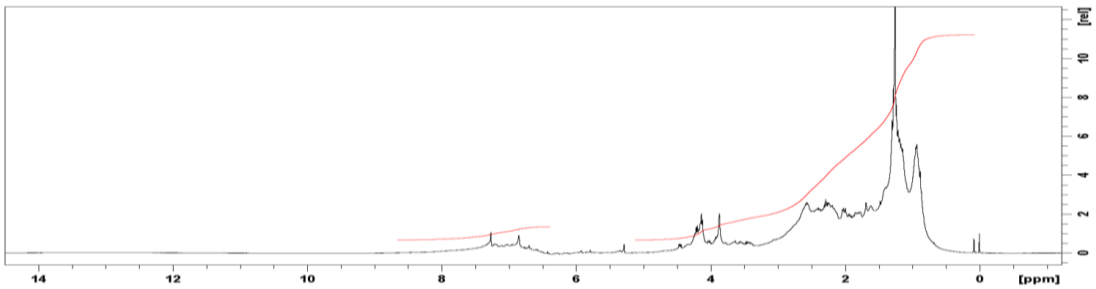


Figure S2: $^{1}$H-NMR spectrum of bio-oil from corn stover liquefaction using $Fe_2O_3$ for 4 hr.

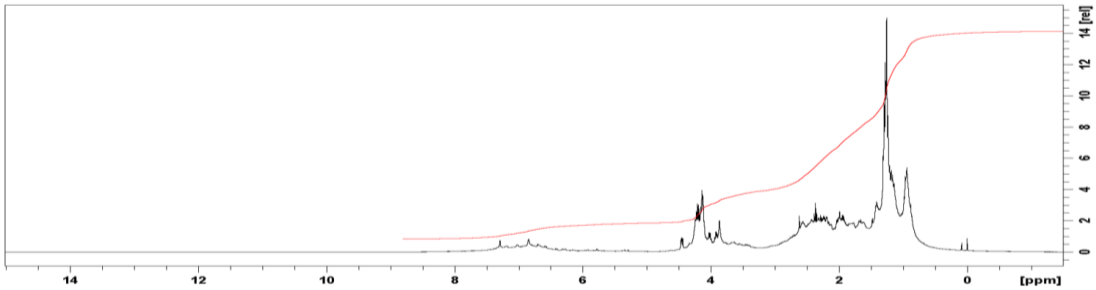


Figure S3: $^{1}$H-NMR spectrum of bio-oil from corn stover liquefaction using $Fe_2O_3$ for 8 hr.

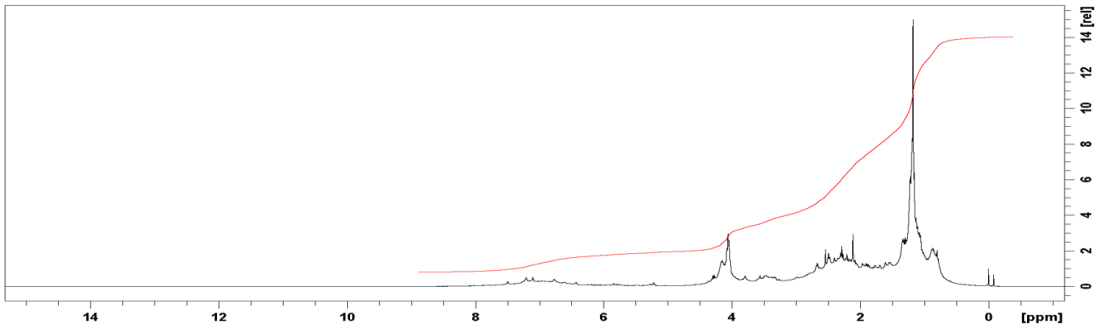


Figure S4: $^{1}$H-NMR spectrum of bio-oil from corn stover liquefaction using $Fe_2O_3$ for 12 hr.

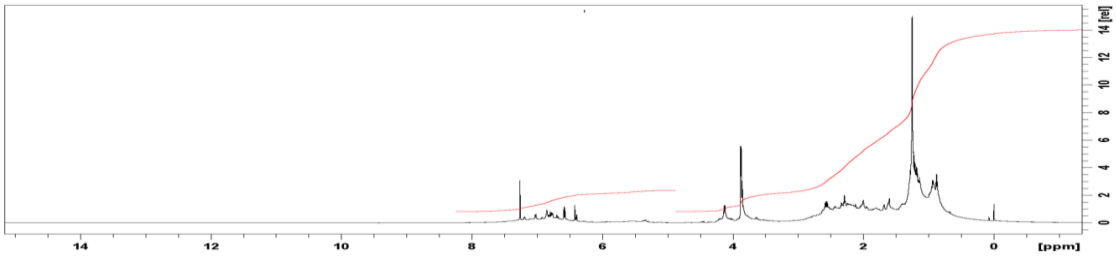


Figure S5:[1]H-NMR spectrum of bio-oil from corn stover liquefaction using $TiO_2$ and NaOH.

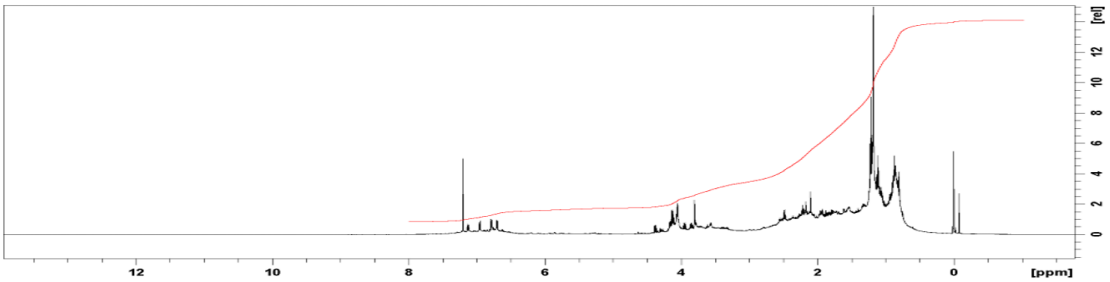


Figure S6:[1]H-NMR spectrum of bio-oil from corn stover liquefaction using MgO and NaOH.

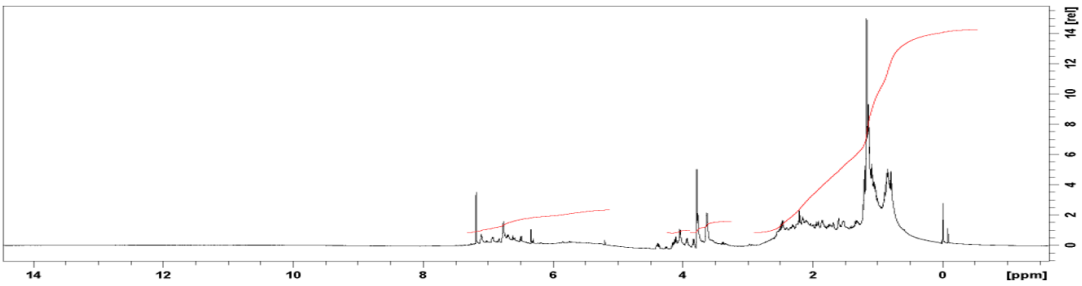


Figure S7:[1]H-NMR spectrum of bio-oil from corn stover liquefaction using ZnO and NaOH.

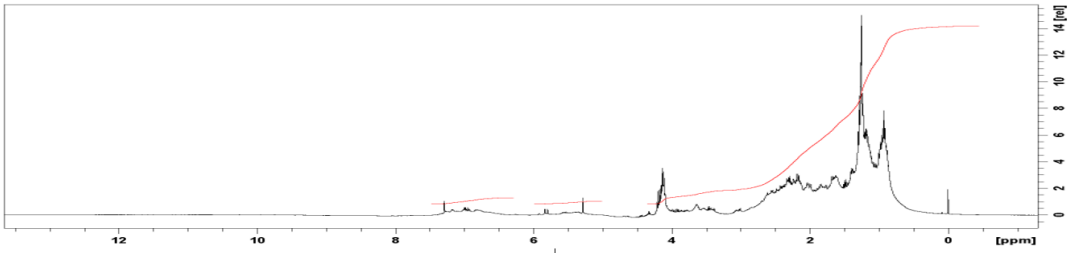


Figure S8:[1]H-NMR spectrum of bio-oil from corn stover liquefaction using $V_2O_5$ and NaOH.

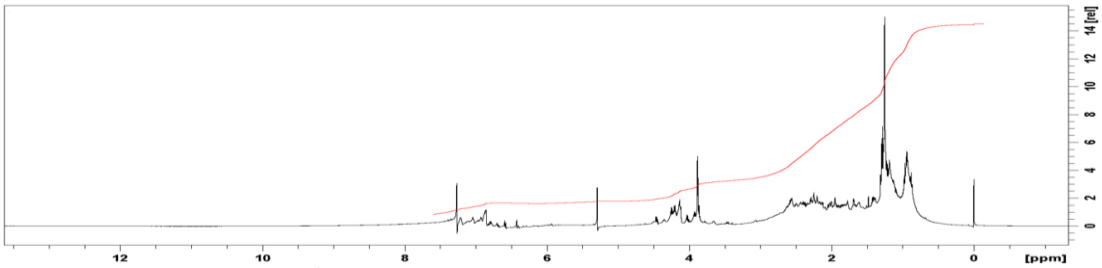


Figure S9:[1]H-NMR spectrum of bio-oil from corn stover liquefaction using $Fe_3O_4$ and NaOH.

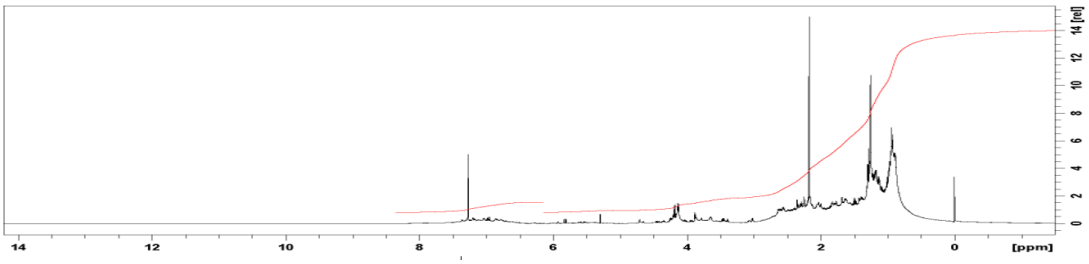


Figure S10:[1]H-NMR spectrum of bio-oil from corn stover liquefaction using $MnO_2$ and NaOH.

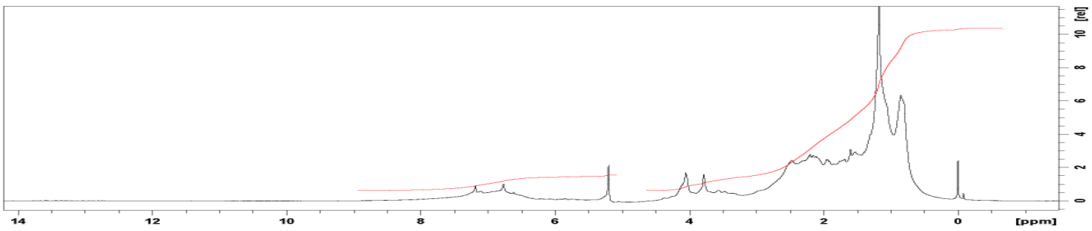


Figure S11:[1]H-NMR spectrum of bio-oil from corn stover liquefaction using $Fe_2O_3$ and NaOH for 8hr.

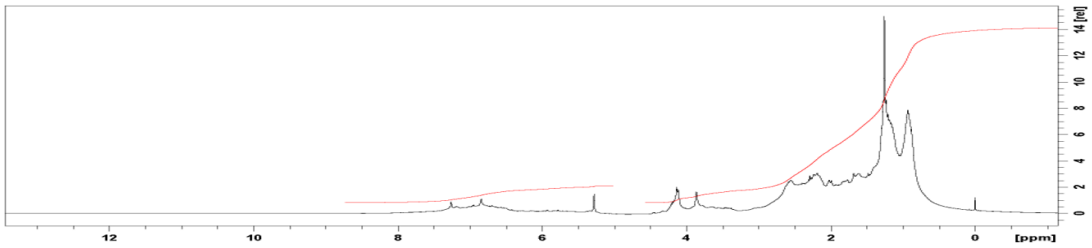


Figure S12:[1]H-NMR spectrum of bio-oil from corn stover liquefaction using Fe metal and NaOH for 8 hr.

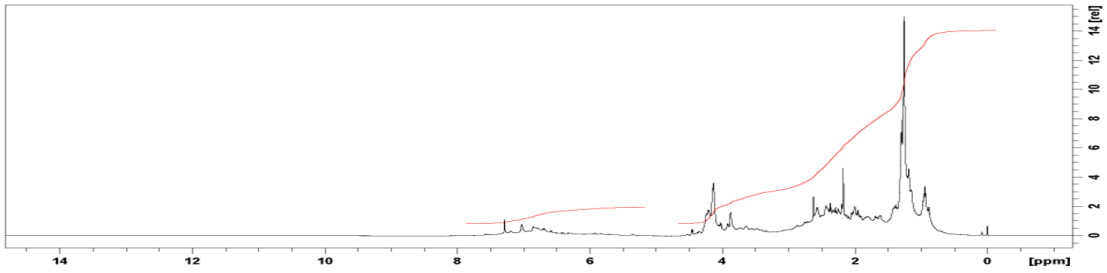


Figure S13:[1]H-NMR spectrum of bio-oil from corn stover liquefaction using NiO, $Fe_2O_3$, and NaOH.

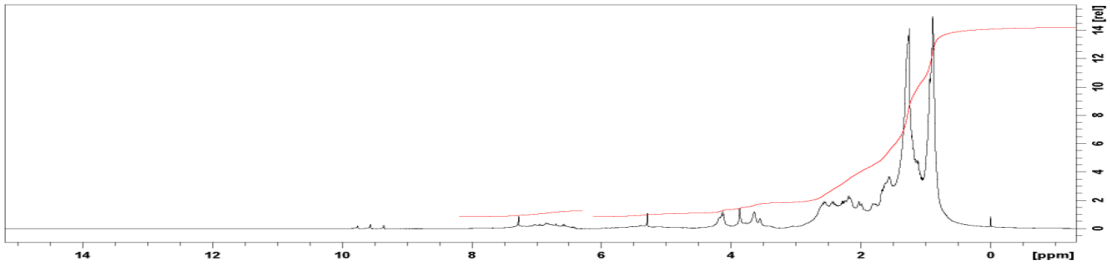


Figure S14:[1]H-NMR spectrum of bio-oil from corn stover liquefaction using Ni/C, $Fe_2O_3$, and NaOH.

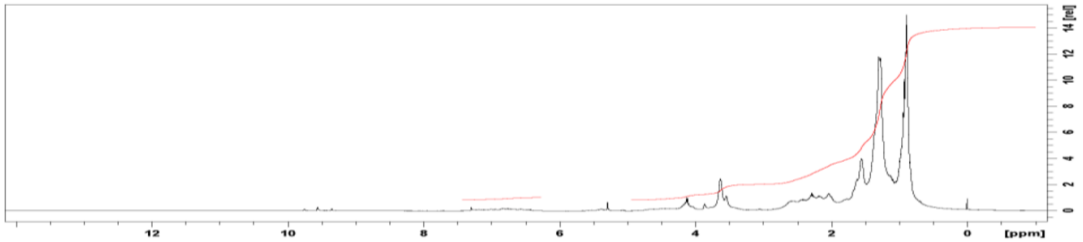


Figure S15:[1]H-NMR spectrum of bio-oil from corn stover liquefaction using Ni ($H_2$), $Fe_2O_3$, and NaOH.

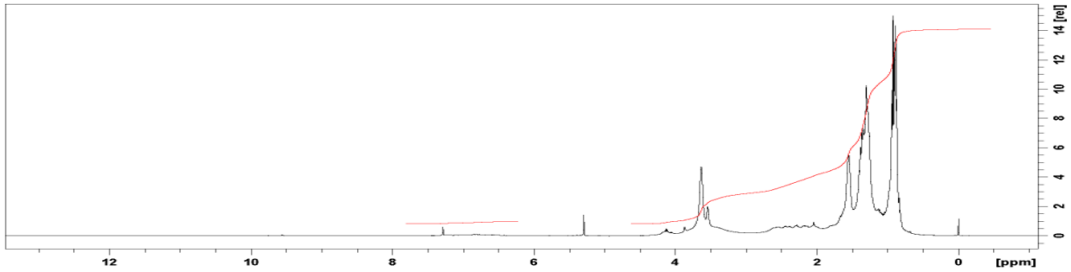


Figure S16:[1]H-NMR spectrum of bio-oil from corn stover liquefaction using Ni (270 °C), $Fe_2O_3$, and NaOH.

# CHAPTER 4: SOLVOLYTIC LIQUEFACTION OF DIFFERENT BIOMASS USING Ni-BASED CATALYSTS COMBINED WITH DIFFERENT METAL OXIDES

## 4.1 Introduction

Lignocellulosic biomass is an efficient and renewable alternative energy source to replace fossil fuels because of the abundant agricultural and forestry biomass generated annually around the world. According to a joint study by the US Department of Energy and the US Department of Agriculture, 344 million dry tons of agricultural and forestry resources could be produced and dedicated to biofuel production yearly in the US.[82] Numerous research works have paid attention to the direct liquefaction method due to being effective for transforming whole solid biomass into liquid fuel in a single step . For instance, various biomass (e.g., Empty fruit bunch,[83] corncob, [84] sugarcane bagasse,[85] white pine sawdust,[44, 56, 86] bamboo shoot shell,[87] sorghum,[88] wheat straw,[88] kenaf,[88] corn stover,[89] and switchgrass[90]) has been liquefied under different operative conditions to enhance the yield and quality of bio-oil. However, HTL bio-oil is needed to improve its physical and chemical properties to meet the standard values of transportation fuels.[91]

Besides the effect of liquefaction process parameters, the use of a suitable catalyst can play a crucial role in achieving the high conversion of biomass and selectivity production of value-added chemicals under mild conditions. For instance, homogenous catalysts, including alkalies ($Na_2CO_3$, NaOH, $K_2CO_3$, KOH, LiOH, RbOH, CsOH, $Rb_2CO_3$)[7, 92, 93] and acids ($HCO_2H$, $CH_3CO_2H$, HCl, $H_2SO_4$, $HClO_4$, $H_3PO_4$)[94] have been widely utilized in the biomass liquefaction. They are used to not only suppress the

formation of char and enhance the yield of bio-oil but also to improve the properties of the bio-oil composition.[7, 94] However, the separation and reuse of homogenous catalysts are no easy task.[95] In contrast, heterogeneous catalysts show high recyclability, stability, and hydrogen selectivity.[96, 97] Several types of heterogeneous catalysts, such as transition metals, metal oxides, and zeolite, have been reported in the literature to improve bio-oil yield and quality.[94] Metal catalysts, such as Pd,[96-98] Pt,[96, 99] Ni,[99] Ru,[96, 99] and Ir[96] can effectively promote the hydrogenation reactions to saturate bonds and improve the stability of the oxy-intermediates.[94] Besides, these metals with solid acids such as $Al_2O_3$, $WO_3$, $NbOPO_4$, $TaOPO_4$, polyoxometalates, acidic zeolites[100, 101] exhibit excellent activity for Hydrodeoxygenation reaction (HDO). For instance, Ni-based catalyst showed high performance in reductive depolymerization of birch lignin giving propylguaiacol and propylsyringol with selectivity >90% at a lignin conversion of about 50%.[61] According to Chen, Zhang et al., the efficient depolymerization of hydrolyzed lignin and char elimination was achieved using a mesoporous Ni/Al-SBA-15(20) catalyst.[102] Lignin-derived phenolics such as guaiacol over Ni/$SiO_2$, Ni/$\gamma$-$Al_2O_3$ Ni/$SiO_2$-$ZrO_2$, Ni/HZSM-5, Pt/HZSM-5, Ru/H-Beta and Pt/H-Beta and eugenol, cresol, and anisole over Ni/$SiO_2$ and Ni/$\gamma$-$Al_2O_3$ have been efficiently converted into hydrocarbon.[103]

Apart from a metal catalyst, a variety of basic, acidic, and amphoteric oxide metal oxides have been used for the promotion of ketonization and aldol condensation reactions, [104, 105] which are recognized as a crucial pathway to upgrade the bio-oil quality and avoid the negative effects of carboxylic acids in bio-oil. For instance, Yakerson et al.[105] observed that oxides with low lattice energies (e.g., MgO, CaO, BaO, SrO, and CdO) can actively interact with acetic acid and form bulk carboxylate salts, which

decompose into acetone, $H_2O$, and $CO_2$. In contrast, on oxides with high lattice energies (e.g., $TiO_2$, $CeO_2$, $ZrO_2$, $SnO_2$, and so forth), the reaction proceeds on the catalyst surface. Moreover, Kuriacose and Jewur[105] investigated the influence of iron oxides on the acetic acid ketonization in the presence of $H_2$. According to the activation energy change observed, two mechanistic pathways were proposed: at < 400 °C; Ketonization proceeds through the interaction of two adsorbed molecules of acetic acid on the catalyst surface while at a higher temperature, the ketonization reaction takes place through the bulk acetate decomposition.

To the best of the authors' knowledge, no previous study describing the liquefaction characteristics of biomass in ethanol with different loadings of Ni metal and transition metal oxide has been reported. In this work, the catalytic effects of various combinations ( metal-NaOH, metal oxide, metal oxide-NaOH, Ni metal-metal oxide, and Ni metal-metal oxide-NaOH) were investigated for liquefaction of pine sawdust. Thereafter, the combinations with higher synergistic effects were selected for liquefaction of corn stover under the same condition, but different masses of Ni metal and metal oxide were employed. To examine the catalytic power of these combinations with various biomass, the liquefaction of birch, switchgrass, and sugarcane bagasse using Ni metal + $Fe_2O_3$ in NaOH's presence and absence was conducted under identical conditions. Furthermore, the obtained bio-oils were characterized using $^1$H-NMR and gas chromatography-mass spectrometry (GC–MS).

## 4.2 Experimental

### 4.2.1 Materials

All biomass used were obtained from a local farm and reduced in size using a blender to 18-50 mesh. The chemical compositions of biomass used are presented in Table 4.1.

| Plant biomass material | Cellulose% | Hemicellulose% | Lignin% |
|---|---|---|---|
| Corn stover | 28-51.2 | 19.1-30.7 | 11-16.9 |
| Pine sawdust | 45-50 | 25-35 | 35-35 |
| Switch grass | 30-50 | 10-40 | 5-20 |
| Sugarcane bagasse | 25-45 | 28-32 | 15-25 |
| Hardwood stems (birch) | 40-55 | 24-40 | 18-25 |

Metal oxides: Titanium (IV) oxide ($TiO_2$), vanadium**(**V**)** oxide ($V_2O_5$), zinc (II) oxide (ZnO), iron(III) oxide ($Fe_2O_3$), iron(II,III) oxide ($F_3O_4$) were used as provided by the chemical suppliers. Base chemical and solvent: Sodium hydroxide and ethanol were purchased from Fisher Scientific and Pharmco-AAPER company, respectively.

### 4.2.2 Preparation of catalysts

Ni/C and Ni (270 °C) metals were prepared as described in the chapter 3.

### 4.2.3 Liquefaction procedure

The general procedure of corn stover liquefaction: To a stainless-steel pressure reactor in a glovebox were added a magnet stirring bar, catalyst, biomass, and EtOH. The closed reactor was transferred into a fume-hood and heated in a molten salt bath for the desired time. After reactor was cooled down, the mixture was filtered and washed with EtOH. The EtOH solution was condensed by rotary evaporation under a reduced pressure

of 80 mbar using a 50°C water bath. To the residue, 1 mL of $CH_2Cl_2$ (DCM) and 0.5 ml of water were added. The DCM solution was separated, and the water phase was extracted by DCM (0.5 mL × 2). The combined DCM solution was neutralized with $NaHCO_3$, dried with $MgSO_4$ powder, and condensed on a rotary evaporator to yield oil product.

The percentage yield of oil, solid residue, and corn stover conversion was calculated based on the weight of corn stover feed by the following formula:

$$\text{Bio oil yield (wt\%)} = \frac{\text{Weight of bio-oil}}{\text{Biomass weight}} \times 100\%$$

$$\text{Solid bio residue (SR) yield (wt\%)} = \frac{\text{Weight of solid bio residue}}{\text{Biomass wieght}} \times 100\%$$

$$\text{Un repolymerization yield (wt\%) of bio oil} = 100\% - \text{Solid bio residue \%}$$

$$\text{Gas + water soluble species (wt\%)} = 100\% - \text{Bio oil \%} - \text{Solid bio residue \%}$$

### 4.2.4 Characterization

It was performed for bio-oil obtained from each biomass liquefaction on a Bruker AVANCE-400 and 600 MHz NMR spectrometer in $CDCl_3$ using TMS as the internal standard. Percentage of protons in different types of chemical groups were calculated from the relative intensity of protons.

GC-MS analysis was performed on a Shimadzu GCMS-QP2010SE. GC column temperature program was set as follows: the temperature was held at 40 $^oC$ for 1 minute, then increased to 240 $^oC$ at a heating rate of 25 $^oC$/min, and then maintained at 240 $^oC$ for 3 minutes. To facilitate the bio-oil derivatization, the bio-oil samples were treated with a common TMS derivatizing reagent - N,O-bis(trimethylsilyl)trifluoroacetamide – BSTFA.

## 4.3 Results and discussion

### 4.3.1 Pine sawdust liquefaction

Six types of catalytic systems were used to enhance the bio-oil production from pine sawdust liquefaction under the following liquefaction condition: 12.66 wt% biomass, 4 mL EtOH, 260 °C, 8 hr. Thus, six cases were generated, i.e., the blank where no catalyst, Ni metal + NaOH, metal oxide alone, metal oxide + NaOH, Ni metal + metal oxide, and Ni metal + metal oxide + NaOH. The catalytic systems applied showed different behaviors toward biomass liquefaction products, as shown in Table 4.2. A low bio-oil yield of 28.48% and 33.1% of SR were achieved using $Fe_2O_3$ alone ( run 4.9), which are comparable to the results obtained by no catalyst (run 4.1). In contrast, the largest SR yield was obtained by $Fe_2O_3$-NaOH (run 4.10), which resulted in the lowest biomass conversion rate. Transition metal oxides are more acidic than their metals; thus, the metal oxide can react with oxygenated species of decomposed biomass to enhance the elimination of hydroxyl group and carboxylic group. In contrast, Ni metal can react with π-system as hydrogen transfer and do reduction reaction. Thus, the synergistic effect of Ni metals prepared by different methods and different metal oxides such as ZnO (run 4.4, 4.8, and 4.12), $V_2O_5$ (run 4.7), $TiO_2$ (run 4.3 and 4.6), and $Fe_2O_3$ ( run 4.11) were also examined. The results showed that the combination of Ni metal and metal oxide gave higher bio-oil, and lower SR yields compared to the yields obtained by metal oxide alone or combined with NaOH . It is interesting to note that more than 100% of bio-oil was generated by employing Ni (270 °C) + ZnO + NaOH, Ni/C + $V_2O_5$ + NaOH, Ni/C + ZnO + NaOH, and $Fe_2O_3$ + NaOH under run 4.4, 4.7, 4.8, and 4.10, respectively. This phenomenon is possibly caused by that NaOH combined with Ni metal, metal oxide, or both can activate Guerbet condensation reactions of not only EtOH but also alcoholic

products formed from biomass. Both Ni/C + $Fe_2O_3$ and Ni/C + ZnO under runs 4.11 and 4.12 exhibited the best performance among the tested catalysts under the same liquefaction condition, giving > 97% of pine sawdust conversion and < 3 % of SR yield. This achievement is better than the results reported by Xu et al. [106] and Li, Liu et al. [107] from woody biomass liquefaction in ethanol under $H_2$ (g) using iron-based catalysts (FeS and $FeSO_4$) and ionic liquid nickel catalyst ([BMIM]Cl–$NiCl_2$), respectively. Moreover, it can be seen from the liquefaction using the combination of Ni metal and metal oxide with and without NaOH; the liquefaction was more improved with an increase of Lewis acidity of metal oxide, which is consistent with the results obtained from empty fruit bunch liquefaction by different metal oxides.[83] From the previous results of this investigation; it can be concluded that Ni metal-metal oxide-NaOH and Ni metal-metal oxide gave better results compared to using Ni metal or metal oxide alone depending on the type of metal and metal oxide.

Table 4.2: Bio-oil production from 400 mg pine sawdust liquefied in 4 mL EtOH at 260 °C for 8 h.

| **Run No** | **Catalyst** | **Bio-oil%** | **Un-repolymerization %** | **SR%** | **Gas + aqueous products%** |
|---|---|---|---|---|---|
| 4.1 | No catalyst | 28.77 | 64.92 | 35.08 | 36.15 |
| 4.2 | 100 mg Ni (270 °C), 50 mg NaOH | 74.25 | 81.92 | 18.08 | 7.67 |
| 4.3 | 100 mg Ni(270 °C), 100 mg $TiO_2$, 50 mg NaOH | 66.37 | 83.4 | 16.6 | 17.02 |
| 4.4 | 100 mg Ni(270 °C), 100 mg ZnO, 50 mg NaOH | 102.27 | 90.62 | 9.37 | - |
| 4.5 | 69 mg Ni/C, 50 mg NaOH | 89.15 | 80.3 | 19.7 | - |

| | | | | | |
|---|---|---|---|---|---|
| 4.6 | 69 mg Ni/C, 300 mg $TiO_2$, 50 mg NaOH | 76 | 80.4 | 19.6 | 4.4 |
| 4.7 | 69 mg Ni/C, 250 mg $V_2O_5$, 50 mg NaOH | 103.95 | 77.92 | 22.08 | - |
| 4.8 | 69 mg Ni/C, 249 mg ZnO, 50 mg NaOH | 124.95 | 95.45 | 4.55 | - |
| 4.9 | 300 mg $Fe_2O_3$ | 28.47 | 66.9 | 33.1 | 38.42 |
| 4.10 | 300 mg $Fe_2O_3$, 50 mg NaOH | 142.32 | 48.67 | 51.33 | - |
| 4.11 | 69 mg Ni/C, 75 wt% $F_2O_3$ | 89.72 | 100 | 0 | 10.27 |
| 4.12 | 69 mg Ni/C, 249 mg ZnO | 80.9 | 97 | 3 | 16.1 |

### 4.3.2 Corn stover liquefaction

As indicated, biomass liquefaction was more promoted using Ni metal-metal oxide in the presence and absence of base than other catalysts. Consequently, this type of catalytic system was selected for biofuels production from corn stover under the following condition: 400 mg corn stover, 4 mL EtOH, 260 °C, 8 h. The results of biomass liquefaction catalyzed by different loadings of Ni metal and $Fe_2O_3/Fe_3O_4$ under runs 4.13-4.22 are shown in Table 4.3. Higher biofuel yields and lower gas and SR production were achieved under basic conditions (runs 4.13-4.15) compared to those obtained by their parallels under neutral conditions ( runs 4.19-4.21). The investigation results could be explained by that small Na ion of NaOH can penetrate the biomass texture, leading to break the linkages between cellulose and lignin, and weaken C—C bond resulting in a decreased activation energy.[84, 108] Moreover, the retro-aldol cleavage, ketonization, and condensation reactions could be more promoted by the addition of Ni

metal and metal oxide in the presence of NaOH, as seen by manipulating the mass of Ni metal and $Fe_2O_3$. A significant change in bio-oil production was seen by reducing the loading of Ni/C from 140 to 70 mg (runs 4.16 and 4.17) and $Fe_2O_3$ from 300 to 100 mg (runs 4.14 and 4.15) under basic condition; however, a slight change was observed in the yields of bio-liquid generated by increasing the mass of Ni/C from 100 to 300 mg (runs 4.18 and 4.19) and Ni (270 °C) from 50 to 100 mg (runs 4.21 and 4.22), and reducing the mass of $Fe_2O_3$ from 100 to 300 mg (runs 4.19 and 4.20) in the absence of NaOH.

Table 4.3: 400 mg corn stover liquefied in 4 mL EtOH at 260 °C for 8 h.

| **Run. No** | **Catalyst** | **Bio-oil%** | **Un-repolymerization %** | **SR%** | **Gas and water-soluble species%** |
|---|---|---|---|---|---|
| 4.13 | 50 mg Ni (270 °C), 150 mg $Fe_2O_3$, 50 mg NaOH | 83.275 | 72.7 | 27.3 | - |
| 4.14 | 140 mg Ni/C, 300 mg $Fe_2O_3$, 50 mg NaOH | 64.07 | 79.73 | 20.27 | 15.65 |
| 4.15 | 140 mg Ni/C, 100 mg $Fe_2O_3$, 50 mg NaOH | 61.42 | 82.97 | 17.03 | 21.55 |
| 4.16 | 140 mg Ni/C, 300 mg $Fe_3O_4$, 50 mg NaOH | 51.8 | 72.85 | 27.15 | 21.05 |
| 4.17 | 70 mg Ni/C, 300 mg $Fe_3O_4$, 50 mg NaOH | 42.87 | 77.47 | 22.53 | 34.6 |
| 4.18 | 70 mg Ni/C, 300 mg $Fe_2O_3$ | 38.47 | 80.08 | 19.92 | 41.6 |
| 4.19 | 140 mg Ni/C, 300 mg $Fe_2O_3$ | 40.5 | 81.75 | 18.25 | 41.25 |

| | | | | | |
|---|---|---|---|---|---|
| 4.20 | 140 mg Ni/C, 100 mg $Fe_2O_3$ | 40.63 | 86.47 | 13.53 | 45.85 |
| 4.21 | 50 mg Ni (270 °C), 150 mg $Fe_2O_3$ | 39.35 | 83.15 | 16.85 | 43.8 |
| 4.22 | 100 mg Ni (270 °C), 150 mg $Fe_2O_3$ | 40.875 | 86.7 | 13.3 | 45.825 |

### 4.3.3 Liquefaction of different biomass

Three types of biomass (birch, sugarcane bagasse, and switchgrass) were selected to investigate the catalytic power of Ni (270 °C)-$Fe_2O_3$ in the presence and absence of NaOH under the following condition: 15.19 wt% biomass, 4.17 wt% $Fe_2O_3$, 8.33 wt% Ni (270 °C), 5 mL EtOH, 6h, 260 °C. The results of this investigation are presented in Figure 4.1. Bio-oil production was higher, and the SR was lower under the basic than under neutral liquefaction. The yield of SR was around 30% for birch and sugarcane bagasse and was 2.25% for switchgrass, while the slight difference was observed in the yields of bio-oil obtained for all biomass liquefied in the absence of NaOH. The highest bio-oil yield of 65.32% was obtained from sugarcane bagasse, while birch and switchgrass gave nearly the same bio-oil yields under basic condition. According to Minowa et al., Zhong et al., Huang et al.[11, 92, 109] the distribution of liquefaction products is mainly determined by the lignin content of biomass. The phenoxy radicals formed from lignin of biomass during liquefaction can condense and repolymerize to a solid mass. Therefore, the higher the lignin content in the feedstock resulted in the lower the conversion rate and bio-oil yield. Moreover, Wang et al.[110] conducted the deoxy-liquefaction process of four agriculture residues (legume straw, cornstalk, cotton stalk,

and wheat straw) for bio-oil production. They found that the highest conversion rate (65.7%) and the lowest yield of bio-oil (5.2%) were obtained by a cotton stalk, which contained the highest holocellulose content among the four samples. However, according to our investigation results and that found by de Caprariis, B., et al.,[111] higher bio-oil production was achieved from the biomass, which has greater lignin content, which may be ascribed to that optimal liquefaction condition may differ based on the chemical composition of biomass. Consequently, no remarkable correlation between the biomass composition and the yield and quality of bio-oil could be concluded. These results confirmed preliminarily that the proposed catalytic system was more effective for the liquefaction of the three different feedstocks under basic condition than under neutral condition.

Figure 4.1: Bio-oil production from diverse biomass using Ni (270 °C) and $Fe_2O_3$ in the presence and absence of NaOH.

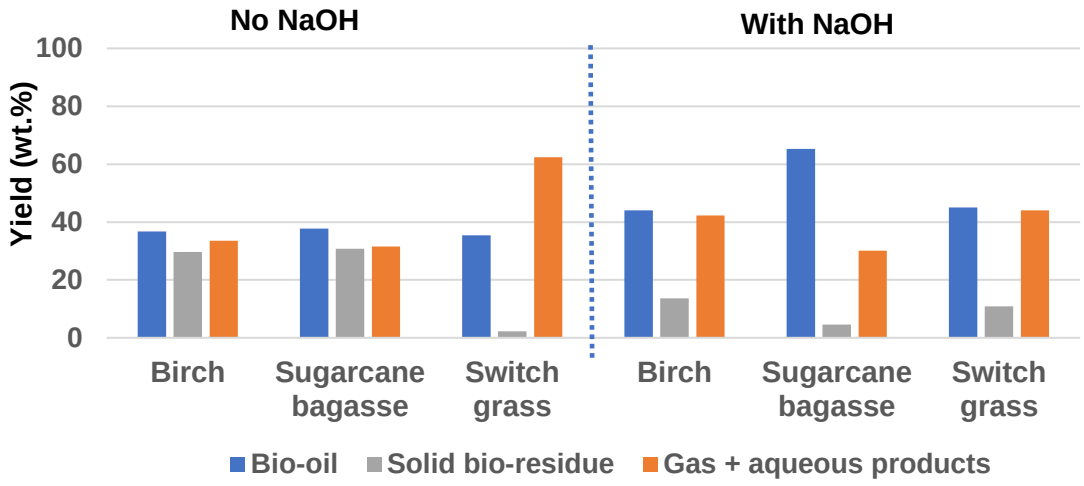

### 4.3.4 Characterization of bio-oil composition

#### 4.3.4.1 $^{1}$H-NMR analysis of bio-oil

To investigate the chemical structural changes of bio-oil produced, a $^{1}$H-NMR analysis was carried out. The percentages of proton types were calculated on the basis of the integration values obtained from the $^{1}$H-NMR spectra (S1-S28), as shown in Figures 4.2, 4.3, and 4.4. The region of the spectrum from (0.5 to 3.0 ppm), (3.0 to 4.0 ppm), (4.1 to 4.3 ppm), and (6.0 to 8.0 ppm) represent aliphatic protons of non-oxygenated carbon atoms (—$CH_3$, —$CH_n$—), protons of carbon atoms bonded to hydroxyl or ether group (—$CH_n$—O—), protons of $CH_n$ connected to ester group (—$COOCH_n$—), and the aromatic protons ( Ar—H), respectively.

$^{1}$H-NMR analysis of bio-oils from pine sawdust liquefaction under different conditions (runs 4.1-4.12, S1-S12) is presented in Figure 4.2. Bio-oil produced by no catalyst contained 29.46% of undesirable protons (protons of oxygenated carbons), while the remaining percentage is about protons of non-oxygenated aliphatic carbon. The percent of ester protons is higher than the percent of aromatic, ether, and alcohol protons, the highest ester proton percentage among bio-oils produced from pine sawdust liquefaction. Compared to the results obtained by no catalyst, all the catalytic liquefaction gave lower percents of undesirable protons. In the catalytic liquefaction using Ni (270 °C)- metal oxide-NaOH (runs 4.2-4.4), the aromatic and oxygenated carbon protons were more reduced by ZnO than $TiO_2$ and the last showed a lower reduction of aromatic and ester protons compared to using Ni (270 °C) + NaOH. For the catalytic liquefaction using Ni/C- metal oxide-NaOH (runs 4.5-4.8), the reduction of aromatic protons and the formation of ether and alcohol protons were more enhanced by the addition of $TiO_2$,

$V_2O_5$, and ZnO compared to using Ni/C alone with NaOH. Whereas, the ester protons were more reduced by Ni/C and NaOH without metal oxide. The influence of Ni/C metal and NaOH addition were noticed in bio-oils generated under reaction runs 4.9-4.12. The aromatics and esters in the catalytic liquefaction using $Fe_2O_3$-NaOH were more reduced than using Ni/C-$Fe_2O_3$, Ni/C-ZnO, and $Fe_2O_3$ alone. In contrast, liquefaction using $Fe_2O_3$ alone showed the lowest reduction of aromatic and ester protons.

The bio-oils generated from corn stover liquefaction were also analyzed using $^1$H-NMR. The analysis results are presented in Figure 4.3 (S13-S22). The bio-oils produced from corn stover using Ni (270 °C) and Ni/C with metal oxide contained lower undesirable proton percents under basic liquefaction than under neutral liquefaction. The percentages of undesirable protons were further suppressed by reducing the loadings of $Fe_2O_3$ from 75 wt% (run 4.14) to 25 wt% (run 4.15) and Ni/C from 35 wt% (run 4.16) to 17.5 wt% (run 4.17) , respectively. Significant changes were also observed in neutral runs 4.18-4.22 by varying the loadings of Ni/C and metal oxide. Reduction in Ni/C and metal oxide loadings clearly caused an increase in the proportion of ester protons.

As shown in Figure 4.4 (S23-S28), the bio-oils produced from birch, sugarcane bagasse, and switch grass liquefaction using the same catalytic system consisting of Ni (270 °C)-$Fe_2O_3$ contained higher percentages of protons on aromatic and oxygenated carbons under neutral conditions than that those obtained under basic conditions. Consequently, lower proton percentages of non-oxygenated carbons were obtained from birch, sugarcane bagasse, and switchgrass under neutral condition than that obtained under basic conditions.

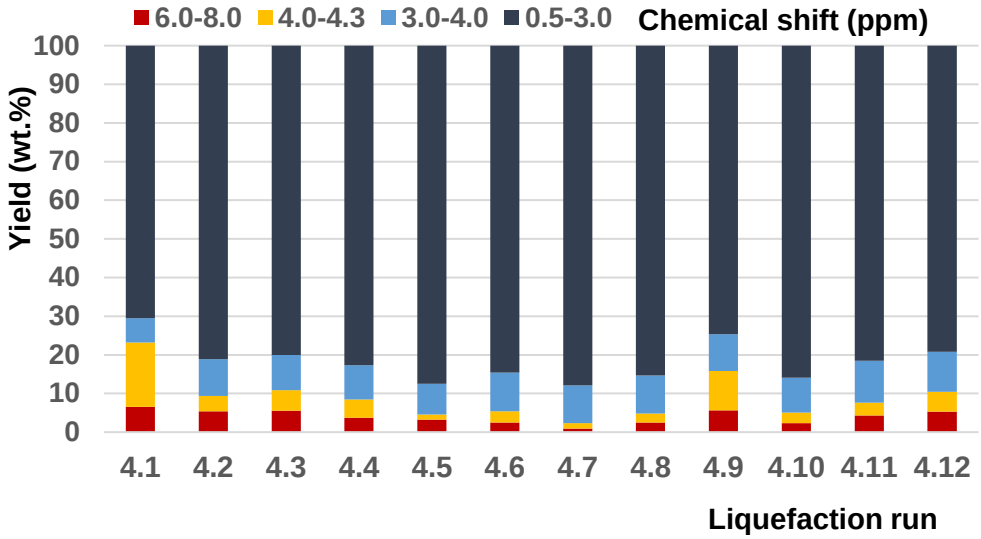


Figure 4.2: H-NMR analysis of bio-oil produced from pine sawdust in runs 4.1-4.12.

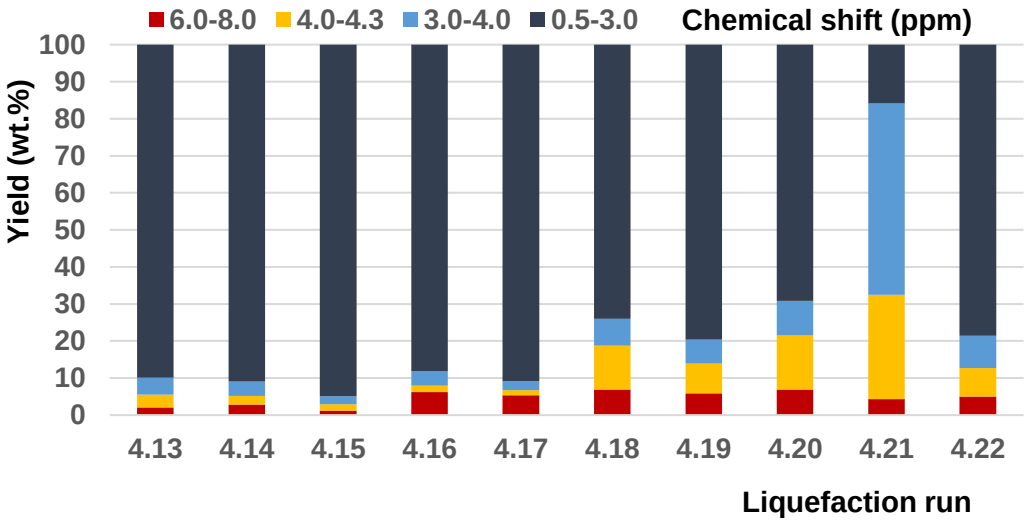


Figure 4.3: H-NMR analysis of bio-oil produced from corn stover in runs 4.13-4.22

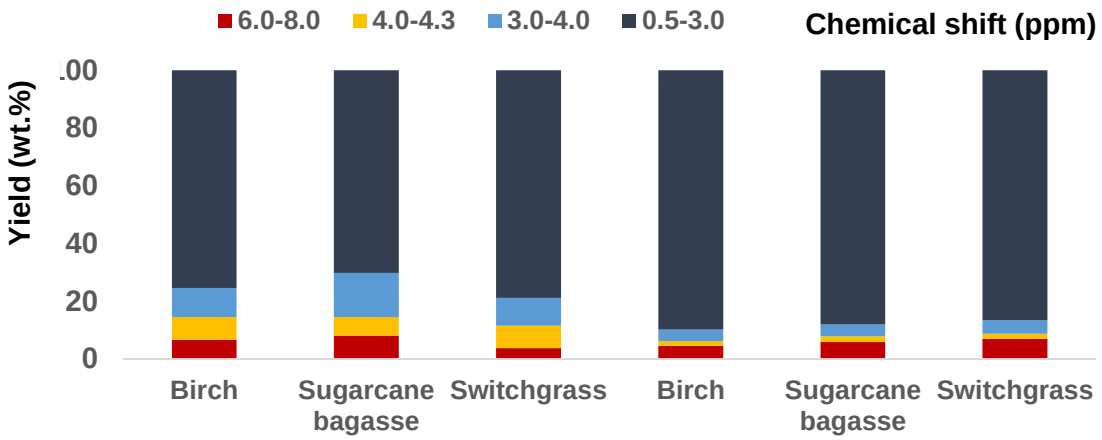


Figure 4.4: H-NMR analysis of bio-oil produced from diverse biomass.

#### 4.3.4.2 GC-MS analysis of ethanol distillate and bio-oil

GC-MS analysis was carried out to detect the volatile compounds in EtOH distillates and bio-oils produced from direct liquefaction of different biomass under different conditions as shown in Tables 4.4-4.27. Aliphatic alcohols (mostly primary) accounted for the largest proportion of the identified derivatives in bio-oils and EtOH distillates from pine sawdust liquefaction (runs 4.5-4.8 and 4.11), except EtOH distillate of run 4.5 as illustrated in Tables 4.4-4.13 (S29-S38). The primary alcohols were derived from ethanol and alcoholic products formed from biomass via Guerbet reaction. The Guerbet reaction involves the coupling of two alcohol molecules to produce the unbranched and β-branched heavier alcohols via a number of sequential steps, as shown in Scheme 1.

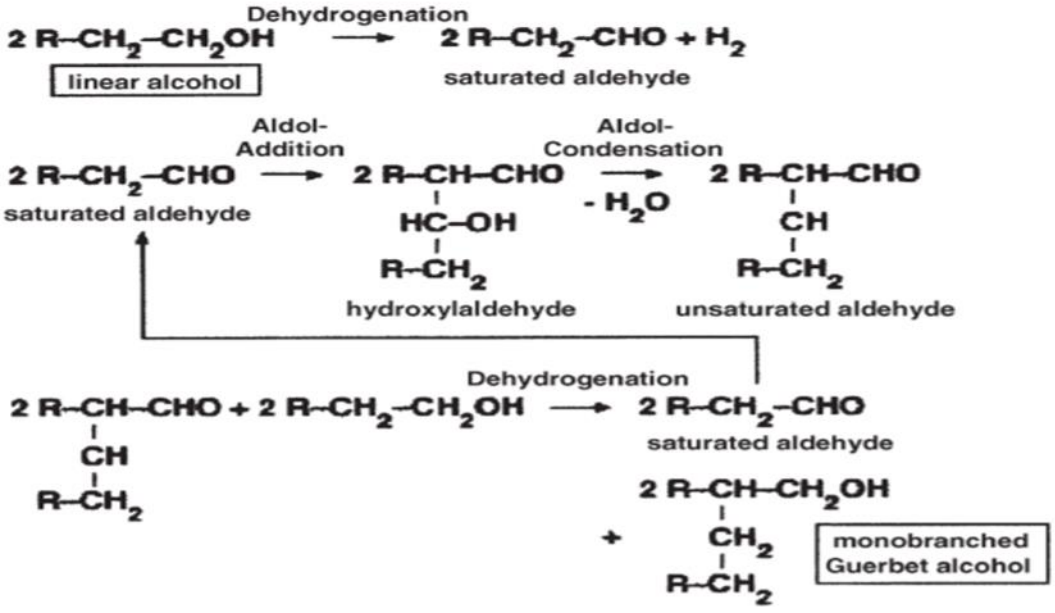


Scheme 1: Guerbet reaction sequence for alcohol coupling.[112]

Compared to other runs (4.5-4.8), derivatives such as acid, ester, aromatic, furan, and ether were detected in bio-oil obtained from pine sawdust using Ni/C-$Fe_2O_3$ in run 4.11, which indicated a marked level of reduction reactions occurred during the liquefaction process. More products of ester, ether, aldehyde, ketone, and furan were measured in EtOH distillates obtained from pine sawdust liquefaction.

The major compounds identified in the bio-oils from corn stover liquefaction were alcohols, acids, esters, ethers, ketones, hydrocarbons, and aromatics, as shown in Tables 4.14-4.17 (S39-S42). Higher relative abundances of aromatic were measured for runs 4.14 and 4.18 than runs 4.15 and 4.16, which indicated that employing 75 wt.% of $Fe_2O_3$ was more effective for the lignin decomposition than $Fe_3O_4$ (75 wt.%) and $Fe_2O_3$ (25 wt.%) in the presence of Ni/C and NaOH. Moreover, the lignin liquefaction was more promoted under neutral than basic conditions.

The bio-oils and EtOH distillates from birch, sugarcane bagasse, and switchgrass liquefaction under a neutral and basic condition were also analyzed. The analysis results (Tables 4.18-4.27, S43-S52) showed similar compounds to what was recognized in the previous analysis. Of the bio-oils from the liquefaction of birch and sugarcane bagasse under neutral conditions, the most abundant volatiles are esters and alcohols, respectively. However, no biomass-derived products were detected in the bio-oils from birch and sugarcane bagasse liquefaction under basic conditions. On the other hand, aromatic products formed the most significant percentage of the bio-oil from switchgrass under both neutral and basic conditions. In EtOH distillates, ester and ether derivatives dominate under neutral condition, while ester, alcohol, aldehyde, and ether derivatives dominate under basic condition.

Table 4.4: Main compounds identified and their contents in bio-oils generated from pine sawdust liquefaction of run 4.5.

| Ret.Time (min) | Area% | Similarity | Compound name |
|---|---|---|---|
| 2.075 | 19.0478 | 96 | n-Hexane |
| 2.457 | 21.428571 | 84 | Cyclohexane |
| 3.421 | 9.5238095 | 95 | Butan-1-ol |
| 4.517 | 11.904762 | 94 | 2-Methyl-pentan-1-ol |
| 4.895 | 21.428571 | 96 | Hexan-1-ol |
| 5.694 | 9.5238095 | 96 | 2-Ethyl-hexan-1-ol |
| 6.193 | 7.1428571 | 93 | Octan-1-ol |

Table 4.5: Main compounds identified and their contents in bio-oils generated from pine sawdust liquefaction of run 4.6.

| Ret.Time (min) | Area% | Similarity | Compound name |
|---|---|---|---|
| 2.765 | 2.36693433 | 93 | Acetic acid |
| 3.436 | 35.4764233 | 98 | Butan-1-ol |
| 4.532 | 14.241641 | 96 | 2-Methyl-pentan-1-ol |
| 4.91 | 34.1132044 | 97 | Hexan-1-ol |
| 5.709 | 7.28630302 | 96 | 2-Ethyl-hexan-1-ol |
| 6.204 | 6.51549395 | 95 | Octan-1-ol |

Table 4.6: Main compounds identified and their contents in bio-oils generated from pine sawdust liquefaction of run 4.7.

| Ret.Time (min) | Area% | Similarity | Compound name |
|---|---|---|---|
| 3.436 | 32.4274857 | 98 | Butan-1-ol |
| 4.532 | 16.4882412 | 97 | 2-Methyl-pentan-1-ol |
| 4.91 | 30.8708735 | 97 | Hexan-1-ol |
| 5.709 | 9.0785633 | 97 | 2-Ethyl-hexan-1-ol |
| 5.984 | 2.47292575 | 82 | 8-Bromo-1-octanol |
| 6.204 | 5.46119939 | 97 | Octan-1-ol |
| 6.849 | 1.42459992 | 84 | 2-Butyl-octan-1-ol |
| 7.341 | 1.32422225 | 94 | Decan-1-ol |

Table 4.7: Main compounds identified and their contents in bio-oils generated from pine sawdust liquefaction of run 4.8.

| Ret.Time (min) | Area% | Similarity | Compound name |
|---|---|---|---|
| 3.439 | 25.14771 | 98 | Butan-1-ol |
| 4.534 | 15.05095 | 97 | 2-Methyl-pentan-1-ol |
| 4.911 | 26.5238 | 97 | Hexan-1-ol |
| 5.709 | 10.99963 | 97 | 2-Ethyl-hexan-1-ol |
| 5.986 | 2.237727 | 74 | 2-Propylpentanol |
| 6.206 | 6.433052 | 97 | Octan-1-ol |
| 6.851 | 2.325473 | 84 | 2-Butyloctanol |
| 7.343 | 1.857978 | 93 | Decan-1-ol |

Table 4.8: Main compounds identified and their contents in bio-oils generated from pine sawdust liquefaction of run 4.11.

| Ret.Time (min) | Area% | Similarity | Compound name |
|---|---|---|---|
| 3.438 | 26.6519111 | 97 | Butan-1-ol |
| 4.192 | 1.59186721 | 86 | Pentan-1-ol |
| 4.257 | 1.28785088 | 86 | Butane, 1,1-diethoxy- |
| 4.534 | 4.9128449 | 95 | 2-Methyl-pentan-1-ol |
| 4.775 | 2.10891997 | 74 | 2,4-Pentanediol, 3-methyl- |
| 4.911 | 30.6626206 | 97 | Hexan-1-ol |

| | | | |
|---|---|---|---|
| 5.232 | 1.10715662 | 53 | Cyclopropane, 1-methylene-2-(4,4-diethoxybutyl)- |
| 5.346 | 1.94861533 | 88 | (Tetrahydro-furan-2-yl)-methanol |
| 5.449 | 1.59482019 | 75 | 2,2-Dimethylglutaric anhydride |
| 5.495 | 1.62814668 | 73 | 2-Hydroxybutanoic acid |
| 5.58 | 3.98272647 | 63 | 4-Methylvleric acid |
| 5.622 | 1.34402781 | 82 | Hexane, 1,1-diethoxy- |
| 5.669 | 1.00541942 | 76 | Phenol, 2-methoxy- |
| 5.709 | 2.24960838 | 90 | 2-Ethyl-hexan-1-ol |
| 5.767 | 1.29881909 | 52 | 1-(1-Ethoxy-ethoxy)-hexane |
| 5.854 | 1.07249426 | 69 | 4-Methyl-3-heptanol |
| 6.094 | 1.34297317 | 58 | 1,2,4-Cyclopentanetriol |
| 6.207 | 4.11462625 | 94 | Octan-1-ol |
| 7.92 | 2.54272681 | 69 | 3-Hydroxy-propionic acid 4-hydroxy-3-methoxy-benzyl ester |
| 10.618 | 3.08368464 | 70 | Methyl dehydroabietate |

Table 4.9: Main compounds identified and their contents in EtOH distillate generated from pine sawdust liquefaction of run 4.5.

| Ret.Time (min) | Area% | Similarity | Compound name |
|---|---|---|---|
| 1.573 | 19.1489362 | 99 | Acetaldehyde |
| 2.75 | 17.0212766 | 96 | Propanoic acid, ethyl ester |

| | | | |
|---|---|---|---|
| 2.878 | 42.5531915 | 97 | Ethane, 1,1-diethoxy- |
| 3.45 | 6.38297872 | 94 | Butanoic acid, ethyl ester |
| 3.56 | 4.25531915 | 72 | 5-Methoxymethoxyhexa-2,3-diene |
| 3.637 | 6.38297872 | 91 | 2-Ethoxytetrahydrofuran |
| 4.242 | 2.12765957 | 82 | Propane, 1,1-diethoxy-2-methyl- |

Table 4.10: Main compounds identified and their contents in EtOH distillate generated from pine sawdust liquefaction of run 4.6.

| Ret.Time (min) | Area% | Similarity | Compound name |
|---|---|---|---|
| 1.569 | 2.50896 | 98 | Acetaldehyde |
| 1.94 | 2.15054 | 82 | 1-Propanol, 2-methyl- |
| 2.075 | 6.09319 | 97 | n-Hexane |
| 2.435 | 61.2903 | 97 | 1-Butanol |
| 2.592 | 0.71685 | 91 | 2-Pentanone |
| 2.882 | 5.37634 | 97 | Ethane, 1,1-diethoxy- |
| 3.164 | 11.1111 | 98 | Butanal, 2-ethyl- |
| 3.458 | 4.6595 | 87 | Hexanal |
| 3.795 | 1.43369 | 92 | 1-Pentanol, 2-methyl- |
| 4.242 | 1.79211 | 90 | Butane, 1,1-diethoxy- |
| 4.686 | 2.86738 | 94 | Hexanal, 2-ethyl- |

Table 4.11: Main compounds identified and their contents in EtOH distillate generated from pine sawdust liquefaction of run 4.7.

| Ret.Time (min) | Area% | Similarity | Compound name |
|---|---|---|---|
| 2.438 | 70.5608 | 97 | 1-Butanol |
| 2.589 | 1.8445 | 97 | 2-Pentanone |
| 2.75 | 2.08725 | 98 | Propanoic acid, ethyl ester |
| 2.882 | 1.48547 | 96 | Ethane, 1,1-diethoxy- |
| 3.161 | 5.70589 | 98 | Butanal, 2-ethyl- |
| 3.329 | 2.57365 | 98 | 3-Hexanone |
| 3.45 | 4.79901 | 94 | Butanoic acid, ethyl ester |
| 3.791 | 2.3302 | 94 | 2-Methylpentanol |
| 4.037 | 2.43316 | 93 | Butanoic acid ethenyl ester |
| 4.242 | 1.5932 | 89 | Pentanoic acid, ethyl ester |
| 4.682 | 2.44166 | 96 | Hexanal, 2-ethyl- |

Table 4.12: Main compounds identified and their contents in EtOH distillate generated from pine sawdust liquefaction of run 4.8.

| Ret.Time (min) | Area% | Similarity | Compound name |
|---|---|---|---|
| 1.94 | 1.293171 | 91 | Butane, 2,3-dimethyl- |
| 2.003 | 1.579557 | 97 | Pentane, 3-methyl- |
| 2.074 | 10.71269 | 97 | n-Hexane |
| 2.438 | 59.7499 | 97 | 1-Butanol |
| 2.88 | 2.086584 | 96 | Ethane, 1,1-diethoxy- |
| 3.162 | 8.593411 | 98 | Butanal, 2-ethyl- |

| | | | |
|---|---|---|---|
| 3.456 | 3.63379 | 89 | Hexanal |
| 3.793 | 3.529103 | 96 | 1-Butanol, 2-ethyl- |
| 4.011 | 2.389386 | 97 | 1-Hexanol |
| 4.242 | 1.146074 | 88 | Butane, 1,1-diethoxy- |
| 4.683 | 3.470834 | 97 | Hexanal, 2-ethyl- |

Table 4.13: Main compounds identified and their contents in EtOH distillate generated from pine sawdust liquefaction of run 4.11.

| Ret.Time (min) | Area% | Similarity | Compound name |
|---|---|---|---|
| 1.569 | 3.026114 | 98 | Acetaldehyde |
| 2.075 | 2.106826 | 97 | n-Hexane |
| 2.438 | 52.03898 | 97 | 1-Butanol |
| 2.75 | 1.363759 | 97 | Propanoic acid, ethyl ester |
| 2.878 | 23.18016 | 97 | Ethane, 1,1-diethoxy- |
| 3.164 | 2.3415 | 98 | Butanal, 2-ethyl- |
| 3.454 | 3.825454 | 83 | Butanoic acid, ethyl ester |
| 3.557 | 0.65386 | 85 | Levulic acid |
| 3.619 | 1.169159 | 82 | 2-Butenal, 2-ethyl- |
| 4.239 | 6.65218 | 94 | Butane, 1,1-diethoxy- |
| 4.338 | 1.635204 | 93 | Butane, 1-(1-ethoxyethoxy)- |

Table 4.14: Main compounds identified and their contents in bio-oils generated from corn stover liquefaction of run 4.14.

| Ret.Time (min) | Area% | Similarity | Compound name |
|---|---|---|---|
| 3.418 | 1.0762 | 95 | 1-Butanol |
| 4.515 | 2.0754 | 96 | 3-Methylpentanol |
| 4.78 | 4.85463 | 93 | 2-Propylpentanol |
| 4.893 | 6.14245 | 97 | 1-Hexanol |
| 5.477 | 1.00953 | 83 | Hexanoic acid |
| 5.689 | 2.69891 | 97 | 1-Hexanol, 2-ethyl- |
| 5.84 | 1.40932 | 83 | 2-Hydroxy-2-methyl-1-phenylpropan-1-one |
| 6.186 | 2.13246 | 96 | Octane-1-ol |
| 6.322 | 1.01965 | 84 | 2,4-Dimethyl-3-pentanol |
| 7.279 | 3.04629 | 87 | Propanoic acid, 2-methyl-, 2,2-dimethyl-1-(2-hydroxy-1-methylethyl)propyl ester |
| 7.392 | 3.1571 | 93 | Propanoic acid, 2-methyl-, 3-hydroxy-2,4,4-trimethylpentyl ester |
| 7.58 | 1.14205 | 87 | Heneicosane |
| 7.899 | 3.67883 | 88 | Hexadecane, 1,16-dichloro- |
| 7.979 | 3.87067 | 72 | Oxalic acid, 2-ethylhexyl isohexyl ester |
| 8.499 | 50.9332 | 79 | Phthalic acid, monoethyl ester |
| 8.672 | 1.5316 | 77 | Eicosane |

Table 4.15: Main compounds identified and their contents in bio-oils generated from corn stover liquefaction of run 4.15.

| Ret.Time (min) | Area% | Similarity | Compound name |
|---|---|---|---|
| 2.749 | 2.82043 | 93 | Acetic acid |
| 3.422 | 5.86564 | 95 | Butan-1-ol |
| 4.099 | 1.90143 | 86 | Isobutyric acid |
| 4.518 | 4.84487 | 95 | 2-Methyl-pentan-1-ol |
| 4.789 | 1.71413 | 62 | 3-Methyl-2-buten-1-ol |
| 4.895 | 14.08 | 96 | Hexan-1-ol |
| 4.95 | 1.30977 | 55 | 2-Ethyl-butane-1,3-diol |
| 5.023 | 1.39451 | 61 | cis-2-Hexen-1-ol |
| 5.313 | 2.0428 | 77 | 2-Hydroxy-2-methyl-1-phenyl-propan-1-one |
| 5.384 | 1.13614 | 74 | Phenol |
| 5.483 | 2.16761 | 75 | Octan-3-ol |
| 5.694 | 6.51174 | 94 | 2-Propyl-1-pentanol |
| 5.755 | 1.98961 | 76 | 2-Hydroxybutanoic acid |
| 5.846 | 6.53463 | 81 | 2-Hydroxy-2-methyl-1-phenyl-propan-1-one |
| 5.969 | 3.67421 | 64 | 2-Ethyl-hexan-1-ol |
| 6.087 | 3.90001 | 76 | 2-Hydroxypentanoic acid |
| 6.192 | 5.22072 | 92 | Octan-1-ol |
| 6.257 | 1.54643 | 59 | 2-Hydroxy-3-methyl-butyric acid |
| 6.328 | 2.72974 | 84 | 3-Methyl-3-pentanol |
| 6.505 | 2.39748 | 61 | 4-Phenoxy-butan-1-ol |

| | | | |
|---|---|---|---|
| 6.585 | 2.59603 | 81 | 3-Ethylphenol |
| 6.674 | 1.55018 | 62 | 4-Methyl-hexane-1,5-diol |
| 6.835 | 1.45809 | 71 | 3-Methyl-pentan-1-ol |
| 6.861 | 1.58134 | 69 | Octan-4-ol |
| 7.041 | 1.54104 | 50 | 2-Hydroxyoctadecanoic acid methyl ester |
| 7.099 | 1.27321 | 54 | beta.-D-Mannofuranoside, 1-O-(10-undecenyl)- |
| 7.291 | 1.25517 | 65 | Benzene |
| 7.345 | 1.72209 | 60 | Undecan-6-ol |
| 7.38 | 1.47856 | 65 | 2-Ketoisohexanoic acid |
| 7.466 | 1.20971 | 69 | 4-Hydroxy-3-methoxy-benzaldehyde |

Table 4.16: Main compounds identified and their contents in bio-oils generated from corn stover liquefaction of run 4.16.

| **Ret.Time (min)** | **Area%** | **Similarity** | **Compound name** |
|---|---|---|---|
| 2.749 | 2.13988 | 82 | Acetic acid |
| 3.423 | 3.00396 | 85 | Butan-1-ol |
| 4.519 | 4.82004 | 90 | 2-Methyl-pentan-1-ol |
| 4.843 | 1.68968 | 71 | Malonic acid |
| 4.897 | 14.3717 | 94 | Hexan-1-ol |
| 5.251 | 2.35276 | 64 | Pentane-1,2,4-triol |
| 5.384 | 2.09296 | 59 | Phenol |

| | | | |
|---|---|---|---|
| 5.484 | 1.7233 | 73 | 2-Hydroxy-butyric acid |
| 5.695 | 10.0845 | 92 | 2-Propyl-1-pentanol |
| 5.756 | 3.64294 | 76 | 1,3-Pentanediol |
| 6.088 | 3.07768 | 75 | 2-Hydroxypentanoic acid |
| 6.193 | 8.18628 | 91 | Octan-1-ol |
| 6.232 | 2.3274 | 72 | 2-Methylpentane-1,3-diol |
| 6.329 | 4.00306 | 77 | Octan-4-ol |
| 6.505 | 3.94535 | 55 | 7-Oxo-octanoic acid |
| 6.602 | 5.38135 | 62 | 2-Phenyl-ethanol |
| 6.835 | 1.82327 | 65 | 2-Ethyl-decan-1-ol |
| 6.864 | 1.60518 | 64 | Dodecan-4-ol |
| 6.952 | 2.81608 | 62 | Decane-1,7-diol |
| 7.295 | 2.03884 | 65 | 62% 2-Isopropyl-5-methyl-phenol |
| 7.38 | 3.52212 | 57 | 2-Ketoisohexanoic acid |
| 7.468 | 2.35347 | 72 | 4-Hydroxy-3-methoxy-benzaldehyde |
| 8.35 | 1.67332 | 57 | 2-tert-Butyl-6-methylphenol |

Table 4.17: Main compounds identified and their contents in bio-oils generated from corn stover liquefaction of run 4.18.

| **Ret.Time (min)** | **Area%** | **Similarity** | **Compound name** |
|---|---|---|---|
| 2.458 | 24.9314 | 72 | Formic acid, hexyl ester |
| 4.957 | 21.0354 | 86 | 3-Hydroxy-2-butanone |

| | | | |
|---|---|---|---|
| 4.99 | 7.60702 | 86 | Hydroxy-acetic acid ethyl ester |
| 5.333 | 2.50143 | 72 | Hexan-2-ol |
| 5.385 | 1.42117 | 84 | Phenol |
| 5.45 | 18.6623 | 84 | 2-Hydroxy-2-methyl-1-phenyl-propan-1-one |
| 5.566 | 1.30358 | 57 | 2-Hydroxy-succinic acid diethyl ester |
| 5.964 | 6.70675 | 83 | 2,4-Dimethyl-3-pentanol |
| 6.507 | 2.71854 | 62 | 2-Methoxyphenol |
| 6.585 | 4.23126 | 82 | 3-Ethylphenol |
| 6.823 | 1.2751 | 65 | 3-Oxo-1-cyclohexene-1-carboxylic acid |
| 6.901 | 1.25127 | 46 | 4-Methylmannitol |
| 6.94 | 1.56614 | 66 | 3-Oxo-1-cyclohexene-1-carboxylic acid |
| 7.315 | 2.0509 | 63 | 3,4-Methoxyphenol |
| 7.466 | 1.18111 | 60 | 4-Hydroxy-3-methoxy-benzaldehyde |
| 7.91 | 1.55671 | 58 | (4-Hydroxy-3-methoxy-phenyl)-acetic acid methyl ester |

Table 4.18: Main compounds identified and their contents in bio-oils generated from birch liquefaction under a neutral condition.

| Ret.Time (min) | Area% | Similarity | Compound name |
|---|---|---|---|
| 3.831 | 4.878049 | 98 | Propanoic acid, 2-hydroxy-, ethyl ester, (S)- |
| 4.406 | 8.536585 | 97 | Butanoic acid, 2-hydroxy-, ethyl ester |

| | | | |
|---|---|---|---|
| 4.978 | 6.097561 | 90 | Furan-2-yl-methanol |
| 5.009 | 7.317073 | 95 | Hydroxy-acetic acid ethyl ester |
| 5.559 | 6.097561 | 92 | Butanoic acid, anhydride |
| 6.352 | 2.439024 | 89 | Benzene-1,2-diol |
| 8.515 | 21.95122 | 95 | Diethyl Phthalate |
| 10.517 | 15.85366 | 95 | Hexadecanoic acid, ethyl ester |
| 11.799 | 18.29268 | 94 | 9,12-Octadecadienoic acid, ethyl ester |
| 11.853 | 4.878049 | 76 | Ethyl Oleate |

Table 4.19: Main compounds identified and their contents in bio-oils generated from sugarcane bagasse liquefaction under a neutral condition.

| Ret.Time (min) | Area% | Similarity | Compound name |
|---|---|---|---|
| 4.714 | 3.96825 | 83 | 2-Oxo-butyric acid |
| 4.953 | 14.2857 | 81 | Propane-1,2-diol |
| 4.988 | 5.55556 | 96 | Hydroxy-acetic acid ethyl ester |
| 5.298 | 4.76191 | 81 | 2,3-Dimethyl-pentan-3-ol |
| 5.329 | 11.9048 | 93 | (Tetrahydro-furan-2-yl)-methanol |
| 5.449 | 13.4921 | 86 | 2-Methyl-pentan-3-ol |
| 5.478 | 4.76191 | 90 | Butane-1,2-diol |
| 5.839 | 3.1746 | 76 | 4-Methyl-2-oxo-pentanoic acid |
| 5.962 | 7.14286 | 84 | 2,4-Dimethyl-pentan-3-ol |
| 6.581 | 14.2857 | 91 | 3-Ethyl-phenol |

| | | | |
|---|---|---|---|
| 7.314 | 3.96825 | 79 | 3,3,5,5-Tetramethyl-cyclohex-1-enol |
| 7.81 | 3.1746 | 77 | Pentane-1,2,5-triol |
| 8.643 | 4.76191 | 79 | (3-Hydroxy-4-methoxy-phenyl)-acetic acid methyl ester |
| 9.04 | 4.76191 | 86 | 4-Hydroxyphenylpropionic acid, ethyl ester |

Table 4.20: Main compounds identified and their contents in bio-oils generated from switchgrass liquefaction under a neutral condition.

| Ret.Time (min) | Area% | Similarity | Compound name |
|---|---|---|---|
| 1.579 | 11.25 | 79 | Ethyl formate |
| 4.324 | 2 | 95 | Butanoic acid, 2-hydroxy-, ethyl ester |
| 5.004 | 1.75 | 78 | Hydroxy-acetic acid ethyl ester |
| 5.533 | 12.5 | 96 | Nonanal |
| 5.565 | 3 | 90 | Butanoic acid, anhydride |
| 6.162 | 21.75 | 96 | Benzoic acid |
| 6.592 | 3.5 | 65 | 2-(4-tert-Butyl-phenoxy)-ethanol |
| 6.636 | 5 | 87 | Benzoylformic acid |
| 6.723 | 10 | 93 | Nonanoic acid |
| 7.906 | 5.25 | 90 | 1-Dodecanol |
| 8.512 | 8 | 80 | Diethyl Phthalate |
| 8.912 | 2.25 | 93 | 1-Hexadecanol |

| | | | |
|---|---|---|---|
| 10.121 | 3.25 | 84 | 7,9-Di-tert-butyl-1-oxaspiro(4,5)deca-6,9-diene-2,8-dione |
| 10.327 | 6.5 | 89 | Pentadecanoic acid |
| 10.828 | 1.75 | 94 | Hexadecanoic acid |
| 11.782 | 2.25 | 84 | Octadecanoic acid |

Table 4.21: Main compounds identified and their contents in bio-oils generated from sugarcane bagasse liquefaction under a basic condition.

| Ret.Time (min) | Area% | Similarity | Compound name |
|---|---|---|---|
| 3.417 | 15 | 91 | Butan-1-ol |
| 4.892 | 45 | 94 | Hexan-1-ol |
| 6.188 | 20 | 93 | Octan-1-ol |
| 6.326 | 20 | 78 | 2,4-Dimethyl-pentan-3-ol |

Table 4.22: Main compounds identified and their contents in bio-oils generated from switchgrass liquefaction under a basic condition.

| Ret.Time (min) | Area% | Similarity | Compound name |
|---|---|---|---|
| 3.417 | 12.94719 | 93 | Butan-1-ol |
| 4.892 | 15.3322 | 91 | Hexan-1-ol |
| 4.952 | 6.984668 | 59 | 7-Hydroxy-octanoic acid |
| 5.381 | 9.199319 | 94 | Phenol |

| | | | |
|---|---|---|---|
| 5.808 | 4.940375 | 72 | 2-Hydroxy-butyric acid |
| 6.001 | 15.50256 | 76 | (Tetrahydro-furan-2-yl)-methanol |
| 6.256 | 4.940375 | 77 | 2-Hydroxy-pentanoic acid |
| 6.505 | 17.54685 | 84 | 2-Methoxy-phenol |
| 7.465 | 7.836457 | 75 | 4-Hydroxy-3-methoxy-benzaldehyde |
| 7.988 | 4.770017 | 53 | 5-tert-Butyl-isophthalic acid |

Table 4.23: Main compounds identified and their contents in EtOH distillate generated from birch liquefaction under a neutral condition.

| Ret.Time (min) | Area% | Similarity | Compound name |
|---|---|---|---|
| 2.141 | 43.65994 | 97 | Ethyl Acetate |
| 2.237 | 15.27378 | 93 | Tetrahydrofuran |
| 2.75 | 4.178674 | 96 | Propanoic acid, ethyl ester |
| 2.878 | 20.60519 | 94 | Ethane, 1,1-diethoxy- |
| 3.296 | 1.152738 | 97 | Acetic acid, hydroxy-, ethyl ester |
| 3.557 | 4.178674 | 89 | Propanoic acid, 2-hydroxy-, ethyl ester, (S)- |
| 3.637 | 4.322767 | 96 | 2-Ethoxytetrahydrofuran |
| 4.297 | 2.017291 | 97 | Butanoic acid, 2-hydroxy-, ethyl ester |

Table 4.24: Main compounds identified and their contents in EtOH distillate generated from sugarcane bagasse liquefaction under a neutral condition.

| Ret.Time (min) | Area% | Similarity | Compound name |
|---|---|---|---|
| 1.562 | 4.364326 | 92 | Acetaldehyde |
| 2.061 | 1.42315 | 90 | Butanal |
| 2.141 | 19.11765 | 98 | Ethyl Acetate |
| 2.237 | 2.182163 | 96 | Tetrahydrofuran |
| 2.394 | 7.495256 | 85 | 2-Propanol, 1-methoxy- |
| 2.46 | 4.222011 | 87 | 1-Butanol |
| 2.757 | 4.222011 | 85 | 3-Hydroxy-butan-2-one |
| 2.878 | 32.25806 | 95 | Ethane, 1,1-diethoxy- |
| 3.201 | 1.185958 | 84 | Diethyl carbonate |
| 3.293 | 1.660342 | 97 | Acetic acid, hydroxy-, ethyl ester |
| 3.465 | 2.182163 | 90 | 1,2-Butanediol |
| 3.553 | 5.502846 | 96 | Propanoic acid, 2-hydroxy-, ethyl ester |
| 3.637 | 4.032258 | 96 | 2-Ethoxytetrahydrofuran |
| 4.239 | 3.98482 | 94 | Butane, 1,1-diethoxy- |
| 4.294 | 3.036053 | 96 | Butanoic acid, 2-hydroxy-, ethyl ester |
| 4.363 | 1.42315 | 80 | 2-Ethoxypentane |

Table 4.25: Main compounds identified and their contents in EtOH distillate generated from birch liquefaction under a basic condition.

| Ret.Time (min) | Area% | Similarity | Compound name |
|---|---|---|---|
| 2.061 | 2.414231 | 90 | Propanal, 2-methyl- |

| | | | |
|---|---|---|---|
| 2.141 | 45.23507 | 97 | Ethyl Acetate |
| 2.237 | 12.96061 | 96 | Tetrahydrofuran |
| 2.391 | 9.52986 | 84 | 2-Propanol, 1-methoxy- |
| 2.46 | 4.955527 | 95 | 1-Butanol |
| 2.662 | 1.143583 | 85 | 3-Pentanone |
| 2.746 | 6.226175 | 96 | Propanoic acid, ethyl ester |
| 2.878 | 5.209657 | 94 | Ethane, 1,1-diethoxy- |
| 2.966 | 1.905972 | 94 | 1H-Pyrrole, 1-methyl- |
| 3.084 | 1.016518 | 87 | Pyrrole |
| 3.45 | 2.668361 | 95 | Butanoic acid, ethyl ester |
| 3.557 | 1.143583 | 84 | 1H-Pyrrole, 1-ethyl- |
| 3.612 | 1.397713 | 96 | 2-Butenal, 2-ethyl- |
| 4.239 | 1.016518 | 83 | Propane, 1,1-diethoxy-2-methyl- |

Table 4.26: Main compounds identified and their contents in EtOH distillate generated from sugarcane bagasse liquefaction under a basic condition.

| Ret.Time (min) | Area% | Similarity | Compound name |
|---|---|---|---|
| 2.053 | 5.039096 | 95 | Butanal |
| 2.134 | 23.80539 | 97 | Ethyl Acetate |
| 2.233 | 1.650738 | 94 | Tetrahydrofuran |
| 2.372 | 1.650738 | 85 | 2-Propanol, 1-methoxy- |
| 2.442 | 21.4596 | 96 | 1-Butanol |

| | | | |
|---|---|---|---|
| 2.581 | 1.216334 | 91 | 2-Pentanone |
| 2.743 | 4.517811 | 96 | Propanoic acid, ethyl ester |
| 2.871 | 4.170287 | 94 | Ethane, 1,1-diethoxy- |
| 3.153 | 9.470026 | 98 | Butanal, 2-ethyl- |
| 3.45 | 8.166811 | 87 | Hexanal |
| 3.553 | 1.476977 | 80 | Acetic acid, butyl ester |
| 3.604 | 3.040834 | 97 | 2-Butenal, 2-ethyl- |
| 3.791 | 1.129453 | 94 | 1-Pentanol, 2-methyl- |
| 4.004 | 1.390096 | 95 | 1-Hexanol |
| 4.235 | 2.69331 | 88 | Butane, 1,1-diethoxy- |
| 4.679 | 3.735882 | 96 | Hexanal, 2-ethyl- |
| 4.979 | 1.476977 | 95 | Hexanoic acid, ethyl ester |
| 5.016 | 1.476977 | 90 | 2-Hexenal, 2-ethyl- |
| 5.071 | 2.432667 | 86 | 1,2,4-Trimethylcyclohexane |

Table 4.27: Main compounds identified and their contents in EtOH distillate generated from switchgrass liquefaction under a basic condition.

| Ret.Time (min) | Area% | Similarity | Compound name |
|---|---|---|---|
| 2.06 | 8.145447 | 94 | Butanal |
| 2.141 | 32.04023 | 96 | Ethyl Acetate |
| 2.24 | 1.713086 | 96 | Tetrahydrofuran |
| 2.39 | 3.370911 | 84 | 2-Propanol, 1-methoxy- |

| | | | |
|---|---|---|---|
| 2.46 | 17.61715 | 96 | 1-Butanol |
| 2.75 | 7.780725 | 96 | Propanoic acid, ethyl ester |
| 2.878 | 7.283378 | 94 | Ethane, 1,1-diethoxy- |
| 3.16 | 3.348806 | 98 | Butanal, 2-ethyl- |
| 3.45 | 7.581786 | 94 | Butanoic acid, ethyl ester |
| 3.556 | 1.934129 | 80 | 6-Methyl-2-heptyne |
| 3.611 | 3.426172 | 98 | 2-Butenal, 2-ethyl- |
| 4.238 | 2.696729 | 87 | Butane, 1,1-diethoxy- |
| 4.682 | 1.127321 | 90 | Hexanal, 2-ethyl- |
| 4.906 | 1.934129 | 84 | 1-Nonanol |

**4.4 Conclusions**

Liquefaction of different biomass using various catalytic systems was investigated. Among other catalysts applied, the synergistic effect of Ni metal-metal oxide in the presence/absence of NaOH showed a more substantial influence on biomass liquefaction. Based on pine liquefaction yield results, the catalytic power of metal oxides is ranked in the following order: $Fe_2O_3 > ZnO > V_2O_5 > TiO_2$. In corn stover, birch, sugarcane bagasse, and switchgrass liquefaction, higher bio-oil and lower SR were achieved under basic than neutral conditions. Based on the $^1$H-NMR analysis, lower abundances of aromatic, ester, ether, and alcohol were present in bio-oils generated under basic conditions compared to those obtained under neutral conditions. The distribution of bio-oil components is highly dependent on the type of biomass and catalysts used. However, no remarkable correlation can be concluded between the biomass composition and the yield and quality of bio-oil obtained. In liquefactions catalyzed by metal + metal

oxide + NaOH, Guerbet condensation is still the dominant reaction, and not much decline was seen for the repolymerized SR. To catalyze the ketonic decarboxylation reactions and reduce the alcohol condensation reactions, reducing reaction time and a weaker base such as KOAc are recommended. Thus, in future work, the influence study of KOAc combined with Ni metal and metal oxide are suggested for the liquefaction of corn stover for a shorter time at a higher temperature of 300°C.

## 4.5 Appendix

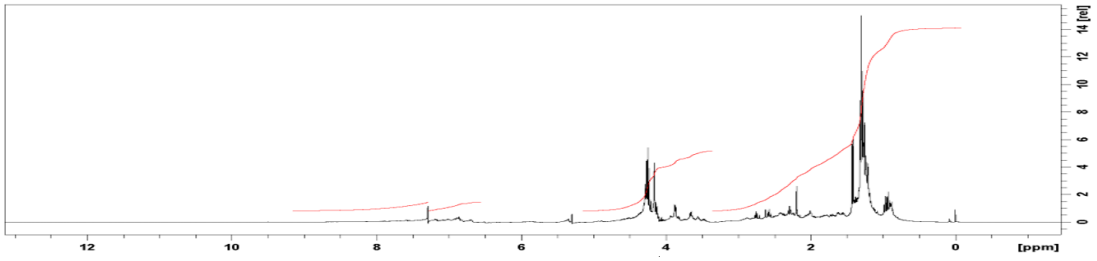


Figure S1: The proton NMR spectrum of bio-oil product of pine sawdust liquefaction of Run 4.1.

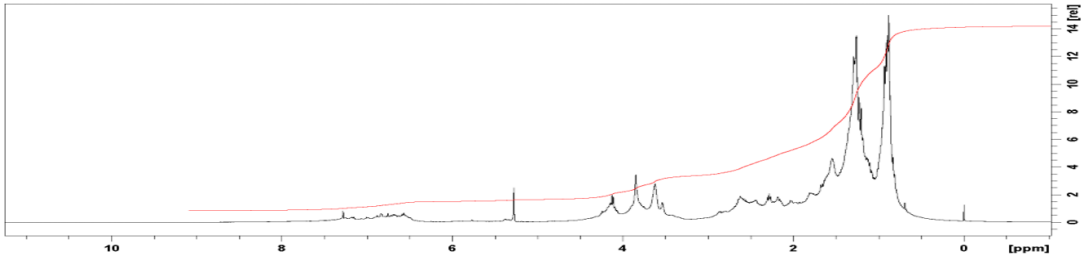


Figure S2: The proton NMR spectrum of bio-oil product of pine sawdust liquefaction of Run 4.2.

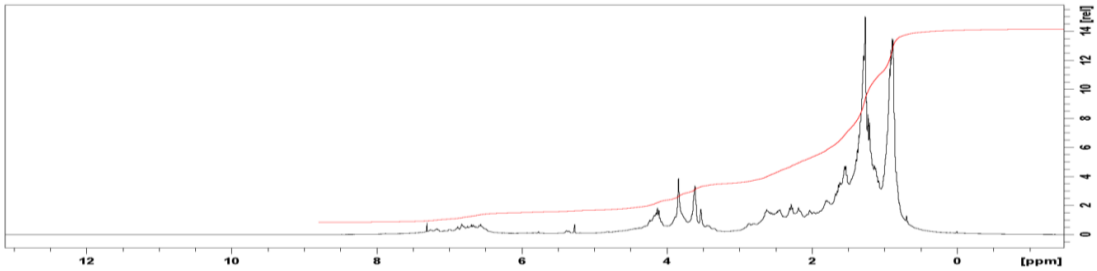


Figure S3: The proton NMR spectrum of bio-oil product of pine sawdust liquefaction of Run 4.3.

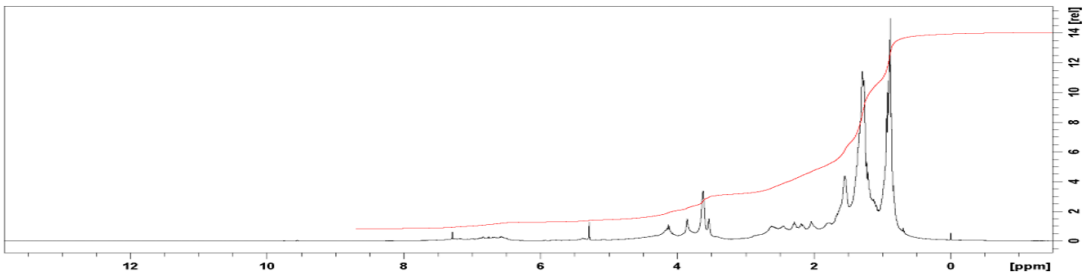


Figure S4: The proton NMR spectrum of bio-oil product of pine sawdust of Run 4.4.

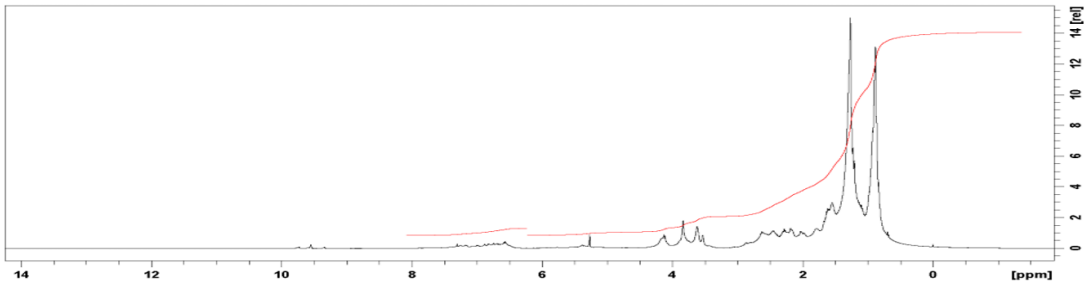


Figure S5: The proton NMR spectrum of bio-oil product of pine sawdust liquefaction of Run 4.5.

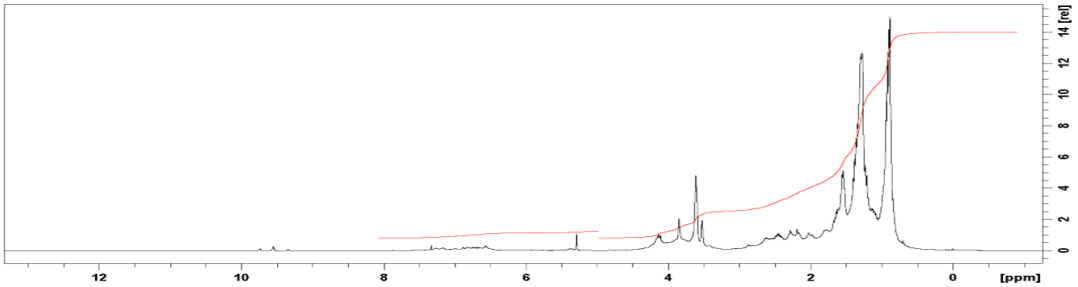


Figure S6: The proton NMR spectrum of bio-oil product of pine sawdust liquefaction of Run 4.6.

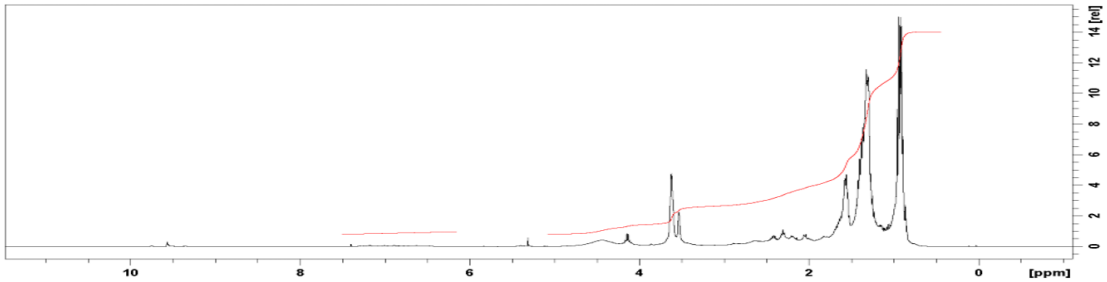


Figure S7: The proton NMR spectrum of bio-oil product of pine sawdust liquefaction of Run 4.7.

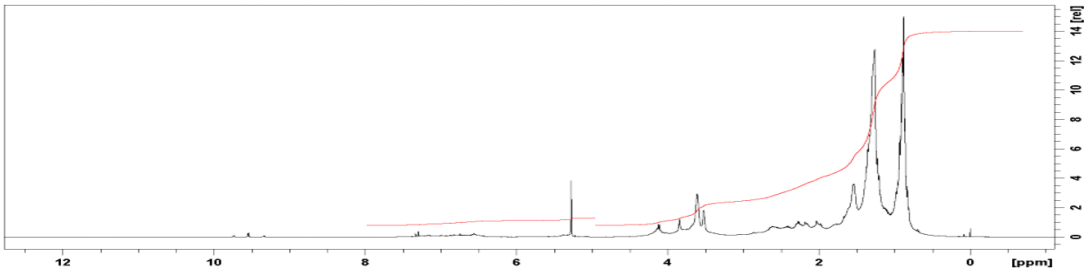


Figure S8: The proton NMR spectrum of bio-oil product of pine sawdust liquefaction of Run 4.8.

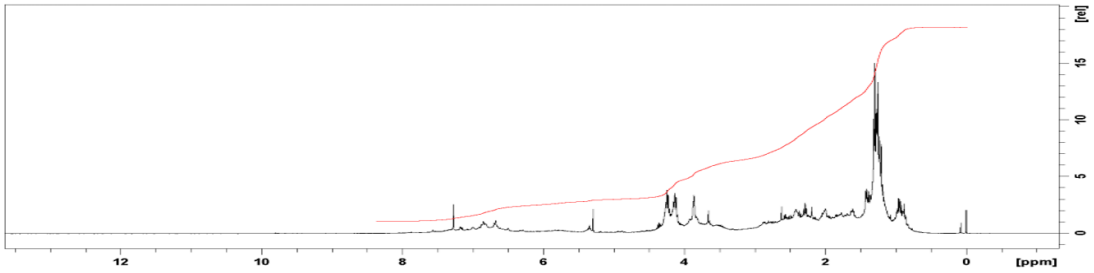


Figure S9: The proton NMR spectrum of bio-oil product of pine sawdust liquefaction of Run 4.9.

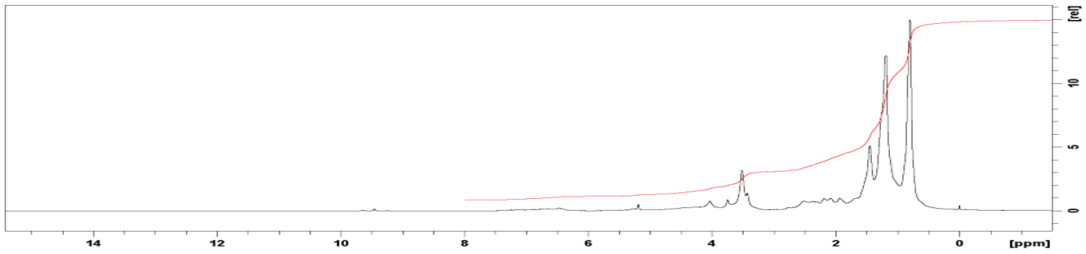


Figure S10: The proton NMR spectrum of bio-oil product of pine sawdust liquefaction of Run 4.10.

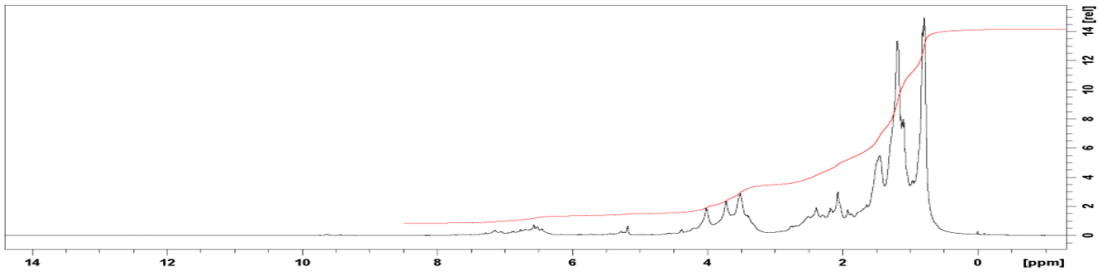


Figure S11: The proton NMR spectrum of bio-oil product of pine sawdust liquefaction of Run 4.11.

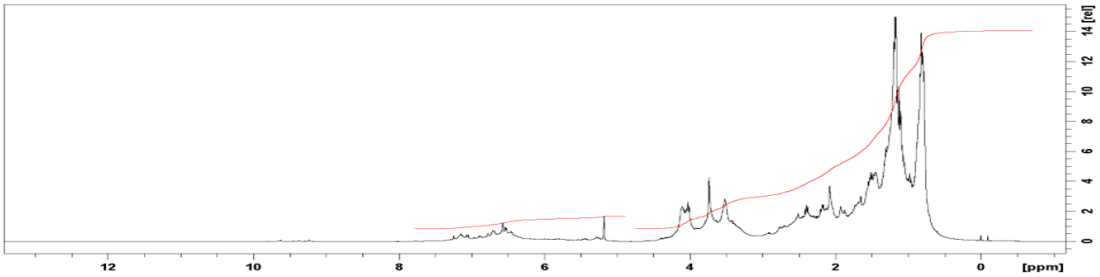


Figure S12: The proton NMR spectrum of bio-oil product of pine sawdust liquefaction of Run 4.12.

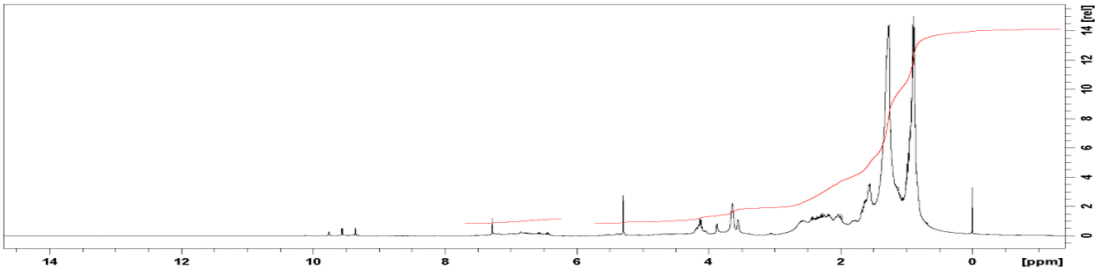


Figure S13: The proton NMR spectrum of bio-oil product of corn stover liquefaction of Run 4.13.

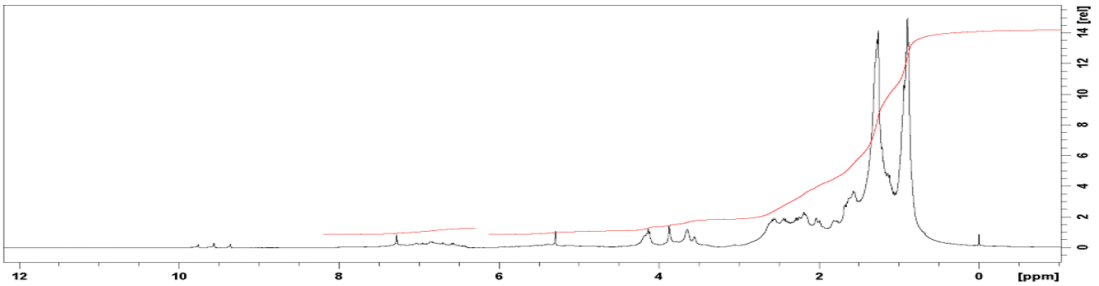


Figure S14: The proton NMR spectrum of bio-oil product of corn stover liquefaction of Run 4.14.

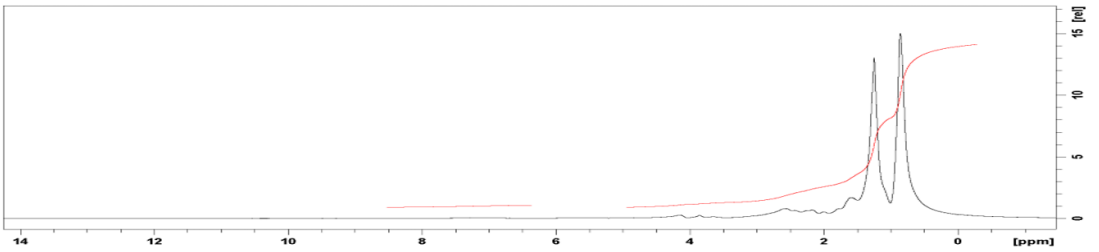


Figure S15: The proton NMR spectrum of bio-oil product of corn stover liquefaction of Run 4.15.

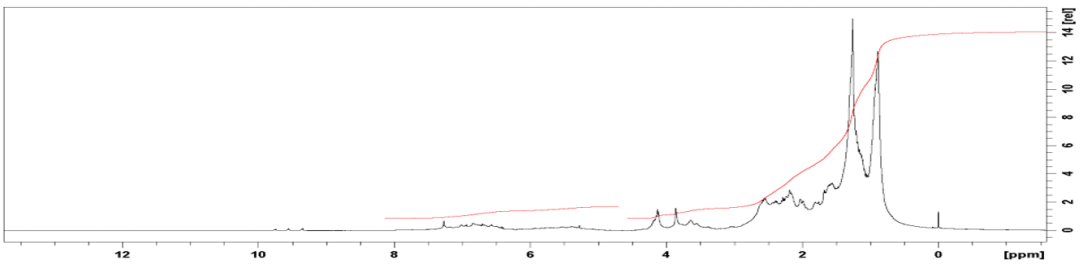


Figure S16: The proton NMR spectrum of bio-oil product of corn stover liquefaction of Run 4.16.

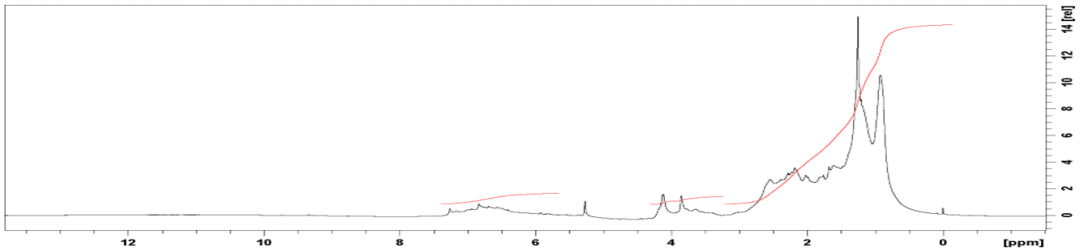


Figure S17: The proton NMR spectrum of bio-oil product of corn stover liquefaction of Run 4.17.

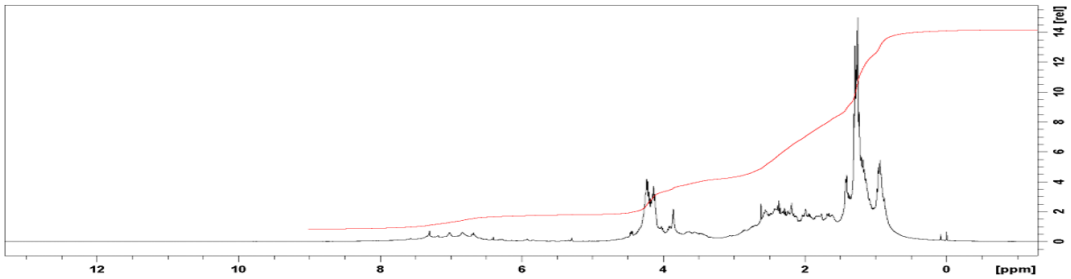


Figure S18: The proton NMR spectrum of bio-oil product of corn stover liquefaction of Run 4.18.

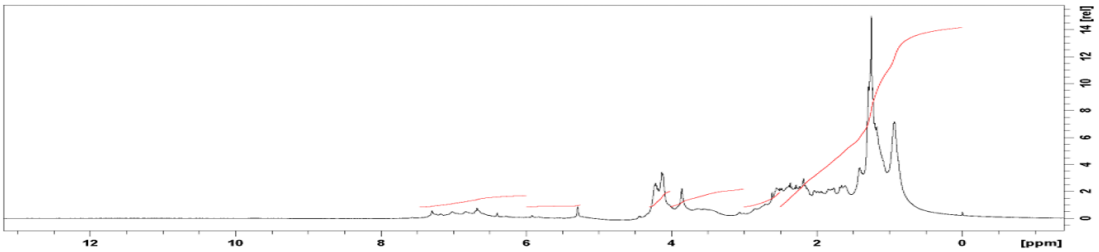


Figure S19: The proton NMR spectrum of bio-oil product of corn stover liquefaction of Run 4.19.

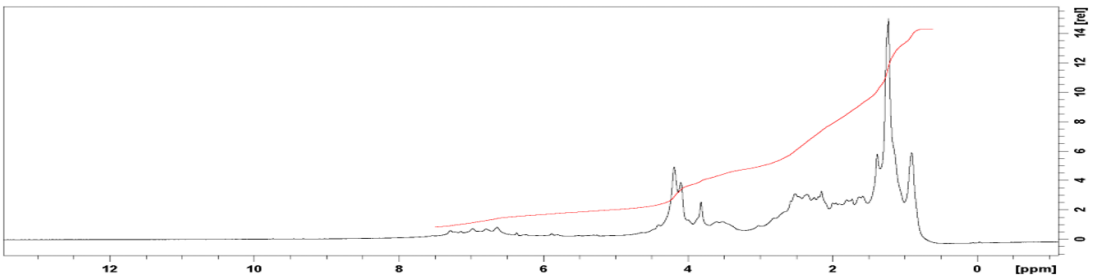


Figure S20: The proton NMR spectrum of bio-oil product of corn stover liquefaction of Run 4.20.

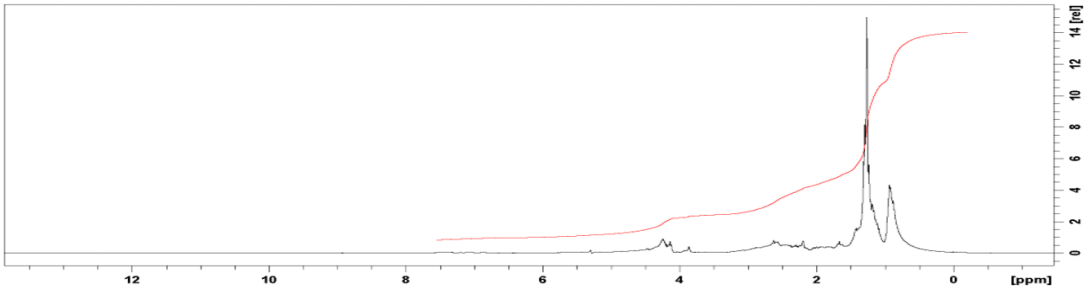


Figure S21: The proton NMR spectrum of bio-oil product of corn stover liquefaction of Run 4.21.

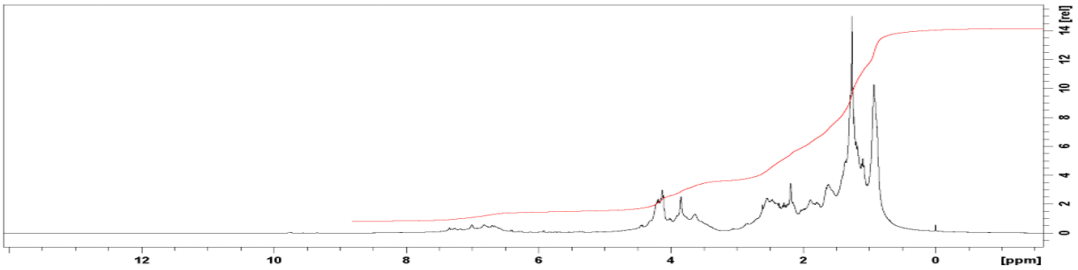


Figure S22: The proton NMR spectrum of bio-oil product of corn stover liquefaction of Run 4.22.

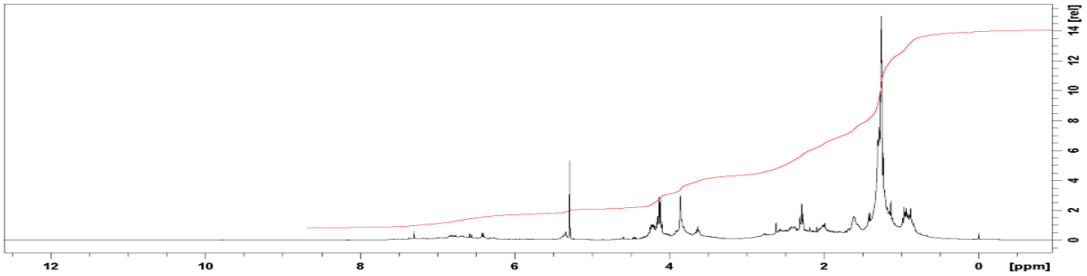


Figure S23: The proton NMR spectrum of bio-oil product of birch liquefaction under a neutral condition.

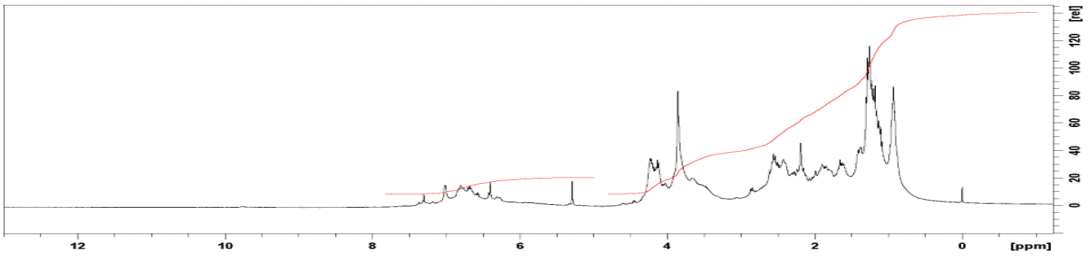


Figure S24: The proton NMR spectrum of bio-oil product of sugarcane bagasse liquefaction under a neutral condition.

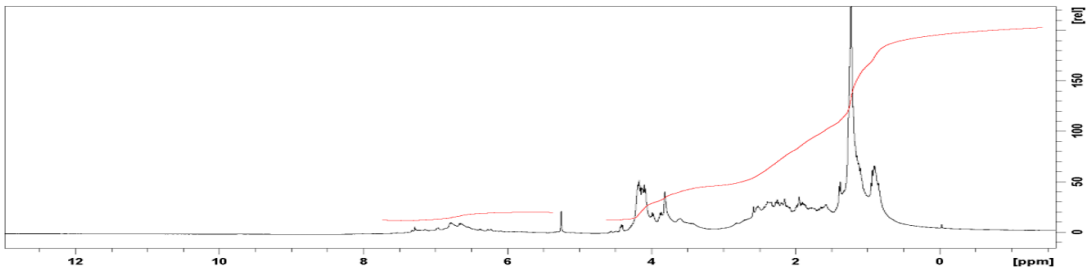


Figure S25: The proton NMR spectrum of bio-oil product of switchgrass liquefaction under a neutral condition.

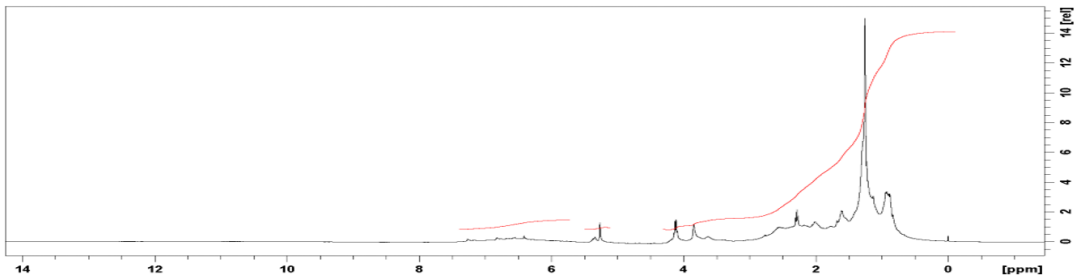


Figure S26: The proton NMR spectrum of bio-oil product of birch liquefaction under a basic condition.

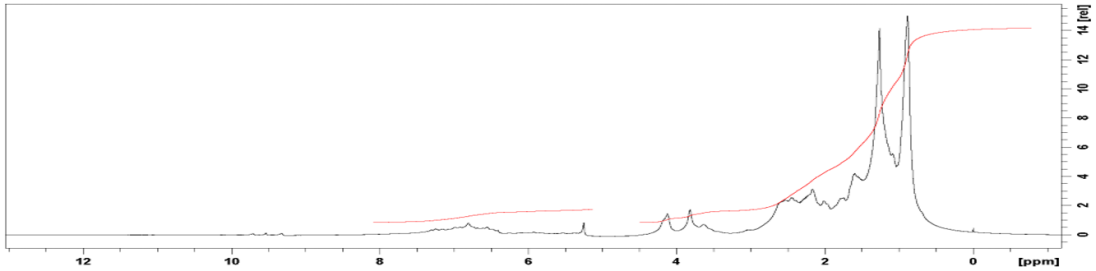


Figure S27: The proton NMR spectrum of bio-oil product of sugarcane bagasse liquefaction under a basic condition.

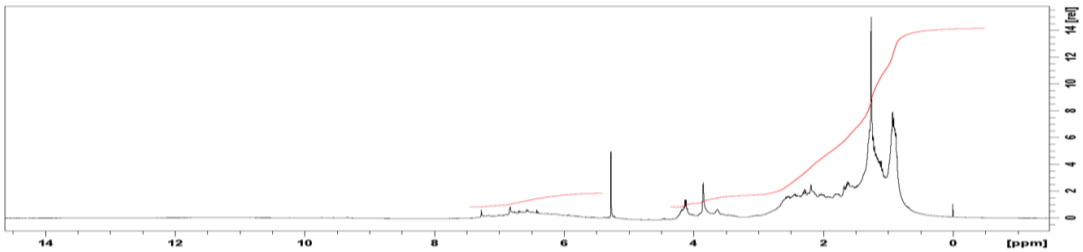


Figure S28: The proton NMR spectrum of bio-oil product of switchgrass liquefaction under a basic condition.

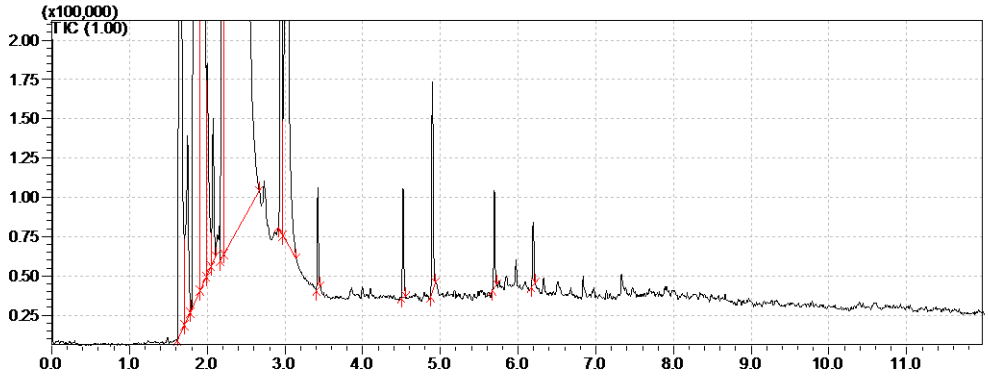


Figure S29: The GC-MS chromatogram of bio-oil product of pine sawdust liquefaction of Run 4.5.

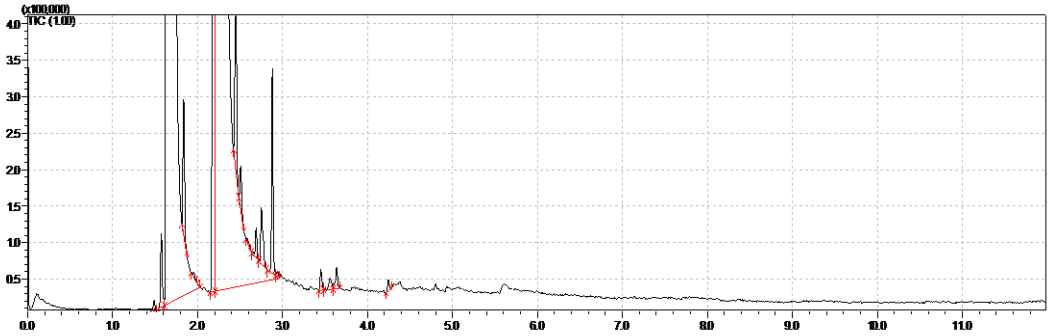

Figure S30: The GC-MS chromatogram of EtOH distillate product of pine sawdust liquefaction of Run 4.5.

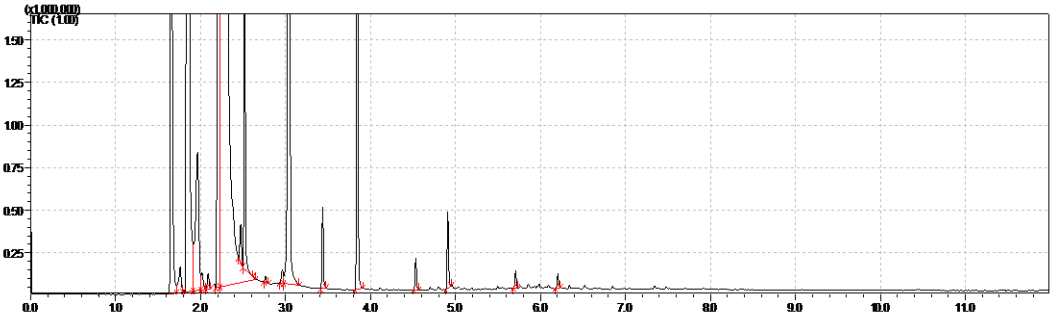

Figure S31: The GC-MS chromatogram of bio-oil product of pine sawdust liquefaction of Run 4.6.

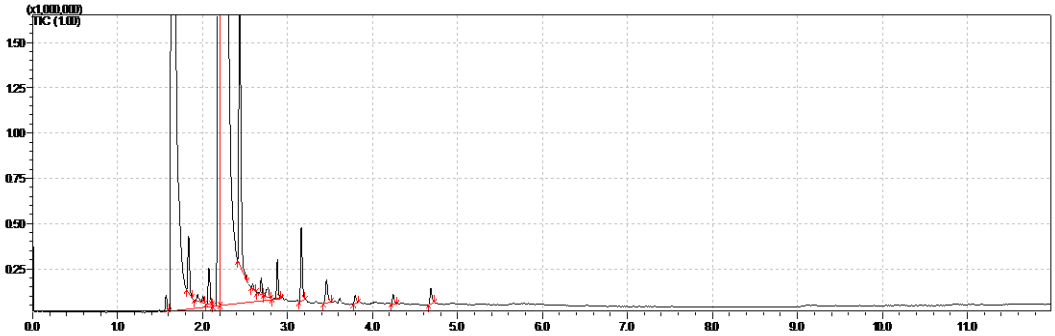


Figure S32: The GC-MS chromatogram of EtOH distillate product of pine sawdust liquefaction of Run 4.6.

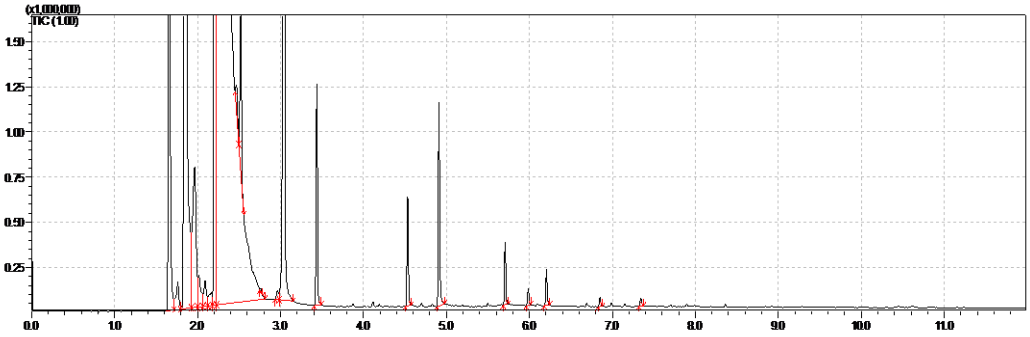


Figure S33: The GC-MS chromatogram of bio-oil product of pine sawdust liquefaction of Run 4.7.

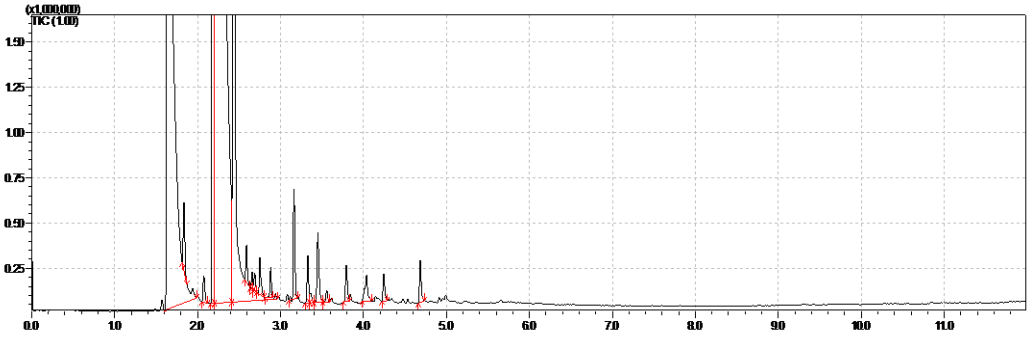


Figure S34: The GC-MS chromatogram of EtOH distillate product of pine sawdust liquefaction of Run 4.7.

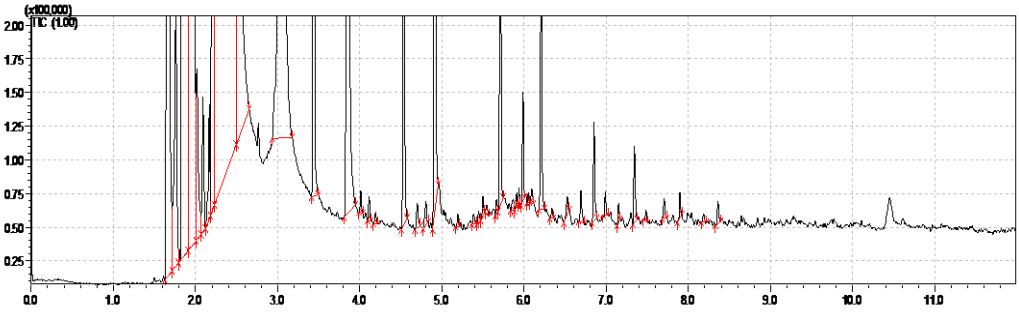


Figure S35: The GC-MS chromatogram of bio-oil product of pine sawdust liquefaction of Run 4.8.

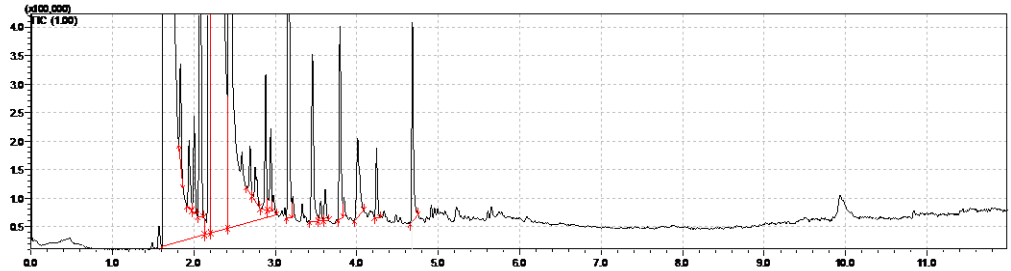


Figure S36: The GC-MS chromatogram of EtOH distillate product of pine sawdust liquefaction of Run 4.8.

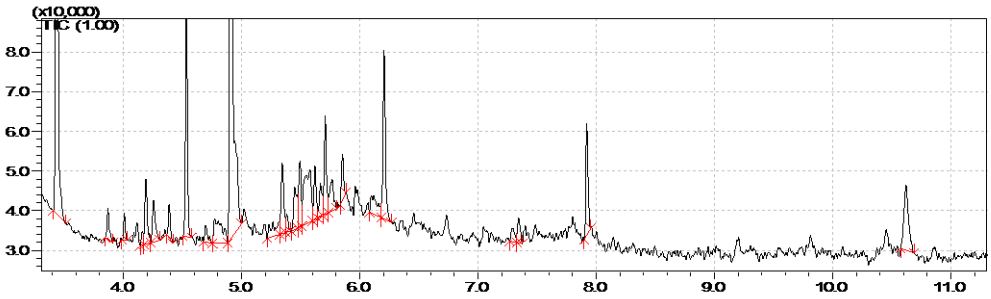


Figure S37: The GC-MS chromatogram of bio-oil product of pine sawdust liquefaction of Run 4.11.

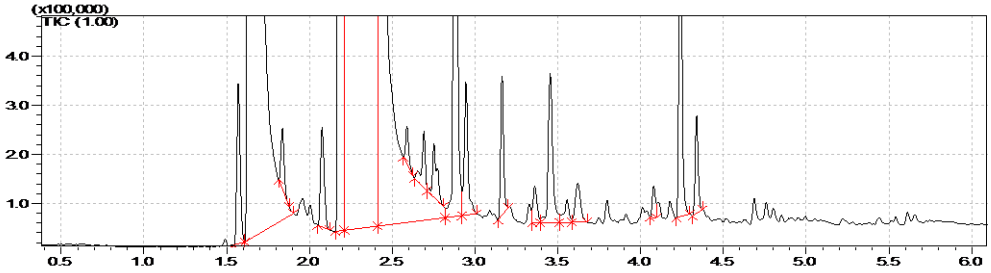


Figure S38: The GC-MS chromatogram of EtOH distillate product of pine sawdust liquefaction of Run 4.11.

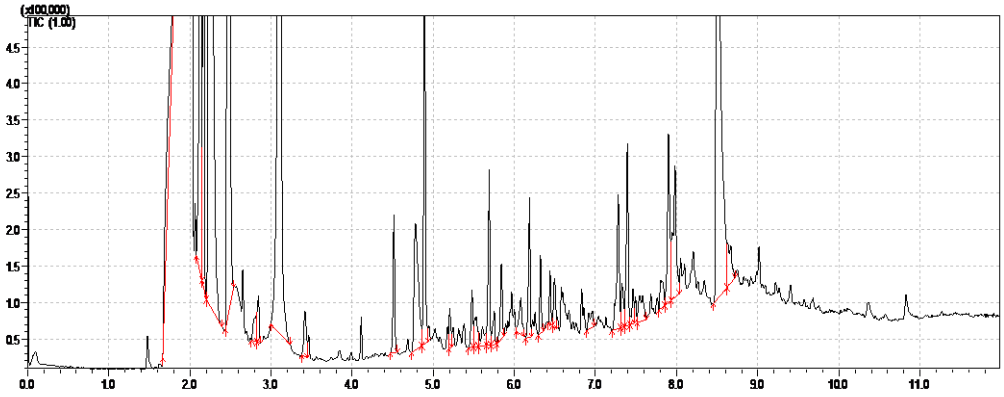


Figure S39: The GC-MS chromatogram of bio-oil product of corn stover liquefaction of Run 4.14.

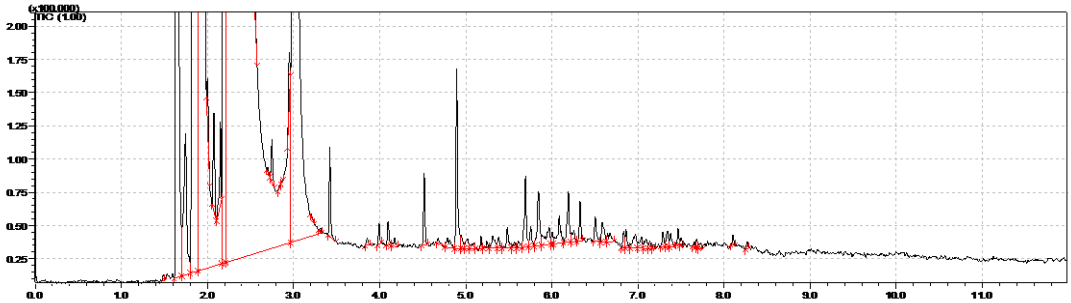


Figure S40: The GC-MS chromatogram of bio-oil product of corn stover liquefaction of Run 4.15.

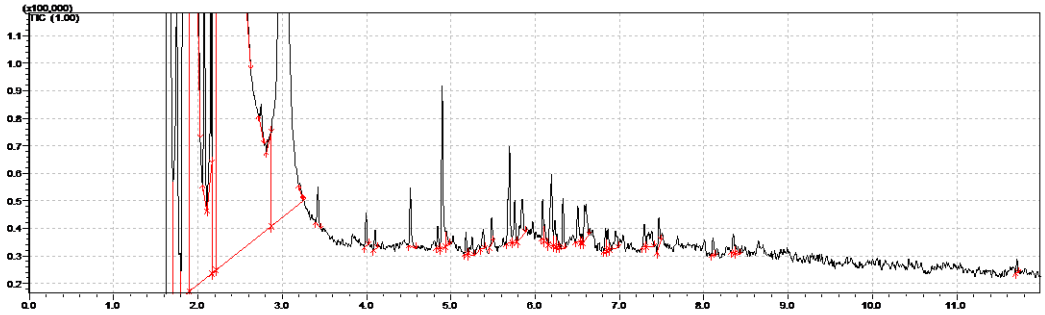


Figure S41: The GC-MS chromatogram of bio-oil product of corn stover liquefaction of Run 4.16.

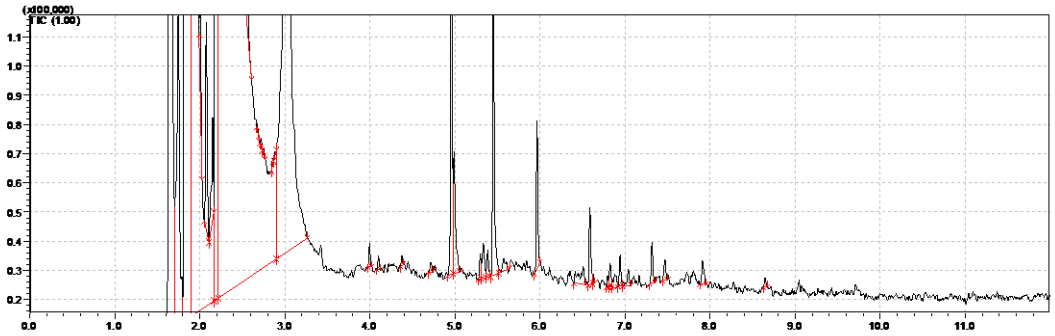

Figure S42: The GC-MS chromatogram of bio-oil product of corn stover liquefaction of Run 4.18.

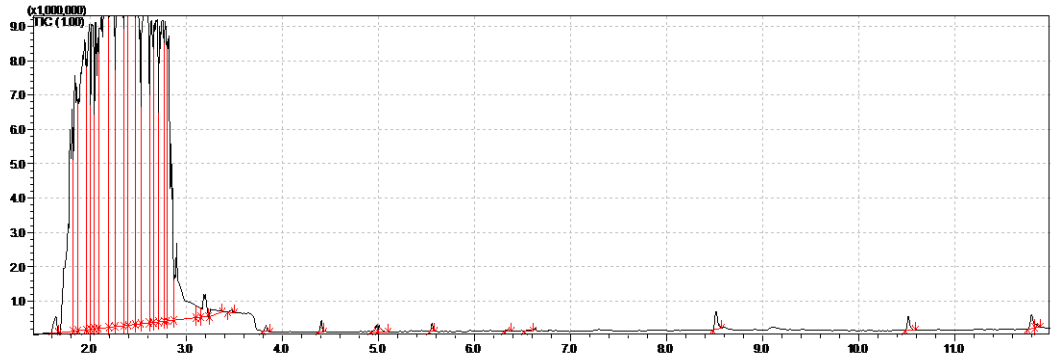

Figure S43: The GC-MS chromatogram of bio-oil product of birch liquefaction under a neutral condition.

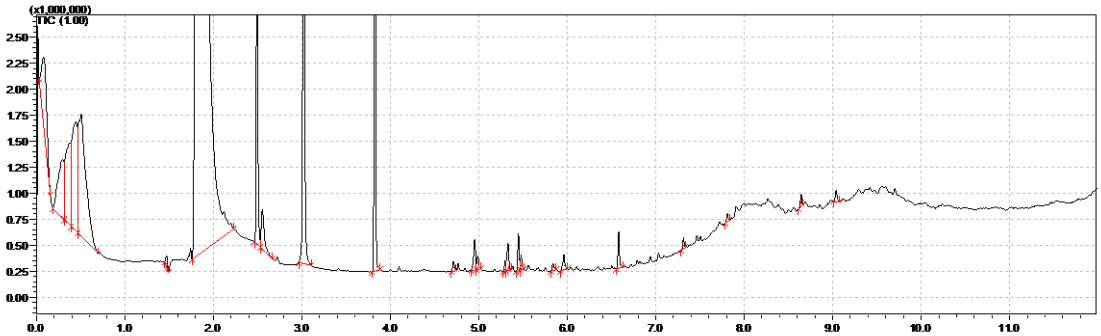

Figure S44: The GC-MS chromatogram of bio-oil product of sugarcane bagasse liquefaction under a neutral condition.

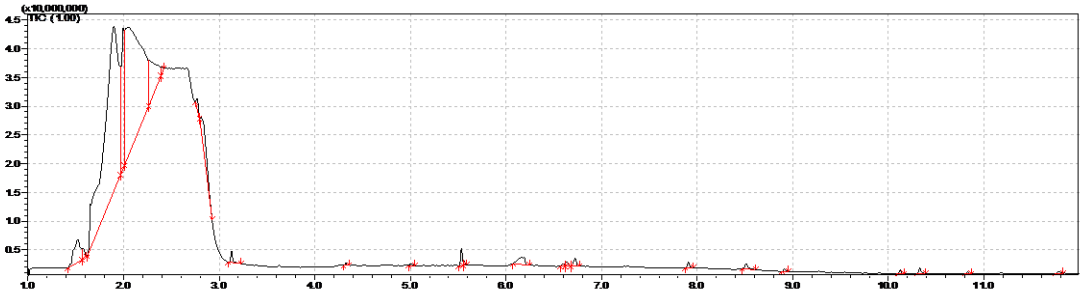

Figure S45: The GC-MS chromatogram of bio-oil product of switchgrass liquefaction under a neutral condition.

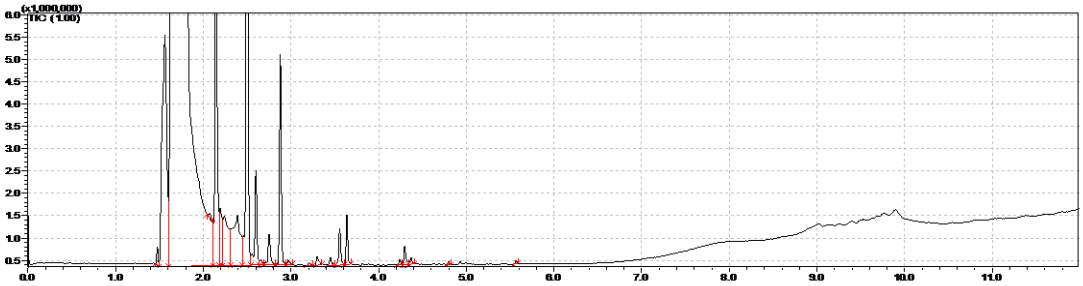

Figure S46: The GC-MS chromatogram of EtOH distillate product of birch liquefaction under a neutral condition.

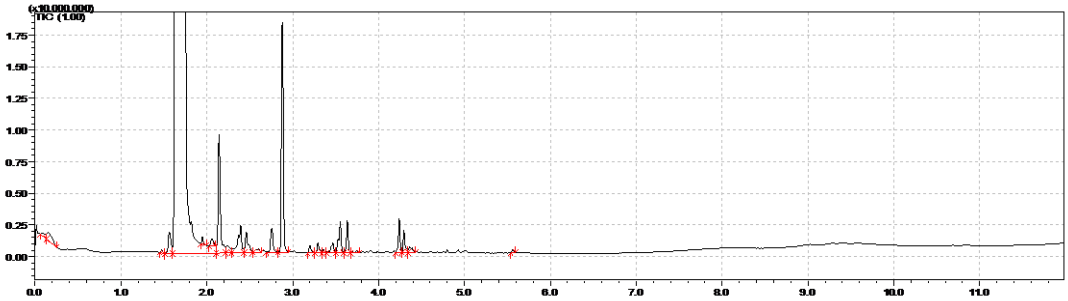

Figure S47: The GC-MS chromatogram of EtOH distillate product of sugarcane bagasse liquefaction under a neutral condition.

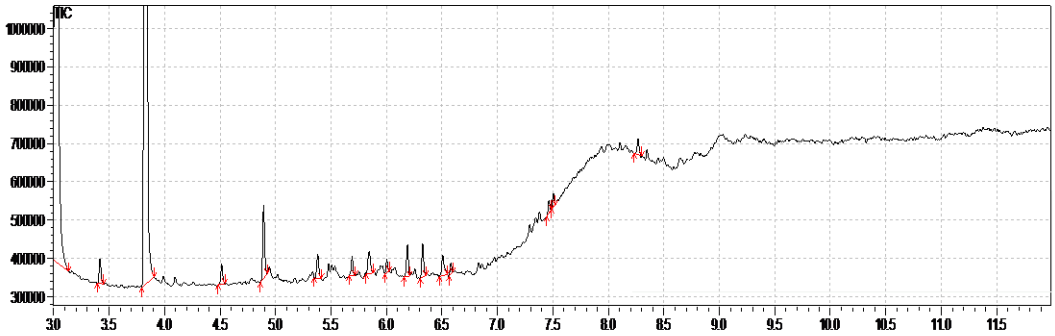

Figure S48: The GC-MS chromatogram of bio-oil product of sugarcane bagasse liquefaction under a basic condition.

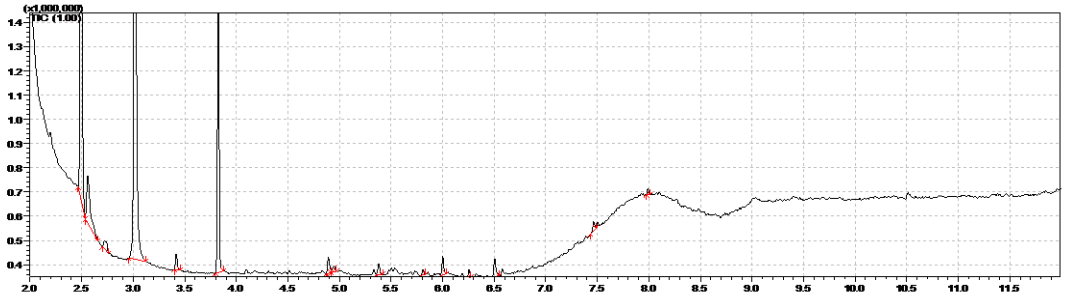

Figure S49: The GC-MS chromatogram of bio-oil product of switchgrass liquefaction under a basic condition.

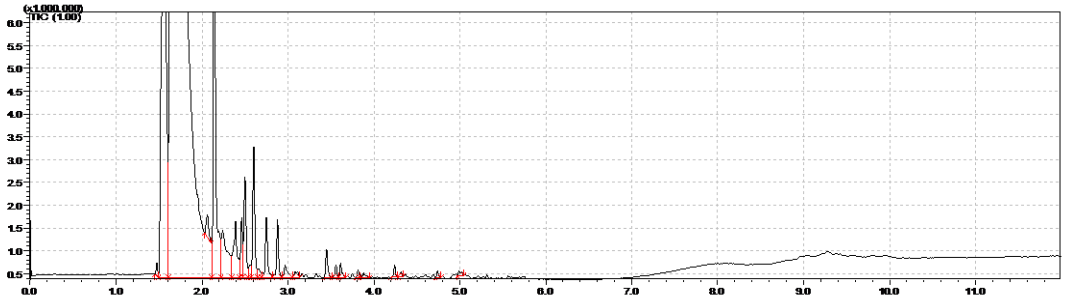

Figure S50: The GC-MS chromatogram of EtOH distillate product of birch liquefaction under a basic condition.

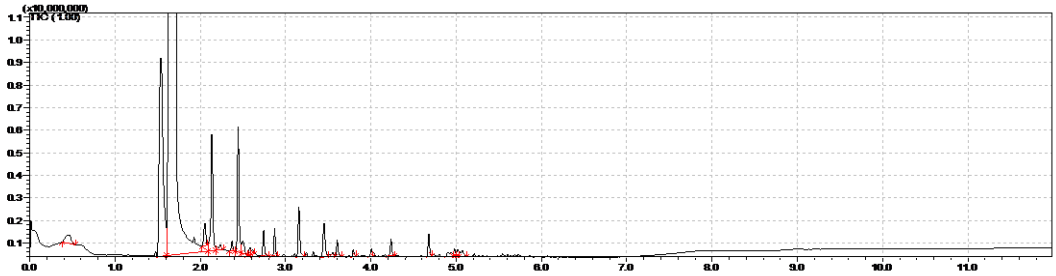

Figure S51: The GC-MS chromatogram of EtOH distillate product of sugarcane bagasse liquefaction under a basic condition.

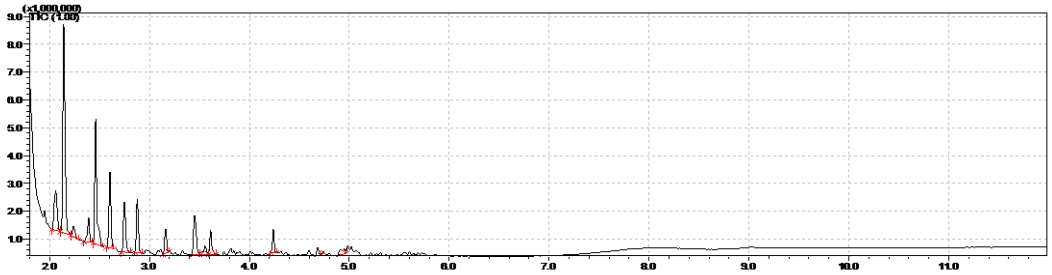

Figure S52: The GC-MS chromatogram of EtOH distillate product of switchgrass liquefaction under a basic condition.

# CHAPTER 5: ENHANCEMENT OF CORN STOVER LIQUEFACTION BY EMPLOYING Ni METAL, KOAc, AND $Fe_2O_3$/ZnO

## 5.1 Introduction

A variety of lignocellulosic materials were converted to oily products by liquefaction process. However, the typical yields of bio-oil produced by liquefaction processes reported in the literature[106, 111, 113, 114] are 20–60%, and the oxygen content is still high. Several types of catalysts have been employed in order to improve the bio-oil yield and quality. Alkaline catalysts, such as NaOH, $K_2CO_3$, $Na_2CO_3$, KOH and $Ca(OH)_2$ have been widely used to enhance liquid products yield and suppress char formation.[84, 106, 115] Moreover, NaOH was found effective in increasing the content of aldehydes, phenols, and hydrocarbons,[116] while $K_2CO_3$ was found useful in increasing phenolic and carboxylic acid compounds[117]. Supply of an external reducing agent such as hydrogen gas has been proved effective in reducing char formation by inhibiting the re-condensation of resulted intermediates and enhancing the liquefaction products.[106, 113, 118] Thus, the catalysts used for promoting the hydrogenation reactions during the conversion process were investigated to increase yields and also bio-oil quality. Zhang, Yang et al.[119] investigated the catalytic effect of potassium salts in biomass gasification, founding that $K_2CO_3$ and KOAc was highly beneficial for improving hydrogen production and carbon conversion efficiency. According to Li, Wenjing et al.[120] nickel acetate salt offers the best catalytic performance in the deoxygenation of stearic acid into alkanes under hydrogen-free conditions compared to other metal salts applied. Duan et al.[19] studied the effects of transition metals (i.e., Pt/C, Pd/C, Ni/$SiO_2$-$Al_2O_3$, Ru/C, and zeolites) on hydrothermal

liquefaction of microalgae, obtaining an increase in oil yield by 10–22 wt% compared to liquefaction without catalysts. The production of 2,5-hexanedione and 3-methyl-2-cyclopenten-1-one was achieved successfully by hydrothermal liquefaction of 5-hydroxymethylfurfural using a number of transition metals such as Fe, Mn, Ni, Zn [121].

In the present work, to enhance bio-oil yields further and obtain liquefied products with lower oxygenated carbons, different catalytic combinations of Ni metal + $Fe_2O_3$ and $Ni(OAc)_2$ + reducing agent (Zn and Fe metals) in the presence of other additives such as KOAc, NaOH, and activated carbon were examined for corn stover liquefaction under different conditions. In Table 5.1, catalytic liquefaction using Ni metal + $Fe_2O_3$ + KOAc was conducted for different reaction times in a range of 260-300°C. The influence of KOAc and time was examined at 260°C, followed by doubling the amount of KOAc and increasing the reaction temperature to 300 °C for achieving the optimum yield of bio-oil production in a shorter time. To promote oxygen removal and reduce repolymerization reactions, further study of Ni metal reduction surface was carried out by rising Ni ($H_2$) metal amount. In Table 5.2, to investigate the catalytic system of Ni metal + ZnO + NaOH under reductive conditions, corn stover liquefaction was conducted in 7:1 and 15:1 EtOH:$H_2O$ mixture. Moreover, the influence of KOAc on the synergy of Ni metal and ZnO was investigated in 100% EtOH at 200, 260, and 300 °C for liquefaction times of 6, 8, and 2 h, respectively. In Table 5.3, the synergy of Ni metal + FeO was studied in the presence and absence of NaOH alone or combined with activated carbon. To characterize bio-oils produced, $^1$H-NMR was used to measure the relative intensity of aromatic protons and those linked to oxygenated and non-oxygenated

carbons. Furthermore, GC–MS was employed to identify the products of bio-oil and EtOH distillates.

## 5.2 Experimental

### 5.2.1 Materials

Corn stover was obtained from a local farm and reduced in size using a blender to 18-50 mesh. Corn stover has cellulose ( 28-51.2 wt.%), hemi-cellulose (19.1-30.7 wt.%), and lignin (11-16.9 wt.%).[73] Potassium acetate, nickel(II) acetate tetrahydrate, and sodium hydroxide were purchased from Fisher Scientific. Iron (III) oxide ($Fe_2O_3$), activated carbon, and Zn and Fe metals were used as provided by the chemical suppliers. Ethanol was purchased from Pharmco-AAPER company.

### 5.2.2 Preparation of catalyst

Ni/C, Ni ($H_2$), and Ni (270 °C) metals were prepared as described in the chapter 2 and 3.

### 5.2.3 Liquefaction procedure

The general procedure of corn stover liquefaction: To a stainless-steel pressure reactor in a glovebox were added a magnet stirring bar, catalyst, corn stover, and EtOH. The closed reactor was transferred into a fume-hood and heated in a molten salt bath for the desired time. After reactor was cooled down, the mixture was filtered and washed with EtOH. EtOH solution was condensed by rotary evaporation under a reduced pressure of 80 mbar using a 50°C water bath. To the residue, 1 mL of $CH_2Cl_2$ (DCM) and 0.5 ml of water were added. The DCM solution was separated, and the water phase was extracted by DCM (0.5 mL × 2). The combined DCM solution was neutralized with

$NaHCO_3$, dried with $MgSO_4$ powder, and condensed on a rotary evaporator to yield oil product.

The percentage yields of liquefaction products were calculated based on the weight of corn stover feed by the following formula [74]:

$$\text{Bio oil yield (wt\%)} = \frac{\text{Weight of bio-oil}}{\text{Biomass weight}} \times 100\%$$

$$\text{Solid bio residue (SR) yield (wt\%)} = \frac{\text{Weight of solid bio residue}}{\text{Biomass wieght}} \times 100\%$$

$$\text{Un repolymerization yield (wt\%) of bio oil} = 100\% - \text{Solid bio residue \%}$$

$$\text{Gas + water soluble species (wt\%)} = 100\% - \text{Bio oil \%} - \text{Solid bio residue \%}$$

### 5.2.4 Characterization

$^1$H-NMR analysis was performed for oil obtained from each corn stover liquefaction on a Bruker AVANCE-400 MHz NMR spectrometer in $CDCl_3$ using TMS as the internal standard. Percentage of protons in different types of chemical groups were calculated from the relative intensity of protons.

GC-MS analysis was performed on a Shimadzu GCMS-QP2010SE. GC column temperature program was set as follows: the temperature was held at 40 $^oC$ for 1 minute, then increased to 240 $^oC$ at a heating rate of 25 $^oC$/min, and then maintained at 240 $^oC$ for 3 minutes. Chloroform, methanol, and acetonitrile were used as a solvent for diluting bio-oil samples. To facilitate the bio-oil derivatization, the bio-oil samples were treated with a common TMS derivatizing reagent - N,O-bis(trimethylsilyl)trifluoroacetamide – BSTFA.

## 5.3 Results and discussion

### 5.3.1 The synergy of hematite, Ni metal, and potassium acetate

The Corn stover liquefaction catalyzed by $Fe_2O_3$, Ni-based catalysts, and KOAc was investigated under different conditions. The liquefaction conditions and yields of conversion, SR, and liquified products for this investigation are illustrated in Table 5.1. The use of each catalytic system showed significantly different liquefaction results. The conversion of biomass in the runs 5.1-5.6 of $Fe_2O_3$, Ni (270°C), and KOAc increased with an increase in reaction temperature: from 89.15%-90.13% at 260°C to 93.22-93.97% at 300°C. The SR decreased accordingly from (9.87-10.85%) to (6.03-6.78%), and the formation of volatile compounds also increased with an increase in temperature and reached 59.47% at 300°C. It was observed in the literature [122-124] that the yield of biomass liquefaction and conversion improves with an increase in temperature to a certain point. Though increasing KOAc amount from 50 mg to 175 mg and residence time from 6 h to around 12 h under runs 5.1-5.3, corn stover liquefaction in the presence of 30 mg of $Fe_2O_3$ and 30 mg of Ni (270°C) at 260°C gave similar yields. However, bio-oil yield was enhanced from 33.9% to 40.86%, and gas yield declined from 59.47% to 52.36% when the mass of KOAc was doubled from 100 mg to 200 mg under runs 5.4-5.6 at 260°C for around 4 h. After the higher conversion and bio-crude yield from liquefaction at 60 mg of $Fe_2O_3$ and Ni (270°C), and 200 mg of KOAc was achieved, the synergistic effects of $Fe_2O_3$, Ni ($H_2$), and KOAc were also investigated under runs 5.7-5.10 by varying the amount of Ni metal and keeping the amounts of other catalysts unchanged. The results of biomass liquefaction showed that bio-oil yields increased while residual solid and gas yields reduced by increasing amount of Ni metal. Bio-oil yields are

greater than 50% and sold residue yields were below 3% when biomass was liquefied by 300 and 600 mg of Ni metal for 12 h and 2 h 40 min, respectively (runs 5.7 and 5.8). In contrast, bio-oils are in a range of 41.2- 43.48% and SRs are in a range of 4.53-4.21% when 60 and 120 mg of Ni metal was used (runs 5.9 and 5.10). The results obtained from this investigation were better than that achieved using $Fe_2O_3$, Ni (270°C), and KOAc. A significantly higher oil yield was achieved with Ni ($H_2$) than that with Ni (270°C). Moreover, the influence of Ni metal loading on liquefaction was stronger than that of KOAc.

| Run | Catalyst | Liquefaction condition | Bio-oil% | Un-repolymerization % | SR% | Gas + Water-soluble species% |
|---|---|---|---|---|---|---|
| 5.1 | 30 mg $Fe_2O_3$, 30 mg Ni (270°C), 175 mg KOAc | 260°C, 8 h | 38.07 | 89.15 | 10.85 | 51.08 |
| 5.2 | 30 mg $Fe_2O_3$, 30 mg Ni (270°C), 100 mg KOAc | 260°C, 11 h 30 min | 37.8 | 90.13 | 9.87 | 52.33 |
| 5.3 | 30 mg $Fe_2O_3$, 30 mg Ni (270°C), 50 mg KOAc | 260°C, 6 h | 37 | 89.86 | 10.14 | 52.86 |
| 5.4 | 60 mg $Fe_2O_3$, 60 mg Ni (270°C), 100 mg KOAc | 300°C, 4 h | 33.9 | 93.37 | 6.63 | 59.47 |
| 5.5 | 60 mg $Fe_2O_3$, 60 mg Ni (270°C), 200 mg KOAc | 300°C, 4 h | 38.6 | 93.97 | 6.03 | 55.37 |
| 5.6 | 60 mg $Fe_2O_3$, 60 mg Ni (270°C), 200 mg KOAc | 300°C, 3 h 30 min | 40.86 | 93.22 | 6.78 | 52.36 |
| 5.7 | 60 mg $Fe_2O_3$, 300 mg Ni ($H_2$), 200 mg KOAc | 300°C, 11 h 40 min | 57.47 | 97.65 | 2.35 | 40.18 |
| 5.8 | 60 mg $Fe_2O_3$, 600 mg Ni ($H_2$), 200 mg KOAc | 300°C, 2 h 40 min | 53.77 | 97.37 | 2.63 | 43.6 |
| 5.9 | 60 mg $Fe_2O_3$, 60 mg Ni ($H_2$), 200 mg KOAc | 300°C, 2 h 40 min | 41.2 | 95.47 | 4.53 | 54.27 |
| 5.10 | 60 mg $Fe_2O_3$, 120 mg Ni ($H_2$), 200 mg KOAc | 300°C, 2 h 40 min | 43.48 | 95.79 | 4.21 | 52.31 |

Table 5.1: Corn stover liquefaction employing $Fe_2O_3$, Ni (270°C)/ Ni ($H_2$) and KOAc.[a,b]

[a]Biomass: 3 g Corn stover was used as a substrate for all experiments, except that under reaction run (5.6), 4.5 g of corn was used.
[b]Solvent: (7/1 ), (7/0.7 ), and (7/0.7 ) mL of EtOH/$H_2O$ mixture were used under reaction runs 5.1, 5.2, and 5.3, respectively. 7 mL EtOH was used under reaction runs (5.4-5.10).

### 5.3.2 The synergistic effect of Zn and Fe with nickel acetate.

Zn metal is a potent reducing agent which can reduce $Ni^{2+}$ ions in nickel salt to Ni (s) metal atoms. Due to being are non-noble, the surface of Zn and Ni metals is usually oxidized in non-reductive conditions (absence of $H_2$ supply), which means that they can also function as Lewis acids. The combination effect of ZnO as Lewis acid and Ni metal as a reduction catalyst on corn stover liquefaction was examined under different conditions, as seen in Table 5.2. The mass of Ni metal used was fixed at 40 mg, and other amounts of ZnO were applied in the presence of NaOH/KOAc. The synergy of Ni metal + ZnO + NaOH catalysts from runs 5.11 to 5.13 and the synergy of Ni metal + ZnO + KOAc catalysts in runs 5.15 and 5.17 enhanced the bio-oil yields and suppressed the formation of volatile and aqueous compounds in the liquefaction at high temperatures of 260 and 300 °C, as compared to the results obtained from runs 5.18 and 5.19 at a low temperature of 200°C and low amount of ZnO metal (800 mg). The influence of the catalytic system used on bio-oil formation becomes more significant at a higher ZnO loading and temperature. The results of this investigation are consistent with results reported by Xu et al., where the catalytic effects of 5 wt% FeS and $FeSO_4$ on bio-oil production increased at a higher temperature.[106] The high un-repolymerization and bio-oil yields, and low residual bio-solid confirm that the biomass was effectively converted into liquid fuels.

Based on the results obtained from runs 5.11-5.13, it seems time influence was more pronounced than solvent and NaOH concentration, which may be ascribed to that

slight difference in the change of solvent and NaOH amount. It is interesting to note that solid bio-residue and bio-oil yields were much lower than the results obtained from liquefaction catalyzed by Ni metal + different metal oxide in chapter 4. This observation indicates that a mixture of EtOH and $H_2O$ gave better results than those obtained in only EtOH regarding deactivation of alcoholic product condensation and bio-residue formation. We can conclude that using a mix of ethanol and water instead of only ethanol is better for liquefaction catalyzed by Ni metal and metal oxide. Because in only ethanol, more condensation reactions would occur, leading to getting % of oil> 100 and high residual biosolid, as we mentioned in chapter 4.

An increment of gas + water % on account of oil production in neutral runs 5.14 and 5.16, where no KOAc added is likely because more dehydration and dehydrogenation reactions would occur. It means that 100% EtOH is not a suitable solvent either for the catalytic system of ZnO and Ni metal under neutral conditions also. The influence of KOAc is seen clearly in the results achieved from run 5.15 as compared to that obtained in run 5.14. The comparison of results between them indicates that dehydrogenation and dehydration reactions were less activated in the case of KOAc. Moreover, KOAc is better than NaOH for increasing oil % because, unlike NaOH, acetate anion functions as a nucleophile more than as a base, which causes lower aldol condensation. Moreover, acetic acid's enolate resulting from ethyl acetate's hydrolysis can facilitate the formation of β-keto carboxylic acid, which is readily decarboxylated over metal oxide. As a result, dehydrogenation and dehydration interactions of liquefied products will be less catalyzed over ZnO and NiO.

In runs 5.18 and 5.19, lower masses of ZnO were used for liquefaction at a low temperature of 200 C compared to Zn amounts and temperatures of runs 5.11-5.17. As a result, Ni metal's reduction surface reduced while the oxidation surface of ZnO and NiO increased, leading to more dehydration. Consequently, lower production of bio-oil was generated in runs 5.18 and 5.19.

Table 5.2: Bio-oil production from Corn stover liquefied using Zn and $Ni(OAc)_2$ under different conditions. [a, b]

| Reaction run | Catalyst | Liquefaction condition | Bio-oil% | SR% | Gas + water-soluble species% |
|---|---|---|---|---|---|
| 5.11 | 1110 mg Zn, 40 mg $Ni(OAc)_2$, 100 mg NaOH | 260°C, 8 h | 39.78 | 5.75 | 54.47 |
| 5.12 | 1110 mg Zn, 40 mg $Ni(OAc)_2$, 70 mg NaOH | 260°C, 8 h | 41.6 | 10.9 | 47.5 |
| 5.13 | 1110 mg Zn, 40 mg $Ni(OAc)_2$, 70 mg NaOH | 260°C, 12 h | 52.15 | 8.82 | 39.03 |
| 5.14 | 2400 mg Zn, 40 mg $Ni(OAc)_2$ | 300°C, 2 h | 28.29 | 0 | 71.71 |
| 5.15 | 2400 mg Zn, 40 mg $Ni(OAc)_2$, 200 mg KOAc | 300°C, 2 h | 56.13 | 0 | 43.87 |
| 5.16 | 2400 mg Zn, 40 mg $Ni(OAc)_2$, | 260°C, 8 h | 31.3 | 0 | 68.7 |
| 5.17 | 2000 mg Zn, 40 mg $Ni(OAc)_2$, 60 mg $Fe_2O_3$, 200 mg KOAc | 300°C, 2 h | 51.5 | 0 | 48.5 |
| 5.18 | 800 mg Zn, 40 mg $Ni(OAc)_2$ | 200°C, 6 h | 11.23 | 0 | 88.76 |
| 5.19 | 800 mg Zn, 40 mg $Ni(OAc)_2$, 200 mg KOAc | 200°C, 6 h | 9.30 | 0 | 90.69 |

[a] Biomass: 0.4 g, 1.5 g, and 1.2 g Corn stover was used under reaction runs (5.11-5.13), (5.14-5.17), and (5.18-5.19), respectively.
[b] Solvent: (7/1 ) mL $EtOH/H_2O$ mixture was used under reaction run 5.11 and (7.5/0.5 ) mL $EtOH/H_2O$ mixture was used under reaction runs 5.12, and 5.13, respectively. For the rest runs, 8 mL EtOH was used.

Fe metal as a reducing agent was employed for the reduction of $Ni^{2+}$ ions, as seen in corn stover liquefaction in Table 5.3. Increasing Ni metal loading from 16 to 32 mg in runs 5.24 and 5.25, respectively, in the presence of Fe metal, resulted in an increase of the bio-oil yield from 29.75% to 36.13% and a decrease in gas and aqueous formation from 51.05% to 37.13%. However, the repolymerized solids were also promoted. Ni metal and NiO atoms were probably more formed after incrementing in the mass of nickel salt, which leads to higher reduction reactions as well as repolymerization reactions. Moreover, a slow release of $H_2$ produced by reacting Fe metal with EtOH can suppress the reduction of radicals formed. In contrast, the addition of carbon in runs 5.21 and 5.23 enhanced the bio-oil and reduced the bio-residue, aqueous, and gas production for the catalytic liquefaction using 300 mg Fe, 4 and 8 mg Ni metal under basic condition compared to that achieved in runs 5.20 and 5.22. These yields may be ascribed to that carbon added may increase the surface area of Ni metal catalyst. The use of NaOH can facilitate the hydrolysis of hydrophobic esters with high molecular weight. As a result, higher improvement in un-repolymerized oil was achieved.

The results obtained using NaOH and activated carbon with a lower amount of Ni metal in runs 5.24 and 5.25 were similar to that achieved by increasing Ni metal from 16 to 32 mg. This combination of NaOH and activated carbon can give an equivalent influence of that achieved from increasing Ni metal amount. Low bio-oil yields generated in this investigation could be attributed to two possible reasons: Fe metal is not a potent reducing agent as Zn metal, and the amount of Ni metal was insufficient. However, a closer mass of Ni metal was used in run 5.15, and high oil % was obtained. So, the second reason is likely avoided, which indicates to Ni metal + metal oxide either in the

presence of NaOH or not in 100% EtOH is not an excellent catalytic system. Moreover, oil% can be increased by condensation reactions as Ni amount raised, but this is not seen, which hint that not all $Ni^{2+}$ ions were reduced by Fe metal.

Table 5.3: Corn stover liquefaction employing Fe and $Ni(OAc)_2$.[a]

| run | Catalyst | Bio-oil% | Un-repolymerization% | SR% | Gas + Water-soluble species % |
|---|---|---|---|---|---|
| 5.20 | 300 mg Fe, 8 mg $Ni(OAc)_2$, 50 mg NaOH | 31.15 | 63 | 37 | 31.85 |
| 5.21 | 300 mg Fe, 8 mg $Ni(OAc)_2$, 50 mg carbon, 50 mg NaOH | 36.92 | 63.5 | 31.63 | 31.45 |
| 5.22 | 300 mg Fe, 4 mg $Ni(OAc)_2$, 50 mg NaOH | 28.07 | 99.9 | 36.5 | 71.83 |
| 5.23 | 300 mg Fe, 4 mg $Ni(OAc)_2$, 50 mg carbon, 50 mg NaOH | 35.15 | 64.32 | 35.67 | 29.18 |
| 5.24 | 300 mg Fe, 16 mg $Ni(OAc)_2$ | 29.75 | 80.8 | 19.2 | 51.05 |
| 5.25 | 300 mg Fe, 32 mg $Ni(OAc)_2$ | 36.12 | 73.25 | 26.75 | 37.13 |

[a] Reaction condition: 400 mg corn stover, 4 mL EtOH, 260°C, 6h.

### 5.3.3 Characterization of bio-oil composition

#### 5.3.3.1 $^1$H-NMR analysis of bio-oil

The chemical structure changes of the bio-oils produced were investigated by $^1$H-NMR analysis. The proton percentages were measured based on the integral values of selected regions as presented in Figure 5.1 (S5.1-5.10), 5.2 (S5.11-5.19), and 5.3 (S5.20-5.25). According to the chemical shifts of functional groups interested, the reduction of oxygenated species in bio-oils was investigated in four different regions. The most upfield region of the spectra, from 0.5 to 3.0 ppm, represents aliphatic protons that are attached to non-oxygenated carbon atoms (—$CH_3$, —$CH_n$—). The next region, from 3.0

to 4.0 ppm, represents proton on aliphatic carbon atoms bonded to hydroxyl or alkoxyl group (—$CH_n$—O—). The next region of 4.1-4.3 ppm represents protons on the $sp^3$ carbon of ester groups (—$COOCH_n$—). The last region of 6.0-8.5 ppm corresponds to the aromatic protons of lignin-derived products.

From Figure 5.1, it was observed that oxygenated species in bio-oils generated from corn stover were significantly reduced using $Fe_2O_3$, Ni (270°C)/Ni ($H_2$) and KOAc. The lowest contents of oxygenated and aromatic compounds of bio-oils were obtained under runs 5.6, 5.7, and 5.8 where high loadings of Ni metal and KOAc were employed. Increasing Ni ($H_2$) loading is more effective on the reduction of aromatic and oxygenated compounds under reaction runs 5.8, 5.9, and 5.10 compared to the influence of KOAc. The abundance of aromatic protons in all bio-oils produced are higher than the protons of ether, alcohol, and ester derivatives.

The bio-oils produced using Zn and $Ni(OAc)_2$ showed also high proton percentages of non-oxygenated carbons and low proton percentages of aromatic and oxygenated carbons except for that obtained under runs 5.18 and 5.19 as shown in Figure 5.2. The lower Zn loading ( 800 mg) and temperature (200°C) may cause to have high proton percentage of  aromatic and oxygenated carbons. The liquefaction at 260°C and 300°C under runs 5.11-5.17 gave low proton percents of both aromatic and oxygenated carbons. The percentages of ether and alcohol protons were more promoted in the presence of NaOH while the percentages of ester protons were more suppressed at 300°C.

As shown in Figure 5.3, bio-oils generated using Fe and $Ni(OAc)_2$ contained higher proton percentages of aromatic and oxygenated carbons under neutral condition (runs 5.24 and 5.25) than under basic condition (runs 5.20-5.23). No significant change

was observed in proton percentages by increasing the loading of $Ni(OAc)_2$ from 4 to 8 mg in runs 5.22 and 5.20 and from 16 to 32 mg under runs 5.24 and 5.25 in the presence and absence of NaOH, respectively. However, the addition of carbon suppressed the proton percentages of ethers, alcohols, and aromatics in bio-oil obtained from run 5.23.

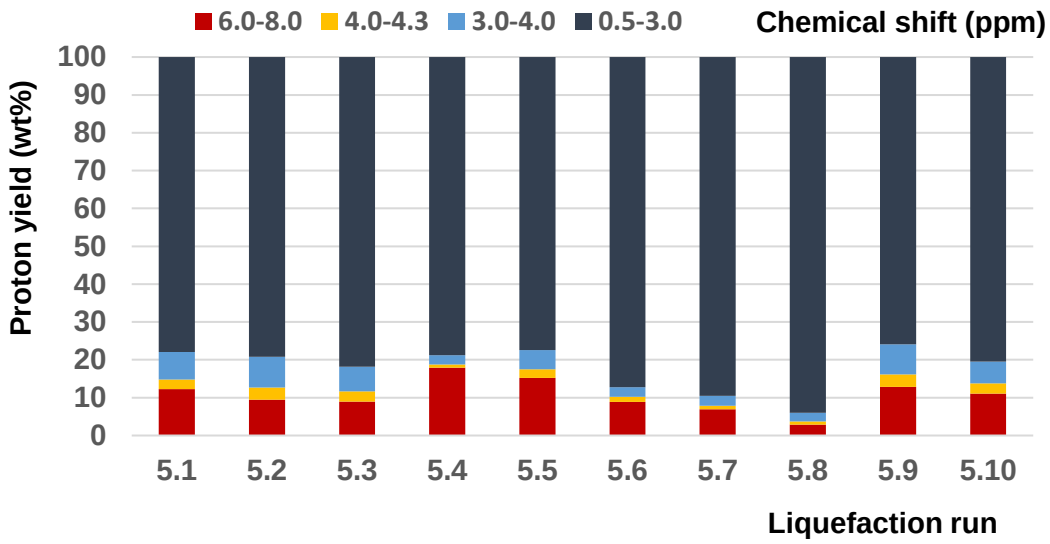


Figure 5.1: $^1$H-NMR analysis of bio-oils produced in runs 5.1-5.10 from corn stover liquefaction employing $Fe_2O_3$, Ni (270°C)/ Ni ($H_2$), and KOAc.

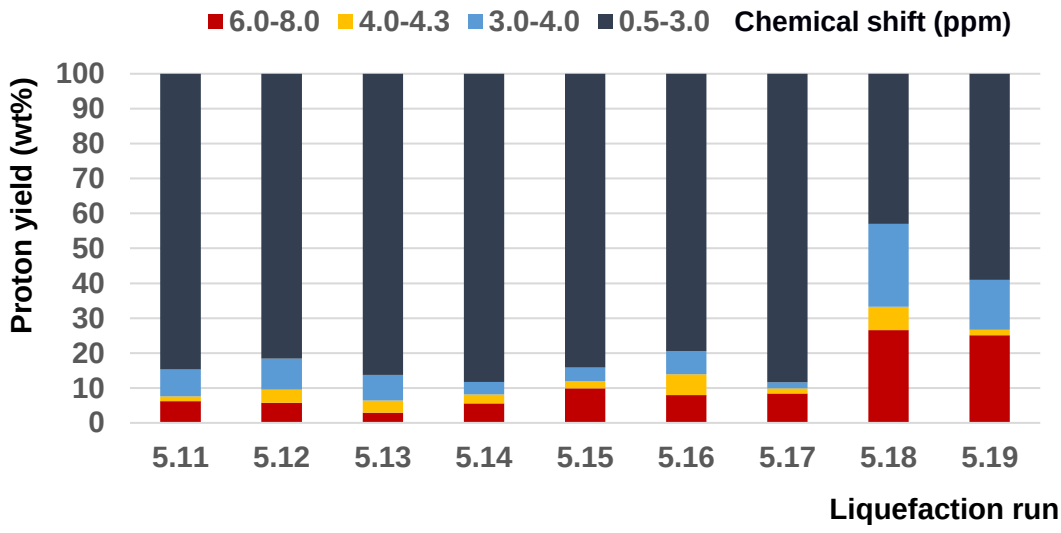


Figure 5.2: $^1$H-NMR analysis of bio-oils produced from corn stover liquefaction in runs 5.11-5.19 using Zn and $Ni(OAc)_2$.

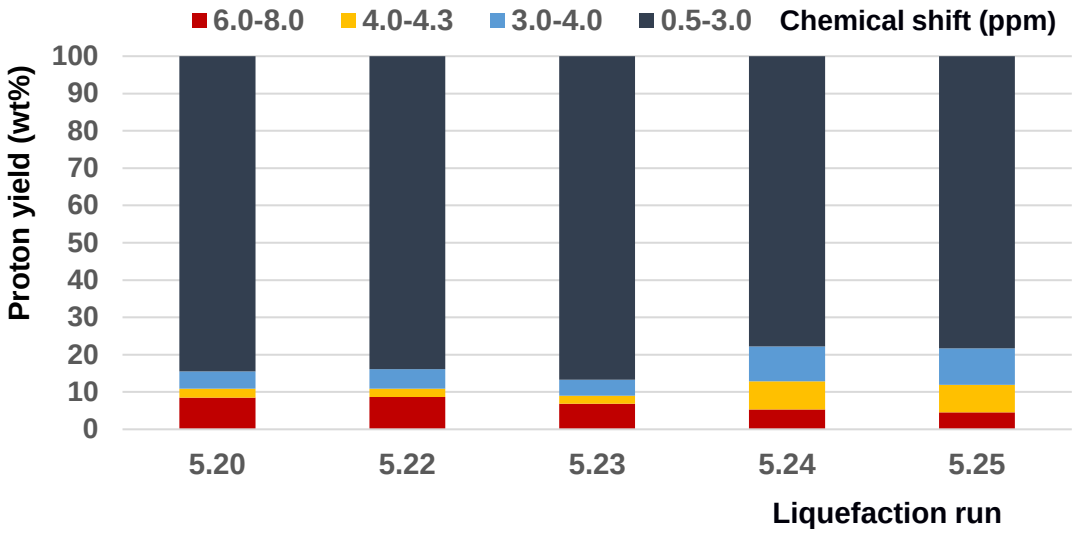


Figure 5.3: $^{1}$H-NMR analysis of bio-oils produced from corn stover liquefaction in runs 5.20-5.25 using Fe metal and $Ni(OAc)_2$.

### 5.3.3.2 GC-MS analysis of bio-oil

To identify the bio-oil products, the GC−MS analysis was carried out. The identification of the bio-oil products was performed using a NIST mass spectral database. The relative percent area for each volatile product was determined by the percentage of the chromatographic area of the compound out of the total area. As illustrated in Tables 5.4-5.13 (S26-S35) of EtOH distillates of biomass liquefaction using Ni metal and KOAc under runs 5.1-5.10, the major categories identified were alcohol, ester, furan, ether, and ketone/aldehyde derivatives. Ester and alcohol derivatives constituted the dominant content of compounds detected compared to other categories. Alcohols were likely produced from alcohol condensation and esters were formed from reactions of alcohols with carboxylic acids. For bio-oil generated in runs 5.1-5.10 using Ni metal and KOAc,

aromatic and acidic derivatives were the dominant compounds identified as seen in Tables 5.14-5.23 (S36-S45). Furan, ether, and alcohol were also detected but with lower abundances. In bio-oils produced in runs 5.14-5.19 using Zn metal and $Ni(OAc)_2$, alcohol, aromatic, acid, and its derivatives were the main compounds identified as presented in Tables 5.24-5.29 (S46-S51). Furan products with low relative portion were also found. High contents of acid and its derivatives were formed under runs 5.14-5.17 compared to that obtained under runs 5.18 and 5.19. The highest content (73.47%) of aromatic compounds was detected under run 5.18. While in EtOH distillates of runs 5.14, 5.1 6, and 5.17, the dominant components are esters, ethers, alcohols, acids, ketones, and hydrocarbons as shown in Tables 5.30-5.32 (S52-S54).

Table 5.4 : The GC-MS analysis of EtOH distillate products of corn stover liquefaction using $Fe_2O_3$, Ni (270°C), and KOAc of Run 5.1.

| Ret. Time (min) | Area% | Similarity% | Compound name |
|---|---|---|---|
| 2.082 | 2.733768 | 86 | 2-Butanone |
| 2.152 | 41.59677 | 93 | Ethyl Acetate |
| 2.249 | 4.53557 | 96 | Tetrahydrofuran |
| 2.407 | 2.85803 | 89 | 2-Propanol, 1-methoxy- |
| 2.473 | 1.584343 | 97 | 1-Butanol |
| 2.755 | 6.461634 | 98 | Propanoic acid, ethyl ester |
| 2.887 | 1.988195 | 97 | Ethane, 1,1-diethoxy- |
| 3.004 | 1.087294 | 91 | 1-Butanol, 2-methyl- |
| 3.453 | 3.541473 | 93 | Butanoic acid, ethyl ester |

| | | | |
|---|---|---|---|
| 3.566 | 1.429015 | 78 | 1H-Pyrrole, 1-ethyl- |
| 3.826 | 1.335819 | 87 | (R)-(+)-3-Methylcyclopentanone |
| 4.252 | 2.081392 | 75 | Furfuryl pentanoate |
| 4.324 | 1.460081 | 86 | Acetic acid, ethoxy-, ethyl ester |
| 4.374 | 10.1895 | 90 | Butane, 2-ethoxy- |
| 4.756 | 1.149425 | 84 | 3-Ethylcyclopentanone |
| 5.565 | 1.366884 | 91 | Butanoic acid, anhydride |

Table 5.5 : The GC-MS analysis of EtOH distillate products of corn stover liquefaction using $Fe_2O_3$, Ni (270°C), and KOAc of Run 5.2.

| Ret. Time (min) | Area% | Similarity% | Compound name |
|---|---|---|---|
| 1.572 | 4.672096 | 95 | Methyl Alcohol |
| 2.076 | 2.400343 | 93 | 2-Butanone |
| 2.152 | 41.36305 | 96 | Ethyl Acetate |
| 2.248 | 6.258037 | 96 | Tetrahydrofuran |
| 2.409 | 1.114445 | 86 | 2-hydroxyethyl ether |
| 2.608 | 2.271753 | 87 | Propane, 1-(1-methylethoxy)- |
| 2.755 | 8.444063 | 98 | Propanoic acid, ethyl ester |
| 2.887 | 1.757394 | 97 | Ethane, 1,1-diethoxy- |
| 3.454 | 3.771967 | 95 | Butanoic acid, ethyl ester |
| 3.565 | 1.328761 | 87 | 1H-Pyrrole, 1-ethyl- |
| 3.827 | 1.628804 | 92 | Cyclopentanone, 3-methyl- |
| 4.327 | 1.457351 | 76 | 2,4-Dimethylfuran |

| | | | |
|---|---|---|---|
| 4.373 | 6.600943 | 89 | Ethane, 1,1-diethoxy- |
| 4.757 | 1.071582 | 83 | 3-Ethylcyclopentanone |
| 5.566 | 1.585941 | 90 | Butanoic acid, anhydride |

Table 5.6: The GC-MS analysis of EtOH distillate products of corn stover liquefaction using $Fe_2O_3$, Ni (270°C), and KOAc of Run 5.3.

| Ret. Time (min) | Area% | Similarity% | Compound name |
|---|---|---|---|
| 1.571 | 9.669582 | 97 | Methyl Alcohol |
| 1.957 | 10.15549 | 96 | 1-Propanol |
| 2.083 | 5.490768 | 88 | Butanal, 2-ethyl- |
| 2.152 | 34.74247 | 94 | Ethyl Acetate |
| 2.249 | 4.810496 | 95 | Tetrahydrofuran |
| 2.401 | 2.478134 | 86 | 2-Propanol, 1-methoxy- |
| 2.471 | 1.020408 | 97 | 1-Butanol |
| 2.756 | 8.98931 | 98 | Propanoic acid, ethyl ester |
| 2.888 | 1.214772 | 96 | Ethane, 1,1-diethoxy- |
| 3.456 | 3.741497 | 95 | Butanoic acid, ethyl ester |
| 3.827 | 1.020408 | 90 | (R)-(+)-3-Methylcyclopentanone |
| 4.251 | 1.603499 | 73 | Furfuryl pentanoate |
| 4.373 | 4.033042 | 88 | 2-Ethoxypentane |
| 5.566 | 1.166181 | 90 | Furan, tetrahydro-2-(methoxymethyl)- |

Table 5.7: The GC-MS analysis of EtOH distillate products of corn stover liquefaction using $Fe_2O_3$, Ni (270°C), and KOAc of Run 5.4.

| Ret. Time (min) | Area% | Similarity% | Compound name |
|---|---|---|---|
| 1.91 | 55.78947 | 95 | Methanol |
| 2.063 | 4.210526 | 91 | 2-Butanone |
| 2.14 | 22.94737 | 97 | Ethyl Acetate |
| 2.364 | 3.578947 | 89 | Propane, 2,2-dimethoxy- |
| 2.657 | 4.421053 | 81 | 2-Hexanone, 4-hydroxy-5-methyl-3-propyl- |
| 3.119 | 9.052632 | 90 | 2,2-Dimethoxybutane |

Table 5.8: The GC-MS analysis of EtOH distillate products of corn stover liquefaction using $Fe_2O_3$, Ni (270°C), and KOAc of Run 5.5.

| Ret. Time (min) | Area% | Similarity% | Compound name |
|---|---|---|---|
| 1.911 | 34.36893 | 95 | Methanol |
| 2.066 | 3.495146 | 91 | 2-Butanone |
| 2.141 | 42.3301 | 97 | Ethyl Acetate |
| 2.238 | 1.941748 | 84 | Tetrahydrofuran |
| 2.365 | 4.07767 | 88 | Propane, 2,2-dimethoxy- |
| 2.749 | 4.854369 | 84 | Propanoic acid, ethyl ester |
| 3.119 | 8.932039 | 89 | 2,2-Dimethoxybutane |

Table 5.9: The GC-MS analysis of EtOH distillate products of corn stover liquefaction using $Fe_2O_3$, Ni (270°C) and KOAc of Run 5.6.

| Ret. Time (min) | Area% | Similarity% | Compound name |
|---|---|---|---|
| 1.91 | 21.89586 | 97 | Methanol |
| 2.068 | 3.204272 | 92 | 2-Butanone |
| 2.142 | 58.21095 | 98 | Ethyl Acetate |
| 2.24 | 1.869159 | 81 | Tetrahydrofuran |
| 2.367 | 3.070761 | 90 | Propane, 2,2-dimethoxy- |
| 2.748 | 4.138852 | 94 | Propanoic acid, ethyl ester |
| 3.119 | 7.610147 | 91 | 2,2-Dimethoxybutane |

Table 5.10: The GC-MS analysis of EtOH distillate products of corn stover liquefaction using $Fe_2O_3$, Ni ($H_2$), and KOAc of Run 5.7.

| Ret. Time (min) | Area% | Similarity% | Compound name |
|---|---|---|---|
| 1.913 | 6.324111 | 94 | Methanol |
| 2.063 | 3.030303 | 87 | Butanal |
| 2.144 | 6.192358 | 96 | Ethyl Acetate |
| 2.24 | 1.581028 | 89 | Tetrahydrofuran |
| 2.369 | 1.844532 | 88 | Propane, 2,2-dimethoxy- |
| 2.446 | 65.34914 | 98 | 1-Butanol |
| 2.881 | 1.317523 | 90 | Ethane, 1,1-diethoxy- |
| 3.12 | 3.952569 | 91 | 2,2-Dimethoxybutane |
| 3.164 | 4.611331 | 97 | Butanal, 2-ethyl- |

| | | | |
|---|---|---|---|
| 3.799 | 5.797101 | 95 | 1-Butanol, 2-ethyl- |

Table 5.11: The GC-MS analysis of EtOH distillate products of corn stover liquefaction using $Fe_2O_3$, Ni ($H_2$), and KOAc of Run 5.8.

| Ret. Time (min) | Area% | Similarity% | Compound name |
|---|---|---|---|
| 1.911 | 3.734896 | 95 | Methanol |
| 2.144 | 6.371293 | 97 | Ethyl Acetate |
| 2.446 | 58.76968 | 98 | 1-Butanol |
| 2.748 | 2.087148 | 92 | Propanoic acid, ethyl ester |
| 2.881 | 1.025265 | 91 | Ethane, 1,1-diethoxy- |
| 2.986 | 1.281582 | 93 | 1-Butanol, 2-methyl- |
| 3.12 | 1.391432 | 90 | 2,2-Dimethoxybutane |
| 3.454 | 2.270231 | 95 | Butanoic acid, ethyl ester |
| 3.563 | 2.233614 | 95 | Acetic acid, butyl ester |
| 3.797 | 8.275357 | 96 | 1-Butanol, 2-ethyl- |
| 4.036 | 1.904064 | 90 | Formic acid, 2-methylpentyl ester |
| 4.244 | 1.830831 | 91 | Butane, 1,1-diethoxy- |
| 5.218 | 1.061882 | 85 | 2-Diethoxymethyl-3-methyl-butan-1-ol |

Table 5.12: The GC-MS analysis of EtOH distillate products of corn stover liquefaction using $Fe_2O_3$, Ni ($H_2$) and KOAc of Run 5.9.

| Ret. Time (min) | Area% | Similarity% | Compound name |
|---|---|---|---|
| 1.91 | 19.11967 | 96 | Methanol |

| | | | |
|---|---|---|---|
| 2.07 | 3.713893 | 92 | 2-Butanone |
| 2.143 | 59.42228 | 98 | Ethyl Acetate |
| 2.241 | 1.788171 | 86 | Tetrahydrofuran |
| 2.368 | 3.026135 | 90 | Propane, 2,2-dimethoxy- |
| 2.749 | 3.988996 | 93 | Propanoic acid, ethyl ester |
| 2.881 | 2.200825 | 90 | Ethane, 1,1-diethoxy- |
| 3.12 | 6.740028 | 90 | 2,2-Dimethoxybutane |

Table 5.13: The GC-MS analysis of EtOH distillate products of corn stover liquefaction using $Fe_2O_3$, Ni ($H_2$) and KOAc of Run 5.10.

| Ret. Time (min) | Area% | Similarity% | Compound name |
|---|---|---|---|
| 1.911 | 25.21459 | 96 | Methanol |
| 2.068 | 8.798283 | 92 | 2-Butanone |
| 2.143 | 52.14592 | 98 | Ethyl Acetate |
| 2.244 | 2.145923 | 84 | Tetrahydrofuran |
| 2.368 | 2.038627 | 90 | Propane, 2,2-dimethoxy- |
| 2.749 | 3.540773 | 93 | Propanoic acid, ethyl ester |
| 2.882 | 1.180258 | 93 | Ethane, 1,1-diethoxy- |
| 3.121 | 4.935622 | 85 | 2,2-Dimethoxybutane |

Table 5.14: The GC-MS analysis of bio-oil products of corn stover liquefaction using $Fe_2O_3$, Ni (270°C) and KOAc of Run 5.1.

| Ret. Time (min) | Area% | Similarity% | Compound name |
|---|---|---|---|

| | | | |
|---|---|---|---|
| 2.766 | 19.54023 | 94 | Acetic acid |
| 3.436 | 2.873563 | 95 | Propionic acid |
| 4.379 | 1.149425 | 86 | 2-(1-Ethoxy-ethoxy)-propionic acid ethyl ester |
| 4.84 | 10.34483 | 86 | (2-Ethoxyethoxy)acetic acid |
| 4.9 | 1.724138 | 93 | Ethoxy-acetic acid |
| 4.961 | 1.149425 | 87 | Butane-2,3-diol |
| 5.39 | 2.873563 | 95 | Phenol |
| 5.456 | 1.436782 | 82 | 2-Hydroxy-2-methyl-1-phenyl-propan-1-one |
| 5.524 | 1.149425 | 78 | Butane, 1,1-diethoxy- |
| 5.564 | 6.034483 | 90 | Furan, tetrahydro-2-(methoxymethyl)- |
| 5.819 | 1.149425 | 92 | 2-Hydroxy-butyric acid |
| 5.862 | 2.011494 | 77 | 4-Oxoheptanedioic acid |
| 6.007 | 12.64368 | 80 | (Tetrahydro-furan-2-yl)-methanol |
| 6.05 | 1.149425 | 84 | 4-Methyl-phenol |
| 6.588 | 4.597701 | 89 | 3-Ethylphenol |
| 7.382 | 1.149425 | 73 | Butanedioic acid, 3-hydroxy-2,2-dimethyl-, diethyl ester |
| 7.47 | 1.724138 | 83 | 4-Hydroxy-3-methoxy-benzaldehyde |
| 7.509 | 1.149425 | 86 | 2,6-Dimethoxyphenol |
| 7.55 | 1.436782 | 65 | Pentanoic acid, 2-methyl-, 1,2,3-propanetriyl ester |

| | | | |
|---|---|---|---|
| 7.724 | 2.298851 | 72 | 4-Hydroxy-pent-1-en-3-one |
| 7.809 | 3.16092 | 80 | 4-Methyl-benzene-1,2-diol |
| 7.925 | 3.448276 | 73 | Benzene-1,2-diol |
| 7.99 | 1.149425 | 72 | 2-Ketoglutaric acid |
| 8.059 | 1.149425 | 74 | (3-Hydroxy-phenyl)-acetic acid |

Table 5.15: The GC-MS analysis of bio-oil products of corn stover liquefaction using $Fe_2O_3$, Ni (270°C) and KOAc of Run 5.2.

| Ret. Time (min) | Area% | Similarity% | Compound name |
|---|---|---|---|
| 2.769 | 23.14815 | 96 | Acetic acid |
| 3.436 | 4.012346 | 94 | Butan-1-ol |
| 4.378 | 1.234568 | 88 | Ethane, 1,1-diethoxy- |
| 4.841 | 5.555556 | 87 | (2-Ethoxyethoxy)acetic acid |
| 4.901 | 1.234568 | 91 | Ethoxy-acetic acid |
| 5.341 | 8.024691 | 80 | Propane, 1,1-diethoxy- |
| 5.389 | 4.320988 | 96 | Phenol |
| 5.563 | 7.098765 | 90 | Furan, tetrahydro-2-(methoxymethyl)- |
| 5.861 | 1.234568 | 77 | 2-Oxopentanedioic acid |
| 6.007 | 11.41975 | 79 | (Tetrahydro-furan-2-yl)-methanol |
| 6.111 | 1.234568 | 85 | 2-Ethyl-malonic acid |
| 6.511 | 1.851852 | 94 | 2-Methoxyphenol |
| 6.588 | 5.864198 | 89 | 3-Ethylphenol, trimethylsilyl ether |
| 7.469 | 2.160494 | 83 | 4-Hydroxy-3-methoxy-benzaldehyde |

| | | | |
|---|---|---|---|
| 7.509 | 1.234568 | 90 | 2,6-Dimethoxyphenol |
| 7.808 | 1.54321 | 82 | 4-Methyl-benzene-1,2-diol |
| 7.924 | 1.234568 | 71 | Hydroxy-(3-methoxy-phenyl)-acetic acid |

Table 5.16: The GC-MS analysis of bio-oil products of corn stover liquefaction using $Fe_2O_3$, Ni (270°C) and KOAc of Run 5.3.

| Ret. Time (min) | Area% | Similarity% | Compound name |
|---|---|---|---|
| 2.768 | 41.38413 | 90 | Acetic acid |
| 3.436 | 3.187721 | 96 | Butan-1-ol |
| 4.841 | 4.012575 | 86 | (2-Ethoxyethoxy)acetic acid |
| 5.343 | 5.533259 | 81 | Propane, 1,1-diethoxy- |
| 5.389 | 3.789229 | 95 | Phenol |
| 5.457 | 1.090232 | 81 | 2-Hydroxy-2-methyl-1-phenyl-propan-1-one |
| 5.567 | 4.897219 | 89 | Furan, tetrahydro-2-(methoxymethyl)- |
| 5.861 | 1.031208 | 77 | 2-Oxopentanedioic acid |
| 6.007 | 10.40969 | 79 | (Tetrahydro-furan-2-yl)-methanol |
| 6.05 | 1.076475 | 70 | 4-Methyl-phenol |
| 6.512 | 1.379619 | 93 | 2-Methoxyphenol |
| 6.588 | 5.017216 | 90 | 3-Ethylphenol |
| 7.471 | 1.583329 | 83 | 4-Hydroxy-3-methoxy-benzaldehyde |
| 7.809 | 1.095779 | 77 | 4-Methyl-benzene-1,2-diol |

Table 5.17: The GC-MS analysis of bio-oil products of corn stover liquefaction using $Fe_2O_3$, Ni (270°C) and KOAc of Run 5.4.

| Ret. Time (min) | Area% | Similarity% | Compound name |
|---|---|---|---|
| 2.808 | 25.21441 | 96 | Acetic acid |
| 3.478 | 6.689537 | 98 | Propionic acid |
| 4.844 | 5.145798 | 85 | Ethane-1,2-diol |
| 5.388 | 11.32075 | 95 | Phenol |
| 5.482 | 1.543739 | 90 | Butane-1,2-diol |
| 6.009 | 12.00686 | 80 | (Tetrahydro-furan-2-yl)-methanol |
| 6.329 | 1.02916 | 87 | 2-Ethylphenol |
| 6.585 | 9.605489 | 91 | 3-Ethylphenol |
| 7.034 | 3.773585 | 95 | Benzene-1,2-diol |
| 7.43 | 2.401372 | 93 | 4-Methyl-benzene-1,2-diol |
| 7.472 | 2.744425 | 75 | 4-Hydroxy-3-methoxy-benzaldehyde |
| 7.806 | 8.233276 | 81 | 2-Hydroxyphenylethyl alcohol |
| 7.924 | 2.401372 | 72 | 2-Hydroxy-benzoic acid |
| 8.056 | 4.116638 | 77 | (3-Hydroxy-phenyl)-acetic acid |
| 8.212 | 3.773585 | 75 | (4-Hydroxy-phenyl)-acetic acid |

Table 5.18: The GC-MS analysis of bio-oil products of corn stover liquefaction using $Fe_2O_3$, Ni (270°C) and KOAc of Run 5.5.

| Ret. Time (min) | Area% | Similarity% | Compound name |
|---|---|---|---|
| 2.798 | 46.15385 | 96 | Acetic acid |

| | | | |
|---|---|---|---|
| 3.474 | 12.82051 | 97 | Propionic acid |
| 5.389 | 17.30769 | 95 | Phenol |
| 6.588 | 14.10256 | 90 | 3-Ethylphenol |
| 7.809 | 9.615385 | 77 | 4-Methyl-benzene-1,2-diol |

Table 5.19: The GC-MS analysis of bio-oil products of corn stover liquefaction using $Fe_2O_3$, Ni (270°C), and KOAc of Run 5.6.

| Ret. Time (min) | Area% | Similarity% | Compound name |
|---|---|---|---|
| 2.805 | 12.34043 | 95 | Acetic acid |
| 3.464 | 3.971631 | 97 | Propionic acid |
| 4.113 | 2.695035 | 91 | Butyric acid |
| 4.835 | 3.546099 | 87 | (2-Ethoxyethoxy)acetic acid |
| 4.946 | 1.41844 | 84 | Butane-2,3-diol |
| 5.337 | 4.539007 | 82 | Propane, 1,1-diethoxy- |
| 5.382 | 5.815603 | 96 | Phenol |
| 5.502 | 3.829787 | 80 | 2-Oxopentanoic acid |
| 5.559 | 1.843972 | 65 | 3-Acetoxybutyric acid |
| 5.675 | 1.41844 | 65 | 1,3-Pentanediol |
| 5.809 | 1.843972 | 80 | 2-Hexenoic acid |
| 5.856 | 1.985816 | 75 | Succinic acid monopropyl ester |
| 6.003 | 6.808511 | 80 | (Tetrahydro-furan-2-yl)-methanol |
| 6.046 | 2.269504 | 72 | 2-Methyl-phenol |
| 6.087 | 1.41844 | 56 | 4-Methyl-2-oxo-pentanoic acid |

| | | | |
|---|---|---|---|
| 6.326 | 2.411348 | 92 | 2-Ethylphenol |
| 6.506 | 2.269504 | 82 | 2-Methoxyphenol |
| 6.582 | 7.51773 | 91 | 3-Ethylphenol |
| 6.719 | 1.276596 | 73 | Succinic acid |
| 7.291 | 3.829787 | 85 | 2-Isopropyl-5-methyl-phenol |
| 7.467 | 1.134752 | 80 | 4-Hydroxy-3-methoxy-benzaldehyde |
| 7.804 | 1.134752 | 76 | 2-(2-Hydroxy-ethyl)-phenol |
| 7.993 | 3.546099 | 76 | 1-(2-Hydroxy-phenyl)-propan-1-one |
| 8.158 | 1.276596 | 64 | (4-Hydroxy-phenyl)-acetic acid |
| 8.208 | 1.134752 | 75 | (3-Hydroxy-phenyl)-acetic acid |
| 8.245 | 1.276596 | 69 | 4-Hydroxy-3-methyl-benzoic acid |
| 8.4 | 1.41844 | 57 | Benzene-1,3,5-tricarboxylic acid trimethyl ester |
| 8.463 | 1.41844 | 66 | 4-tert-Butyl-benzene-1,2-diol |

Table 5.20: The GC-MS analysis of bio-oil products of corn stover liquefaction using $Fe_2O_3$, Ni ($H_2$), and KOAc of Run 5.7.

| Ret. Time (min) | Area% | Similarity% | Compound name |
|---|---|---|---|
| 4.126 | 9.883721 | 93 | Butyric acid |
| 5.486 | 22.09302 | 96 | Hexanoic acid |
| 5.696 | 10.46512 | 97 | 2-Ethyl-hexan-1-ol |
| 6.009 | 10.46512 | 81 | (Tetrahydro-furan-2-yl)-methanol |
| 6.189 | 6.976744 | 96 | Octan-1-ol |

| | | | |
|---|---|---|---|
| 6.947 | 2.906977 | 80 | 1,4-Benzenediol, 2,5-dimethyl- |
| 7.271 | 8.139535 | 71 | 2-Isopropyl-5-methylphenol |
| 7.652 | 3.488372 | 53 | 4-(1,1-Dimethyl-propyl)-phenol |
| 7.784 | 4.651163 | 72 | Decanoic acid |
| 8.007 | 15.11628 | 77 | 3-(3-Hydroxy-phenyl)-acrylic acid methyl ester |
| 8.106 | 5.813953 | 68 | 5-Isopropyl-2-methyl-phenol |

Table 5.21: The GC-MS analysis of bio-oil products of corn stover liquefaction using $Fe_2O_3$, Ni ($H_2$), and KOAc of Run 5.8.

| Ret. Time (min) | Area% | Similarity% | Compound name |
|---|---|---|---|
| 2.847 | 5.714286 | 82 | Propan-2-ol |
| 4.117 | 6.153846 | 93 | Butyric acid |
| 4.819 | 1.538462 | 96 | Pentanoic acid |
| 4.895 | 5.054945 | 97 | Hexanol |
| 4.983 | 1.758242 | 81 | 2-Oxo-pentanoic acid |
| 5.212 | 1.098901 | 85 | 4-Methylvaleric acid |
| 5.333 | 2.857143 | 89 | (Tetrahydro-furan-2-yl)-methanol |
| 5.481 | 6.373626 | 91 | Hexanoic acid |
| 5.687 | 9.010989 | 97 | 2-Propyl-pentan-1-ol |
| 6.083 | 3.296703 | 82 | 2-Ethyl-hexanoic acid |
| 6.193 | 4.835165 | 96 | Octan-1-ol |
| 6.325 | 1.978022 | 78 | 2-Ethylphenol |

| | | | |
|---|---|---|---|
| 6.51 | 3.076923 | 74 | Octan-4-ol |
| 6.589 | 2.637363 | 87 | 3-Ethylphenol |
| 6.699 | 1.978022 | 83 | Octanoic acid |
| 6.84 | 1.758242 | 85 | Decan-1-ol |
| 7.293 | 4.175824 | 84 | 2-Isopropyl-5-methyl-phenol |
| 7.469 | 1.318681 | 71 | 4-Hydroxy-3-methoxy-benzaldehyde |
| 7.667 | 3.076923 | 52 | Butyric acid, 4-ethoxy- |
| 8.004 | 1.538462 | 73 | 3-(4-Hydroxy-phenyl)-acrylic acid methyl ester |
| 8.657 | 2.197802 | 62 | 3-(3-Hydroxy-phenyl)-acrylic acid methyl ester |

Table 5.22: The GC-MS analysis of bio-oil products of corn stover liquefaction using $Fe_2O_3$, Ni ($H_2$), and KOAc of Run 5.9.

| Ret. Time (min) | Area% | Similarity% | Compound name |
|---|---|---|---|
| 2.31 | 7.713499 | 72 | Ethane-1,2-diol |
| 2.8 | 12.02938 | 96 | Acetic acid |
| 3.468 | 1.74472 | 97 | Propionic acid |
| 4.115 | 1.74472 | 92 | Butyric acid |
| 4.837 | 2.571166 | 87 | (2-Ethoxyethoxy)acetic acid |
| 4.948 | 1.101928 | 89 | Propane-1,2-diol |
| 5.338 | 3.673095 | 83 | Propane, 1,1-diethoxy- |
| 5.384 | 4.499541 | 96 | Phenol |

| | | | |
|---|---|---|---|
| 5.503 | 3.030303 | 84 | 2-Methyl-pent-4-enoic acid |
| 5.562 | 1.74472 | 76 | 2-Ethoxytetrahydrofuran |
| 5.675 | 1.101928 | 71 | Benzene-1,4-diol |
| 5.754 | 1.010101 | 70 | 16-Hydroxy-octadec-9-enoic acid methyl ester |
| 5.81 | 1.74472 | 85 | 2-Hexenoic acid |
| 5.857 | 1.928375 | 74 | 1,3-Dioxolane, 2-cyclohexyl-4,5-dimethyl- |
| 6.004 | 3.948577 | 79 | (Tetrahydro-furan-2-yl)-methanol |
| 6.047 | 1.37741 | 79 | 2-Methyl-phenol |
| 6.109 | 1.010101 | 72 | 2-Ethyl-malonic acid |
| 6.327 | 2.203857 | 89 | 2-Ethylphenol |
| 6.506 | 1.652893 | 86 | 2-Methoxyphenol |
| 6.583 | 5.785124 | 90 | 3-Ethylphenol |
| 6.72 | 1.285583 | 79 | Succinic acid |
| 7.153 | 1.469238 | 89 | Pentanedioic acid |
| 7.292 | 3.581267 | 86 | 2-Isopropyl-5-methyl-phenol |
| 7.349 | 1.101928 | 80 | 3-Hydroxy-4-methoxy-benzaldehyde |
| 7.467 | 1.193756 | 82 | 4-Hydroxy-3-methoxy-benzaldehyde |
| 7.713 | 1.193756 | 71 | 3-Ethoxy-4-hydroxy-benzaldehyde |
| 8.004 | 1.193756 | 74 | 3-(4-Hydroxy-phenyl)-acrylic acid methyl ester |
| 8.209 | 1.010101 | 73 | (4-Hydroxy-phenyl)-acetic acid |

| | | | |
|---|---|---|---|
| 8.463 | 2.203857 | 70 | 2-tert-Butyl-benzene-1,4-diol |
| 8.644 | 1.469238 | 61 | 5-Acetyl-2-hydroxy-benzoic acid |
| 8.701 | 1.101928 | 73 | 5-Allyl-3-methoxy-benzene-1,2-diol |

Table 5.23: The GC-MS analysis of bio-oil products of corn stover liquefaction using $Fe_2O_3$, Ni ($H_2$), and KOAc of Run 5.10.

| Ret. Time (min) | Area% | Similarity% | Compound name |
|---|---|---|---|
| 2.801 | 28.46656 | 96 | Acetic acid |
| 3.452 | 6.460822 | 97 | Propionic acid |
| 4.109 | 3.26108 | 92 | Butyric acid |
| 4.839 | 6.753158 | 86 | (2-Ethoxyethoxy)acetic acid |
| 4.899 | 1.558677 | 85 | Ethoxy-acetic acid |
| 5.056 | 1.40369 | 74 | 2-Pentenoic acid |
| 5.34 | 8.364947 | 83 | Propane, 1,1-diethoxy- |
| 5.388 | 2.256575 | 88 | Phenol |
| 5.504 | 4.224136 | 81 | 2-Methyl-pent-4-enoic acid |
| 5.57 | 1.857034 | 74 | Furan, tetrahydro-2-(methoxymethyl)- |
| 5.599 | 1.052712 | 69 | 2-Isopropoxy-2-phenylcyclopropane carboxylic acid,ethyl ester |
| 5.68 | 1.118198 | 67 | 5-Ethyl-2-furaldehyde |
| 5.756 | 1.14743 | 78 | Cyclopentanone, 3-butyl- |
| 5.812 | 2.417292 | 79 | 2-Hexenoic acid |
| 5.858 | 3.75554 | 77 | 4-Oxoheptanedioic acid |

| | | | |
|---|---|---|---|
| 6.004 | 14.05565 | 80 | (Tetrahydro-furan-2-yl)-methanol |
| 6.079 | 1.628712 | 50 | Hexa-2,4-dienoic acid |
| 6.112 | 1.163194 | 66 | 2-Ethyl-malonic acid |
| 6.586 | 2.515689 | 81 | 3-Ethylphenol |
| 7.157 | 1.1883 | 83 | Pentanedioic acid |
| 7.994 | 1.721802 | 74 | 1-(2-Hydroxy-phenyl)-propan-1-one |

Table 5.24: The GC-MS analysis of bio-oil products of corn stover liquefaction using Zn and $Ni(OAc)_2$ of Run 5.14.

| Ret. Time (min) | Area% | Similarity% | Compound name |
|---|---|---|---|
| 2.814 | 3.444667 | 94 | Acetic acid |
| 3.431 | 4.384499 | 96 | Butan-1-ol |
| 3.472 | 1.244458 | 97 | propanoate |
| 3.645 | 1.103498 | 95 | But-2-en-1-ol |
| 4.12 | 1.430633 | 91 | Butanoic acid |
| 4.521 | 1.343647 | 94 | 3-Methyl-pentan-1-ol |
| 4.791 | 2.054133 | 85 | 3-Methyl-but-2-en-1-ol |
| 4.842 | 2.415795 | 86 | (2-Ethoxy-ethoxy)-acetic acid |
| 4.898 | 7.251535 | 92 | Hexan-1-ol |
| 5.026 | 6.45094 | 91 | cis-2-Hexen-1-ol |
| 5.388 | 7.186311 | 97 | Phenol |
| 5.482 | 2.29999 | 77 | Hexanoic acid |
| 5.522 | 5.271685 | 80 | 2-Oxopentanedioic acid |

| | | | |
|---|---|---|---|
| 5.606 | 1.400237 | 66 | Propanoic acid, decyl ester |
| 5.694 | 2.366438 | 83 | 2-Ethyl-hexan-1-ol |
| 5.738 | 2.022212 | 87 | 3-Hexene, 2,2-dimethyl-, (Z)- |
| 5.81 | 2.217405 | 81 | 2-Hexenoic acid |
| 5.858 | 3.385587 | 75 | 4-Oxo-heptanedioic acid |
| 5.92 | 1.131009 | 77 | 2-Methyl-phenol |
| 6.004 | 4.440144 | 78 | (Tetrahydro-furan-2-yl)-methanol |
| 6.057 | 3.409954 | 77 | Phenyl-methanol |
| 6.136 | 1.646281 | 66 | 3-Cyclopentylpropionic acid, 2-methylphenyl ester |
| 6.189 | 2.011481 | 86 | Octan-1-ol |
| 6.258 | 1.857041 | 88 | 2-Hydroxy-pentanoic acid |
| 6.329 | 1.532978 | 82 | 2-Ethylphenol |
| 6.413 | 1.10136 | 59 | 2,3-Dimethylphenol |
| 6.509 | 2.087809 | 68 | 2-Methoxyphenol |
| 6.583 | 8.28653 | 91 | 3-Ethylphenol |
| 7.292 | 1.120165 | 82 | 2-Isopropyl-5-methyl-phenol |

Table 5.25: The GC-MS analysis of bio-oil products of corn stover liquefaction using Zn and $Ni(OAc)_2$ of Run 5.15.

| Ret. Time (min) | Area% | Similarity% | Compound name |
|---|---|---|---|
| 2.796 | 11.40649 | 96 | Acetic acid |

| | | | |
|---|---|---|---|
| 3.422 | 5.842592 | 97 | Butan-1-ol |
| 4.121 | 3.120488 | 92 | Butanoic acid |
| 4.522 | 2.030533 | 95 | 2-Methyl-pentan-1-ol |
| 4.795 | 2.796267 | 87 | 3-Methyl-but-2-en-1-ol |
| 4.901 | 7.890344 | 92 | Hexan-1-ol |
| 5.028 | 5.751844 | 90 | cis-2-Hexen-1-ol |
| 5.342 | 1.857906 | 82 | Propane, 1,1-diethoxy- |
| 5.389 | 2.864284 | 97 | Phenol |
| 5.485 | 8.233333 | 95 | Hexanoic acid |
| 5.696 | 1.557488 | 85 | 2-Ethyl-hexan-1-ol |
| 5.81 | 2.625946 | 85 | 2-Hexenoic acid |
| 5.858 | 1.933509 | 78 | 2-Oxopentanedioic acid |
| 6.007 | 1.452973 | 78 | (Tetrahydro-furan-2-yl)-methanol |
| 6.06 | 3.995984 | 90 | Phenyl-methanol |
| 6.259 | 1.512162 | 88 | 2-Hydroxy-pentanoic acid |
| 6.585 | 2.775992 | 90 | 3-Ethylphenol |
| 6.678 | 1.545358 | 73 | 2-Phenyl-ethanol |

Table 5.26: The GC-MS analysis of bio-oil products of corn stover liquefaction using Zn and $Ni(OAc)_2$ of Run 5.16.

| Ret. Time (min) | Area% | Similarity% | Compound name |
|---|---|---|---|
| 2.807 | 1.518648 | 93 | Acetic acid |
| 4.308 | 1.2784 | 96 | Butanoic acid, 2-hydroxy-, ethyl ester |

| | | | |
|---|---|---|---|
| 4.96 | 5.160213 | 85 | Butane-2,3-diol |
| 5.008 | 3.599178 | 80 | 3-Hexanol, 2-methyl- |
| 5.387 | 6.693567 | 97 | Phenol |
| 5.452 | 5.078389 | 86 | 2-Methyl-3-pentanol |
| 5.482 | 1.027907 | 68 | 2-Hydroxy-butyric acid |
| 5.518 | 2.332244 | 76 | 2-Oxopentanedioic acid |
| 5.562 | 6.166917 | 91 | Butanoic acid, anhydride |
| 5.676 | 1.587879 | 74 | 1,2-Butanediol |
| 5.756 | 1.913055 | 67 | 8-Heptadecene, 1-chloro- |
| 5.815 | 1.585436 | 94 | 2-Hydroxy-butyric acid |
| 5.856 | 2.029971 | 69 | 3-Hydroxypropanoic acid ethyl ester |
| 5.965 | 3.727776 | 84 | 2,4-Dimethyl-3-pentanol |
| 6.005 | 1.797905 | 77 | (Tetrahydro-furan-2-yl)-methanol |
| 6.05 | 1.232946 | 68 | 2-Methyl-phenol |
| 6.107 | 1.706269 | 86 | 2-Ethyl-malonic acid |
| 6.259 | 2.914466 | 92 | 2-Hydroxy-pentanoic acid |
| 6.329 | 1.612891 | 72 | 2-Ethylphenol |
| 6.507 | 3.18726 | 91 | 2-Methoxyphenol |
| 6.584 | 8.574917 | 90 | 3-Ethylphenol |
| 6.733 | 1.689355 | 85 | 2-Hydroxy-3-methyl-pentanoic acid |
| 6.85 | 1.493631 | 55 | 2-Ethoxy-phenol |
| 6.966 | 1.341388 | 64 | Heptanedioic acid |
| 7.095 | 1.590002 | 71 | 2-Decen-1-ol |

| | | | |
|---|---|---|---|
| 7.39 | 1.213777 | 67 | Hexahydro-furo[3,2-b]furan-3,6-diol |
| 7.466 | 1.8273 | 82 | 4-Hydroxy-3-methoxy-benzaldehyde |
| 7.722 | 1.614863 | 70 | 1-[3-(1-Hydroxy-1-methyl-ethyl)-oxiranyl]-pentan-1-ol |

Table 5.27: The GC-MS analysis of bio-oil products of corn stover liquefaction using Zn and $Ni(OAc)_2$ of Run 5.17.

| Ret. Time (min) | Area% | Similarity% | Compound name |
|---|---|---|---|
| 2.784 | 9.5199 | 96 | Acetic acid |
| 3.411 | 4.419609 | 96 | Butan-1-ol |
| 3.627 | 1.443254 | 97 | But-2-en-1-ol |
| 4.104 | 2.044568 | 92 | Butanoic acid |
| 4.779 | 1.937388 | 86 | 3-Methyl-but-2-en-1-ol |
| 4.828 | 1.152668 | 85 | (2-Ethoxy-ethoxy)-acetic acid |
| 4.885 | 3.352859 | 92 | 2-Ethyl-butan-1-ol |
| 4.92 | 1.13149 | 72 | Hex-3-en-1-ol |
| 5.014 | 5.073159 | 88 | cis-2-Hexen-1-ol |
| 5.375 | 4.584914 | 97 | Phenol |
| 5.492 | 8.280775 | 85 | 2-ketohexanoic acid |
| 5.681 | 1.418618 | 73 | 2,4,4-Trimethyl-pentan-1-ol |
| 5.722 | 1.381613 | 83 | 3-Hexene, 2,2-dimethyl-, (E)- |
| 5.797 | 4.188896 | 91 | 2-Hexenoic acid |
| 5.846 | 2.3804 | 77 | 2-Oxopentanedioic acid |

| | | | |
|---|---|---|---|
| 5.937 | 1.025595 | 76 | 2-Methyl-butanediol |
| 5.992 | 3.564239 | 78 | (Tetrahydro-furan-2-yl)-methanol |
| 6.046 | 4.065205 | 88 | Phenyl-methanol |
| 6.169 | 1.481724 | 65 | 15-Hydroxy-octadec-9-enoic acid methyl ester |
| 6.247 | 1.147425 | 92 | 2-Hydroxy-pentanoic acid |
| 6.316 | 1.740026 | 86 | 2-Ethylphenol |
| 6.402 | 1.175096 | 63 | Tetradec-9-en-5-ol |
| 6.498 | 1.91058 | 69 | 4-Phenoxy-butan-1-ol |
| 6.572 | 2.815624 | 90 | 3-Ethylphenol |
| 6.6 | 1.427611 | 91 | o-Tolyl-methanol |
| 6.662 | 1.338694 | 78 | 4-Methylbenzyl alcohol |
| 6.709 | 1.033479 | 74 | Succinic acid monoethyl ester |
| 7.141 | 1.14785 | 88 | Pentanedioic acid monoethyl ester |
| 7.279 | 1.616069 | 81 | 2-Isopropyl-5-methyl-phenol |

Table 5.28: The GC-MS analysis of bio-oil products of corn stover liquefaction using Zn and $Ni(OAc)_2$ of Run 5.18.

| Ret. Time (min) | Area% | Similarity% | Compound name |
|---|---|---|---|
| 5.444 | 2.405112 | 85 | 2-Methyl-pentan-3-ol |
| 6.574 | 2.172408 | 92 | 3-Ethylphenol |
| 6.824 | 13.62842 | 76 | 3-Methyl-phenol |
| 7.279 | 1.603903 | 81 | 3-Hydroxy-butan-2-one |

| | | | |
|---|---|---|---|
| 7.399 | 2.567399 | 92 | 4-Hydroxy-benzaldehyde |
| 7.569 | 12.01864 | 78 | 1-(4-Hydroxy-phenyl)-ethanone |
| 7.703 | 1.137148 | 65 | 4-(3-Hydroxy-phenyl)-butyric acid |
| 7.801 | 2.522639 | 87 | Pentane-1,2,5-triol |
| 8.235 | 1.456708 | 71 | 4-Hydroxy-3-methoxy-benzaldehyde |
| 9.063 | 1.343307 | 67 | (4-Hydroxy-3-methoxy-phenyl)-acetic acid methyl ester |
| 9.12 | 1.93475 | 64 | 2-Methoxy-4-propenyl-phenol |
| 9.845 | 28.12733 | 78 | 3-(3-Hydroxy-phenyl)-acrylic acid ethyl ester |
| 10.502 | 2.679552 | 59 | Hexadecanoic acid, ethyl ester |
| 10.754 | 9.085501 | 60 | 3-(3-Hydroxy-4-methoxy-phenyl)-propionic acid methyl ester |
| 11.83 | 1.106823 | 82 | Ethyl Oleate |

Table 5.29: The GC-MS analysis of bio-oil products of corn stover liquefaction using Zn and $Ni(OAc)_2$ of Run 5.19.

| Ret. Time (min) | Area% | Similarity% | Compound name |
|---|---|---|---|
| 4.951 | 5.368118 | 83 | Propane-1,2-diol |
| 5.444 | 4.413262 | 86 | 2-Methyl-3-pentanol |
| 6.576 | 2.549011 | 91 | 3-Ethylphenol |
| 6.827 | 10.39298 | 75 | 3-Methyl-phenol |
| 7.049 | 1.181683 | 85 | 2,3-Diethoxy-propionic acid, ethyl ester |

| | | | |
|---|---|---|---|
| 7.402 | 1.881571 | 92 | 4-Hydroxy-benzaldehyde |
| 7.498 | 1.332387 | 93 | 2,6-Dimethoxyphenol |
| 7.572 | 10.70402 | 78 | 1-(4-Hydroxy-phenyl)-ethanone |
| 7.704 | 1.423022 | 64 | 4-(3-Hydroxy-phenyl)-butyric acid |
| 7.803 | 3.805951 | 86 | Pentane-1,2,5-triol |
| 8.237 | 1.93846 | 75 | Ethoxy-(4-hydroxy-3-methoxy-phenyl)-acetic acid ethyl ester |
| 8.381 | 1.460725 | 76 | 2-Methoxy-4-propenyl-phenol |
| 9.122 | 2.265187 | 59 | 4-[2-(2-Hydroxy-ethoxy)-ethyl]-2-methoxy-phenol |
| 9.848 | 19.94269 | 66 | P-Hydroxycinnamic acid, methyl ester |
| 10.505 | 1.826047 | 96 | Hexadecanoic acid, ethyl ester |
| 10.758 | 8.21962 | 61 | 3-Hydroxy-4-methoxycinnamic acid, methyl ester |

Table 5.30: The GC-MS analysis of EtOH distillate products of corn stover liquefaction using Zn and $Ni(OAc)_2$ of Run 5.14.

| Ret. Time (min) | Area% | Similarity% | Compound name |
|---|---|---|---|
| 0.191 | 35.01634 | 53 | 1,2-Propadiene-1,3-dione |
| 1.912 | 14.15114 | 96 | Methanol |
| 2.14 | 6.539966 | 97 | Ethyl Acetate |
| 2.364 | 1.045826 | 88 | Propane, 2,2-dimethoxy- |
| 2.451 | 3.064623 | 90 | 1-Butanol |

| | | | |
|---|---|---|---|
| 3.118 | 2.424837 | 88 | 2,2-Dimethoxybutane |
| 10.833 | 3.10489 | 89 | Hexadecanoic acid |

Table 5.31: The GC-MS analysis of EtOH distillate products of corn stover liquefaction using Zn and $Ni(OAc)_2$ of Run 5.16.

| Ret. Time (min) | Area% | Similarity% | Compound name |
|---|---|---|---|
| 1.913 | 18.26331 | 96 | Methanol |
| 1.996 | 1.435841 | 83 | Pentane, 3-methyl- |
| 2.067 | 6.558693 | 90 | Pentane, 2,4-dimethyl- |
| 2.143 | 49.52443 | 98 | Ethyl Acetate |
| 2.236 | 2.522186 | 82 | 1-Pentanol, 4-methyl- |
| 2.368 | 2.380369 | 87 | Propane, 2,2-dimethoxy- |
| 2.457 | 2.797408 | 90 | 1-Butanol |
| 2.75 | 3.465993 | 91 | Propanoic acid, ethyl ester |
| 2.881 | 7.076807 | 93 | Ethane, 1,1-diethoxy- |
| 3.121 | 5.974958 | 89 | 2,2-Dimethoxybutane |

Table 5.32: The GC-MS analysis of EtOH distillate products of corn stover liquefaction using Zn and $Ni(OAc)_2$ of Run 5.17.

| Ret. Time (min) | Area% | Similarity% | Compound name |
|---|---|---|---|
| 1.901 | 42.68004 | 96 | Methanol |
| 2.046 | 5.592696 | 79 | 2-Hexanone, 3,4-dimethyl- |
| 2.129 | 34.31124 | 98 | Ethyl Acetate |

| | | | |
|---|---|---|---|
| 2.352 | 4.40956 | 88 | Propane, 2,2-dimethoxy- |
| 3.106 | 13.00646 | 87 | 2,2-Dimethoxybutane |

## 5.4 Conclusions

The catalytic liquefaction of corn stover by various combinations of Ni metal + $Fe_2O_3$ + KOAc, Ni metal + ZnO + NaOH/KOAc, and Ni metal + FeO + NaOH + activated carbon was conducted under different conditions. The results of liquefaction catalyzed by Ni metal + $Fe_2O_3$ showed that bio-oil yield was enhanced by the addition of KOAc giving ~ 38-40%, and great production of bio-oil was achieved by the increase in the amount of Ni ($H_2$) metal at 300 $^oC$ in less than 4 h. The catalytic liquefaction results using Ni metal + ZnO + KOAc confirmed that KOAc has a better influence on biomass liquefaction than NaOH, giving > 50% of bio-oil at 300 $^oC$ in lower than 2 h. Using a mix of EtOH and water instead of only EtOH is better for liquefaction catalyzed by Ni metal and metal oxide under basic conditions. Moreover, oxygenated carbons, condensation reactions, and repolymerized bio-residues were much reduced in liquefaction catalyzed by Ni metal + $Fe_2O_3$/ZnO + KOAc compared to that obtained from liquefaction catalyzed by Ni metal + metal oxide + NaOH (Chapter 4). The bio-oil yields of corn stover liquefaction by $Ni(OAc)_2$ + Fe were improved by adding activated carbon. The pronounced improvement was observed for runs with NaOH added than under neutral conditions. However, because of Fe metal not being a potent reducing agent as Zn metal, bio-oil production using this catalytic system was lower than that generated by Ni + ZnO + NaOH.

## 5.5 Appendix

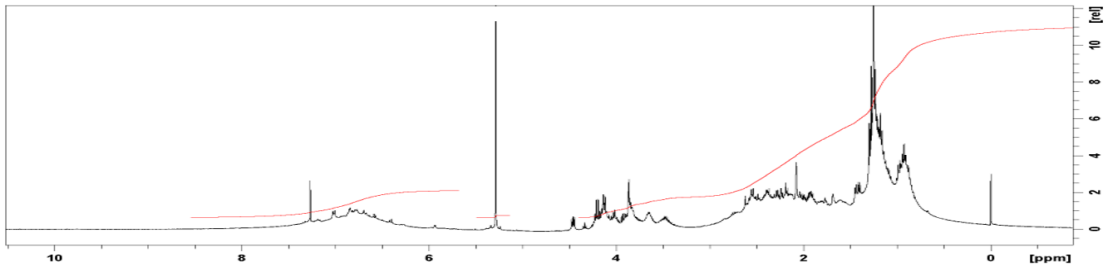


Figure S5.1: The H-NMR spectrum of bio-oil product of corn stover liquefaction using $Fe_2O_3$, Ni (260°C), and KOAc of Run 5.1.

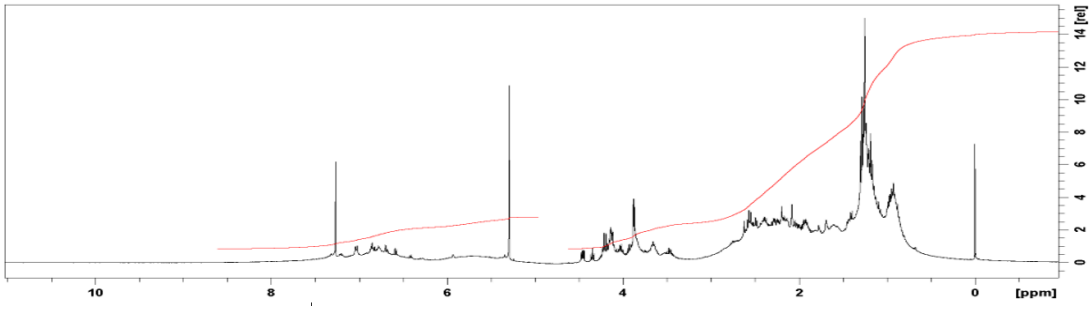


Figure S5.2: The H-NMR spectrum of bio-oil product of corn stover liquefaction using $Fe_2O_3$, Ni (260°C), and KOAc of Run 5.2.

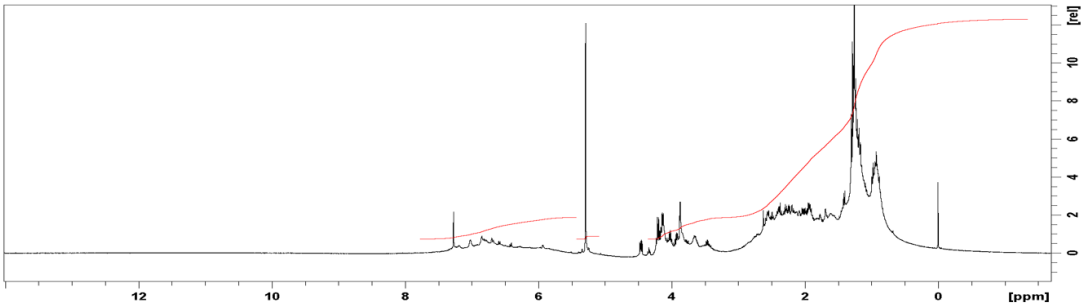


Figure S5.3: The H-NMR spectrum of bio-oil product of corn stover liquefaction using 3.$Fe_2O_3$, Ni (260°C), and KOAc of Run 5.3.

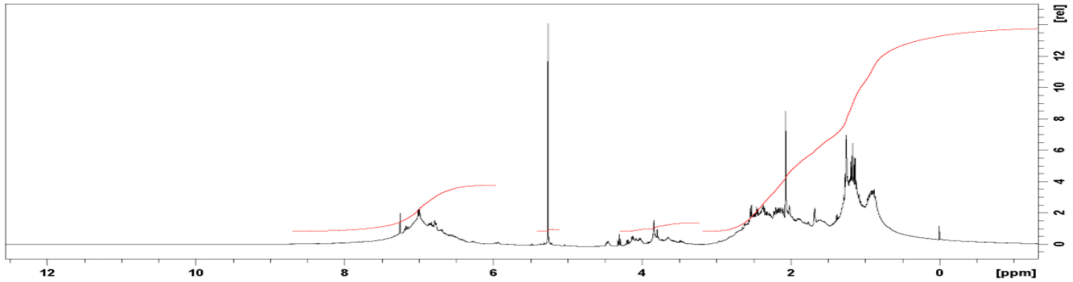


Figure S5.4: The H-NMR spectrum of bio-oil product of corn stover liquefaction using 3.$Fe_2O_3$, Ni (260°C), and KOAc of Run 5.4.

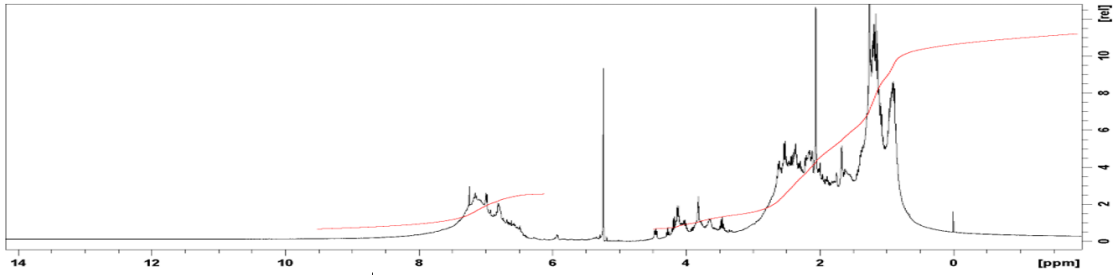


Figure S5.5: The H-NMR spectrum of bio-oil product of corn stover liquefaction using 3.$Fe_2O_3$, Ni (260°C), and KOAc of Run 5.5.

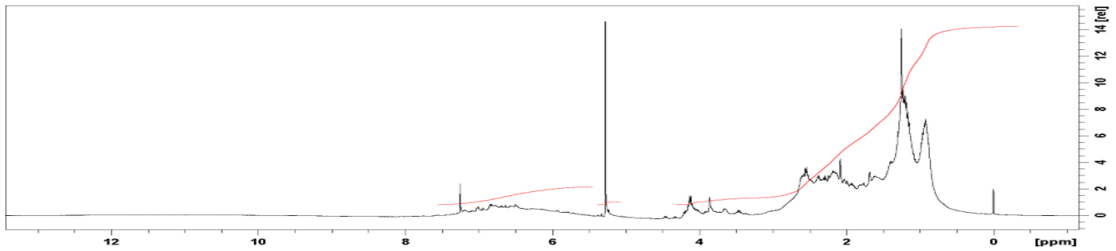


Figure S5.6: The H-NMR spectrum of bio-oil product of corn stover liquefaction using 3.$Fe_2O_3$, Ni (260°C), and KOAc of Run 5.6.

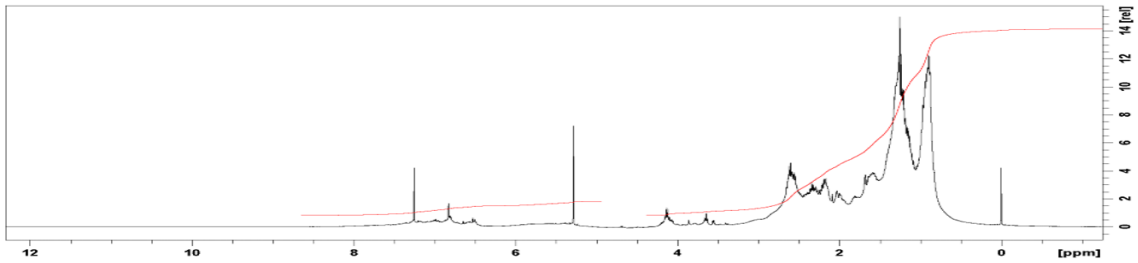


Figure S5.7: The H-NMR spectrum of bio-oil product of corn stover liquefaction using 3.$Fe_2O_3$, Ni ($H_2$), and KOAc of Run 5.7.

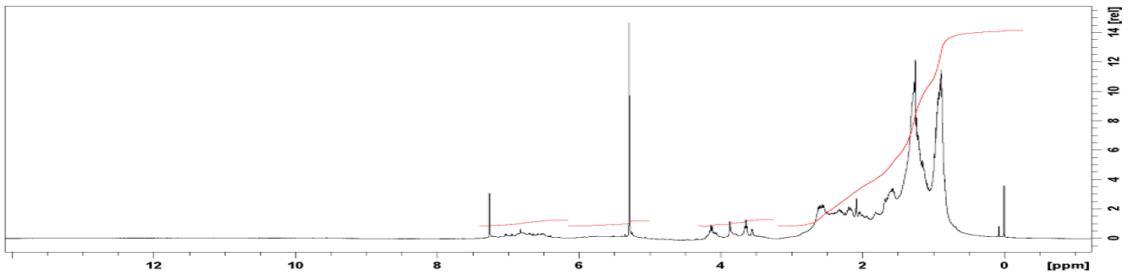


Figure S5.8: The H-NMR spectrum of bio-oil product of corn stover liquefaction using 3.$Fe_2O_3$, Ni ($H_2$), and KOAc of Run 5.8.

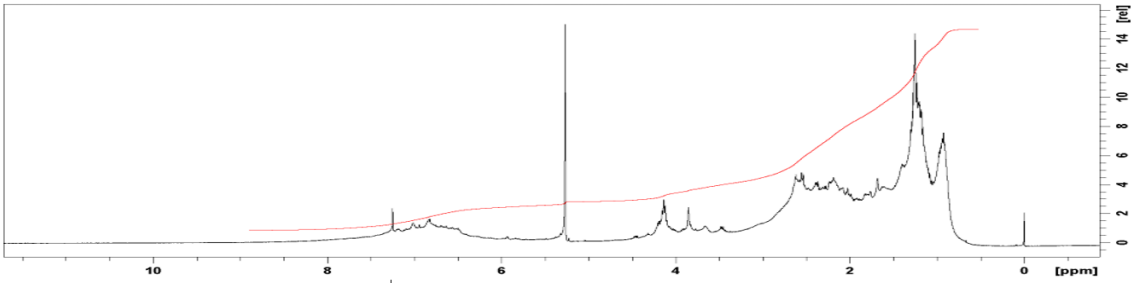


Figure S5.9: The H-NMR spectrum of bio-oil product of corn stover liquefaction using 3.$Fe_2O_3$, Ni ($H_2$), and KOAc of Run 5.9.

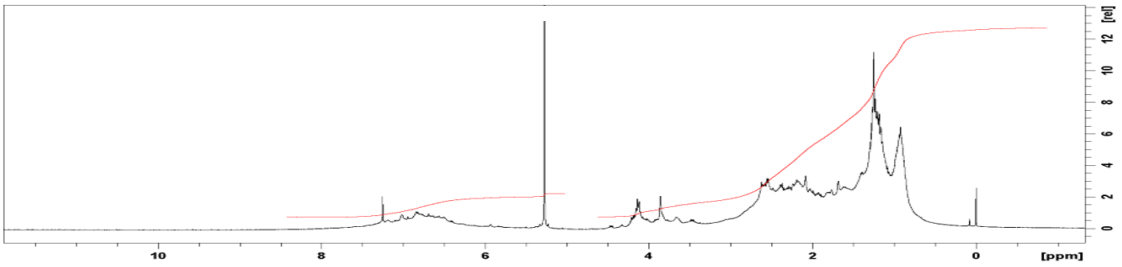


Figure S5.10: The H-NMR spectrum of bio-oil product of corn stover liquefaction using 3.$Fe_2O_3$, Ni ($H_2$), and KOAc of Run 5.10.

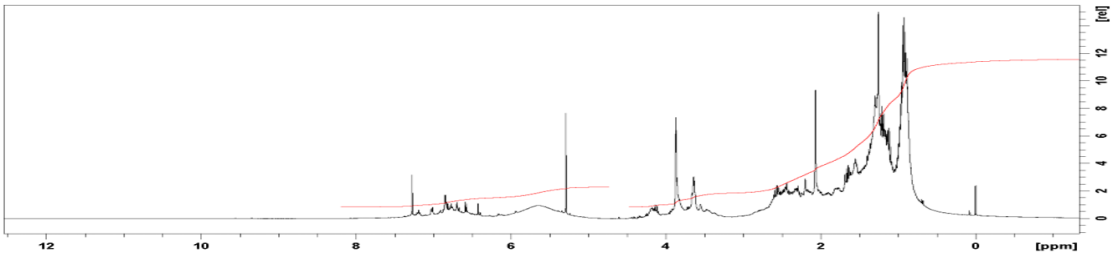


Figure S5.11: The H-NMR spectrum of bio-oil product of corn stover liquefaction using Zn and $Ni(OAc)_2.4H_2O$ of Run 5.11.

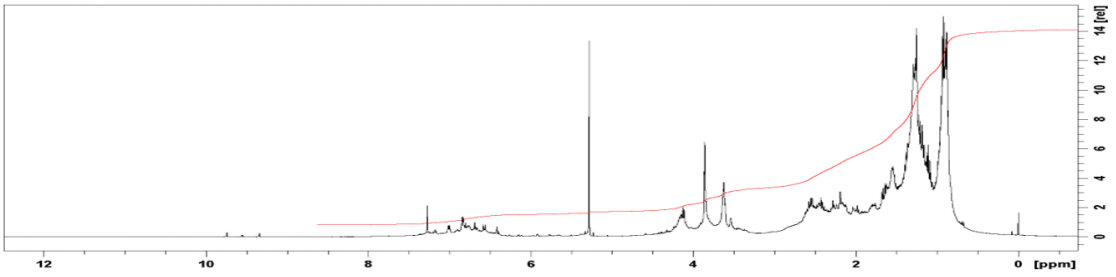


Figure S5.12: The H-NMR spectrum of bio-oil product of corn stover liquefaction using Zn and $Ni(OAc)_2.4H_2O$ of Run 5.12.

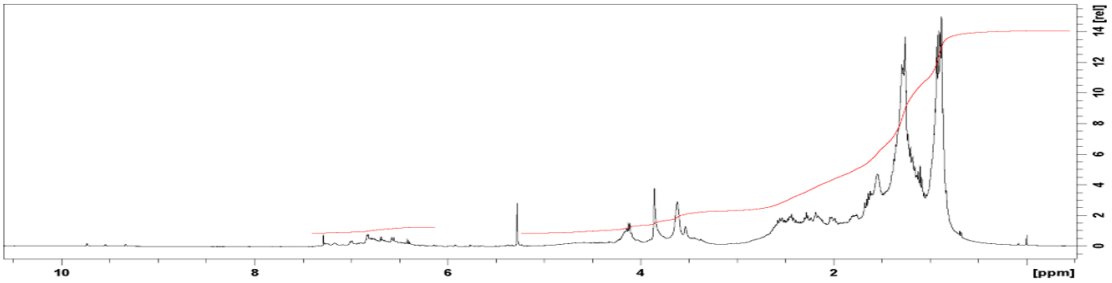


Figure S5.13: The H-NMR spectrum of bio-oil product of corn stover liquefaction using Zn and $Ni(OAc)_2.4H_2O$ of Run 5.13.

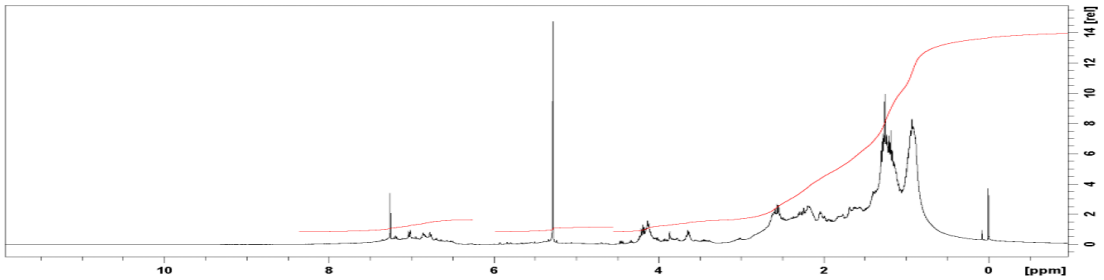


Figure S5.14: The H-NMR spectrum of bio-oil product of corn stover liquefaction using Zn and $Ni(OAc)_2.4H_2O$ of Run 5.14.

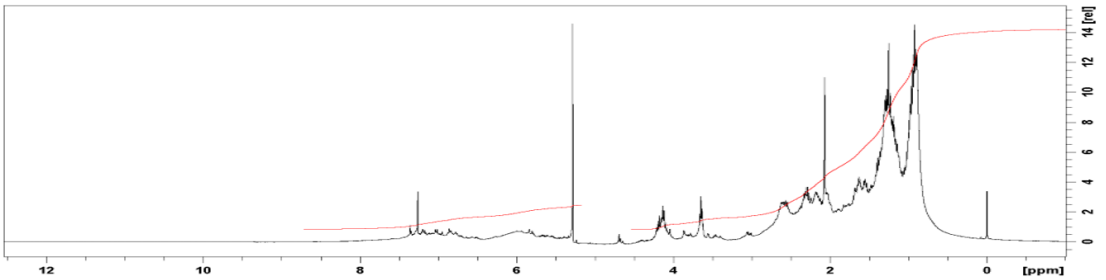


Figure S5.15: The H-NMR spectrum of bio-oil product of corn stover liquefaction using Zn and $Ni(OAc)_2.4H_2O$ of Run S5.15.

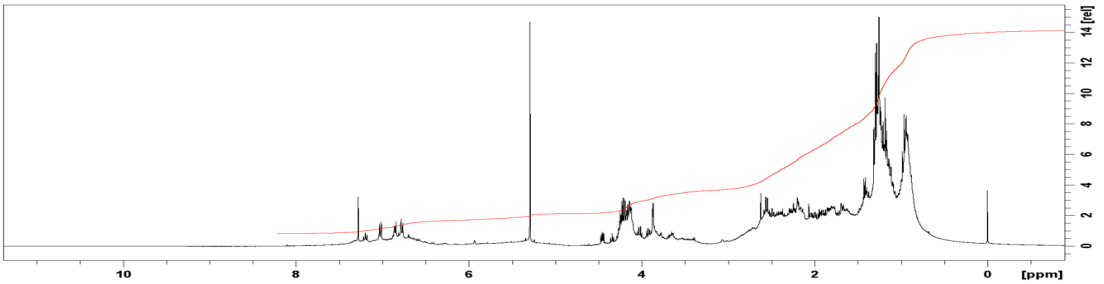


Figure S5.16: The H-NMR spectrum of bio-oil product of corn stover liquefaction using Zn and $Ni(OAc)_2.4H_2O$ of Run 5.16.

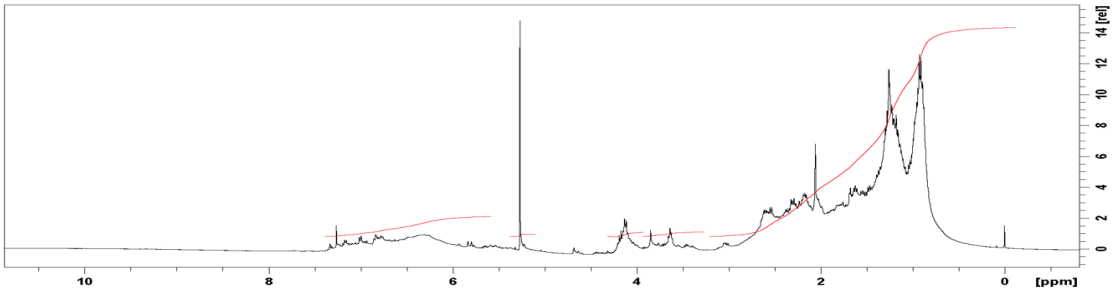


Figure S5.17: The H-NMR spectrum of bio-oil product of corn stover liquefaction using Zn and $Ni(OAc)_2.4H_2O$ of Run 5.17.

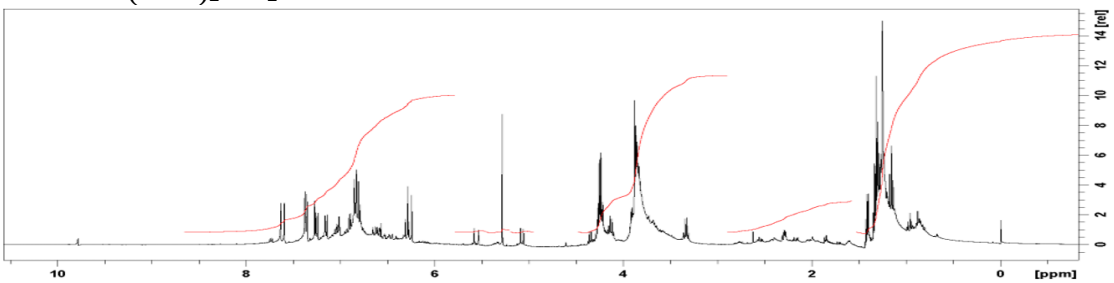


Figure S5.18: The H-NMR spectrum of bio-oil product of corn stover liquefaction using Zn and $Ni(OAc)_2.4H_2O$ of Run 5.18.

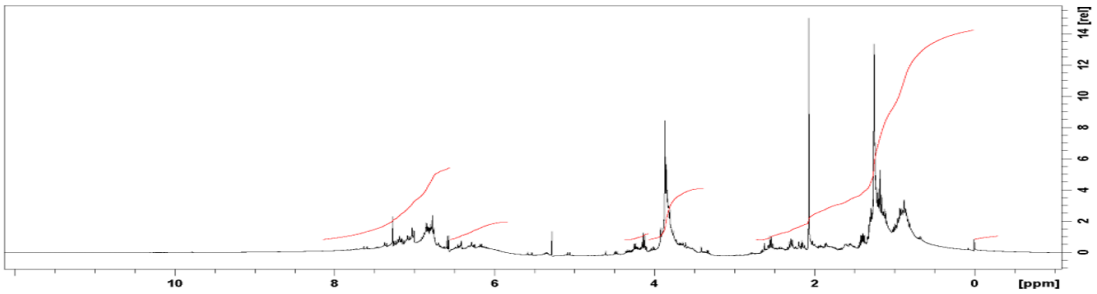


Figure S5.19: The H-NMR spectrum of bio-oil product of corn stover liquefaction using Zn and $Ni(OAc)_2.4H_2O$ of Run 5.19.

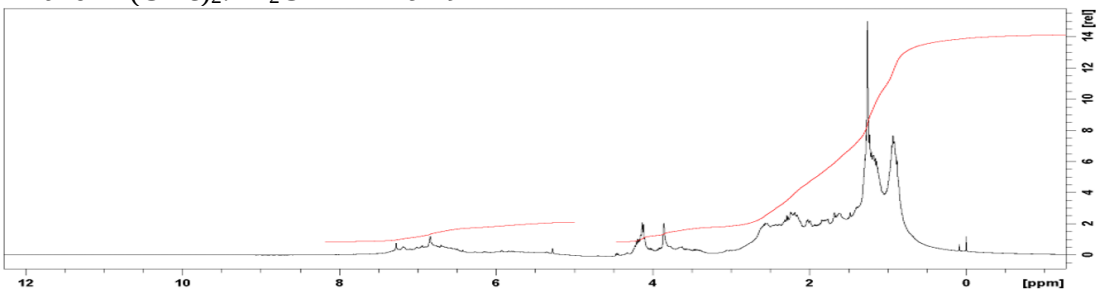


Figure S5.20: The H-NMR spectrum of bio-oil product of corn stover liquefaction using Fe and $Ni(OAc)_2.4H_2O$ of Run 5.20.

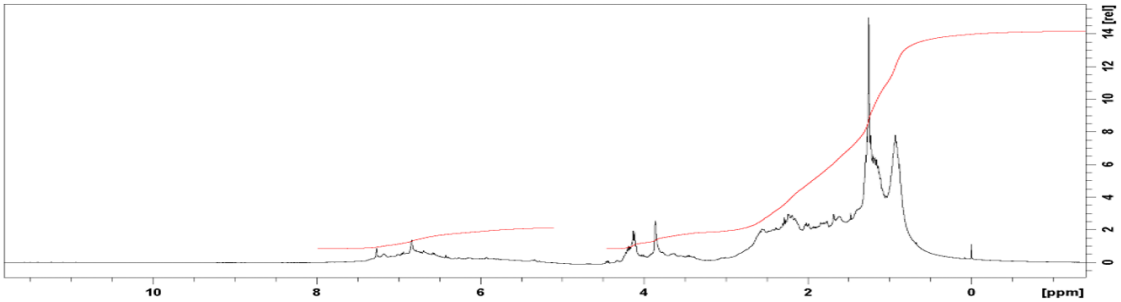


Figure S5.22: The H-NMR spectrum of bio-oil product of corn stover liquefaction using Fe and $Ni(OAc)_2.4H_2O$ of Run 5.22.

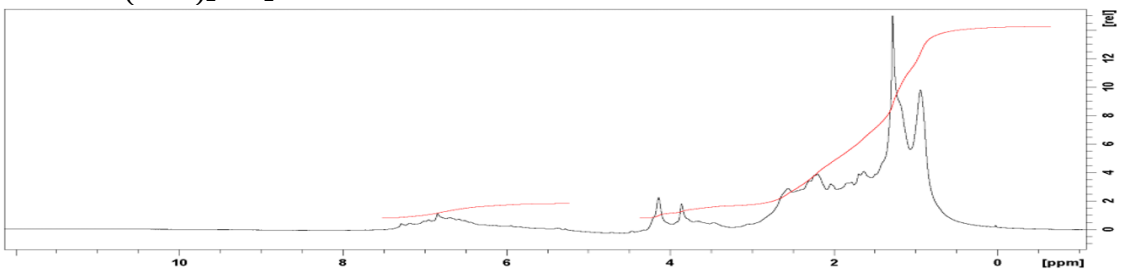


Figure S5.23: The H-NMR spectrum of bio-oil product of corn stover liquefaction using Fe and $Ni(OAc)_2.4H_2O$ of Run 3.

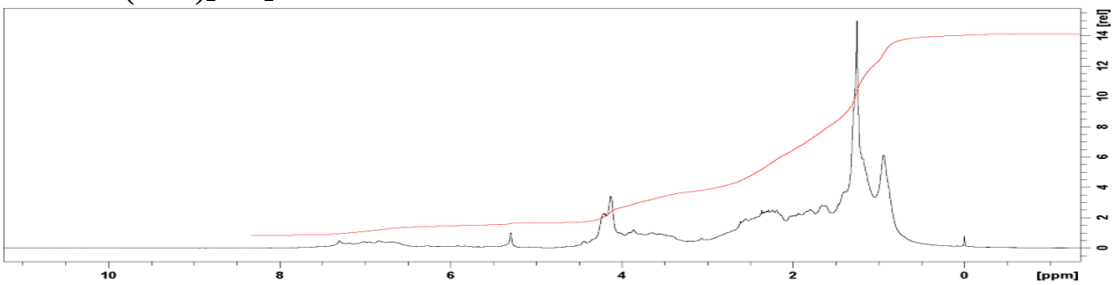


Figure S5.24: The H-NMR spectrum of bio-oil product of corn stover liquefaction using Fe and $Ni(OAc)_2.4H_2O$ of Run 5.24.

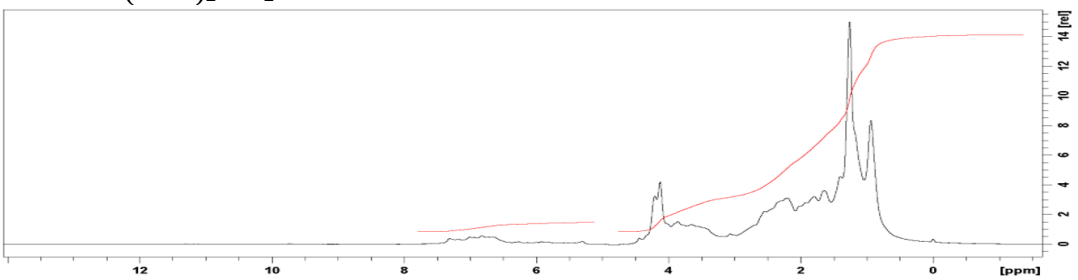


Figure S5.25: The H-NMR spectrum of bio-oil product of corn stover liquefaction using Fe and $Ni(OAc)_2.4H_2O$ of Run 5.25.

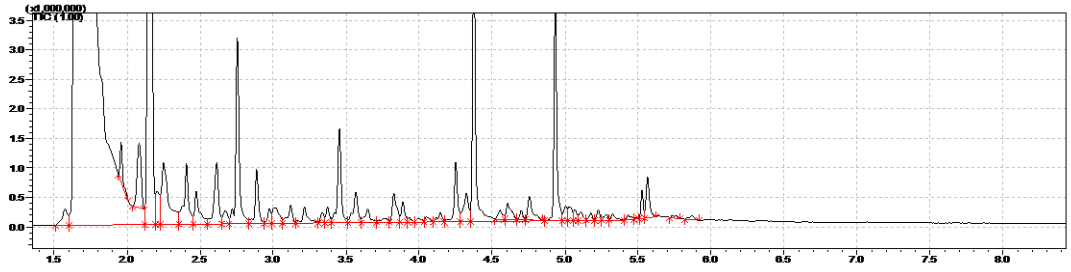

Figure S26: The GC-MS chromatogram of EtOH distillate product of corn stover liquefaction using $Fe_2O_3$, Ni (260°C) and KOAc of Run 5.1.

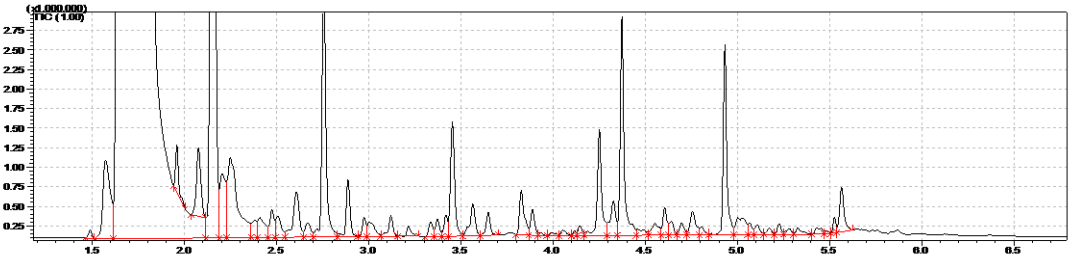

Figure S27: The GC-MS chromatogram of EtOH distillate product of corn stover liquefaction using $Fe_2O_3$, Ni (260°C) and KOAc of Run 5.2.

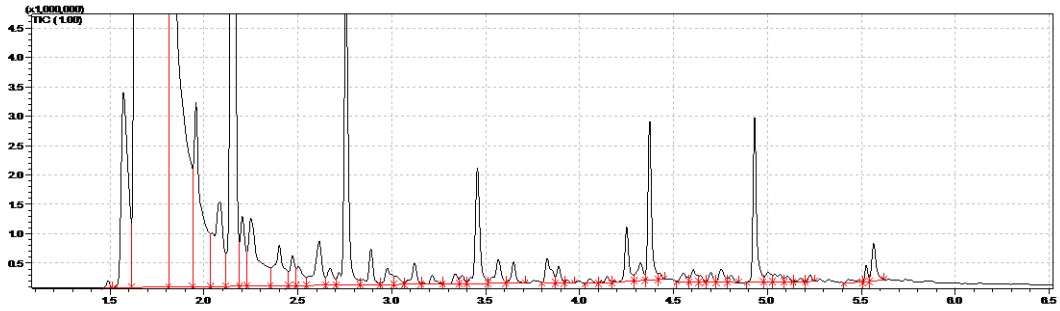

Figure S28: The GC-MS chromatogram of EtOH distillate product of corn stover liquefaction using $Fe_2O_3$, Ni (260°C) and KOAc of Run 5.3.

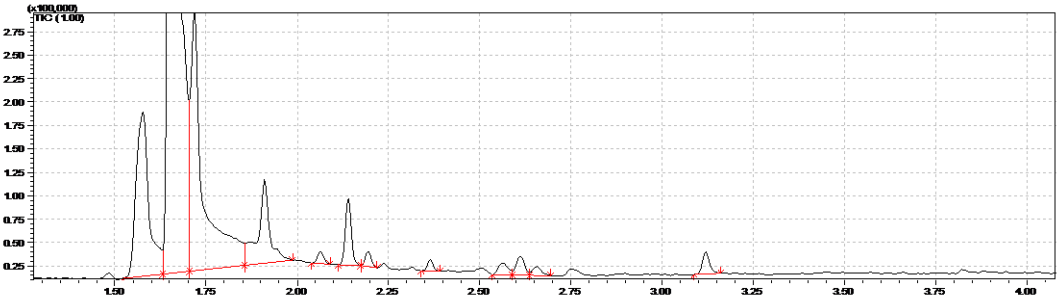

Figure S29: The GC-MS chromatogram of EtOH distillate product of corn stover liquefaction using $Fe_2O_3$, Ni (260°C) and KOAc of Run 5.4.

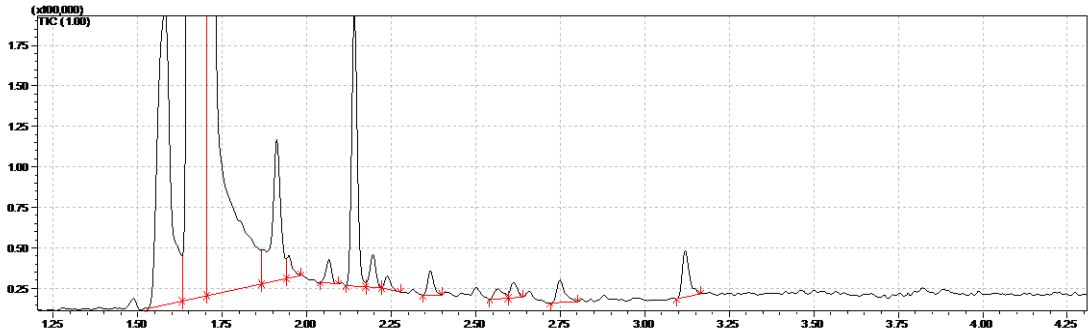

Figure S30: The GC-MS chromatogram of EtOH distillate product of corn stover liquefaction using $Fe_2O_3$, Ni (260°C), and KOAc of Run 5.5.

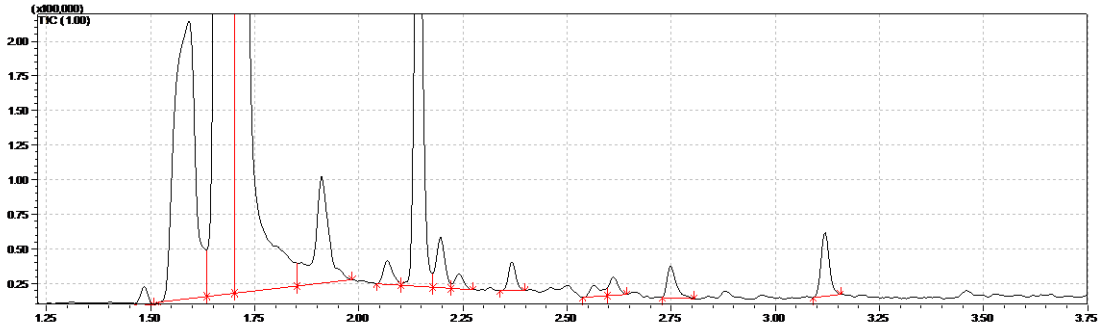

Figure S31: The GC-MS chromatogram of EtOH distillate product of corn stover liquefaction using $Fe_2O_3$, Ni (260°C), and KOAc of Run 5.6.

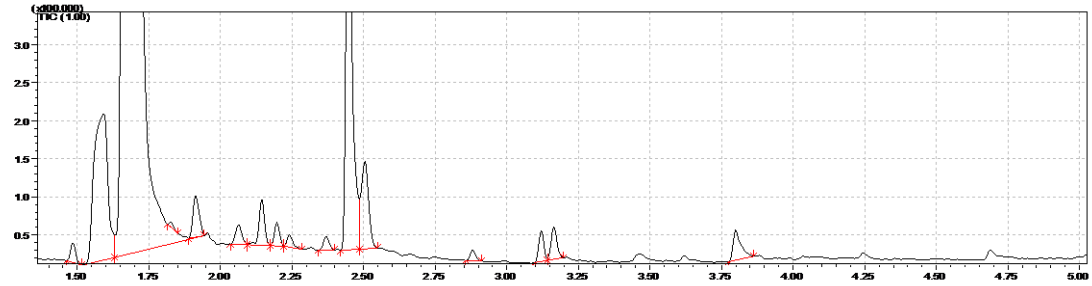

Figure S32: The GC-MS chromatogram of EtOH distillate product of corn stover liquefaction using $Fe_2O_3$, Ni ($H_2$) and KOAc of Run 5.7.

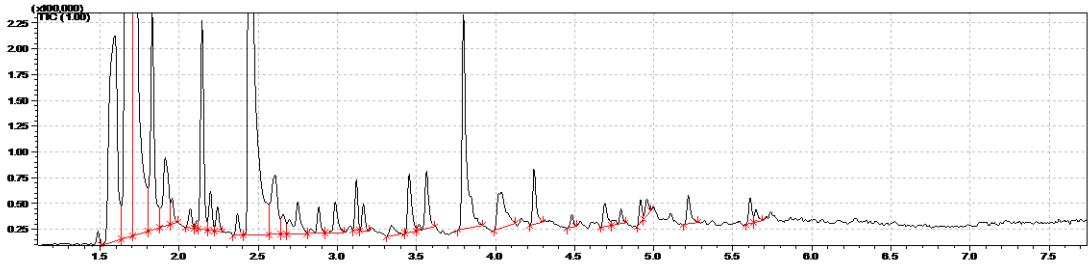

Figure S33: The GC-MS chromatogram of EtOH distillate product of corn stover liquefaction using $Fe_2O_3$, Ni ($H_2$) and KOAc of Run 5.8.

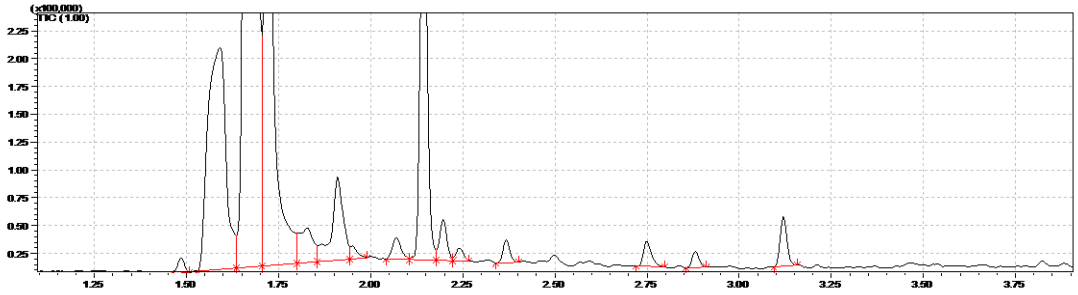

Figure S34: The GC-MS chromatogram of EtOH distillate product of corn stover liquefaction using $Fe_2O_3$, Ni ($H_2$) and KOAc of Run 5.9.

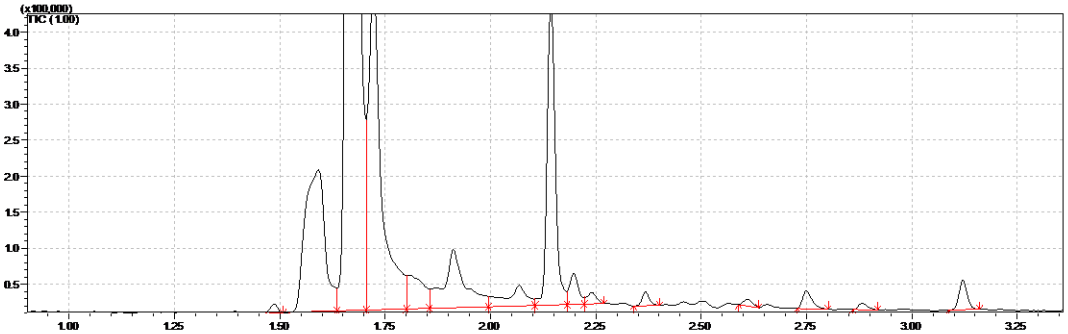

Figure S35: The GC-MS chromatogram of EtOH distillate product of corn stover liquefaction using $Fe_2O_3$, Ni ($H_2$), and KOAc of Run 5.10.

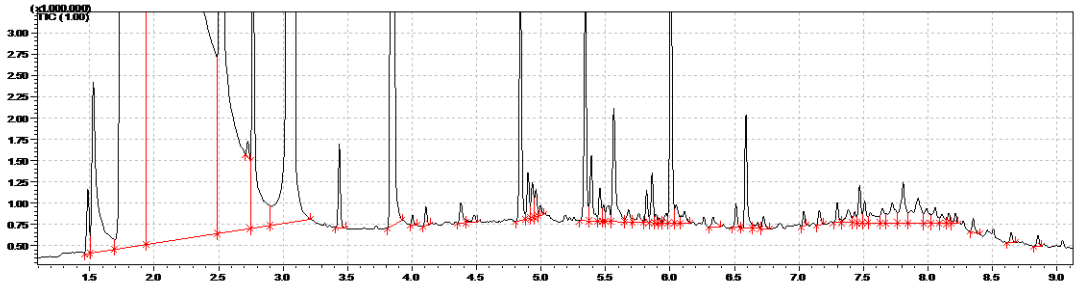

Figure S36: The GC-MS chromatogram of bio-oil product of corn stover liquefaction using $Fe_2O_3$, Ni (260°C), and KOAc of Run 5.1.

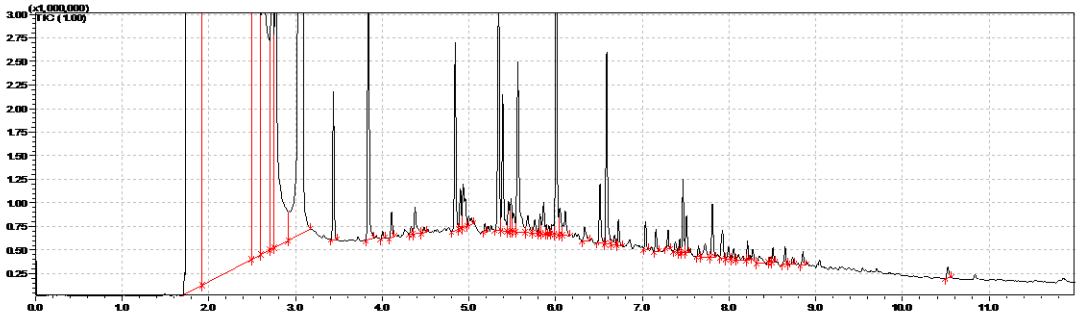

Figure S37: The GC-MS chromatogram of bio-oil product of corn stover liquefaction using $Fe_2O_3$, Ni (260°C), and KOAc of Run 5.2.

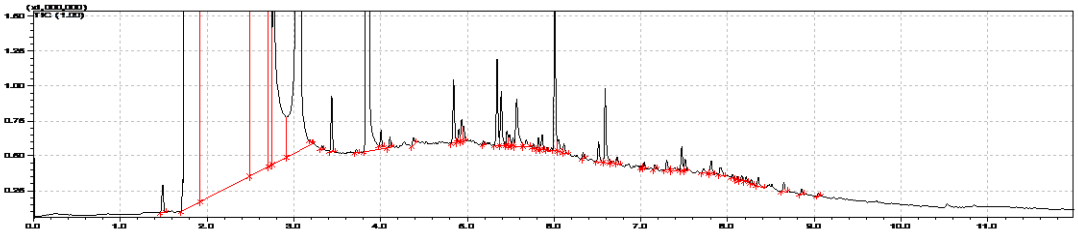

Figure S38: The GC-MS chromatogram of bio-oil product of corn stover liquefaction using $Fe_2O_3$, Ni (260°C) and KOAc of Run 5.3.

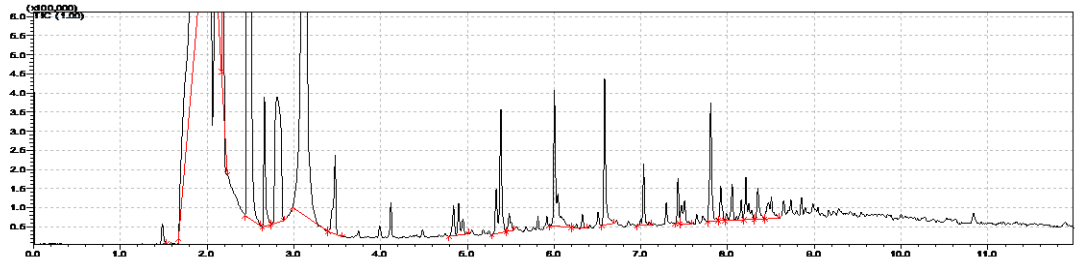

Figure S39: The GC-MS chromatogram of bio-oil product of corn stover liquefaction using $Fe_2O_3$, Ni (260°C), and KOAc of Run 5.4.

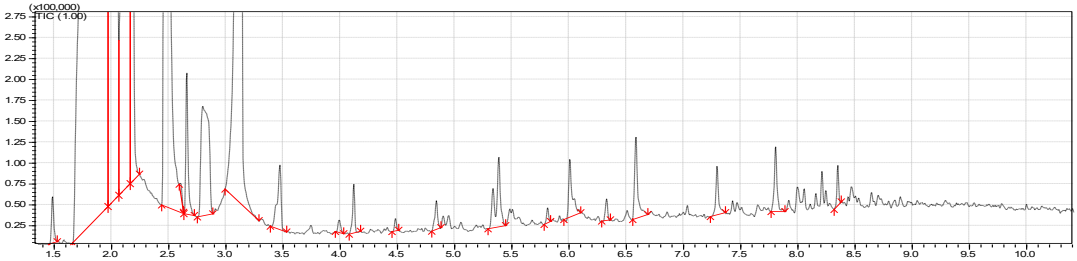

Figure S40: The GC-MS chromatogram of bio-oil product of corn stover liquefaction using $Fe_2O_3$, Ni (260°C), and KOAc of Run 5.5.

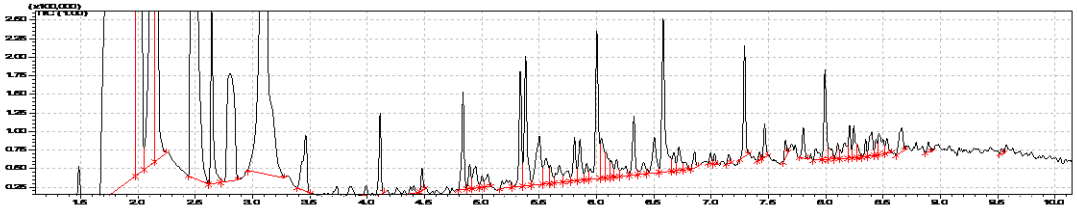

Figure S41: The GC-MS chromatogram of bio-oil product of corn stover liquefaction using $Fe_2O_3$, Ni (260°C), and KOAc of Run 5.6.

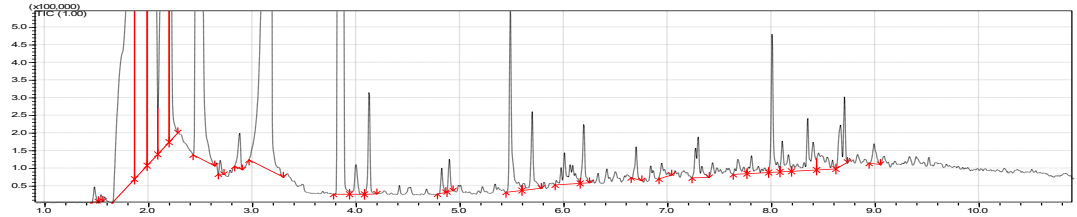

Figure S42: The GC-MS chromatogram of bio-oil product of corn stover liquefaction using $Fe_2O_3$, Ni ($H_2$), and KOAc of Run 5.7.

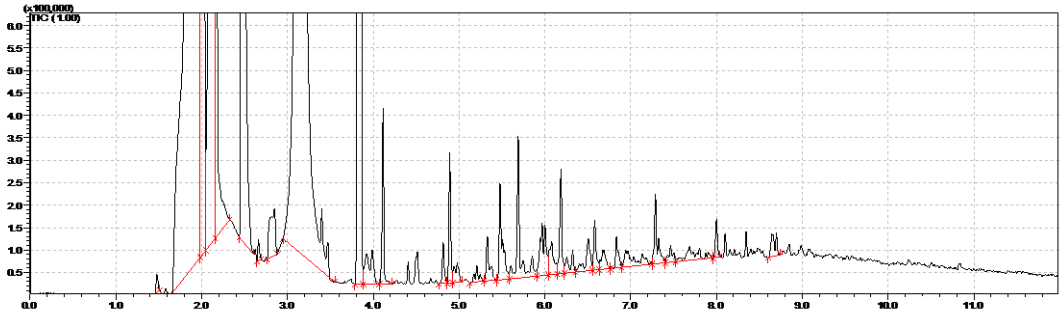

Figure S43: The GC-MS chromatogram of bio-oil product of corn stover liquefaction using $Fe_2O_3$, Ni ($H_2$), and KOAc of Run 5.8.

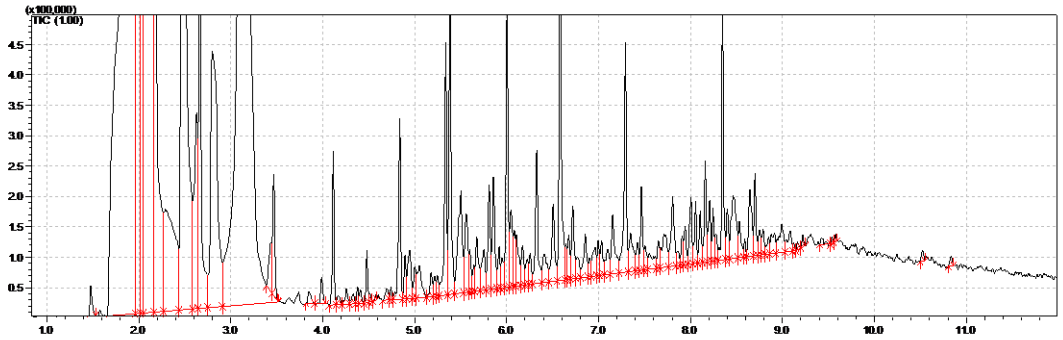

Figure S44: The GC-MS chromatogram of bio-oil product of corn stover liquefaction using $Fe_2O_3$, Ni ($H_2$), and KOAc of Run 5.9.

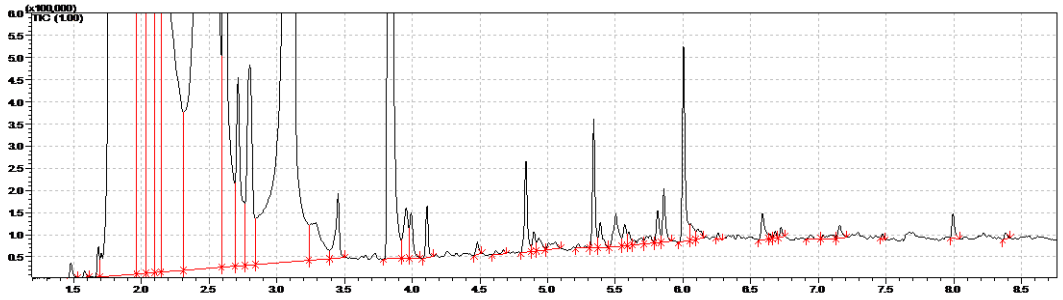

Figure S45: The GC-MS chromatogram of bio-oil product of corn stover liquefaction using $Fe_2O_3$, Ni ($H_2$) and KOAc of Run 5.10.

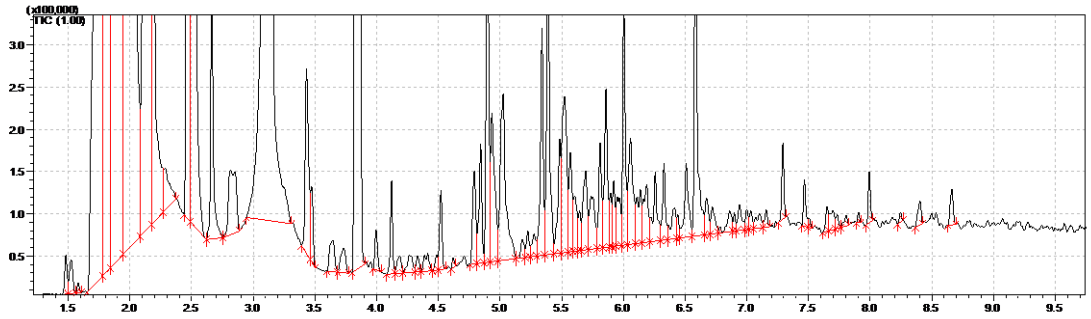

Figure S46: The GC-MS chromatogram of bio-oil product of corn stover liquefaction using Zn and $Ni(OAc)_2.4H_2O$ of Run 5.14.

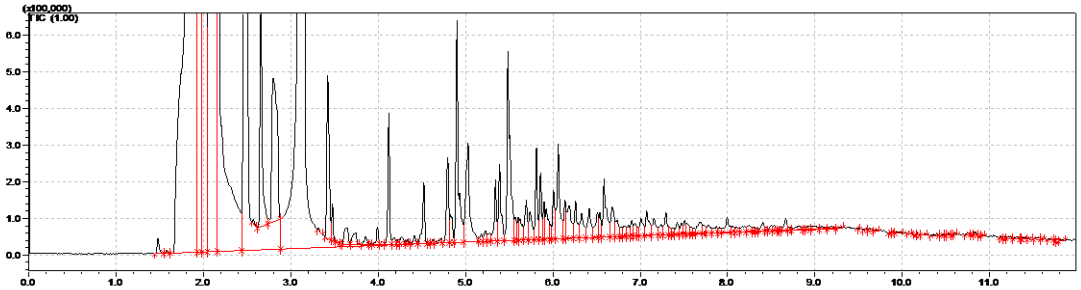

Figure S47: The GC-MS chromatogram of bio-oil product of corn stover liquefaction using Zn and $Ni(OAc)_2.4H_2O$ of Run 5.15.

Figure S48: The GC-MS chromatogram of EtOH distillate product of corn stover liquefaction using Zn and $Ni(OAc)_2.4H_2O$ of Run 5.16.

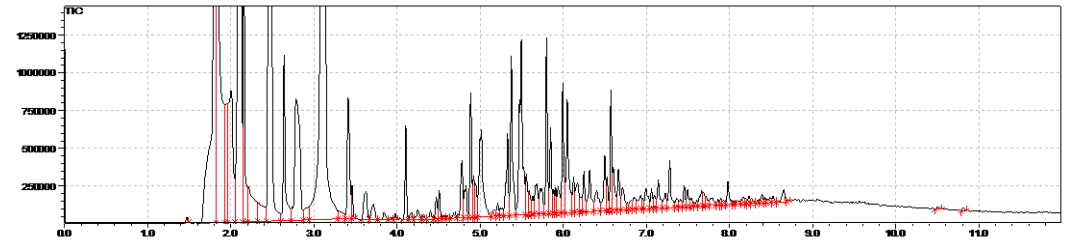

Figure S49: The GC-MS chromatogram of bio-oil product of corn stover liquefaction using Zn and $Ni(OAc)_2.4H_2O$ of Run 5.17.

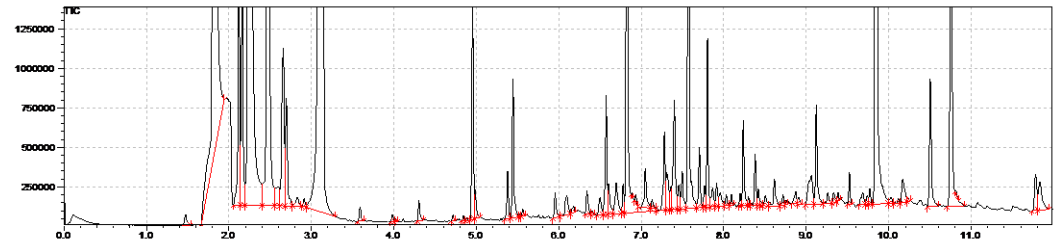

Figure S50: The GC-MS chromatogram of bio-oil product of corn stover liquefaction using Zn and $Ni(OAc)_2.4H_2O$ of Run 5.18.

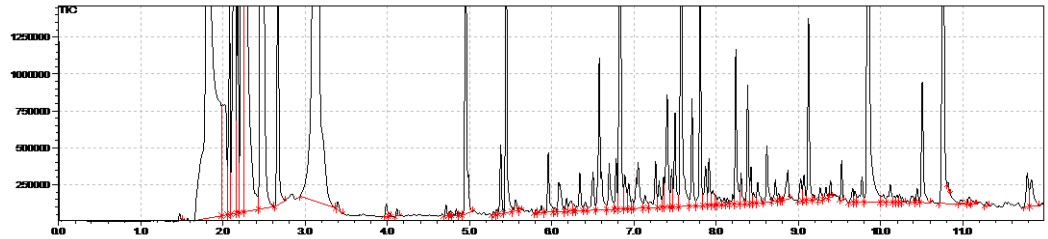

Figure S51: The GC-MS chromatogram of bio-oil product of corn stover liquefaction using Zn and $Ni(OAc)_2.4H_2O$ of Run 5.19.

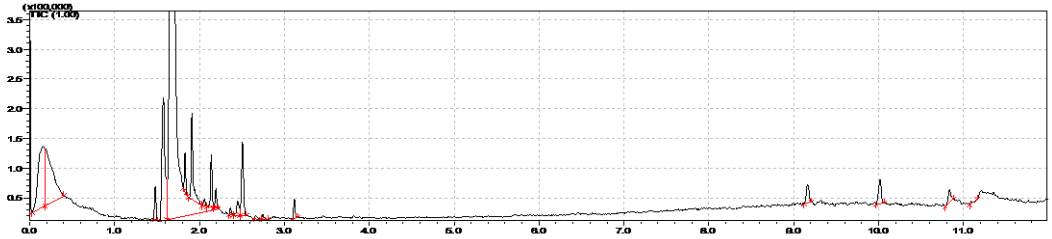

Figure S52: The GC-MS chromatogram of EtOH distillate product of corn stover liquefaction using Zn and $Ni(OAc)_2.4H_2O$ of Run 5.14.

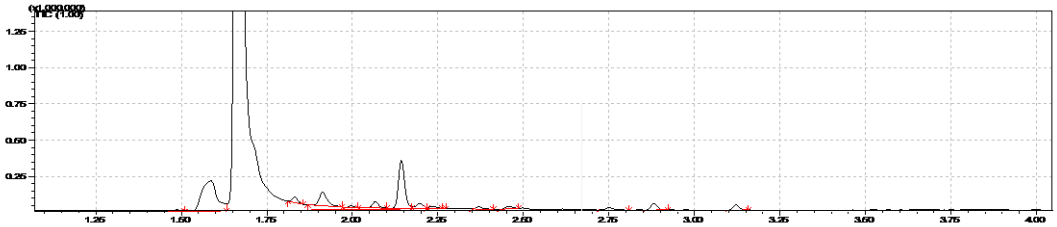

Figure S53: The GC-MS chromatogram of bio-oil product of corn stover liquefaction using Zn and $Ni(OAc)_2.4H_2O$ of Run 5.16.

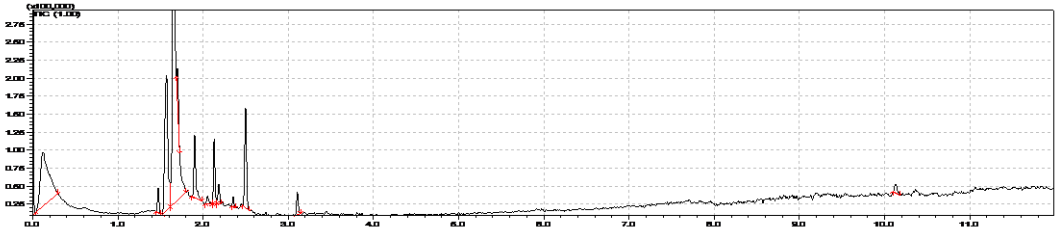

Figure S54: The GC-MS chromatogram of EtOH distillate product of corn stover liquefaction using Zn and $Ni(OAc)_2.4H_2O$ of Run 5.17.

# CHAPTER 6: SUMMARY

The presented work in this dissertation has aimed to study the direct-liquefaction of lignocellulosic biomass for bio-oil production, focusing on the effect of temperature, residence time, biomass, solvent, and catalysts on the yield, composition, and quality of bio-oil. Based on the liquefaction results presented in this work, the following specific conclusions can be summarized:

1) Hydrothermal liquefaction of pine sawdust under basic condition at low temperature of 200 °C was insufficient. Cellulose was mostly recovered. Thus, biomass liquefaction in $H_2O$ should be conducted at higher temperatures.

2) Co-solvent pine sawdust liquefaction using Zn metal and $Ni(OAc)_2$ in 1:1 solvent:$H_2O$ at different temperatures and residence times could provide bio-oils with high yields. Compared to the bio-oils from solvolytic liquefaction, the aromatic and oxygenated species were found in higher amounts in the bio-oils generated from both hydrothermal and co-solvent liquefaction.

3) Metallic salts applied in pine sawdust liquefaction in EtOH showed synergistic effect with Zn, Mn, and Fe metals under basic condition. The effect of metal alone, metal-NaOH, metal oxide, metal oxide, metal oxide-NaOH, Ni metal-metal oxide, and Ni metal-metal oxide-NaOH were investigated in chapter 3 and 4. Based on the results, the last two catalytic systems exhibited better performance on liquefaction of biomass than others. The results obtained from different biomass liquefaction using $Fe_2O_3$-Ni (260°C) under neutral and basic conditions indicate to that bio-oil production was more promoted under basic than neutral conditions and aromatic and oxygenated species were greatly reduced by addition of NaOH.

4) The major components of bio-oil may be alcoholic compounds from EtOH condensation under basic condition when EtOH was used as the solvent. The distribution of bio-oil components is highly determined by the type of biomass, solvent, and catalysts used.

5) The effect of KOAc on corn stover liquefaction was investigated under different conditions (Zn or Fe- NiOAc and Ni metal-$Fe_2O_3$). The results showed that KOAc was more effective than NaOH.

6) Bio-oil yields greater than 40% were obtained using Ni metal-$Fe_2O_3$- KOAc or Zn metal-$Ni(OAc)_2$-KOAc at 300 $^oC$ in less than 4 hr.

## REFERENCES

1. Guo, M.; Song, W.; Buhain, J., Bioenergy and biofuels: history, status, and perspective. *Renewable and Sustainable Energy Reviews* **2015,** *42*, 712-725.

2. Huber, G. W.; Iborra, S.; Corma, A., Synthesis of transportation fuels from biomass: chemistry, catalysts, and engineering. *Chemical reviews* **2006,** *106* (9), 4044-4098.

3. Lynd, L. R.; Cushman, J. H.; Nichols, R. J.; Wyman, C. E., Fuel ethanol from cellulosic biomass. *Science* **1991,** *251* (4999), 1318-1323.

4. Zhang, Y.-H. P., Reviving the carbohydrate economy via multi-product lignocellulose biorefineries. *Journal of industrial microbiology & biotechnology* **2008,** *35* (5), 367-375.

5. Tilman, D.; Socolow, R.; Foley, J. A.; Hill, J.; Larson, E.; Lynd, L.; Pacala, S.; Reilly, J.; Searchinger, T.; Somerville, C., Beneficial biofuels—the food, energy, and environment trilemma. *Science* **2009,** *325* (5938), 270-271.

6. Alonso, D. M.; Bond, J. Q.; Dumesic, J. A., Catalytic conversion of biomass to biofuels. *Green chemistry* **2010,** *12* (9), 1493-1513.

7. Baloch, H. A.; Nizamuddin, S.; Siddiqui, M.; Riaz, S.; Jatoi, A. S.; Dumbre, D. K.; Mubarak, N.; Srinivasan, M.; Griffin, G., Recent advances in production and upgrading of bio-oil from biomass: A critical overview. *Journal of environmental chemical engineering* **2018,** *6* (4), 5101-5118.

8. Akia, M.; Yazdani, F.; Motaee, E.; Han, D.; Arandiyan, H., A review on conversion of biomass to biofuel by nanocatalysts. *Biofuel Research Journal* **2014,** *1* (1), 16-25.

9. Kim, J.-Y.; Lee, H. W.; Lee, S. M.; Jae, J.; Park, Y.-K., Overview of the recent advances in lignocellulose liquefaction for producing biofuels, bio-based materials and chemicals. *Bioresource technology* **2019,** *279*, 373-384.

10. Gollakota, A.; Kishore, N.; Gu, S., A review on hydrothermal liquefaction of biomass. *Renewable and Sustainable Energy Reviews* **2018,** *81*, 1378-1392.

11. Huang, H.-j.; Yuan, X.-z., Recent progress in the direct liquefaction of typical biomass. *Progress in Energy and Combustion Science* **2015,** *49*, 59-80.

12. Alonso, D. M.; Wettstein, S. G.; Dumesic, J. A., Bimetallic catalysts for upgrading of biomass to fuels and chemicals. *Chemical Society Reviews* **2012,** *41* (24), 8075-8098.

13. Joffres, B.; Laurenti, D.; Charon, N.; Daudin, A.; Quignard, A.; Geantet, C., Thermochemical conversion of lignin for fuels and chemicals: A review. *Oil & Gas Science and Technology–Revue d'IFP Energies nouvelles* **2013,** *68* (4), 753-763.

14. Kim, J.-Y.; Heo, S.; Choi, J. W., Effects of phenolic hydroxyl functionality on lignin pyrolysis over zeolite catalyst. *Fuel* **2018,** *232*, 81-89.

15. Chundawat, S. P.; Beckham, G. T.; Himmel, M. E.; Dale, B. E., Deconstruction of lignocellulosic biomass to fuels and chemicals. *Annual review of chemical and biomolecular engineering* **2011,** *2*, 121-145.

16. Zakzeski, J.; Bruijnincx, P. C.; Jongerius, A. L.; Weckhuysen, B. M., The catalytic valorization of lignin for the production of renewable chemicals. *Chemical reviews* **2010,** *110* (6), 3552-3599.

17. Mitrović, D. M.; Janevski, J. N.; Laković, M. S., Primary energy savings using heat storage for biomass heating systems. *Thermal Science* **2012,** *16* (suppl. 2), 423-431.

18. Kumar, A.; Jones, D. D.; Hanna, M. A., Thermochemical biomass gasification: a review of the current status of the technology. *Energies* **2009,** *2* (3), 556-581.

19. Ong, H. C.; Chen, W.-H.; Farooq, A.; Gan, Y. Y.; Lee, K. T.; Ashokkumar, V., Catalytic thermochemical conversion of biomass for biofuel production: A comprehensive review. *Renewable and Sustainable Energy Reviews* **2019,** *113*, 109266.

20. Sınağ, A., Catalysts in thermochemical biomass conversion. In *Biomass Conversion*, Springer: 2012; pp 187-197.

21. Hansen, A. C.; Kyritsis, D. C.; Lee, C. f. F., Characteristics of biofuels and renewable fuel standards. *Biomass to biofuels: strategies for global industries* **2010**, 1-26.

22. Jalkh, R.; El-Rassy, H.; Chehab, G. R.; Abiad, M. G., Assessment of the physico-chemical properties of waste cooking oil and spent coffee grounds oil for potential use as asphalt binder rejuvenators. *Waste and Biomass Valorization* **2018,** *9* (11), 2125-2132.

23. Guo, Y.; Yeh, T.; Song, W.; Xu, D.; Wang, S., A review of bio-oil production from hydrothermal liquefaction of algae. *Renewable and Sustainable Energy Reviews* **2015,** *48*, 776-790.

24. Isa, K. M.; Abdullah, T. A. T.; Ali, U. F. M., Hydrogen donor solvents in liquefaction of biomass: A review. *Renewable and Sustainable Energy Reviews* **2018,** *81*, 1259-1268.

25. Pan, Z.; Wang, L., Novel reversible data hiding scheme for two-stage VQ compressed images based on search-order coding. *Journal of Visual Communication and Image Representation* **2018,** *50*, 186-198.

26. Feng, S.; Wei, R.; Leitch, M.; Xu, C. C., Comparative study on lignocellulose liquefaction in water, ethanol, and water/ethanol mixture: Roles of ethanol and water. *Energy* **2018,** *155*, 234-241.

27. Zhang, L.; Xu, C. C.; Champagne, P., Overview of recent advances in thermo-chemical conversion of biomass. *Energy Conversion and Management* **2010,** *51* (5), 969-982.

28. Rogelj, J.; McCollum, D. L.; Riahi, K., The UN's' Sustainable Energy for All'initiative is compatible with a warming limit of 2 C. *Nature Climate Change* **2013,** *3* (6), 545-551.

29. Cadenas, A.; Cabezudo, S., Biofuels as sustainable technologies: perspectives for less developed countries. *Technological Forecasting and Social Change* **1998,** *58* (1-2), 83-103.

30. Demiral, I.; Eryazıcı, A.; Şensöz, S., Bio-oil production from pyrolysis of corncob (Zea mays L.). *Biomass and Bioenergy* **2012,** *36*, 43-49.

31. Zabaniotou, A.; Kantarelis, E.; Theodoropoulos, D., Sunflower shells utilization for energetic purposes in an integrated approach of energy crops: Laboratory study pyrolysis and kinetics. *Bioresource technology* **2008,** *99* (8), 3174-3181.

32. McKendry, P., Energy production from biomass (part 1): overview of biomass. *Bioresource technology* **2002,** *83* (1), 37-46.

33. McKendry, P., Energy production from biomass (part 2): conversion technologies. *Bioresource technology* **2002,** *83* (1), 47-54.

34. Xu, C.; Lad, N., Production of heavy oils with high caloric values by direct liquefaction of woody biomass in sub/near-critical water. *Energy & Fuels* **2008,** *22* (1), 635-642.

35. Maldas, D.; Shiraishi, N., Liquefaction of biomass in the presence of phenol and H2O using alkalies and salts as the catalyst. *Biomass and Bioenergy* **1997,** *12* (4), 273-279.

36. Karagöz, S.; Bhaskar, T.; Muto, A.; Sakata, Y., Hydrothermal upgrading of biomass: Effect of K2CO3 concentration and biomass/water ratio on products distribution. *Bioresource technology* **2006,** *97* (1), 90-98.

37. Ogi, T.; Yokoyama, S.-y.; Koguchi, K., Direct liquefaction of wood by alkali and alkaline earth salt in an aqueous phase. *Chemistry letters* **1985,** *14* (8), 1199-1202.

38. Chianelli, R.; Berhault, G.; Raybaud, P.; Kasztelan, S.; Hafner, J.; Toulhoat, H., Periodic trends in hydrodesulfurization: in support of the Sabatier principle. *Applied Catalysis A: General* **2002,** *227* (1-2), 83-96.

39. Sughrue, E. L.; Yao, J., Hydrotreating carbohydrates. Google Patents: 2014.

40. Nguyen, H.; Nikolakis, V.; Vlachos, D. G., Mechanistic insights into Lewis acid metal salt-catalyzed glucose chemistry in aqueous solution. *ACS catalysis* **2016,** *6* (3), 1497-1504.

41. van Putten, R.-J.; Van Der Waal, J. C.; De Jong, E.; Rasrendra, C. B.; Heeres, H. J.; de Vries, J. G., Hydroxymethylfurfural, a versatile platform chemical made from renewable resources. *Chemical reviews* **2013,** *113* (3), 1499-1597.

42. Zhao, H.; Holladay, J. E.; Brown, H.; Zhang, Z. C., Metal chlorides in ionic liquid solvents convert sugars to 5-hydroxymethylfurfural. *Science* **2007,** *316* (5831), 1597-1600.

43. Hu, S.; Zhang, Z.; Song, J.; Zhou, Y.; Han, B., Efficient conversion of glucose into 5-hydroxymethylfurfural catalyzed by a common Lewis acid SnCl 4 in an ionic liquid. *Green Chemistry* **2009,** *11* (11), 1746-1749.

44. Cheng, S.; D'cruz, I.; Wang, M.; Leitch, M.; Xu, C., Highly efficient liquefaction of woody biomass in hot-compressed alcohol− water co-solvents. *Energy & Fuels* **2010,** *24* (9), 4659-4667.

45. Singh, R.; Balagurumurthy, B.; Prakash, A.; Bhaskar, T., Catalytic hydrothermal liquefaction of water hyacinth. *Bioresource technology* **2015,** *178*, 157-165.

46. Yuan, Z.; Cheng, S.; Leitch, M.; Xu, C. C., Hydrolytic degradation of alkaline lignin in hot-compressed water and ethanol. *Bioresource technology* **2010,** *101* (23), 9308-9313.

47. Chen, Z.; Wan, C., Biological valorization strategies for converting lignin into fuels and chemicals. *Renewable and Sustainable Energy Reviews* **2017,** *73*, 610-621.

48. Amada, Y.; Watanabe, H.; Hirai, Y.; Kajikawa, Y.; Nakagawa, Y.; Tomishige, K., Production of biobutanediols by the hydrogenolysis of erythritol. *ChemSusChem* **2012,** *5* (10), 1991-1999.

49. Nakagawa, Y.; Kasumi, T.; Ogihara, J.; Tamura, M.; Arai, T.; Tomishige, K., Erythritol: Another C4 Platform Chemical in Biomass Refinery. *ACS omega* **2020,** *5* (6), 2520-2530.

50. Naik, S. N.; Goud, V. V.; Rout, P. K.; Dalai, A. K., Production of first and second generation biofuels: a comprehensive review. *Renewable and sustainable energy reviews* **2010,** *14* (2), 578-597.

51. Isikgor, F. H.; Becer, C. R., Lignocellulosic biomass: a sustainable platform for the production of bio-based chemicals and polymers. *Polymer Chemistry* **2015,** *6* (25), 4497-4559.

52. Mettler, M. S.; Vlachos, D. G.; Dauenhauer, P. J., Top ten fundamental challenges of biomass pyrolysis for biofuels. *Energy & Environmental Science* **2012,** *5* (7), 7797-7809.

53. French, R.; Czernik, S., Catalytic pyrolysis of biomass for biofuels production. *Fuel Processing Technology* **2010,** *91* (1), 25-32.

54. Su-Ping, Z., Study of hydrodeoxygenation of bio-oil from the fast pyrolysis of biomass. *Energy Sources* **2003,** *25* (1), 57-65.

55. Wang, A.; Austin, D.; Song, H., Investigations of thermochemical upgrading of biomass and its model compounds: Opportunities for methane utilization. *Fuel* **2019,** *246*, 443-453.

56. Wang, Y.; Wang, H.; Lin, H.; Zheng, Y.; Zhao, J.; Pelletier, A.; Li, K., Effects of solvents and catalysts in liquefaction of pinewood sawdust for the production of bio-oils. *Biomass and bioenergy* **2013,** *59*, 158-167.

57. Chornet, E.; Overend, R. P., Biomass liquefaction: an overview. In *Fundamentals of thermochemical biomass conversion*, Springer: 1985; pp 967-1002.

58. Akhtar, J.; Amin, N. A. S., A review on process conditions for optimum bio-oil yield in hydrothermal liquefaction of biomass. *Renewable and Sustainable Energy Reviews* **2011,** *15* (3), 1615-1624.

59. Kobayashi, H.; Hosaka, Y.; Hara, K.; Feng, B.; Hirosaki, Y.; Fukuoka, A., Control of selectivity, activity and durability of simple supported nickel catalysts for hydrolytic hydrogenation of cellulose. *Green chemistry* **2014,** *16* (2), 637-644.

60. Jin, S.; Xiao, Z.; Chen, X.; Wang, L.; Guo, J.; Zhang, M.; Liang, C., Cleavage of lignin-derived 4-O-5 aryl ethers over nickel nanoparticles supported on niobic acid-activated carbon composites. *Industrial & Engineering Chemistry Research* **2015,** *54* (8), 2302-2310.

61. Song, Q.; Wang, F.; Cai, J.; Wang, Y.; Zhang, J.; Yu, W.; Xu, J., Lignin depolymerization (LDP) in alcohol over nickel-based catalysts via a fragmentation–hydrogenolysis process. *Energy & Environmental Science* **2013,** *6* (3), 994-1007.

62. Toledano, A.; Serrano, L.; Pineda, A.; Romero, A. A.; Luque, R.; Labidi, J., Microwave-assisted depolymerisation of organosolv lignin via mild hydrogen-free hydrogenolysis: Catalyst screening. *Applied Catalysis B: Environmental* **2014,** *145*, 43-55.

63. He, J.; Zhao, C.; Lercher, J. A., Ni-catalyzed cleavage of aryl ethers in the aqueous phase. *Journal of the American Chemical Society* **2012,** *134* (51), 20768-20775.

64. Wang, X.; Rinaldi, R., Solvent effects on the hydrogenolysis of diphenyl ether with Raney nickel and their implications for the conversion of lignin. *ChemSusChem* **2012,** *5* (8), 1455-1466.

65. Molinari, V.; Giordano, C.; Antonietti, M.; Esposito, D., Titanium nitride-nickel nanocomposite as heterogeneous catalyst for the hydrogenolysis of aryl ethers. *Journal of the American Chemical Society* **2014,** *136* (5), 1758-1761.

66. Barta, K.; Warner, G. R.; Beach, E. S.; Anastas, P. T., Depolymerization of organosolv lignin to aromatic compounds over Cu-doped porous metal oxides. *Green Chemistry* **2014,** *16* (1), 191-196.

67. Barta, K.; Matson, T. D.; Fettig, M. L.; Scott, S. L.; Iretskii, A. V.; Ford, P. C., Catalytic disassembly of an organosolv lignin via hydrogen transfer from supercritical methanol. *Green Chemistry* **2010,** *12* (9), 1640-1647.

68. Macala, G. S.; Matson, T. D.; Johnson, C. L.; Lewis, R. S.; Iretskii, A. V.; Ford, P. C., Hydrogen transfer from supercritical methanol over a solid base catalyst: A model for lignin depolymerization. *ChemSusChem: Chemistry & Sustainability Energy & Materials* **2009,** *2* (3), 215-217.

69. Jongerius, A. L.; Jastrzebski, R.; Bruijnincx, P. C.; Weckhuysen, B. M., CoMo sulfide-catalyzed hydrodeoxygenation of lignin model compounds: An extended reaction network for the conversion of monomeric and dimeric substrates. *Journal of catalysis* **2012,** *285* (1), 315-323.

70. Rensel, D. J.; Rouvimov, S.; Gin, M. E.; Hicks, J. C., Highly selective bimetallic FeMoP catalyst for C–O bond cleavage of aryl ethers. *Journal of catalysis* **2013,** *305*, 256-263.

71. Ma, R.; Hao, W.; Ma, X.; Tian, Y.; Li, Y., Catalytic ethanolysis of Kraft lignin into high-value small-molecular chemicals over a nanostructured α-molybdenum carbide catalyst. *Angewandte Chemie* **2014,** *126* (28), 7438-7443.

72. Qi, S.; Jiaying, C.; ZHANG, J.; Weiqiang, Y.; Feng, W.; Jie, X., Hydrogenation and cleavage of the CO bonds in the lignin model compound phenethyl phenyl ether over a nickel-based catalyst. *Chinese Journal of Catalysis* **2013,** *34* (4), 651-658.

73. Kumar, A.; Wang, L.; Dzenis, Y. A.; Jones, D. D.; Hanna, M. A., Thermogravimetric characterization of corn stover as gasification and pyrolysis feedstock. *Biomass and Bioenergy* **2008,** *32* (5), 460-467.

74. Li, Q.; Liu, D.; Song, L.; Wu, P.; Yan, Z., Direct liquefaction of sawdust in supercritical alcohol over ionic liquid nickel catalyst: effect of solvents. *Energy & Fuels* **2014,** *28* (11), 6928-6935.

75. Zanchet, D.; Santos, J. B. O.; Damyanova, S.; Gallo, J. M. R.; Bueno, J. M. C., Toward understanding metal-catalyzed ethanol reforming. *ACS Catalysis* **2015,** *5* (6), 3841-3863.

76. Konsolakis, M.; Ioakimidis, Z.; Kraia, T.; Marnellos, G. E., Hydrogen production by ethanol steam reforming (ESR) over CeO2 supported transition metal (Fe, Co, Ni, Cu) catalysts: Insight into the structure-activity relationship. *Catalysts* **2016,** *6* (3), 39.

77. Choi, Y.; Liu, P., Understanding of ethanol decomposition on Rh (1 1 1) from density functional theory and kinetic Monte Carlo simulations. *Catalysis Today* **2011,** *165* (1), 64-70.

78. Zhang, P.; Dong, S.-J.; Ma, H.-H.; Zhang, B.-X.; Wang, Y.-F.; Hu, X.-M., Fractionation of corn stover into cellulose, hemicellulose and lignin using a series of ionic liquids. *Industrial Crops and Products* **2015,** *76*, 688-696.

79. Yang, H.; Yan, R.; Chen, H.; Lee, D. H.; Zheng, C., Characteristics of hemicellulose, cellulose and lignin pyrolysis. *Fuel* **2007,** *86* (12), 1781-1788.

80. Wei Kong, X.; Liang Zhang, R.; Kui Zhong, S.; Wu, L., Electrospinning synthesis of 3D porous NiO nanorods as anode material for lithium-ion batteries. *Materials Science-Poland* **2016,** *34* (2), 227-232.

81. Drobná, H.; Kout, M.; Sołtysek, A.; González-Delacruz, V. M.; Caballero, A.; Čapek, L., Analysis of Ni species formed on zeolites, mesoporous silica and alumina supports and their catalytic behavior in the dry reforming of methane. *Reaction Kinetics, Mechanisms and Catalysis* **2017,** *121* (1), 255-274.

82. Langholtz, M.; Stokes, B.; Eaton, L., 2016 Billion-ton report: Advancing domestic resources for a thriving bioeconomy, Volume 1: Economic availability of feedstock. *Oak Ridge National Laboratory, Oak Ridge, Tennessee, managed by UT-Battelle, LLC for the US Department of Energy* **2016,** *2016*, 1-411.

83. Yim, S. C.; Quitain, A. T.; Yusup, S.; Sasaki, M.; Uemura, Y.; Kida, T., Metal oxide-catalyzed hydrothermal liquefaction of Malaysian oil palm biomass to bio-oil under supercritical condition. *The Journal of Supercritical Fluids* **2017,** *120*, 384-394.

84. Khampuang, K.; Boreriboon, N.; Prasassarakich, P., Alkali catalyzed liquefaction of corncob in supercritical ethanol–water. *Biomass and Bioenergy* **2015,** *83*, 460-466.

85. Govindasamy, G.; Sharma, R.; Subramanian, S., Studies on the effect of heterogeneous catalysts on the hydrothermal liquefaction of sugarcane bagasse to low-oxygen-containing bio-oil. *Biofuels* **2019,** *10* (5), 665-675.

86. Liu, Z.; Zhang, F.-S., Effects of various solvents on the liquefaction of biomass to produce fuels and chemical feedstocks. *Energy conversion and management* **2008,** *49* (12), 3498-3504.

87. Ye, L.; Zhang, J.; Zhao, J.; Tu, S., Liquefaction of bamboo shoot shell for the production of polyols. *Bioresource technology* **2014,** *153*, 147-153.

88. Meryemoğlu, B.; Hasanoğlu, A.; Irmak, S.; Erbatur, O., Biofuel production by liquefaction of kenaf (Hibiscus cannabinus L.) biomass. *Bioresource technology* **2014,** *151*, 278-283.

89. Yu, F.; Liu, Y.; Pan, X.; Lin, X.; Liu, C.; Chen, P.; Ruan, R. In *Liquefaction of corn stover and preparation of polyester from the liquefied polyol*, Twenty-Seventh Symposium on Biotechnology for Fuels and Chemicals, Springer: 2006; pp 574-585.

90. Wu, H.; Zheng, J.; Wang, G., Catalytic liquefaction of switchgrass in isobutanol/water system for bio-oil development over bifunctional Ni-HPMo/Fe3O4@ Al-MCM-41 catalysts. *Renewable Energy* **2019,** *141*, 96-106.

91. Ramirez, J. A.; Brown, R. J.; Rainey, T. J., A review of hydrothermal liquefaction bio-crude properties and prospects for upgrading to transportation fuels. *Energies* **2015,** *8* (7), 6765-6794.

92. Minowa, T.; Kondo, T.; Sudirjo, S. T., Thermochemical liquefaction of Indonesian biomass residues. *Biomass and Bioenergy* **1998,** *14* (5-6), 517-524.

93. Karagöz, S.; Bhaskar, T.; Muto, A.; Sakata, Y., Effect of Rb and Cs carbonates for production of phenols from liquefaction of wood biomass. *Fuel* **2004,** *83* (17-18), 2293-2299.

94. Cao, L.; Zhang, C.; Chen, H.; Tsang, D. C.; Luo, G.; Zhang, S.; Chen, J., Hydrothermal liquefaction of agricultural and forestry wastes: state-of-the-art review and future prospects. *Bioresource technology* **2017,** *245*, 1184-1193.

95. Deuss, P. J.; Barta, K.; de Vries, J. G., Homogeneous catalysis for the conversion of biomass and biomass-derived platform chemicals. *Catalysis Science & Technology* **2014,** *4* (5), 1174-1196.

96. Chng, L. L.; Erathodiyil, N.; Ying, J. Y., Nanostructured catalysts for organic transformations. *Accounts of chemical research* **2013,** *46* (8), 1825-1837.

97. Molnar, A., Efficient, selective, and recyclable palladium catalysts in carbon− carbon coupling reactions. *Chemical reviews* **2011,** *111* (3), 2251-2320.

98. Yang, J.; Li, N.; Li, S.; Wang, W.; Li, L.; Wang, A.; Wang, X.; Cong, Y.; Zhang, T., Synthesis of diesel and jet fuel range alkanes with furfural and ketones from lignocellulose under solvent free conditions. *Green chemistry* **2014,** *16* (12), 4879-4884.

99. Shrotri, A.; Kobayashi, H.; Fukuoka, A., Cellulose depolymerization over heterogeneous catalysts. *Accounts of chemical research* **2018,** *51* (3), 761-768.

100. Corma, A.; de la Torre, O.; Renz, M., Production of high quality diesel from cellulose and hemicellulose by the Sylvan process: catalysts and process variables. *Energy & Environmental Science* **2012,** *5* (4), 6328-6344.

101. Bohre, A.; Saha, B.; Abu-Omar, M. M., Catalytic Upgrading of 5-Hydroxymethylfurfural to Drop-in Biofuels by Solid Base and Bifunctional Metal–Acid Catalysts. *ChemSusChem* **2015,** *8* (23), 4022-4029.

102. Chen, P.; Zhang, Q.; Shu, R.; Xu, Y.; Ma, L.; Wang, T., Catalytic depolymerization of the hydrolyzed lignin over mesoporous catalysts. *Bioresource technology* **2017,** *226*, 125-131.

103. Zhang, X.; Tang, W.; Zhang, Q.; Wang, T.; Ma, L., Hydrodeoxygenation of lignin-derived phenoic compounds to hydrocarbon fuel over supported Ni-based catalysts. *Applied Energy* **2018,** *227*, 73-79.

104. Gliński, M.; Kijeński, J.; Jakubowski, A., Ketones from monocarboxylic acids: catalytic ketonization over oxide systems. *Applied Catalysis A: General* **1995,** *128* (2), 209-217.

105. Pham, T. N.; Sooknoi, T.; Crossley, S. P.; Resasco, D. E., Ketonization of carboxylic acids: mechanisms, catalysts, and implications for biomass conversion. *Acs Catalysis* **2013,** *3* (11), 2456-2473.

106. Xu, C.; Etcheverry, T., Hydro-liquefaction of woody biomass in sub-and super-critical ethanol with iron-based catalysts. *Fuel* **2008,** *87* (3), 335-345.

107. Li, Q.; Liu, D.; Li, M.; Song, L.; Li, M.; Yan, Z.; Geng, Y., Hydro-liquefaction of woody biomass for bio-oil in supercritical solvent with [BMIM] Cl/NiCl 2 catalyst. *Applied Petrochemical Research* **2015,** *5* (4), 363-369.

108. Kumar, S.; Surendra, K., Role of sodium hydroxide for hydrogen gas production and storage. *College of Engineering and Computing, Florida International University, Miami, Florida* **2013,** *33199*.

109. Zhong, C.; Wei, X., A comparative experimental study on the liquefaction of wood. *Energy* **2004,** *29* (11), 1731-1741.

110. Wang, C.; Pan, J.; Li, J.; Yang, Z., Comparative studies of products produced from four different biomass samples via deoxy-liquefaction. *Bioresource technology* **2008,** *99* (8), 2778-2786.

111. de Caprariis, B.; De Filippis, P.; Petrullo, A.; Scarsella, M., Hydrothermal liquefaction of biomass: Influence of temperature and biomass composition on the bio-oil production. *Fuel* **2017,** *208*, 618-625.

112. O'Lenick, A. J., Guerbet chemistry. *Journal of Surfactants and Detergents* **2001,** *4* (3), 311-315.

113. Shuping, Z.; Yulong, W.; Mingde, Y.; Kaleem, I.; Chun, L.; Tong, J., Production and characterization of bio-oil from hydrothermal liquefaction of microalgae Dunaliella tertiolecta cake. *Energy* **2010,** *35* (12), 5406-5411.

114. de Caprariis, B.; Bavasso, I.; Bracciale, M. P.; Damizia, M.; De Filippis, P.; Scarsella, M., Enhanced bio-crude yield and quality by reductive hydrothermal liquefaction of oak wood biomass: Effect of iron addition. *Journal of analytical and applied pyrolysis* **2019,** *139*, 123-130.

115. Arturi, K. R.; Kucheryavskiy, S.; Søgaard, E. G., Performance of hydrothermal liquefaction (HTL) of biomass by multivariate data analysis. *Fuel processing technology* **2016,** *150*, 94-103.

116. Yang, L.; Havard, P.; Corscadden, K.; Xu, C. C.; Wang, X., Co-liquefaction of spent coffee grounds and lignocellulosic feedstocks. *Bioresource technology* **2017,** *237*, 108-121.

117. Zhu, Z.; Toor, S. S.; Rosendahl, L.; Yu, D.; Chen, G., Influence of alkali catalyst on product yield and properties via hydrothermal liquefaction of barley straw. *Energy* **2015,** *80*, 284-292.

118. Lancas, F. M.; Ruggiero, M. A.; Donate, P. M., Upgrading of Sugar Cane Bagasse by Thermal Processes 10. Catalytic Liquefaction in Aqueous Medium. *Energy sources* **1999,** *21* (4), 309-318.

119. Zhang, Y.; Gong, X.; Zhang, B.; Liu, W.; Xu, M., Potassium catalytic hydrogen production in sorption enhanced gasification of biomass with steam. *international journal of hydrogen energy* **2014,** *39* (9), 4234-4243.

120. Li, W.; Gao, Y.; Yao, S.; Ma, D.; Yan, N., Effective deoxygenation of fatty acids over Ni (OAc) 2 in the absence of H 2 and solvent. *Green Chemistry* **2015,** *17* (8), 4198-4205.

121. Ren, D.; Song, Z.; Li, L.; Liu, Y.; Jin, F.; Huo, Z., Production of 2, 5-hexanedione and 3-methyl-2-cyclopenten-1-one from 5-hydroxymethylfurfural. *Green Chemistry* **2016,** *18* (10), 3075-3081.

122. Zhao, Y.-P.; Zhu, W.-W.; Wei, X.-Y.; Fan, X.; Cao, J.-P.; Dou, Y.-Q.; Zong, Z.-M.; Zhao, W., Synergic effect of methanol and water on pine liquefaction. *Bioresource technology* **2013,** *142*, 504-509.

123. Qian, Y.; Zuo, C.; Tan, J.; He, J., Structural analysis of bio-oils from sub-and supercritical water liquefaction of woody biomass. *Energy* **2007,** *32* (3), 196-202.

124. Fang, Z.; Sato, T.; Smith Jr, R. L.; Inomata, H.; Arai, K.; Kozinski, J. A., Reaction chemistry and phase behavior of lignin in high-temperature and supercritical water. *Bioresource Technology* **2008,** *99* (9), 3424-3430.